

TH-6016

QUANTITATIVE DESCRIPTION OF DEPRESSION STORAGE AND ROUGHNESS
PROPERTIES USING A DIGITAL SURFACE MODEL

A Thesis

Presented to

The Faculty of Graduate Studies

of

The University of Guelph

by

WASI ULLAH

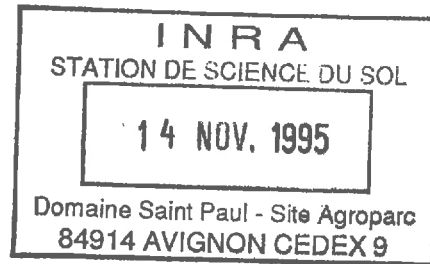
In partial fulfilment of requirements

for the degree of

Doctor of Philosophy

May, 1974

© WASI ULLAH, 1974



UNIVERSITY OF GUELPH
FACULTY OF GRADUATE STUDIES

ULLAH	
surname	
Wasi	9801460
given names	I.D. number
Agricultural Engineering	Ph.D.
department	degree

CERTIFICATE OF APPROVAL (DOCTORAL THESIS)

We, the undersigned, hereby certify that the thesis presented by the above-named candidate in partial fulfilment of the requirements for the degree of
Doctor of Philosophy
is worthy of acceptance and may now be formally submitted to the Dean of Graduate Studies.

Title: Quantitative Description of Depression Storage and Roughness
Properties Using A Digital Surface Model

External Examiner

Truman Adkinson
Candidate's Research Supervisor

J. W. Kitchison
Supervisory Committee

Stanley H. Collins
Supervisory Committee

Supervisory Committee

Supervisory Committee

Merit Rating

- Distinguished
- Satisfactory

Date: May 12/74

Received by [Signature]
Dean of Graduate Studies

Date: 10/10/74

ABSTRACT

QUANTITATIVE DESCRIPTION OF DEPRESSION STORAGE AND ROUGHNESS — PROPERTIES USING A DIGITAL SURFACE MODEL

Wasi Ullah, Ph.D.
University of Guelph, 1974

Supervisor:
Dr. W.T. Dickinson

Considering a surface runoff system, there exists a mechanism of retention in storage and surface flow which is characterized by the geometry of the watershed surface. This thesis is an investigation of the physical properties of a surface in terms of depression storage and surface roughness. Depression storage is a dominating storage element which accounts for most of the retention on a watershed surface. Surface roughness controls the hydraulics of overland flow.

The above two properties depend upon the surface configuration which can be modelled with a set of elevation values given as a function of horizontal coordinates. These values constitute a digital surface model. A photogrammetric technique has been used to develop digital surface models for 15 sample plots, of about 160 cm. by 200 cm. size having similar physiographic conditions.

A simple digital technique has been developed and used to determine the geometric properties of individual depressions of all sample plots. The method scans the digital surface model and identifies characteristic points of depressions

such as low points, pour points, etc. The data of volume, depth, and surface area of individual depressions are subsequently analysed.

The spatial distribution of depressions is found to be both random and direction oriented. Depression storage volume decreases with slope of the plot due to a reduction in both the number of depressions and the dimensions of individual depressions. The three geometric properties of depth, surface area, and volume are also related to each other.

The geometric properties of the depressions exhibit frequency distribution of somewhat similar characteristics. The observed frequency distributions can be satisfactorily described by the three parameter Weibull distribution function.

The method of quantitatively describing surface roughness of a microsurface considers roughness as being caused by height, slope, and frequency of occurrence of microrelief features. A microrelief feature is defined as a ridge or depression having horizontal extent of 5 to 60 cm. According to this definition, that part of the Fourier cosine series containing wave lengths $5 \leq \lambda \leq 60$ is assumed to contain all information about the geometric properties of microrelief features associated with any profile. This part of the Fourier series is processed to obtain five roughness components of each profile. A visual comparison indicates that the numerical values of roughness components are compatible with the

physical structure of profiles when plotted on a graph.

Seasonal effects are very pronounced in substantially reducing the total volume of depression storage and the dimensions of individual depressions. The reduction in the number of depressions is also substantial. The roughness components, however, do not exhibit any significant change over the same interval. Therefore, the range of data reported in this study does not indicate any relationship between depression storage and surface roughness.

The results of this study have wide application and will help in developing realistic parameters of hydrologic response models. Application of the results has been examined in a watershed model proposed by Claborn and Moore (1970).

TABLE OF CONTENTS

Chapter	Page
LIST OF TABLES	vii
LIST OF FIGURES	viii
1. INTRODUCTION	1
2. REVIEW OF PREVIOUS WORKS	7
2.1. ESTIMATES OF DEPRESSION STORAGE VOLUMES	7
2.11. General Continuity Equation ...	7
2.12. Hydrograph Analysis	8
2.13. Watershed Simulation Models ...	12
2.14. Urban Runoff Models.....	17
2.2. METHODS OF MEASURING SURFACE ELEVATION	20
2.21. Leveling Instruments	21
2.22. Specially Designed Point Gauges	22
2.23. Aerial and Terrestrial Photo- grammetry	24
2.3. DETERMINATION OF STORAGE VOLUME	26
2.4. ACTIVE POTENTIAL STORAGE VOLUME AND MEASURED STORAGE VOLUME	29
2.5. QUANTITATIVE DESCRIPTION OF SURFACE ROUGHNESS	30
2.51. Definition of Surface Roughness	30
2.52. Methods of Describing Surface Roughness	34
2.521. Surface Roughness Para- meters	34
2.522. Normal Density Functions and Autocorrelation Functions.....	35

Chapter	Page
2.523. Power Spectral Density Function.....	38
2.524. Fourier Series Analysis	40
3. OBJECTIVES.....	46
4. THEORETICAL FRAMEWORK.....	48
4.1. GENERAL.....	48
4.2. ESTIMATION OF GEOMETRIC PROPERTIES OF DEPRESSIONS.....	48
4.21. Basic Considerations.....	48
4.22. Measurable Geometric Properties of Depressions.....	49
4.23. Definition of Terms.....	51
4.24. Identification of Points.....	55
4.25. Computation of Volume of Storage.....	58
4.26. Sample Computation by the Proposed Digital Method.....	59
4.27. Comparison of Results with Contour Area Method.....	62
4.28. Evaluation of the Digital Method.....	66
4.29. Algorithm Design Considerations	67
4.30. Algorithm Design and Computer Programming.....	69
4.3 QUANTITATIVE DESCRIPTION OF SURFACE ROUGHNESS.....	73
4.31. General.....	73
4.32. Basic Considerations in Selection of Methodology.....	74
4.33. Physical Concept of Roughness...	75
4.34. Definition of Microrelief Features of Microsurface.....	77
4.35. Fourier Analysis of a Profile...	79

Chapter	Page
4.36. Mathematical Formulations of Roughness Elements	83
4.361. Relief Factor (M) ...	83
4.362. Slope Factor (P)	84
4.363. Structural Homogeneity Factor (K)	85
4.364. Resistance Factor (ρ)	88
4.365. Cell Length (C_L)	89
4.37. Summary of Roughness Components	91
5. THE STUDY AREA AND DATA ACQUISITION	92
5.1. THE STUDY AREA	92
5.11. Site Selection	92
5.12. Site Description	92
5.13. Sample Plots	95
5.2. DATA ACQUISITION	96
5.21. Sample Plot Layout	96
5.22. Ground Control Points	98
5.23. Camera and Auxiliary Equipment	100
5.231. Camera	101
5.232. Tripod	104
5.233. Photographic Plates .	105
5.24. Field Work	107
5.241. Positioning of Control Points	107
5.242. Camera Setting	107
5.25. Sequence of Observations	110
5.26. Developing Glass Plates	110

Chapter	Page
6. DEVELOPMENT AND ANALYSIS OF DIGITAL SURFACE MODEL	112
6.1. GENERAL	112
6.2. DEVELOPMENT OF DIGITAL SURFACE MODEL	114
6.21. Sample Plot Index	114
6.22. Coding of Photo Plates	115
6.23. Measurement on the Stereo-comparator	117
6.24. Data Processing	119
6.241. General	119
6.242. Data Preparation	121
6.243. Strip Triangulation .	122
6.244. Strip and Block Adjustment	123
6.245. Uniform Grid Data	123
6.246. Accuracy	125
6.3. ANALYSIS OF DIGITAL SURFACE MODEL ..	126
6.31. Geometric Properties of Depressions	126
6.32. Computation of Roughness Components	126
7. ANALYSIS OF DATA AND DISCUSSION OF RESULTS	131
7.1. GENERAL	131
7.2. GEOMETRIC PROPERTIES OF DEPRESSIONS	132
7.21. Number and Spatial Distribution of Depressions	132
7.22. Volume of Depression Storage	134
7.23. Test of Homogeneity of Surface	138
7.24. Storage Volume and Land Slope Relationship	140

Chapter		Page
	7.25. Volume, Depth, Surface Area Relationships	147
	7.26. Frequency Distribution of the Geometric Properties	155
	7.261. General.....	155
	7.262. Volume.....	156
	7.263. Depth.....	160
	7.264. Surface Area	161
	7.27. Theoretical Probability Distribution Models.....	166
	7.271. Exponential Distribution	166
	7.272. The Weibull Distribution	169
	7.28. Goodness of Fit Significance Test	176
7.3.	SURFACE ROUGHNESS.....	180
	7.31. Roughness Components for the Plots	180
	7.32. Correspondence Between Surface Structure and Roughness Components	183
	7.33. Variability of Roughness Components	187
	7.34. Roughness Components and Depression Storage	190
7.4.	SEASONAL CHANGES	192
	7.41. General	192
	7.42. Depression Storage	192
	7.43. Geometric Properties of Depressions	196
	7.44. Surface Roughness	198
	7.45. Depression Storage and Surface Roughness	201
7.5.	APPLICATION OF RESULTS	204

Chapter	Page
8. <u>CONCLUSIONS</u>	216
<u>REFERENCES</u>	218
<u>ACKNOWLEDGEMENTS</u>	225
<u>APPENDIX A</u>	227
Parameters of Probability Distribution Models	228
<u>APPENDIX B</u>	232
Computer Programs	233

LIST OF TABLES

Table		Page
1	Design values of depression storage volume.	12
2	Distribution of watershed area in three groups.....	15
3	Definitions of surface roughness.....	31
4	Depression storage volumes computed by contour area method and digital method.....	64
5	Model numbers of sample plots.....	115
6	Volume of depression storage.....	136
7	Analysis of variance of data of depression storage volume.....	139
8	Results of regression analysis.....	143
9	Mean and standard deviation of the geometric properties of selected depressions.....	148
10	Surface roughness components.....	182
11	Roughness order of the selected profiles...	187
12	Analysis of variance of data of relief factor.....	189
13	Analysis of variance of data of slope factor.....	189
14	Analysis of variance of data of resistance factor.....	190
15	Volume of depression storage of selected plots before and after rains.....	193
16	Roughness components of selected plots before and after rains.....	199

LIST OF FIGURES

Figure		Page
1	A portion of digital surface model consisting of matrix (I,J).....	52
2	Definition of adjacent points or neighbours	52
3	Simple depression (first order basin).....	54
4	Complex depression (second order basin)....	54
5	Complex depression (third order basin).....	54
6	Link and order list.....	56
7	Geometry of a vertical cylinder used for computation of volume.....	56
8	Computation of depression storage volume...	56
9	Grid point elevations of a portion of sample plot for depression storage volume computation by contour area and digital methods.....	60
10	Relationship between volumes computed by contour area method and digital method.....	65
11	System logic flow.....	70
12	Periodic even function $f(x)$ and its periodic extension.....	79
13	Hydrologic station, University of Guelph, Guelph, Ontario.....	94
14	Layout of sample plots.....	97
15	Location of control points in the sample plot.....	99
16	Photograph of a sample plot showing location of control points.....	99
17	Wild stereometric camera.....	102

Figure		Page
18	Tripod of the stereometric camera for vertical photography	102
19	Setting of the camera over a sample plot	109
20	Plates fixed in comparator showing overlapping area.....	120
21	Contact prints of a set of glass plates.	120
22	Location of depressions in plot I/2.....	133
23	Relation between number of depressions and slope of sample plot.....	135
24	Slope-volume relationship.....	142
25	Average maximum depth and slope relationship.....	145
26	Volume-depth relationship.....	149
27	Volume-surface area relationship.....	152
28	Surface area-depth relationship.....	154
29	Histogram of volume and theoretical curves.....	157
30	Histogram of volume and theoretical curves	158
31	Histogram of volume and theoretical curves	159
32	Histogram of depth and theoretical curves	162
33	Histogram of depth and theoretical curves	163
34	Histogram of surface area and theoretical curves.....	165
35	Plottings of profiles for sample plot I/1	184
36	Histograms of volume, depth and surface area.....	197
37	Influence of depression storage characteristics on fraction of area producing runoff	211
38	Normalized area-volume histograms.....	212

1. INTRODUCTION

The results of numerous hydrologic investigations have provided background for an understanding of the basic mechanism of processes involved in the disposition of precipitation as it reaches the land surface. This includes studies on simple sprinkled plots used for infiltration and overland flow analyses, and recently developed sophisticated mathematical models as well as physical models. As regards the usefulness of these results in relation to practical problems, there remains much to be accomplished. The difficulty of this situation is well recognized and is attributed to the complex nature of the hydrologic processes occurring during the land surface phase of the hydrologic cycle. These processes are further complicated by the extreme variability of surface geometry both in space and time.

The complex nature of the watershed surface restricts the extrapolation of results obtained from sprinkled plots to any natural watershed. For the same reason, the application of physical models is severely restricted in modelling the dynamic response of natural watersheds. In the case of mathematical models, surface properties of watersheds cannot be treated objectively, resulting in varying degrees of discrepancies in simulated and observed responses. This adversely reflects on the appropriateness of various parameters of the models selected to define the surface properties. These parameters suffer from severe constraints imposed by various simplifying assumptions that must be made due to lack

of quantitative data on surface properties. Linsley (1967) emphasized this point when he said:

"The model (Stanford watershed model) suggests certain long term data problems which should be seriously considered now. The experience with the model has been that the most important part of the total runoff process is the land surface. If the storage and retention on the surface and the infiltration losses are not correctly modelled it is impossible to reproduce the hydrograph. On the other hand if the land surface model is effective and produces an accurate time distribution of runoff increment, a relatively simple storage routing procedure is sufficient to reproduce the hydrograph with considerable accuracy."

Considering a surface runoff system, there exists a definite mechanism of retention, storage, and surface flow at any time which is characterized by the surface properties of watersheds. The dominating storage elements include depression storage, which accounts for most of the retention on the surface, and detention storage, which controls the surface flow. The appropriateness of the parameter values of a model will depend upon the extent to which these reflect the physical characteristics of the watershed surface. A quantitative evaluation of these elements in relation to surface properties becomes a prerequisite for the success of any model. Furthermore, these characteristics are not stationary but change with time due to aggradation and degradation of the surface configuration taking place under the actions of the raindrops and overland flow. The temporal changes have to be quantitatively treated for the determination of parameter values in a model for a more

realistic simulation of the hydrologic response.

The physical characteristics of the surface can be considered in terms of depression storage and surface roughness. These properties are interrelated but the existence or non existence of any significant functional relationship between the depression storage and surface roughness has to be established by the results of field investigations. The quantitative description of surface roughness may possibly lead to a rational estimate of the hydraulic roughness term of the hydrodynamic equation, and in turn detention storage.

Depression storage, though recognized for its hydrologic importance in reducing both the volume and rate of runoff, unfortunately has been least studied because of practical difficulties in making direct measurement of numerous depressions of different shapes and sizes occurring on a watershed surface. Some information is available on the total volume of depression storage, based on either indirect estimates or on assumptions and conjectures inspired with reasons. Only recently have total volumes of storage been computed on sample plots, using elevation data of the surface. There is no information available on the geometric properties of individual depressions or of their statistical distribution in space, both of which are important for the study of the mechanics of the surface runoff system.

The variability of point values of surface configuration or microrelief features at any time provides a physical

description of the surface structure, known as surface roughness. Surface roughness has been quantitatively described by statistical and mathematical functions, using surface elevation data in problems such as reflection of electromagnetic waves, design of vehicle suspension systems, taxiing efficiency of an aeroplane on a runway, etc. In the case of watersheds, surface roughness has been described mostly in terms of various indices based on the standard deviations of elevation data of sample plots. In a few studies, roughness has been described by spectral density functions and autocorrelation functions.

In view of the fact that direct measurements of the dimensions of individual depressions and numerous microrelief features are not physically possible, indirect determination based on elevation data of the surface seems to be a logical choice. The indirect approach is to model the configuration of the surface with a series of elevation values taken at carefully selected points. The resulting set of elevation values given as a function of horizontal coordinates provide a numerical representation of surface features and constitute a digital surface model. The digital surface model is assumed to contain all the physical details of the surface under study. These are sufficient to permit computation of surface features with the required accuracy.

Elevation measurements of the soil surface at small intervals have been done in the past with the help of specially

designed automatic point gauges. These gauges are expensive, time consuming, and not practical when the size and number of the sampling sites are relatively large and where periodic measurements are required within certain time limits. With the advanced techniques developed in the field of photogrammetry, it is felt that a photogrammetric approach may be used with advantage for developing digital surface models.

According to Moffitt (1968) the ideal measuring system for establishing a three dimensional portrayal of a surface, must meet the following requirements:

- a) it must be fairly simple,
- b) it should be capable of measuring an infinite number of points at one instant of time,
- c) it should not physically disturb the surface, and
- d) it should not be influenced by the time lag and other disturbing elements of the measuring system.

The photogrammetric system ideally meets the above requirements. It is also adaptable to different types of surfaces and various sizes of areas. The exactness of reproduction of surface configurations can be controlled to suit various types of surfaces.

The vital role of depression storage and surface roughness in controlling the runoff system, and the deficiency in knowledge in this area prompted the present study. The investigation of these surface properties requires numerical modelling of the land surface or terrain to be used as basic data. The study envisages an investigation of the adaptability

of a photogrammetric technique for developing digital surface models which can subsequently be used for determining the desired surface properties. Using digital surface models, it is proposed to develop techniques of determining the geometric properties of depressions and quantitatively describing surface roughness. The statistical distributions of the geometric properties of depressions will also be studied. The study also includes the evaluation of seasonal changes in depression storage, frequency distributions of the geometric properties, and surface roughness.

2. REVIEW OF PREVIOUS WORKS

2.1. ESTIMATES OF DEPRESSION STORAGE VOLUMES

2.1.1. General Continuity Equation

In the early stages of hydrologic research hydrologists employed the continuity equation, often referred to as the storage equation, to study the disposition of rainfall on experimental areas. The primary interest of most of the investigators centred around the estimation of infiltration rates and detention storage in relation to hydraulics of overland flow. The storage equation was generally expressed as:

$$P = Q + F + V_d + I + D_a \text{ ----- } 2.1$$

where: P = rainfall for the period Δt ,

Q = runoff for the period Δt ,

F = amount of infiltration for the period Δt ,

V_d = amount of depression storage for the period Δt ,

I = amount of interception loss for the period Δt ,
and

D_a = surface detention, or detention storage, for
the period Δt .

Of the six terms of equation 2.1, only rainfall and runoff can be measured directly. The quantity (P-Q), often referred to as 'losses', constitutes four terms which occur almost simultaneously on the land surface and do not lend themselves to direct measurements. The interception loss in

general is negligibly small and any error in its estimate is considered to be inconsequential. If the interception loss is set to zero, equation 2.1 reduces to:

$$P - Q = F + V_d + D_a \text{ ----- } 2.2$$

The specific magnitude of depression storage is generally assumed, leaving only two unknowns, infiltration and detention storage, to be determined. In some of the studies, depression storage has been considered as part of infiltration (Dunin 1969). Since neither of these terms can be measured reliably, one has to be approximately determined in order to evaluate the other term in equation 2.2.

For the sake of convenience, the review of literature on the estimation of depression storage has been grouped, keeping in view the development stages of scientific hydrology. In the initial stages of hydrologic research, small sprinkled plots were used to determine the infiltration rates and storage-discharge relationships by hydrograph analysis. This was followed by the establishment of an increasing number of experimental watersheds for similar investigations. With the advent of digital computers, several mathematical models have been recently developed to simulate the hydrologic response of natural watersheds. Studies on urban areas have been grouped separately.

2.12. Hydrograph Analysis

Horton (1939), in the analysis of hydrographs obtained

from sprinkled plots, used the following relationship for computing the volume of depression storage.

$$V_d = (i - f'/2)t_d \quad \text{-----} \quad 2.3$$

where: i = intensity of rainfall,

f' = infiltration rate at the time of the beginning of runoff, and

t_d = time required to fill the depressions.

The method is based on the assumption that overland flow starts only after depression storage is satisfied. That is, there is a specific point on the time scale which marks the end of accretion to depression storage and the beginning of runoff.

In addition to practical difficulties in determining the term t_d , and possible uncertainty in the estimation of the infiltration rate f' , the above assumption is not valid on the natural land surface where overland flow may take place even when depression storage is not exhausted.

Using the above equation, Horton (1939) computed the average volume of depression storage of sprinkled plots having slopes ranging from one to sixteen percent. The depression storage volume was found to decrease with increase in slope except in plots with two and twelve percent slopes. For these plots, volume was observed to increase with increasing slope. This reverse trend in the result was attributed to errors in the estimation of f' and t_d .

Sharp and Holtan (1940, 1942) employed the storage equation (i.e. equation 2.2) in establishing a relationship between the runoff rate (q) and detention depth (D_a) in order to determine the infiltration capacity of sprinkled plots. Artificial rainfall was applied a second time on each plot immediately after the cessation of runoff and complete depletion of depression storage. With the infiltration rate set to a constant value, equation 2.2 was solved for V_d to determine the approximate value of depression storage. The authors suggested that these values served as a check for the initial estimates of depression storage made in the analysis of hydrographs obtained in the first run.

Sharp and Holtan (1942) suggested a similar approach for estimating approximate values of depression storage volumes for small homogeneous watersheds. The method envisaged the analysis of another hydrograph produced shortly after the first, when depression storage was back to original capacity but infiltration capacity had not recovered. The availability of such a hydrograph which meets the above conditions is extremely difficult. Also the application of simulated rainfall on a natural watershed is not practical. The requirement of homogeneity of watershed restricts this approach to very small areas.

Graphical techniques had also been attempted for the isolation of various components of the storage equation for the determination of infiltration rates for sprinkled plots. These techniques had been extended to small watersheds

(Horner and Lloyd 1940; Sherman 1940; Sharp and Holtan 1942; and Holtan 1945). The volume of depression storage in all the studies was arbitrarily assumed. The method employed the art of trial and error in drawing mass curves to establish the relationship between surface detention and runoff. This relationship was then used to isolate the infiltration component of the storage equation.

One must be cautious in applying the above subjective methodology and in the interpretation of results from natural watersheds. Holtan (1945) applied this method in the analysis of hydrographs obtained from a few small watersheds and reported some difficulties in verification of the model. The remarks of the author regarding the extension of the technique to natural watersheds are relevant: "In applying this method to watersheds W-I and W-II, it is apparent that we can expect greater success on larger areas where the hydrograph is not so sensitive to small irregularities of the ground surface". A reasonable estimate of depression storage could possibly be made on sprinkled plots, but such estimates may be far from actual in the case of natural watersheds.

Brater and Sangal (1969), in their study of the effect of urbanization on peak flow, emphasized the controlling effect of depression storage which they called 'retention' on the accuracy of the estimates of the infiltration rates. A value of 0.2 inch was suggested for the basins near Detroit, U.S.A., varying in area from 22.9 to 36.5 square miles.

Hills (1971) in his study of the influence of land management and soil characteristics on infiltration and overland flow, assumed the value of depression storage to be 0.05 inches on the bare ground surface and 0.10 inches for all other surfaces. The effect of slope was ignored.

Values of depression storage volume have been suggested in the design and construction of sanitary and storm sewers (A.S.C.E. Manual 1969). These values are presented in Table 2.1.

Table 2.1. Design Values of Depression Storage Volume

Type of surface	Depression storage volume (inches)
Forest litter	0.30
Good pasture	0.20
Smooth cultivated land	0.50 - 0.10
Urban areas	0.05
Lawns and normal urban pervious areas	0.10

2.13. Watershed Simulation Models

The depression storage term has also been utilized in various forms in most of the recently developed watershed simulation models. The conceptual hydrologic model known as the Stanford model (Crawford and Linsley 1966) considers depression

storage as part of the upper storage zone which also includes storage in shallow depths of top soil. These two elements of the upper storage zone have a dominating influence in reducing and delaying runoff produced by small storms. In the case of larger storms, the effect is more pronounced in the early part of rainfall and gradually reduces with reduction in the available storage capacity of the upper storage zone. The initial volume of the upper storage zone is empirically estimated as a function of lower zone storage depending upon the slope, vegetation and volume of depression storage qualitatively grouped as low, moderate and high. According to Crawford (1969), the effect of increase in the depression storage volume incorporated in computer simulation had been very pronounced on the system response, especially at low soil moisture.

Boughton (1966) developed a simulation model which had features similar to the Stanford model. The model considered a storage element which represented interception loss and depression storage. An estimate of the volume of depression storage was not based on actual measurement, but rather an indirect deduction from available data on rainfall and runoff.

Riley and Narayana (1969) developed a simulation model of an urban watershed by means of analog computer. The volume of depression storage, established during the process of testing and verification of the model, was considered to

be appropriate for the area under study.

Claborn and Moore (1970) developed a simulation model which in fact was a modified form of the Stanford model. The model considered depression storage in some detail. The watershed area was divided into three parts:

- a) areas contributing directly to streamflow,
- b) areas contributing to depression storage, and
- c) areas of depressions.

The part of overland flow occurring in the drainage areas of depressions was added to depression storage. The portion of overland flow occurring in areas included under (a) was added to the variable runoff. The surface area of water in the depression was assumed to have a linear relation with the volume of depression storage. This assumption, found useful and effective for the purpose of modelling, was not verified with field observations of depressions.

After the depressions were filled up, the area under (c) started contributing to runoff. Based on the results of a few hypothetical normalized volume-area distribution curves characterizing different basins, a typical relationship between depression storage area producing runoff and the volume of depression storage was assumed to be of the form:

$$X_a = \left(\frac{1}{C} \cdot \frac{D_s}{D_{smax}} \right)^{0.5}$$

where: X_a = the fraction of depression area producing runoff,

D_s = the actual depression volume, in

inches of depth,

D_{smax} = the maximum depression storage volume, in inches of depth, and

C = a constant, normally with a value of 1.

The proportion of the areas falling in each of the three groups obtained in the test area as reported by the authors are given in Table 2.2.

Table 2.2. Distribution of the watershed area in three groups

Month	Proportion of the area		
	a	b	c
Oct.	0.40	0.50	0.10
May	0.30	0.55	0.15
Rest	0.80	0.15	0.05

(a) areas contributing directly to streamflow,
 (b) areas contributing to depression storage, and
 (c) areas of depressions.

Values were presented separately for the months of May and October, to account for tillage operations used in planting of corn and wheat respectively.

Lee (1972) proposed a computer model of surface energy and water budget wherein depression storage was considered as a separate storage element. The author derived a relation-

ship between depression storage, slope and surface conditions using the depression storage figures reported in the Handbook of Hydrology (Chow 1964). The equation was of the form:

$$S_{DETM} = 0.02 + 0.14 e^{-17 S_1}$$

where: S_{DETM} = depression storage for turf in inch depth,
and,

S_1 = slope of the ground surface in ft/ft.

Despite a wide scatter in plotted points the relationship was reported to be consistent. The above equation was used to compute depression storage in the model.

It is evident from the above that the depression storage term has been considered in most hydrologic models either separately or in combination with other storage elements of the model. As regards its importance, the effect of the magnitude of depression storage on simulated response has been demonstrated by the results of studies reported by Crawford (1969). Lack of quantitative data is evident from the above studies. In consequence, the magnitude of depression storage has either been assumed or indirectly estimated from the results of the analysis of hydrographs obtained from plots and small experimental watersheds. In absence of data based on actual measurements the reliability of the model cannot be ensured. It is also felt that the practice of parameter optimization, widely used in such models to force the simulated response to approximate the observed response as

closely as possible, could be made more realistic and meaningful if quantitative data are made available and used.

2.14. Urban Runoff Models

The status of the depression storage term in urban runoff models is similar to that in other hydrologic models. In the case of impervious areas, the problem of evaluating the specific volume of depression storage on any surface is simple and some available experimental data are reviewed here.

The problem of determining the specific volume of depression storage of impervious surfaces reduces to the measurement of rainfall and runoff. The interception and infiltration terms may be dropped from the storage equation. Assuming evaporation loss from depression storage during the period of rainfall to be negligibly small, depression storage can be computed from the relationship:

$$V_d = P - Q \text{ ----- } 2.4$$

This simple approach has been used by a few investigators to determine the volume of depression storage.

Stammers (1956) and Stammers and Ayers (1957) studied the effect of slope and microtopography on the volume of depression storage and surface detention with the help of simulated rainfall on three laboratory developed surfaces. These included flat surface, cultipacked with corrugations along the slope and cultipacked with corrugations across the slope. The size of the plot was four feet by four feet

and slope ranged from two degrees to 16 degrees. The magnitude of depression storage on the flat surface at two degrees slope was 0.0371 inches, compared to 0.149 inches on the cultipacked surface with corrugations across the slope. A general decrease in the depression storage volume was observed with increase in slope on all three surfaces.

Willeke (1966) examined the time distribution of response from four urban areas, using equation 2.4, to determine storm losses. The difference between rainfall and runoff was termed as loss which essentially constituted depression storage. The analysis of several storms, ranging from 0.09 inches to 1.64 inches of rainfall revealed that the losses ranged from 0.04 inches to 0.14 inches. The results also indicated that the losses decreased with increase in slope. The regression equation was of the form:

$$\text{Loss} = 0.162 - 0.0392 S$$

where: S = the mean slope of the watershed in percent.

Viessman (1968) in a similar study investigated the rainfall-runoff relationship on several 100 percent impervious areas ranging from 0.4 to 1.0 acres. The storm losses were calculated using equation 2.4. Average storm losses ranged from 0.04 inches to 0.11 inches. A highly significant relationship was obtained between the storm losses and the land slope. The equation was of the form:

$$\text{Loss} = 0.13 - 0.0301 S$$

where: S = the mean slope of the watershed in percent.

The relationship is similar to that reported by Willeke (1966). The results are reported to be applicable to small impervious areas having mean slopes of 1 to 3 percent. It was observed that depression storage was distributed over the first few minutes of the storm.

The Los Angeles hydrograph method (Hicks 1944) was based on the results of hydraulic investigations, infiltration measurements in urban drainage areas of different types and sizes, and rainfall-runoff studies in the same areas. The rainfall and runoff data had been analysed to determine the relationship between the rainfall rates and loss rates both for pervious and impervious areas. Depression storage was considered as a loss along with infiltration.

The Chicago hydrograph method of sewer design (Tholin and Keifer 1960) evaluated different components of the hydrologic cycle operating in the urban areas. The method recognized the necessity for making an estimate of depression storage to evaluate its effect on the runoff system. Consideration was also given to the relationship that might exist between the mean depth of depression and the proportional area covered by such depressions. The model assumed a summation of the standard normal probability curve to express this relationship. It appears to be a compromise between the assumptions made by some investigators that all

the depressions must be filled before overland flow begins and exponential decay type function suggested by Linsley et al. (1949). On the basis of the observations taken during heavy rainfall, the volume of depression storage was assumed to be 0.25 inches for pervious areas and 0.06 inches for pervious areas with a depth range of 0.0 - 0.50 inches and 0.0 - 0.12 inches respectively. These values were used in the model.

The studies reported so far reveal that the volume of depression storage has been estimated from the rainfall and runoff data collected from small experimental areas. Although direct field measurement of depression storage has not been attempted in the previously reported works, a few attempts have recently been made to measure the volume of depression storage. The general approach used was to characterize the configuration of the surface with a series of point elevation values measured at selected points. The point elevation values have then been used to determine the volume of storage on a surface. The two aspects of the problem, i.e. methods of measuring surface elevation and methods of computing volume with the help of elevation data, are reviewed in the following sections.

2.2 METHODS OF MEASURING SURFACE ELEVATION

The suitability of any method for taking elevation

measurements depends to a great extent on the average size of depressions associated with any surface. The large size depressions associated with macrosurfaces are amenable to direct measurements of geometric properties with the help of levels used for engineering surveys. Topographic maps and aerial photographs with suitable scales can also be used to delineate depressions and compute the volume of storage. The difficulty arises in the case of small size depressions present on natural watershed surfaces. These, because of their vast number, small size, and ill-defined shapes, preclude direct measurement. The small-scale topographic variations require specially designed gauges or special photogrammetric techniques for elevation measurements. The use of conventional leveling instruments, gauges and photogrammetric methods has to be considered in relation to the scale of topographic variations on the surface under study.

2.21. Leveling Instruments

The standard leveling instruments used in engineering surveys can satisfactorily be used for the measurement of geometric properties of individual large size depressions, both natural and artificial. The information collected by topographical surveys also can be used to delineate individual depressions and to determine the storage capacity. The size of the depressions which may be determined depends on the scale of survey. Haan (1967) measured volumes, depths and areas of large size depressions, known as potholes,

having a mean area of 2.29 acres and mean depth of 1.09 feet. For small size depressions, which generally predominate on the land surface of natural watersheds, this method is obviously not suitable.

2.22. Specially Designed Point Gauges

Various types of gauges have been designed and developed for the measurement of elevation of the land surface to describe surface roughness. The gauges vary in sophistication from similar frame mounted linear scales to automatic gauges which measure and record elevations of predetermined points.

Kuipers (1957) used a simple apparatus, which he called a reliefmeter, to measure surface elevation to determine surface roughness. It consisted of a board with vertical scales in centimeters in front of which 20 needles were placed 10 centimeters apart and held in place by a spring mounted brass bar. The board was placed horizontally above the soil surface and the bar actuated to let the pins slide down until they touched the soil surface. On a sloping surface the board was placed parallel to the slope. The heights of the needles were read on the respective scales. The board was turned over to bring the needles back to the original positions for next measurement. The operation was repeated 20 times at fixed distances to measure 400 height values relative to a certain level.

Burwell, Allmaras and Amemiya (1963) and Allmaras et al. (1966) developed a gauge called a microrelief meter. The

gauge was similar in operation to the one developed by Kuipers (1957). The gauge was designed to measure surface elevation on a two inch square grid on a 40 inches by 40 inches area to provide 400 height readings in 20 settings of the gauge. The elevation measurements were made to study porosity and random roughness in relation to tillage operations.

Merva et al. (1970) in an investigation of the roughness characteristics of the microsurface, used a probe with a diameter of 0.283 inches to measure elevations at a distance of 0.788 inches along a 10 feet distance.

Currence and Lovely (1969) developed an automatic recording profilometer which consisted of a mechanical system and a measuring system. The framework covered an area of size 60 inches by 80 inches. Permanent magnet AC - DC motors were used to index a measuring probe carrier over the sample area. The probe carrier was moved in one inch increments in both X and Y directions. At each point of measurement the probe was lowered to the soil surface and stopped. The distance the probe moved from the level datum or its original position to the soil surface was automatically stored and recorded by the measuring system with simultaneous return of the probe to the original position and automatic movement of the probe carrier to the next point. The accuracy of heightreading of the system was of the order of ± 0.05 inches. Depending on the roughness of the plot, three

to four hours were required to measure and record 4800 height readings per plot.

Mitchell and Jones (1971) developed a profile measuring device (PMD) nicknamed the 'clodhopper' which automatically measured and compiled the elevation data of the soil surface. It was similar to the one reported by Currence and Lovely (1969) and operated on the same principle. The design and the operation of the device has been described in detail by Mitchell (1970).

2.23. Aerial and Terrestrial Photogrammetry

Photogrammetric techniques have been extensively applied in the field of topographic surveying and mapping. The application of photogrammetry is also growing rapidly in other fields. Photogrammetric techniques are classified as aerial when the camera is airborne and terrestrial when the camera is mounted on the land surface while taking photographs of the surface. The choice depends on the scale of topographic variations and the desired precision in measurements.

Aerial photographs with relatively large scale may be used for delineating large size natural or artificial depressions and then determining the storage capacity. Haan (1967) used aerial photographs to map four sample areas of 320 acres size to delineate large size depressions and measure their volume, area and depth. The sample topographic maps of the area were also drawn with a contour interval of two

feet. In many cases auxiliary contours were drawn to reduce the interval to one foot. The "average" ground slope was stated to be 0.87 percent.

Merva et al. (1970) in a study of the description of a macrosurface by spectral analysis, used a topographic map with a four foot contour interval. The elevations of the individual points spaced 200 feet apart along a traverse were interpolated from the map.

Although terrestrial photogrammetry has not yet been applied to the problems of depression storage and surface roughness, it has been successfully used in other problems requiring elevation measurements of microsurface. Poulin (1961) used a photogrammetric technique to study the frost formed patterns in soils of arctic and subarctic environments. Stereophotographs of a few selected frost patterns were taken from a height of ten to twenty feet in Greenland and at a high altitude site in Colorado. Motion measurements were made on maps prepared with a scale of one to four and a contour interval of 0.02 feet. The comparison of these maps over a period of several seasons was expected by the author to yield much information about the amount and direction of movement in the soil pattern.

Rosenfield (1966) reported the application of terrestrial photogrammetry to a problem in hydraulics. Terrestrial photographs of residual sand beds in a hydraulic test flume were taken from a height of 65 inches. These photographs were used to make a contour map with a contour interval of

.01 feet to study the nature of the sand bed in relation to hydraulics of flow.

2.3. DETERMINATION OF STORAGE VOLUME

The volume of water stored in depressions on the soil surface can be calculated with the help of surface elevation data. A standard method employed in many engineering problems of volume estimation has been to draw a contour map of the land surface using a suitable contour interval. The volume between a contour and the next higher is given by the average of the two areas multiplied by the contour interval. The procedure is repeated up to the highest contour outlining the depression boundary.

Haan (1967) used the above technique for determining the volume of storage in individual potholes. Mitchell and Jones (1971) also used this method to determine the depression storage for the test plot measured by the profile measuring device. A digital computer has also been used to carry out essentially the same process without the actual labour of drawing a contour map.

Mitchell (1970) developed a technique of computing depression storage using PMD data for a series of reference heights which yielded a stage-storage relationship of the test plot. The computation of a stage-storage relationship consisted of first determining the maximum and minimum values of heights of the plot which provided the stage range.

The volume of storage for each increment of stage was calculated and then accumulated to determine the total volume of storage for the test plot.

Five methods of computing storage for each increment of stage were initially attempted. The first method considered each vertical height reading to represent the centre of a one inch square level surface. The sum of differences between the height of a point and a reference height provided the volume of storage in cubic inches. The second approach used the average end-area method of computing volume. The areas between the reference heights and individual profiles were computed to determine the volume. The third method considered three adjacent points to describe a triangular plane. The volume above the plane and the reference height was computed. The fourth method considered a prismatic formula to compute volume with the help of the area between the individual profile and the reference height. The fifth method used a modified form of the same formula.

The validity of the above methods of volume computation was tested with the help of three synthetic surfaces of three feet by three feet size, constructed of styrofoam and artificially roughened. The actual stage-storage relationship for these plots with varying degrees of roughness was determined in the laboratory. The surface was inverted and securely fastened in a water tank of slightly larger size. The stage-storage relationship was determined by adding

known quantities of water in the tank and measuring the depth with a point gauge. The two increments of stage initially tried were 0.1 inches and 0.01 inches. The stage-storage relationship was reported to be of the following form:

$$S = a \left(\sin \frac{D}{b} \right)^c$$

where: S = storage, inches,

D = depth above the lowest point on the surface, inches, and

a, b, c = equation parameters.

Stage-storage relationships of these artificial surfaces were also determined by taking elevation measurements with the help of a PMD and using the above five methods. These were then compared with the actual stage-storage relationship. The results obtained from all five methods were reported to be comparable with the laboratory results. The first method, using a stage increment of 0.1 inches was finally selected and used to develop stage-storage relationships for a few measured surfaces produced by different tillage equipments.

Barron (1971) in a similar study initially considered four methods of determining stage-storage relationship using different geometric shapes with the help of PMD data. The first method considered each vertical height reading to represent a one inch square vertical column. This was similar to the one used by Mitchell (1970). The second method also considered one inch square column but the height was equal

to the average of heights of four surrounding points. The third method considered 2 x 2 inch vertical column with height reading equal to the average of four height readings at the corner of each column. The fourth method considered three adjacent height readings to describe a prismatic column.

The validity of these methods was tested with the help of three artificial surfaces, as done by Mitchell (1970). The first geometrical shape was finally selected and used for computing stage-storage relationships of tilled soil surfaces.

The above methods of determining stage and storage assume level surfaces. These methods are not valid for sloping surfaces and therefore, cannot be used to compute depression storage on a sloping surface.

2.4. ACTIVE POTENTIAL STORAGE VOLUME AND MEASURED STORAGE VOLUME

It is evident from the results of the above reported studies that the magnitude of depression storage has either been estimated from rainfall-runoff data or directly measured with the help of elevation data. The values of depression storage as obtained by the two methods are theoretically different. The first approach provides an estimate of potentially active depression storage which is assumed to be available for direct abstraction from rainfall. The second approach based on direct measurement provides information on the total volume of storage permitted by the dimensions of the individual depressions. It does not take into account

the effect of any climatic or topographic restraint which may not permit the filling of any depression to its maximum capacity defined by its geometric properties. For example, the catchment area of any depression may be too small compared to its capacity with the result that it may never fill up. In other words the estimate based on direct measurement assumes that all the depressions on the surface will be filled up to their capacities. This assumption may always not be true. The active potential depression storage may in some cases be less than the measured depression storage.

2.5. QUANTITATIVE DESCRIPTION OF SURFACE ROUGHNESS

2.5.1. Definition of Surface Roughness

A principal consideration of any surface is its geometric property or form which has been extensively referred to in scientific literature as surface roughness with a problem oriented definition. In view of the fact that different investigations dealing with surfaces of interest have required specific types of roughness parameters suited to a particular problem, it is almost impossible to provide a single definition for the much used term 'surface roughness'. Each study has its own definition of surface roughness based on those geometric properties of the surface relevant to the study. Information from Stone and Dugundji (1965) has been expanded in Table 2.3 to indicate some of the definitions of the term surface roughness used in various investigations.

Table 2.3. Definitions of Surface Roughness

<u>Source</u>	<u>Date</u>	<u>Definition</u>
LeConte*	1877	Configuration of surface dotted by mounds 6-10 inches higher than adjoining depressions.
Terry and Stevenson*	1957	Mounds, ridges, depressions or undulations on the sea floor. Lower limit 3 feet; maximum limit 10-40 feet.
Dwornik et al.*	1959	Objects of surface irregularity less than 1 inch in height in a 7 ft. plot.
Strahler and Koons*	1959	Surface roughness involving measurements of height difference greater than 0.1 ft.
Sytinskaya*	1959	Limits between 0.1 mm. and 0.1 m. for lunar irregularities.
Van Lopik and Kolb*	1959	Surface geometry associated with terrain features exhibiting less than 10 ft. of relief.
Shipek*	1961	Microrelief on sea floor measured horizontally in meters and tens of meters and vertically in centimeters and meters.
Houbolt	1961	Roughness consists of elevation differences taken at 2 ft. intervals along a runway line.
Green*	1962	Microsurface (of the moon) is "bicycle smooth" and ranges in size from 1 μ to 1 cm.
Saucier and Broughton*	1962	Surface configuration of terrain that exhibits relief of less than 10 ft.
Hobson	1967	Surface irregularities ranging from a few tenths of an inch to several tens of ft.

Stone and Dugundji	1965	Microrelief features which display internal differences of elevation of not more than 10 ft. or less than 3 inches .
Kozin et al.	1964	Hard ground roughness consists of variations in elevation which are stable over reasonably large areas and change gradually with distance.
Allmaras et al.	1966	Random roughness produced by tillage implements is merely a random occurrence of surface peaks and depressions.
Currence and Lovely	1969	Soil surface roughness produced by tillage implements.
Merva et al.	1970	Surface nonuniformity of macro-surface and microsurface classified on the basis of its being described with a contour interval of 1 ft. or more.

(*From Table 1 of Stone and Dugundji (1965)).

As will appear from the definitions given in Table 2.3, the surface roughness in all the cases is expressed in terms of specified variations in point elevations of the surface or terrain. The upper and lower limits are controlled by the problem under study. The lower limit is also influenced by the accuracy of the elevation measuring instruments. A specific definition of the term surface roughness is required before any attempt is made to characterize a surface.

Merva et al. (1970) differentiated between large scale surfaces such as seen on a watershed as a whole, and its

constituent small scale surfaces, forming independent hydrologic units functioning as surface system with overland flow as output. The macrosurface has been generated by the long term geomorphic processes in the geologic and climatic setting and manifests large variations in elevations of various topographic features such as hills, valleys, drainage networks, etc. The microsurface has been caused by short term geomorphic processes and has small topographic variations on which are superimposed the surface irregularities caused by the tillage implements. These two elements of surface irregularities, geomorphic roughness and tillage roughness, constitute the overall roughness of the microsurface.

The macrosurface is of interest in making a hydrologic classification of an area in relation to its runoff and sediment production rate which dictate its economic use and conservation needs. The microsurface constitutes a hydrologic system with roughness properties or microrelief pattern as an important component which transforms the rainfall as input to overland flow as output. Since the roughness properties control the storage and transmission properties of the surface, the hydrologic response is likely to vary with different surface roughness. The microsurface is of equal importance in studies such as hydraulics of irrigation water on sloping surfaces, soil surface conditions in relation to crop production, and operational efficiency of tillage implements. The quantitative description of microsurfaces have been attempted by a number of investigators,

using mathematical and empirical parameters.

2.52. Methods of Describing Surface Roughness

Methods used in the quantitative description of surface roughness can broadly be grouped as surface roughness indices or parameters and mathematical models based on spectral and harmonic analysis.

2.52i. Surface Roughness Parameters

Allmaras et al. (1966) studied the effect of tillage on total porosity and random roughness of interzone areas of the tilled surface. Soil surface height readings were taken with the help of a profilometer. The random roughness index used was the standard error of heights adjusted for slopes and tool marks. The differences in the soil conditions obtained by tillage treatments were reported to be reflected in the estimates of the indices.

Currence and Lovely (1969) used the above index, termed RL, in addition to four other indices for describing soil surface roughness obtained by the application of various tillage treatments. The second index (RM) was based on the method developed by Luttrell (1963) which is calculated by summing absolute differences in slopes between the end points of height readings measured across the direction of tillage. The standard deviation of the heights measured by the profilometer was calculated as a third index (RS). The standard deviation of the differences between the measured heights and a plane of best fit for each plot obtained by linear multiple regression was calculated as the fourth index (RR). The standard deviation of the height readings corrected for row and column effects was calculated as the fifth index of roughness (RC). The index (RR) describing the amplitude variations of the height residuals was considered adequate

to describe the surface where the effects of tool marks were important. The index (RC) was reported to be suitable in studies where the effect of tillage marks was excluded.

The roughness indices based on the standard deviation of the measured heights or adjusted heights are not particularly meaningful for the physical description of a surface in relation to its hydrologic response. These indices do not reveal the pattern of the microrelief features or microtopographic irregularities constituting the surface which give rise to a specific type of surface roughness. Since these indices are insensitive to the spatial distribution of the microrelief features it is not possible to have any idea or image of the physical structure of the surface. Also, it is possible for two surfaces to have equivalent values of indices but completely different patterns of microrelief features and hence different hydrologic responses.

Hobson (1967) suggested a parameter based on the comparison of estimated actual area with corresponding planar area as an index of roughness. Another index of roughness suggested by the author was based on the estimate of bump or elevation frequency distribution. It is true that surface area increases with surface irregularities, but a comparison of the surface areas does not reveal the structure of the surface roughness since different combinations of the number and magnitude of microrelief features can give rise to the same estimate of the parameter. The bump frequency parameter, consisting of mean and variance of elevation readings describing

the size distribution of the surface irregularities, also does not provide a good description of the surface since two surfaces with different roughness properties may give similar values of the variance.

2.522. Normal Density Functions and Autocorrelation Functions

The geometric properties of the surface which give rise to roughness are neither periodic nor explicitly determined. They are a combination of both deterministic and random influences which though deterministic in nature have been described by the statistical properties (Scheidegger 1964, Beckmann and Spizzichino 1963). The actual surface is represented as being a realization of a stochastic process, which implies that the surface properties are random variables, and therefore are definable in terms of their probability distribution.

Merva et al. (1970) described roughness properties of both macrosurfaces and microspheres by normal distribution functions and autocorrelation functions. The geometric property of the surface used as a random variable was the deviation measured in the direction of elevation from a mean plane. The normal density function does not uniquely describe the surface roughness since the two different surfaces may have the same variance. It also does not reveal any information about the pattern of microrelief features or distances between high and low points which determine the density of surface irregularities. For these reasons an

autocorrelation function was also specified which reveals the correlation between any two points on the surface. The proposed statistical distribution was based on the assumptions of homogeneity and isotropy of the surface.

The surface is completely described by the statistical distribution function and correlation function provided that the assumption of normality is not violated. The assumption of normality does not appear to be unrealistic in view of the fact that some of the geomorphic processes have been found to be adequately described by this distribution. The assumption of normal distribution with respect to deviation angles in a study of river meanders and other wiggly lines was found satisfactory (Thakur 1970; Ghosh 1971). The assumption of normality with respect to the slope of microrelief features was also found to hold true in a study when 385 slope values were compiled and graphed on normal probability paper (Merva et al. 1970).

Beckmann and Spizzichino (1963) suggested the use of the normal distribution and autocorrelation functions to describe any type of rough surface in practice, in a study of the scattering of electromagnetic waves from rough surfaces. They also suggested the use of other types of statistical distribution functions and correlation functions in cases where the surface under study does not conform to normal distribution.

2.523. Power Spectral Density Function

Surfaces represented by stationary random or stochastic processes have been characterized by one and two dimensional power spectral density functions (Houbolt 1961; Press and Tukey 1963; Kozin et al. 1964; and others). The power spectral density functions provide information on the general frequency composition of the surface in terms of the spectral density of its variance. The spectral density functions have also been used in other studies dealing with the statistical distribution of stochastic processes such as river meandre and other wiggly lines (Thakur 1970; Ghosh 1971) and daily river flow data (Adamowski 1969), etc.

Houbolt (1961) summarized the results of several studies on the description of runway roughness in relation to the operational response of aeroplanes. For a linear system, the relationship between the input power spectrum $G(f)$ characterizing the roughness, frequency response function or transfer function $T(f)$ characterizing the aeroplane, and the response function $\phi(f)$ was considered to be of the following form:

$$\phi(f) = G(f) |T(f)|^2$$

The output spectrum was then used to develop criteria for smoothness of the runway.

Bogdanoff and Kozin (1962), Kozin et al. (1964), Bogdanoff et al. (1966) and Kozin et al. (1968) used both one

and two dimensional spectral density functions to describe stable ground roughness to study the vehicle dynamic response for the design of suspension system. The pertinent features of the estimated power spectrum had been interpreted in terms of relief features exhibited by the plotted ground profiles.

Application of the power spectral technique for the analysis of the aeroplane dynamic response has been discussed in detail by Press and Tukey (1963). The relation between the power spectra of the atmospheric turbulence and the response of the aeroplane to the disturbance have been studied.

Currence and Lovely (1969) used spectral density functions to characterize roughness of the soil surface treated by different types of tillage operations to provide different degrees of roughness. Tillage tool marks were indicated by spikes in the power spectrum.

Merva et al. (1970) applied the method of spectral analysis to describe the roughness of both macrosurfaces and microspheres. The results were expressed in the form of a plot of the spectral density function against the corresponding fraction of the folding or Nyquist frequency expressed as cycle per unit length. The shape of the power spectrum was interpreted to draw inferences about the roughness of the surface. For example, the occurrence of sharp peaks indicated the existence of microrelief features at some regular intervals

determined by the corresponding frequencies.

2.524. Fourier Series Analysis

Fourier series analysis provides a means of separating a curve into a number of simple harmonics, defined by the amplitude and wave length which when added together can represent any type of curve. A single Fourier series has been used for representing a curve or a profile, whereas the double Fourier series has been used for the analytical description of any surface. Any arbitrary function $f(x)$ defined in the interval $-L$ to L may be represented in terms of Fourier series expansion as follows:

$$f(x) = \frac{a_0}{2} + \sum_{n=1}^{\infty} \left(a_n \cos \frac{n\pi x}{L} + b_n \sin \frac{n\pi x}{L} \right).$$

where: $a_n = \frac{1}{L} \int_{-L}^L f(x) \cos \frac{n\pi x}{L} dx, \quad n=0,1,2,-----\infty$

$$b_n = \frac{1}{L} \int_{-L}^L f(x) \sin \frac{n\pi x}{L} dx, \quad n=1,2,-----\infty$$

It is often convenient to use the exponential form of equation which is given by:

$$f(x) = \sum_{-\infty}^{\infty} C_n e^{-i\omega_n x}$$

where: $\omega_n = \frac{n\pi}{L}$

$$C_n = \frac{1}{2}(a_n - ib_n)$$

$$C_0 = a_0$$

$$C_{-n} = \frac{1}{2}(a_n + ib_n)$$

It can also be represented in terms of amplitudes and phases:

$$f(x) = \sum_{n=0}^{\infty} A_n \cos(\omega_n x - \psi_n)$$

where: $A_n = \sqrt{a_n^2 + b_n^2}$, and

$$\psi_n = \arctan \frac{b_n}{a_n}$$

In several studies reported by Rice (1951) the coefficients a_n and b_n were assumed to be random variables having normal distributions. Also according to Rice (1951), it is also agreed upon that both the coefficients are statistically independent. The phase and amplitude are also independent. The phase of the input does not affect the amplitude of the output of the mechanical system and similarly the amplitude of the input does not affect the phase of the output. (Kozin et al. 1964). In the problem of surface description, the amplitude which reflects the height of the microrelief features is more important than phase. Press and Tukey (1963) has shown that the C_n values are fixed constants and phase shifts ψ_n are independent random variables distributed uniformly over the interval 0 to 2π . Hence, an approximation

to the Gaussian random process can be obtained. The application of the Fourier series has generally been limited to the fitting of profiles and topographic surfaces, using elevation data of the measured points. Its application in geology has been discussed by Harbaugh and Merriam (1968).

Rice (1951) suggested a randomized Rayleigh method for describing a slightly rough surface represented by the function $\zeta = \zeta(x,y)$ which by his definition is almost but not quite flat with small random deviations of this surface from the x-y plane. The equation of the surface was expanded in Fourier series for the application of the Rayleigh method. The coefficients were assumed to be independent random variables with normal distributions about zero. The application of this approach is limited to slightly rough surfaces because of the mathematical difficulties encountered when dealing with rougher surfaces (Beckmann and Spizzichino 1963).

Stone and Dugundji (1965) in their study on the quantitative description of the microrelief features of a terrain in relation to the military vehicle requirements, used Fourier series analysis of the terrain profile. They developed a provocative concept of roughness which in addition to the amplitude of oscillations considered other aspects such as steepness of the oscillations involving wave length and density of microrelief features. This concept of considering the roughness as being built of several surface properties departs from other methods reviewed earlier wherein

roughness had been considered as a single elementary property. The microrelief information of any profile was obtained by representing that profile in terms of Fourier cosine series and using that part of the series having a wave length $4 \leq \lambda \leq 64$ ft. This part of the series was termed as a microrelief packet which was assumed to have all information about the profile. Based on the amplitudes of the predetermined number of harmonics the following components of roughness were computed which in fact represented the specific geometric property of the microrelief features.

Relief factor (M). It refers to the average changes in elevation as a profile is traversed.

Specific relief factor (A). It represents average height of major relief feature.

Slope factor (P). The term represents average steepness of relief features along the direction of movement.

Structural homogeneity factor (K) The term refers to the extent of the repetitive tendency in the microrelief features.

Avoidance factor (ρ) This quantity is a measure of the difficulty encountered in traversing the terrain.

Cell length (C_L) It refers to the distance one must traverse from a given origin in order to encounter all significant features of the terrain.

Several areas consisting of different types of microrelief features in southern California were selected for mapping. These maps were then used to develop fan shaped radial profiles

which in turn were subjected to mathematical analysis to compute roughness components. The magnitude of roughness components were compared to study the relative roughness of different areas.

It is evident from the review of literature that depression storage has been considered in most of the hydrologic investigations. The magnitude of depression storage volume and its time distribution has been arbitrarily assumed because of the lack of data and unavailability of a suitable technique for measuring the geometric properties of depressions. The method of measuring total volume of depression storage suggested by Mitchell (1970) and Barron (1971) are applicable only to level surfaces. The method of determining surface elevations using specially designed point gauges, lacks adaptability to other types of surfaces. There is, therefore, a need for developing techniques for measuring surface elevations which could be adaptable to any type and size of surface, and also for determining the geometric properties of depressions.

The description of surface roughness by various indices suffers from serious limitations pointed out earlier. The method of spectral analysis which has successfully been used in other fields has limited application in describing surface roughness in relation to hydrologic response of a surface system. The concept of roughness

suggested by Stone and Dugundji (1965) is more meaningful in a physical description of surface roughness. It considers different geometric properties of a surface which contribute to roughness. The concept of roughness, though developed for macrosurfaces can be adapted to describe surface roughness associated with microspheres.

In view of the importance of the surface properties in controlling the hydrologic response of a surface system and the lack of adequate techniques and data the present investigation has been proposed with specific objectives outlined in Chapter 3.

3. OBJECTIVES

The specific objectives of the proposed study are as follows:

1. To investigate the adaptability of a photogrammetric technique for developing a digital surface model of a microsurface.
2. To develop a digital technique for determining the geometric properties of depressions using a digital surface model.
3. To investigate the frequency distribution of the geometric properties of depressions and the appropriateness of known probability distribution models to describe the observed distributions.
4. To develop or adapt a method for quantitative description of surface roughness of a microsurface.
5. To investigate the seasonal changes in both surface properties, ie. depression storage and surface roughness.

The plan of operation proposed for the accomplishment of the above objectives starts with the development of a theoretical framework of the techniques for the description of the geometric properties of depressions and surface roughness. The development of these techniques, involving the use of a digital surface model, in fact is the basic objective of the proposed study. A sample digital surface

model is initially used for this purpose. Subsequent to the development of a theoretical framework, a study area is selected for application of the techniques. The description of the study area, sample plots and the method of collecting data are presented in Chapter 5. This is followed by the descriptions of the photogrammetric technique used for the development of digital surface models of the plots selected in the study area and processing of these models to obtain data of the geometric properties of depressions and surface roughness. The analysis of data and discussion of the results are then presented. Finally the conclusions of the study in the light of the above objectives are drawn.

4. THEORETICAL FRAMEWORK

4.1. GENERAL

A digital surface model can be used to determine surface properties such as slope, contours, ridges and valleys, watershed boundaries, drainage channels, storage, roughness parameters, etc. In fact, such models can provide all information which is presently collected from the topographic maps or actual field surveys and measurements. This information could be obtained with the aid of techniques suitable for analysing digital surface models. The present study is confined to the problem of developing suitable techniques for determining the geometric properties of depressions and surface roughness parameters using a digital surface model.

4.2. ESTIMATION OF GEOMETRIC PROPERTIES OF DEPRESSIONS

4.2.1. Basic Considerations

The technique proposed for determining the geometric properties of depressions, including the volume of storage, has been based on the following criteria for evaluating its suitability:

1. the method should allow relatively easy and rapid determination of geometric properties of individual depressions;
2. the method should be accurate and precise;
3. the method should be applicable to any surface from the microrelief of a soil, to the macro-

relief of large areas having large size depressions.

The surface can be described in terms of measurable geometric properties such as surface elevation differences, surface slope or gradient, and a density of stationary points such as maxima, minima and saddle points, etc. All these properties are determined by the point values of elevation taken on any surface. In fact, the variability of these point values gives rise to the above properties. Surface elevation data is therefore, more appropriate for such investigations. Such data may consist of elevations taken at regularly or irregularly spaced points. Irregularly spaced data points are difficult to work with, whereas regularly spaced data, though sometimes operationally expensive, are more readily analysed. This has prompted the use of elevation data of points spaced regularly on a square grid. The digital surface model is of the form of a matrix consisting of M rows and N columns where an element ij is denoted by Z_{ij} . This matrix is the input for the subsequent analysis of the surface properties. A portion of such a matrix is shown in Fig. 4.1a.

4.22. Measurable Geometric Properties of Depressions

The total volume of depression storage on any surface is the sum of the volumes of all individual depressions.

Each depression is characterized by its geometric properties such as depth, surface area^{*}, and volume. The determination of these properties with the help of a digital surface model consisting of a matrix of elevation constitutes a problem of recognition, isolation, and measurement of individual depressions.

In order to recognize a depression it is essential to consider a few characteristic points which fall within its extent. The first such point is the lowest point of a depression which could easily be identified by comparing this point with its adjacent points or neighbours. Therefore, any point that is lower than its neighbours is the lowest point of a depression. This point is termed a low point.

For isolation of a depression it is essential to determine its boundary. Each depression has some specific storage capacity after which it starts overflowing at one or more points. Each overflow point, termed a pour point, defines the boundary of the depression in the sense that all other points associated with any low point having elevations lower than the pour point form part of that depression. And so a depression can be isolated by identifying a low point, a pour point or points and associated depression points.

The information obtained in the process of isolation can be used for computing the geometric properties of depressions. The elevation difference between the low point and the pour point yields the maximum depth of a depression. The

* surface area is defined on page 55.

product of the number of associated depression points including the low point and the grid area gives the maximum surface area. The volume of storage can then be determined from the surface area and depth values.

This general approach is applicable to any type and size of depressions. Depressions may be simple, having only one low point, or complex, having more than one low point. A complex depression consists of two or more simple depressions which operate separately until two or more boundaries coincide with each other at one or more points. Such a point is termed a shared pour point. At this point or points, the associated depression points of the simple depressions are pooled and the depression is considered as one.

Before describing the technique for identifying and characterizing the information on depressions, it is appropriate to provide formal definitions of the characteristic points of a depression described above and some other terms to be used later.

4.23. Definition of Terms

The terms used to denote the properties of depressions are defined below.

Initial low point (ILP). A point Z_{ij} is considered as an initial low point if it is equal to or lower than its four adjacent points located at right ($Z_{i,j+1}$), left ($Z_{i,j-1}$) above ($Z_{i-1,j}$) and below ($Z_{i+1,j}$) as shown in Fig. 4.1b.

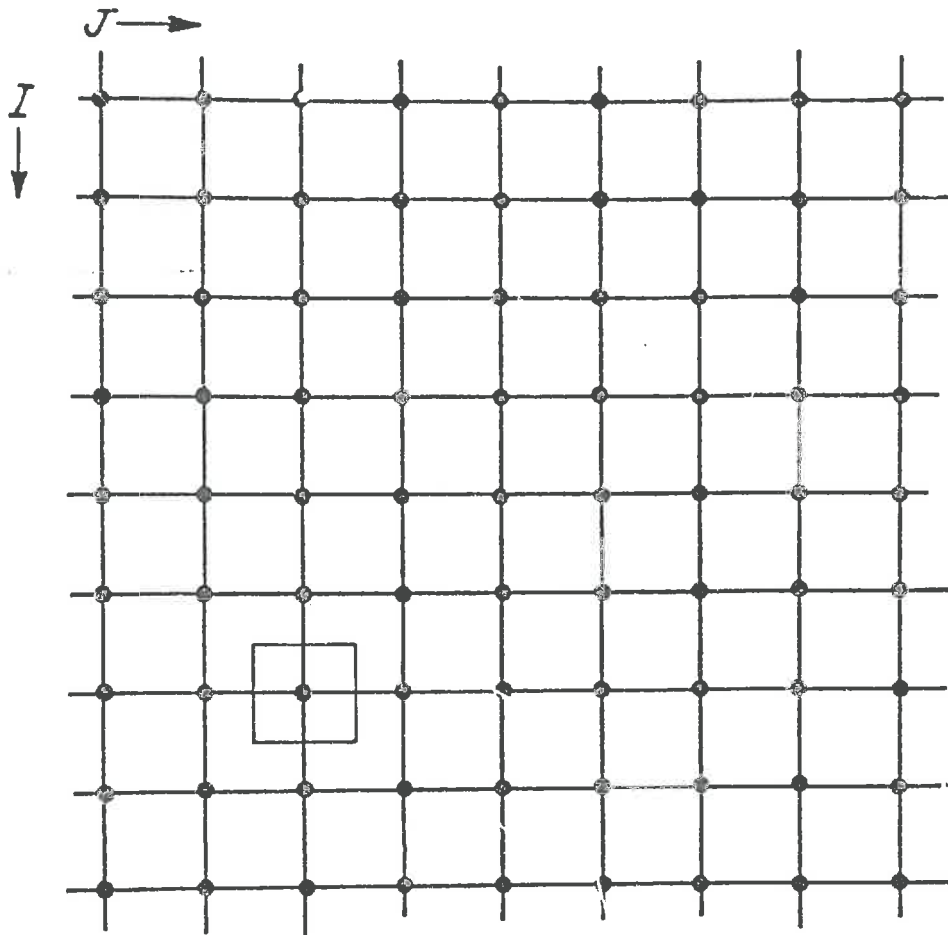


FIG. 4.1(a) A PORTION OF DIGITAL SURFACE MODEL CONSISTING OF MATRIX (IJ)

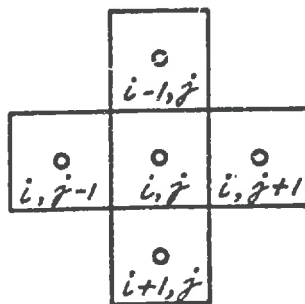


FIG. 4.1(b) DEFINITION OF ADJACENT POINTS OR NEIGHBOURS

It involves a four point comparison. In the case of equal elevations of adjacent point or points, the point with higher coordinates (X,Y) is taken as the low point. This criterion excludes all points along the edge of the matrix and adjacent to an undefined point or element from consideration of an initial low point.

Pour point (PP). It is a point Z_{ij} in the basin area at which the depression overflows its boundary. The pour point may be unique or multiple.

Active pour point (APP). It is a point Z_{ij} at which a complex depression finally overflows its boundary.

Shared pour point (SPP). It is a pour point which is common to two or more depressions.

Associated depression points (ADP). The term refers to all other points lying within the surface area of a depression at the elevation of the pour point.

Basin. The basin definition includes all points associated with a given initial low point up to and including the pour point or points. It has been used interchangeably with depression.

Simple depression (SD). It is a depression which has one low point and has no shared pour point as shown in Fig. 4.2a.

Complex depression (CD). It is a depression which has more than one low point and has one or more shared pour points. It consists of more than one simple depression as

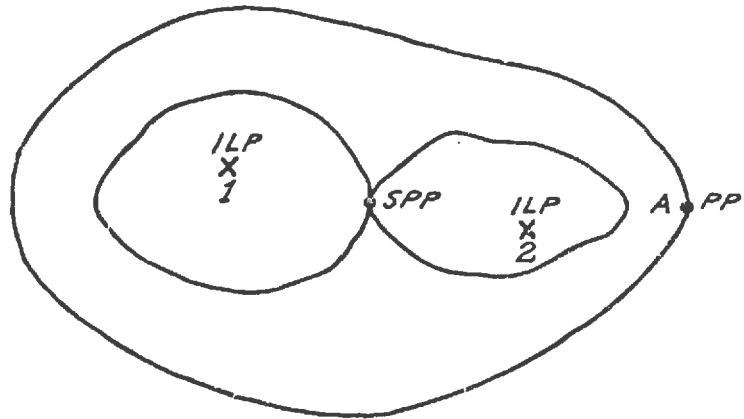
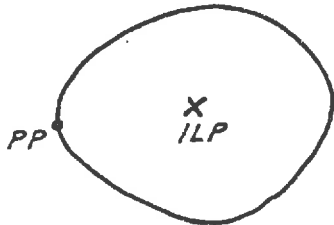
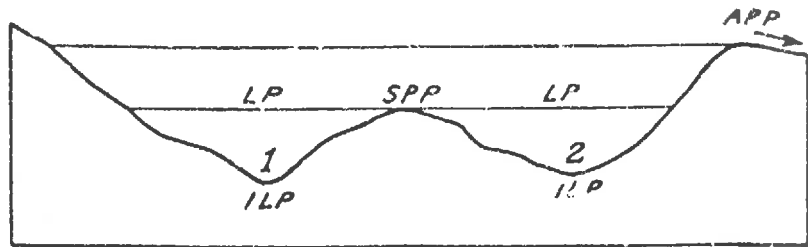
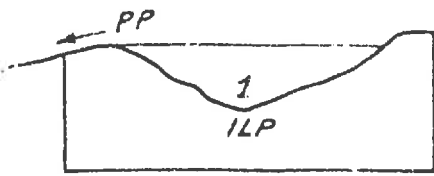


FIG. 4.2 (a) SIMPLE DEPRESSION
(FIRST ORDER BASIN)

FIG. 4.2 (b) COMPLEX DEPRESSION
(SECOND ORDER BASIN)

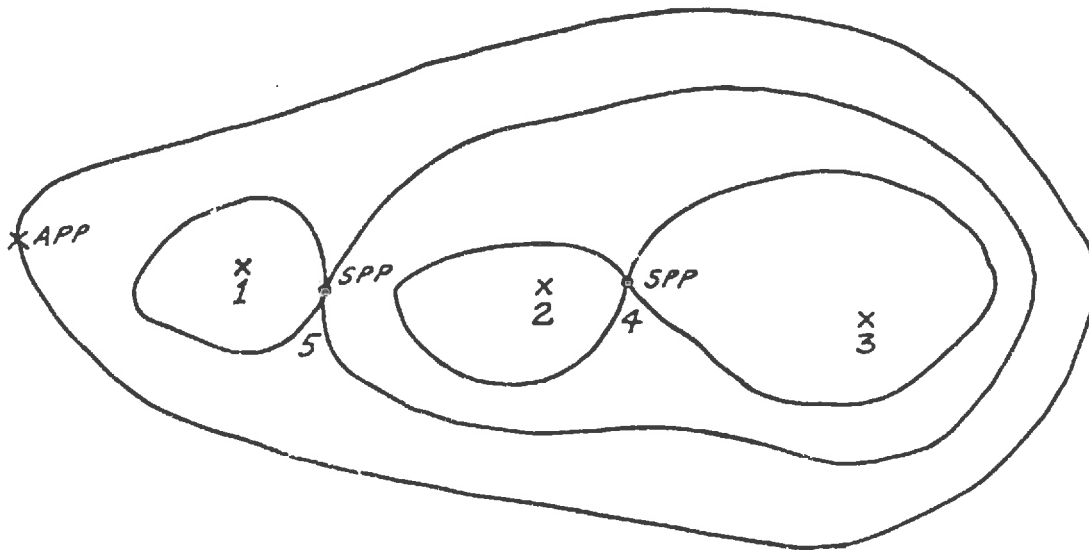
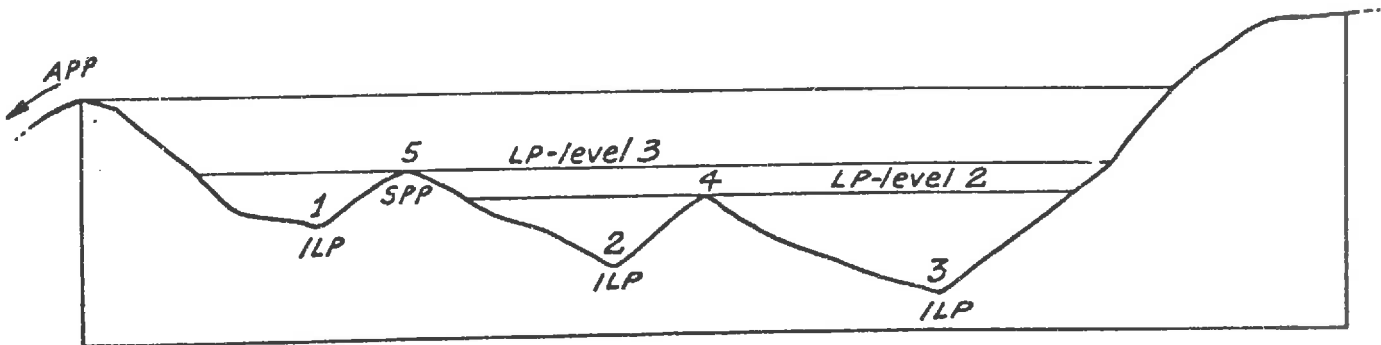


FIG. 4.2 (c) COMPLEX DEPRESSION (THIRD ORDER BASIN)

shown in Fig. 4.2b and c.

Maximum depth. The term represents the difference in elevation between the initial low point and the pour point.

Maximum surface area. It is the water area at the pour point elevation. It is also referred to as the basin area when the depression is full.

Basin order. It is convenient to classify depressions on the basis of their grouping or nesting to study their hierarchic structure in relation to the controlling factors such as soil, slope, topography, management practices, etc. It will also help in the computation of volumes at different levels. A simple depression is designated as the first order basin as shown in Fig. 4.2a. A complex depression with more than one first order basin is designated as second order basin. A third order basin contains one or more second order basins and so on up to K^{th} order which will have an active pour point to drain the water in excess of the storage capacity of the depression.

Level. The number associated with the term 'level' represents the order of the basin and is used to specify the low points. For example, level one is the set of initial low points and level two is the set of low points at the elevation of shared pour points and so on up to the highest order as shown in the link list in Fig. 4.2d.

4.24. Identification of Points

The digital surface model, constituting a matrix of

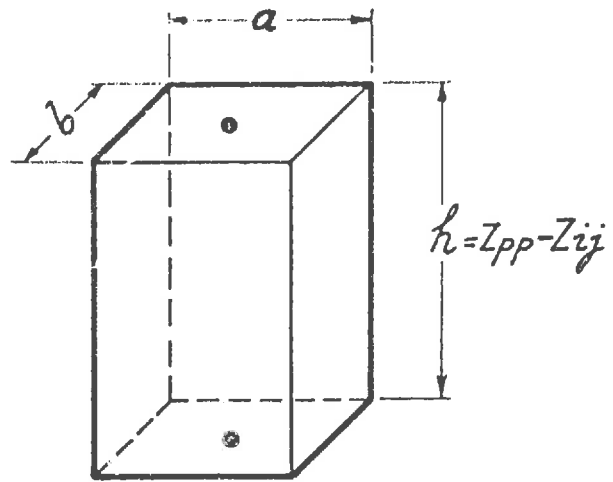
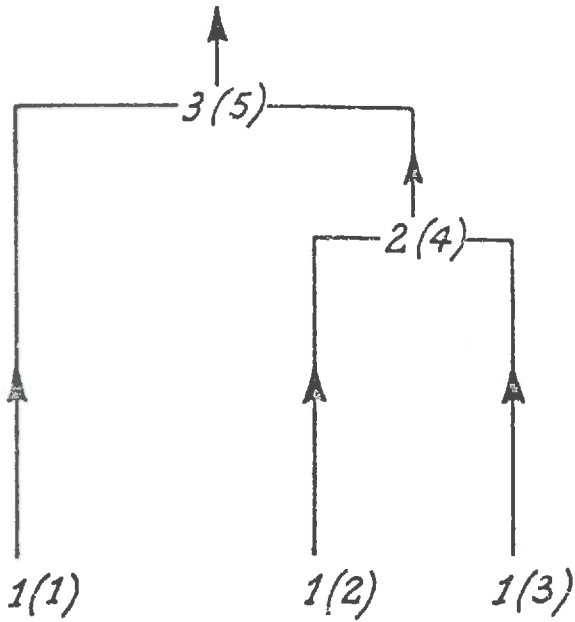


FIG. 4.3(a) - GEOMETRY OF A VERTICAL CYLINDER
USED FOR COMPUTATION OF VOLUME.

FIG. 4.2(d) LINK AND ORDER LIST

THE FIRST NUMBER INDICATES ORDER NUMBER AND
THE NUMBER IN BRACKET INDICATES BASIN NUMBER.

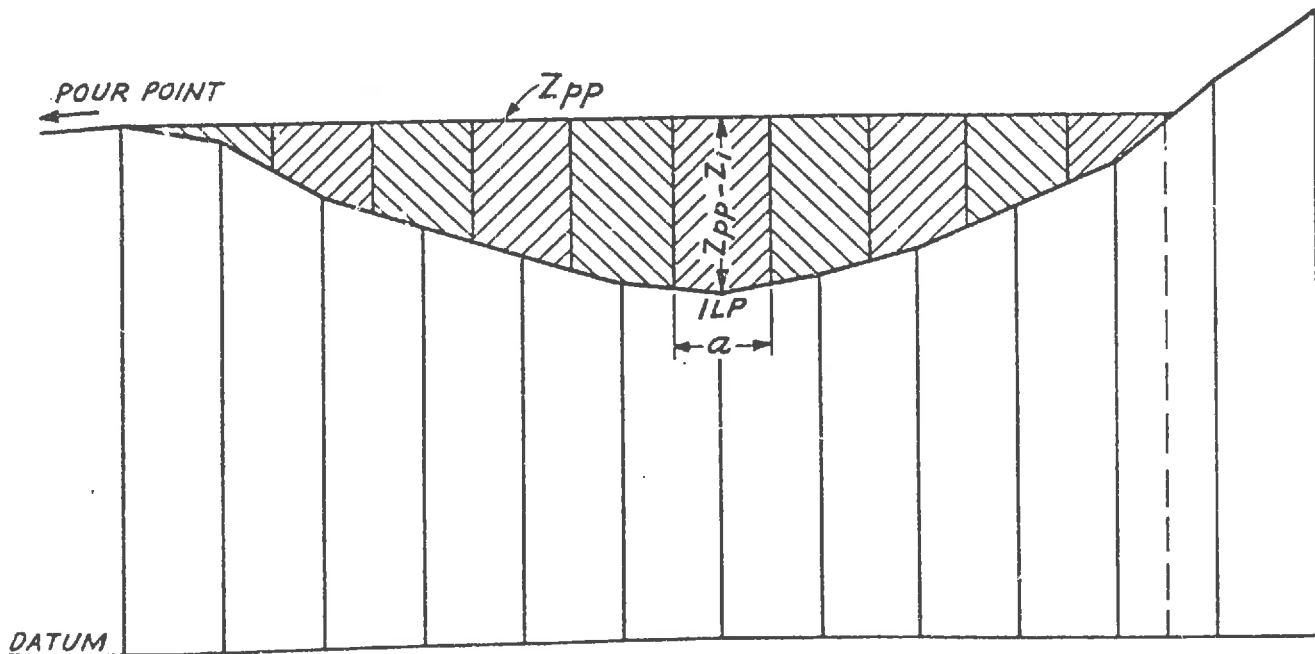


FIG. 4.3(b) - COMPUTATION OF DEPRESSION STORAGE VOLUME

elevation points, is scanned for the initial low points, associated depression points, and pour points. These points are required for computation of surface area, depth, and volume of storage. The procedure is as follows.

1. Identify all the low points and list them as initial low points with their coordinates (X,Y).

2. Go to a low point and find the next higher point by comparing the low point with its four adjacent points. List all five points which have been compared including the low point.

3. Go to the point selected in step 2, and compare it with those of its adjacent points or neighbours which have not been compared earlier to find if any one of these is lower. If so, this point is a pour point and the basin is complete. If not, find the next higher point out of the points listed in step 2 and adjacent points compared. Add the compared points to the list.

4. Go to the point obtained in 3, and search for a lower point by comparing it with its adjacent points. If there is no lower point enter the compared points in the list and find the next higher point in the augmented list.

5. Go to the point obtained in 4, and repeat the process of checking, comparing, and listing all points till a pour point is obtained. This point is the point of overflow and marks the end of the storage zone.

6. Delete all the points higher than the elevation

of the pour point. A listing of points in order of increasing elevation facilitates this step.

7. In the case of complex basins, the same procedure is followed separately for each simple depression up to the level of shared pour point. At this level, the points in the lists associated with each low point of the simple depressions sharing the pour point are combined, and the procedure repeated till an active pour point of the complex basin is obtained.

4.25. Computation of Volume of Storage

Let the points in the list be represented as Z_1, Z_2, \dots, Z_n and Z_{pp} , where Z_1 is the low point, Z_2 to Z_n are the associated depression points and Z_{pp} is the pour point. Consider each point Z_i , where $i = 1, 2, 3, \dots, n$, as the centre of the base of a vertical cylinder having a length equal to the difference between the pour point Z_{pp} and Z_i , as shown in Fig. 4.3a,b. Let the base of the cylinder be represented by 'a' units in the X direction and 'b' units in the Y direction with an area 'ab' equal to the size of the grid. The volume of storage can be computed as follows:

$$\begin{aligned}
 V &= a \times b \sum_{i=1}^n (Z_{pp} - Z_i), \\
 &= a \times b [(Z_{pp} - Z_1) + (Z_{pp} - Z_2) + \dots + (Z_{pp} - Z_n)] \\
 &= a \times b (n Z_{pp} - \sum_{i=1}^n Z_i) \qquad 4.1
 \end{aligned}$$

For the case of a square grid, equation 4.1 becomes,

$$V = a^2 (n Z_{pp} - \sum_{i=1}^n Z_i) \quad 4.2$$

where: V = the storage capacity of a basin, in cc.,
 Z_{pp} = the elevation of the pour point, in cm.,
 Z_i = the elevation of the low point and associated depression points, in cm., and
 n = the number of points up to but excluding the pour point.

The surface area and the depth of each depression may be computed by the following relationships.

$$\text{Surface area (SA)} = n \times a \times b \quad 4.3$$

$$\text{maximum depth (D)} = Z_{pp} - Z_1 \quad 4.4$$

where Z_1 is the elevation of the initial low point. In the case of a complex basin, Z_1 is the elevation of the lowest initial low point.

4.26. Sample Computation by the Proposed Digital Method

Fig. 4.4 shows the grid point elevations of a portion of a sample plot obtained by the photogrammetric technique. Consider a matrix (ij) , where $1 \leq i \leq 10$ and $1 \leq j \leq 6$, and a given elevation Z_{ij} . The point Z_{44} (13.42) is a low point as it is lower than its four adjacent points Z_{45} , Z_{34} , Z_{43} and Z_{54} . The next higher point is Z_{43} (14.??) which is compared with those adjacent points not considered earlier,

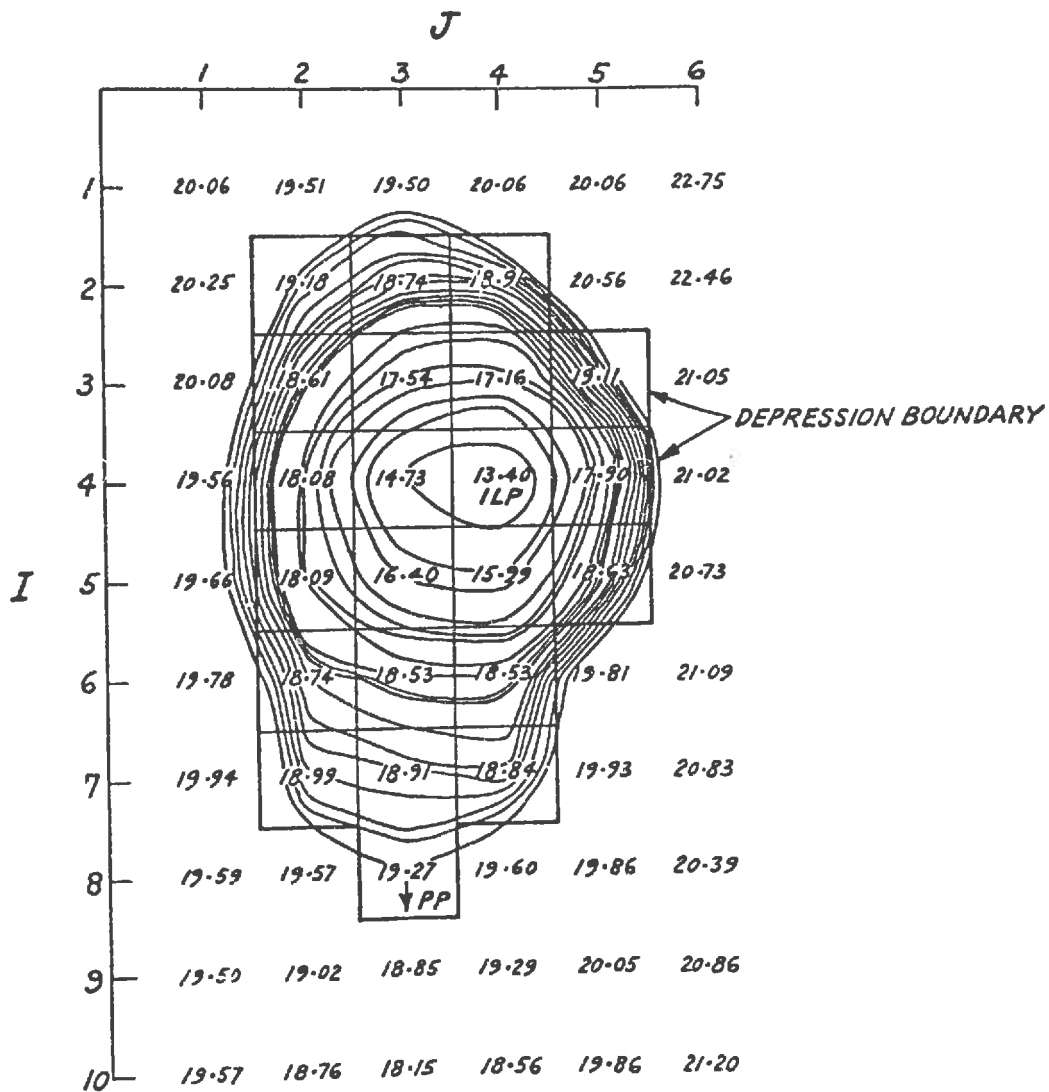


FIG. 4.4 - GRID POINT ELEVATIONS OF A PORTION OF SAMPLE PLOT
FOR DEPRESSION STORAGE VOLUME COMPUTATION
BY CONTOUR AREA AND DIGITAL METHODS.

ie. Z_{42} which is higher. Consider the augmented boundary consisting of Z_{45} , Z_{34} , Z_{43} , Z_{54} and Z_{42} and find the next higher point which is Z_{54} (15.99). Compare this point with its adjacent points Z_{64} , Z_{53} and Z_{55} , all of which are higher. Consider now the augmented boundary consisting of Z_{45} , Z_{34} , Z_{43} , Z_{54} , Z_{42} , Z_{64} , Z_{53} and Z_{55} and find the next higher point which is Z_{53} (16.40). Compare Z_{53} with its new neighbours Z_{52} and Z_{63} which again are higher. Proceed as before until point Z_{83} is reached and compare it with its adjacent points Z_{82} , Z_{84} and Z_{93} for the existence of any lower point. The point Z_{93} (18.85) is lower than the point Z_{83} (19.27) and therefore, the point Z_{83} is a pour point at which the depression will overflow its boundary.

Considering all the points lower than the pour point Z_{83} , the following associated depression points are obtained.

Point	Elevation (Z) cm.	Point	Elevation (Z) cm.
Low point	13.40	ADP	18.63
			18.74
ADP	14.73		18.74
	15.99		18.84
	16.40		18.91
	17.16		18.91
	17.54		18.99
	17.90		19.11
	18.08		19.18
	18.09		
	18.53	PP	19.27
	18.53		
	18.51		

To summarize the information, the required properties have been computed below.

$$z_i = 13.40 \text{ cm.}$$

$$z_{pp} = 19.27 \text{ cm.}$$

$$\sum z_i = 375.01 \text{ cm.}$$

$$n = 21$$

$$ab = 6.25 \text{ cm}^2.$$

$$\begin{aligned} \text{Maximum depth (D)} &= 19.27 - 13.40 \\ &= 5.87 \text{ cm. (From equation 4.4)} \end{aligned}$$

$$\begin{aligned} \text{Surface area (SA)} &= 21 \times 6.25 \\ &= 131.25 \text{ sq. cm. (From equation 4.3)} \end{aligned}$$

$$\begin{aligned} \text{Volume (V)} &= 6.25 (21 \times 19.27 - 375.01) \\ &= 185.37 \text{ cc. (From equation 4.1)} \end{aligned}$$

4.27. Comparison of Results with Contour Area Method

The proposed digital method of computation of volume considers each grid as a vertical cylinder with base equal to the grid area and height equal to the difference between the grid elevation and the pour point. This is a valid calculation and is the best that can be made without assuming continuity of surface. It also includes tilted plane surface elements. The method is likely to introduce some error in the estimation of volume of vertical cylinders along the boundary of a depression. But the resulting error is expected to be too small for any significant effect

on the accuracy of volume estimation.

The reliability of the digital method was studied by a comparison of the estimates of volume with similar estimates obtained by the contour area method. The grid data were used for drawing of contours representing grid elevations, as shown in Fig. 4.4. For example, the contour of 14.73 cm. passed through the point Z_{43} . The water held at this level was assumed to cover an area equivalent to the area enclosed by the contour. Similarly, the contour of 19.27 cm. passing through the pour point Z_{83} , enclosed the maximum water area when the depression was full.

The volume of storage was estimated by planimentering the area enclosed by each contour and computing the volume, equal to half the sum of the areas of two consecutive contours multiplied by the difference in the elevations of the two contours.

Table 4.1 gives the volume of storage as obtained by the two methods for a few selected depressions.

Table 4.1. Depression Storage Volumes Computed by Contour Area Method and Digital Method

Depression No.	Storage Capacity	
	Contour Area Method cc.	Digital Method cc.
1	13.66	13.75
2	14.34	15.37
3	37.21	38.19
4	190.12	185.37
5	62.59	59.10
6	25.24	25.69
7	63.86	62.31
8	22.28	25.75
9	23.81	25.12
10	84.43	94.69
11	2.63	3.50
12	3.37	3.44
Total	543.54	552.28

The difference between the total volumes as obtained by the two methods is negligibly small. The volumes of individual depressions are also comparable. Fig. 4.5 shows the plotting of volumes given in Table 4.1 and the line of best fit obtained by the method of least squares. The

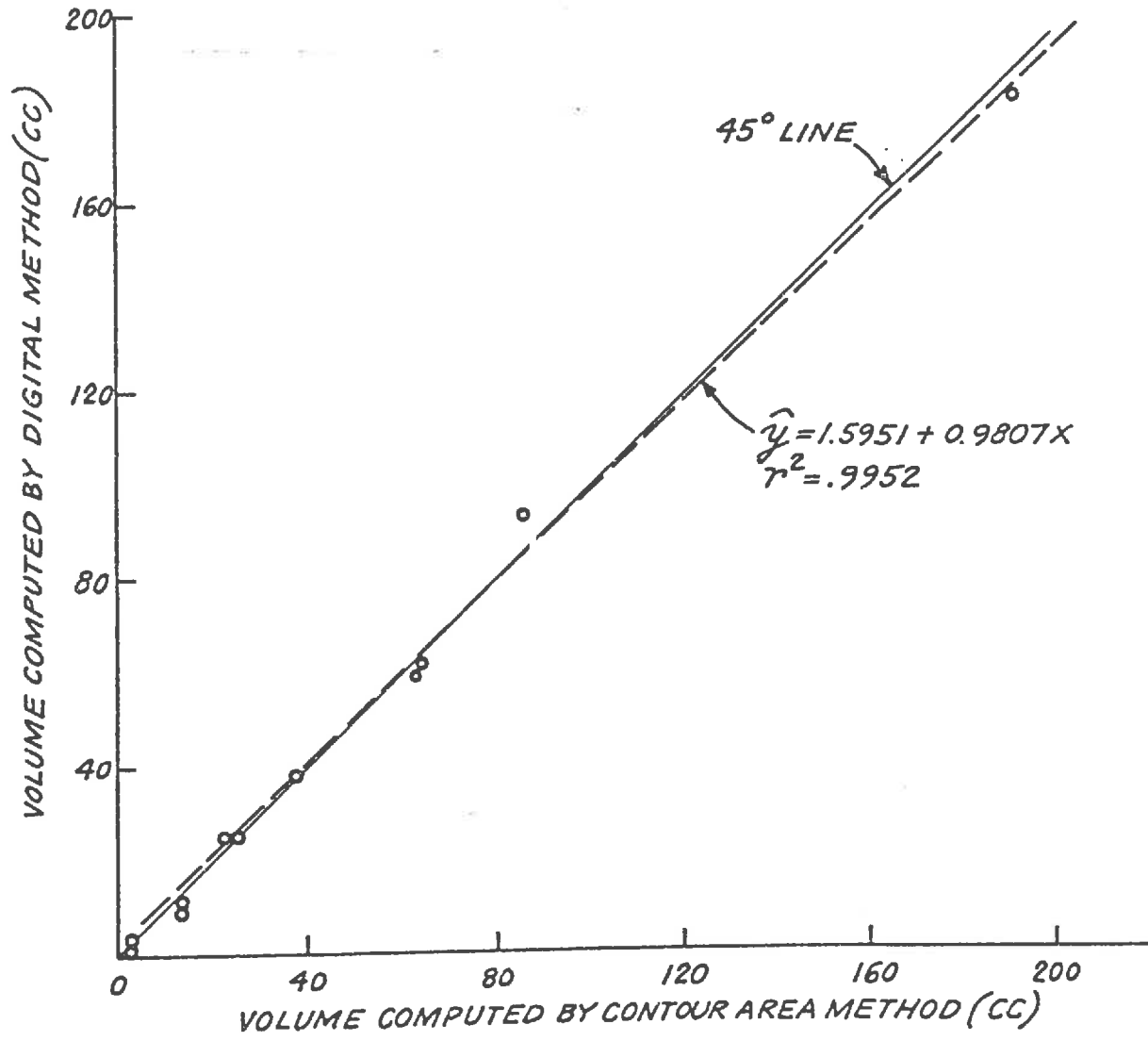


FIG. 4.5 - RELATIONSHIP BETWEEN VOLUMES COMPUTED BY CONTOUR AREA METHOD AND DIGITAL METHOD.

regression line exhibits a slope not significantly different from the equal value line. The relationship is highly significant with a coefficient of determination of 0.9952.

4.28. Evaluation of the Digital Method

It would be appropriate at this stage to evaluate the proposed digital method in light of the criteria of suitability laid down earlier.

From the details given in the preceding sections, it is evident that the digital method may be applied simply and rapidly, allowing the saving of considerable time. The simple logic of the method lends itself to computer programming which, in addition to saving of time and cost, can handle any number of digital surface models.

The results obtained by the proposed method are very close to that obtained by the contour area method for the entire range of data. There is also no evidence of any trend in the two sets of data. It is therefore, reasonable to assume that the proposed digital method is as reliable and precise as the contour area method which is an accepted method of volume estimation. It is difficult to establish the superiority of one over the other in terms of relative accuracy of computed volume of storage because of practical difficulties in directly measuring the actual volume of storage of a depression.

The method is applicable to digital surface models representing both macrosurface and microsurface having any

number and size of depressions. Though the method has not been applied to any other type of surface, characterized by large natural or artificial depressions, there is nothing in the basic approach which may restrict its applicability to macrosurfaces. The only input data needed is a matrix of elevation contained in the digital surface model of any surface.

The proposed method is confined to the estimation of the geometric properties of depressions, but the basic approach could be utilized to develop techniques for determining information on other properties of the surface or terrain.

It is evident from the above discussion that the proposed digital method meets the criteria mentioned earlier. Having ascertained the suitability of the method, a computer program has been developed. The algorithm design considerations and the details of the computer program are discussed in the following sections.

4.29. Algorithm Design Considerations

The problem of volume estimation on a surface by the digital method discussed earlier can be considered in three parts:

1. Identification of initial low points on the surface, indicating the location of depressions,
2. Identification of associated depression points and pour point or points of all simple and complex depressions, and

3. Computation of surface area, depth, and volume of storage for all depressions.

The following design considerations are required in the development of an algorithm for computer programming using a digital surface model.

a. Completeness of Points.

A point must have four adjacent points to be considered as a low point. The algorithm must provide for such situations as edges of the matrix and points adjacent to an undefined area. The undefined area itself has to be identified in some way such as a large negative number.

b. Equalities of Points.

A depression may have more than one pour point, shared pour point, and a few associated depression points with the same elevation. The algorithm design must provide for identification and processing of such points.

c. Level Identification.

In the case of complex basins, a concept of level has been introduced to indicate the order of the basin and compute the volume of storage as it builds up from one level to the next higher level. The first order basins may have a common or shared pour point with a fixed number of associated depression points defining each basin. The two or more simple depressions constituting any complex basin will fill up independently up to the elevation of the shared pour point(s). This is designated as level 1 and represents the volume of

storage of the first order basins. Similarly the shared pour point elevation of the second order depressions is designated as level 2, and so on up to the K^{th} level. The K^{th} level containing K^{th} order basins will have one or more active pour points at which the complex basin overflows after it is filled to its capacity. All the associated depression points up to this level will define the complex basin having initial low points obtained during the first scanning of the matrix. The algorithm must provide for the identification and flagging of each level with its characteristic points.

4.30. Algorithm Design and Computer Programming

The system flow logic, shown in Fig. 4.6, operates in the following four distinct stages.

1. Identification of Initial Low Points

The initial low points are identified and flagged with their coordinates (X,Y) by a scanning of the matrix by row, moving from left to right, and from top to bottom. There is nothing particular about the direction of scanning as other systems could be followed. The scanning involves the comparison of each point with its four adjacent points or neighbours to check for its being a low point. The edges of the matrix and the points adjacent to an unidentified point are not considered for scanning. In the event that two adjacent points have equal values, the point to the right will be defined as a low point. This choice has been

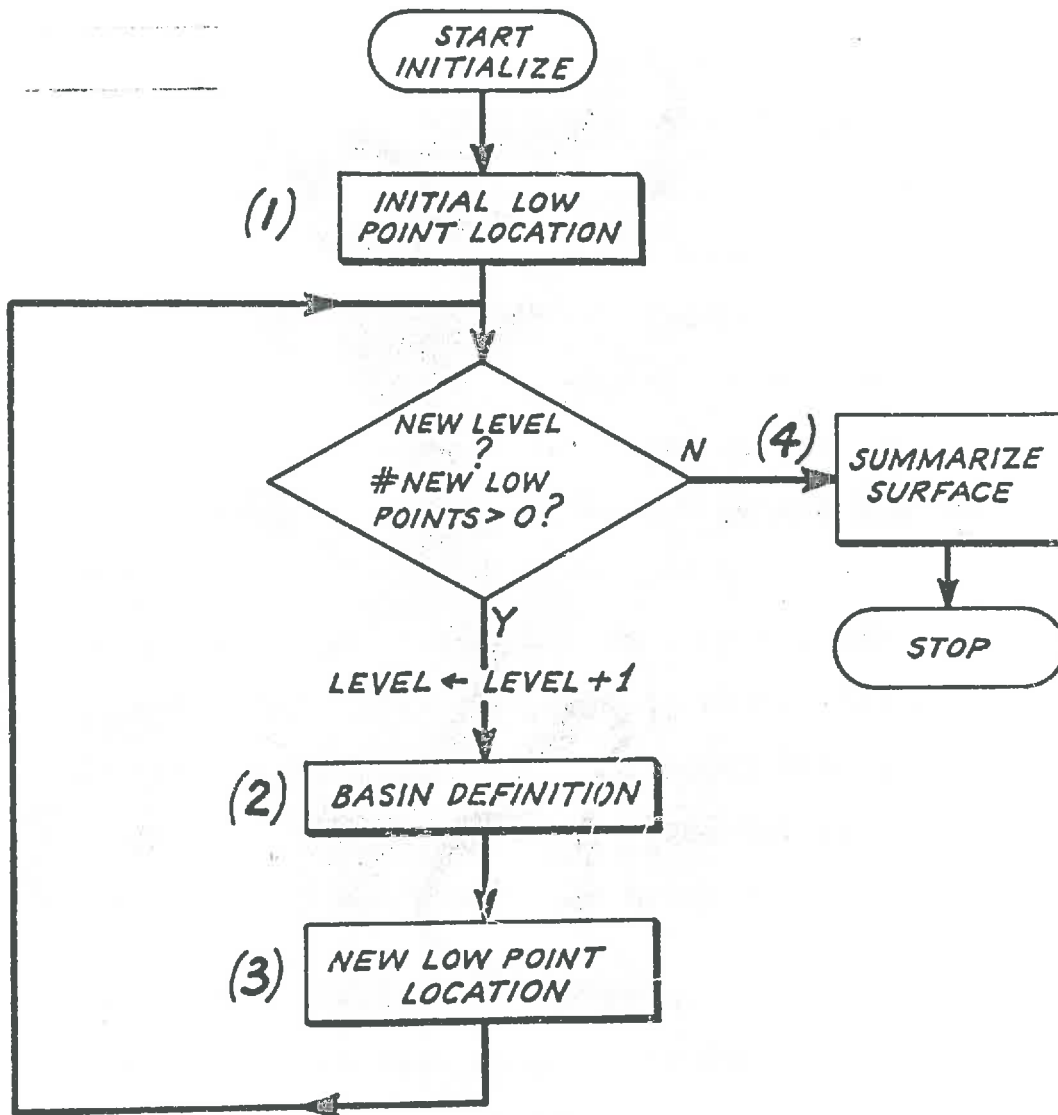


FIG. 4.6-SYSTEM LOGIC FLOW

favoured because of the order of scanning.

2. Basin Definition for Each Initial Low Point

For each initial low point all associated depression points are determined and flagged with their coordinates which constitute or define the basin. The pour point(s) is also flagged. The procedure for determining the associated depression points and the pour points discussed in section 4.24 has been incorporated in the algorithm design. In the case of two or more associated depression points having the same elevation, each is compared with its adjacent points. When the edge of the area is reached, the scanning is stopped and the edge point is taken as a pour point. Each basin thus identified and defined by the associated depression points and pour point(s) is flagged with a serial number for subsequent identification. The volume, surface area, and the maximum depth for each basin are then computed.

3. Low Point Location for Higher Order Basins.

The purpose of this stage is to determine the location of the low point at any level 'K' when $K > 1$ and to build up a link list describing the surface structure of the complex basins. All the flagged points obtained in the first stage are searched to identify the shared pour points indicated by the equal value coordinates. For each complex basin thus identified and flagged, all the associated depression points of the constituent first order basin are pooled to get an

augmented boundary. The associated depression points in the pooled list having elevations equal to or lower than the shared pour point are assigned the elevation of the shared pour point obtained at the first level. The associated depression points having elevations higher than the shared pour point elevation are then selected in order of increasing elevation and compared with their respective adjacent points, as done in stage two, to define the basin at level 2. The above procedure is repeated till all the levels are completed and an active pour point is obtained. The link list as shown in Fig. 4.2d consists of a pair of basins at any level which are found to have shared pour point(s) and a new low list contains the low point number for the basin to be defined at level K.

4. Summary of Geometric Properties of Depressions.

This part of the computer program summarizes the information on storage volume, surface area, and maximum depth for each depression. In the case of complex basins the numbers of the lower order basins are also listed. The total volume of storage on the surface represented by the digital surface model is also computed and given in the end. The computer program developed with the help of the Institute of Computer Science at the University of Guelph is shown in Appendix B. The output consists of the following:

- (i) Print output of the input data.
- (ii) List of initial low points with their coordinates.

- (iii) List of basins with coordinates of low points, pour points and associated depression points along with the computed values of volume, depth and surface area.
- (iv) List of new basins formed from basins sharing pour points along with a link list.
- (v) List of complex basins with constituent lower order basins and computed values of volume, depth and surface area.
- (vi) Volume of storage for the area represented by the digital surface model.

The algorithm design is set up in such a way that the program can suitably be modified to provide the information on other properties of the surface.

4.3. QUANTITATIVE DESCRIPTION OF SURFACE ROUGHNESS

4.31. General

The overall roughness of a microsurface (defined in Chapter two) which controls the hydrologic response of the surface to any rainfall event consists of the following components:

- (i) Particle roughness, due to soil grain on bare areas.
- (ii) Form roughness, due to small scale topographic irregularities caused by the geomorphic processes, geomorphic roughness, on which are superimposed the irregularities caused by the tillage operations, tillage roughness.
- (iii) Vegetative roughness, due to the physical obstruction and retarding influence of plant growth.

The present study is concerned only with a quantitative description of form roughness. The effect of vegetation has been excluded by considering only a bare surface.

4.32. Basic Considerations in Selection of Methodology

Although a power spectral density function has successfully been used for describing surface roughness in a variety of problems, its application has been limited in describing the microsurface of interest to hydrologists. The reason appears to be the lack of information about the form of the transfer function of the surface system which does not permit the evaluation of the response function. For this reason the spectral density approach provides information only on the frequency composition of data as inferred from the shape of the power spectrum.

Also a power spectral density function considers roughness as being contributed only by the height of micro-relief features represented by the point elevation values. In fact, roughness is caused not only by the height but also by other geometric properties of the microrelief features such as slope, number, and areal pattern of distribution, etc. Therefore, surface roughness cannot be completely described by any single property of the microrelief features. For a complete description of surface roughness all the important properties of the microrelief features have to be considered.

The geometric properties of microrelief features which give rise to specific types of roughness can be considered as independent components of roughness. This permits independent comparison of two or more surfaces in terms of one or more components for the determination of the exact nature of differences in surface properties. Knowledge of the nature of surface roughness is important in the analysis of the effect of roughness on the response of a surface system.

The method proposed by Stone and Dugundji (1965) for studying macrosurfaces by considering roughness as being caused by more than one geometric property of the microrelief features, appears to be quite realistic. This method can be adapted for describing the roughness of microspheres.

4.33. Physical Concept of Roughness

The concept of roughness and mathematical formulations that follow have been adapted from the work of Stone and Dugundji (1965) on terrain roughness for the design of vehicle suspension systems. Their approach considers a profile taken on a smooth surface to be represented by a straight line. A rough profile indicates a random occurrence of small ridges and valleys or depressions, termed earlier as microrelief features, which give rise to roughness. What constitutes the roughness of the profile in quantitative terms requires identification and description of the geometric properties of microrelief features. A few of these are height, slope, and frequency of occurrence which are

considered below.

1. Height of microrelief features

The height of ridges and the depth of valleys are the first visual considerations regarding the relative roughness of two profiles representing two surfaces. If a profile is represented by a periodic function, the height of the microrelief features are equivalent to the amplitude of the oscillations. Therefore, the amplitude of any oscillation must be an important component of roughness. This is termed the relief factor (M).

2. Slope of microrelief features

The steepness of the slope of microrelief features is another property which aids in decision about the relative roughness of two profiles. The steeper the slope of the microrelief features, the rougher is the profile. The steepness of the slope is a property associated with the wavelength of the periodic function representing the profile. Therefore, the steepness of any oscillation is another important component of roughness which needs to be accounted for in a meaningful definition of roughness. This is designated as the slope factor (P).

3. Frequency of occurrence

In the case of similarity of two surfaces with respect to height and steepness of the slope, another consideration

is the frequency of occurrence of microrelief features. The profile with a frequent occurrence of microrelief features at more or less regular spacing is rougher than one with less frequent occurrences. Therefore, the periodic repetition of microrelief features is also an important component of roughness. This is known as the structural homogeneity factor (K).

Since each of the height and steepness of a slope provide a measure of the degree of roughness, the product of these two quantities can be used as another term which reflects overall roughness of the surface. This quantity is termed the resistance factor (ρ) which is equivalent to the avoidance factor of Stone and Dugundji (1965).

There is another apparently useful quantity termed the cell length (C_L) which indicates the length of profile where all significant microrelief features are encountered. The usefulness of these quantities with respect to their ability to describe surface roughness will be revealed by the results of the analysis.

4.34. Definition of Microrelief Features of Microsurface

The above described roughness elements can be determined from a Fourier series analysis of profiles taken on any surface. The surface irregularities are caused primarily by high frequency terms of the Fourier series which depends on the horizontal distance of the predominant microrelief features. The microrelief features associated with the

microsurfaces consist of short length topographic variations caused by small scale geomorphic processes and on which are superimposed the microrelief features generated by tillage operations. A horizontal distance of 60 centimeters appears satisfactory as an upper limit to be considered for microrelief features since such distance includes most significant microrelief features contributing to roughness. The lower limit of horizontal extent of microrelief features depends on the relative contribution of small microrelief features to overall roughness, the spacing of available data and the requirements of numerical analysis while using discrete data. A lower limit of 5 centimeters is considered adequate since the contribution to roughness by smaller microrelief features may be negligibly small. This requires elevation data with a spacing of 2.5 centimeters, which has successfully been obtained in the earlier reported studies. This also meets the requirement of the numerical analysis which needs two to three points for the shortest wave length for a reasonable accuracy in the computation of Fourier coefficients.

Using the above limits the microrelief features of any given profile can be quantitatively defined as any ridge or depression having horizontal extent of 5 to 60 centimeters. According to this definition, the part of the Fourier series expansion containing wave lengths $5 \leq \lambda \leq 60$

is assumed to contain all information about the geometric properties of the microrelief features associated with any profile. This part of the Fourier series may be processed to obtain the roughness elements. The microrelief features with horizontal extent of less than five centimeters and more than sixty centimeters need not be considered on the assumption that their contribution to total roughness is insignificantly small.

4.35. Fourier Analysis of a Profile

Let $f(x)$ be defined in the interval $0 \leq x \leq L$ and extended with period $2L$ as shown in Fig. 4.7.

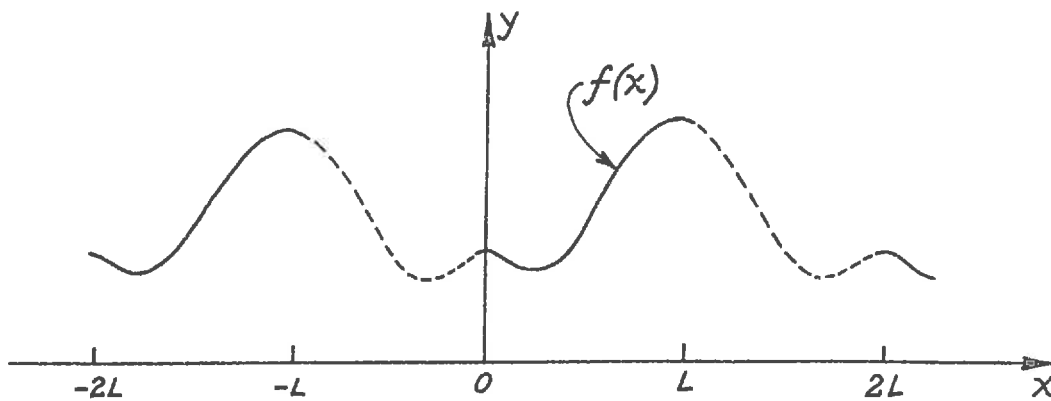


Fig. 4.7. Periodic even function $f(x)$ and its periodic extension.

A Fourier series can be used to represent $f(x)$ in the given interval. It also represents the periodic extension of $f(x)$ outside this interval. The function 'f' is an even function of 'x' in the given interval since,

$$f(-x) = f(x) \quad , \quad 0 \leq x \leq L$$

The function $f(x)$ can therefore, be represented by the Fourier cosine series given below:

$$f(x) = a_0 + \sum_{n=1}^{\infty} a_n \cos \frac{n\pi x}{L} \quad , \quad (-\infty < x < \infty)$$

where: $a_0 = \frac{1}{L} \int_0^L f(x) dx$, and

$$a_n = \frac{2}{L} \int_0^L f(x) \cos \frac{n\pi x}{L} dx, \quad (n=1, 2, \dots)$$

The term a_n is the amplitude of n th harmonic. The frequency is given by $\frac{n\pi}{L}$, and the wave length by $\frac{2L}{n}$. In view of the definition of microrelief features, the smallest wave length for which the harmonic is determined is 5 cm. If the length of the profile is 200 cm., the number of harmonics required to be calculated is $\frac{2 \times 200}{5} = 80$, a rather large number. It appears adequate to use only 12 harmonics with wave length $5 \leq \lambda \leq 60$. The method suggested by Stone and Dugundji (1965) may be used to compute the amplitudes for the entire length of the profile. It is as follows:

- (a) Divide the profile into segments with
 $l = 12 \times 2.5 = 30$ cm.
- (b) For each segment of 30 cm. compute the first 12 harmonics.

$$\begin{matrix} (1) & (1) & (1) & & (1) \\ a_1, & a_2, & a_3, & \text{-----}, & a_{12} \end{matrix} \quad 0 \leq x \leq \ell$$

$$\begin{matrix} (2) & (2) & (2) & & (2) \\ a_1, & a_2, & a_3, & \text{-----}, & a_{12} \end{matrix} \quad \ell \leq x \leq 2\ell$$

$$\begin{matrix} (3) & (3) & (3) & & (3) \\ a_1, & a_2, & a_3, & \text{-----}, & a_{12} \end{matrix} \quad 2\ell \leq x \leq 3\ell$$

$$\begin{matrix} (k) & (k) & (k) & & (k) \\ a_1, & a_2, & a_3, & \text{-----}, & a_{12} \end{matrix} \quad (k-1)\ell \leq x \leq k\ell$$

where k is the number of segment.

(c) Calculate

$$a_s = \frac{\begin{matrix} (1) & (2) & & & (k) \\ a_s & + a_s & + \text{-----} & + a_s \end{matrix}}{k}, \quad s \text{ is even, and}$$

$$a_s = \frac{\begin{matrix} (1) & (2) & & & (k) \\ a_s & - a_s & + \text{-----} & \pm a_s \end{matrix}}{k}, \quad s \text{ is odd.}$$

It can be shown that a_s is the amplitude, with period

$\frac{60}{s}$, for the entire curve $f(x)$, on the interval $0 \leq x \leq k\ell$

(Stone and Dugundji 1965). The above procedure gives the harmonics of period 60, 30, -----, 5 cm. irrespective of the length L . The proof is shown below.

$$(1) \quad a_s = \frac{2}{l} \int_0^l f(x) \cos \frac{s\pi x}{l} dx$$

$$(2) \quad a_s = \frac{2}{l} \int_l^{2l} f(x) \cos \frac{s\pi(x-l)}{l} dx$$

$$= (-1)^s \frac{2}{l} \int_l^{2l} f(x) \cos \frac{s\pi x}{l} dx$$

Adding, gives

$$a_s = \frac{a_s^{(1)} + \dots + (-1)^{s(k-1)} a_s^{(k)}}{k}$$

$$= \frac{1}{k} \cdot \frac{2}{l} \int_0^{kl} f(x) \cos \frac{s\pi x}{l} dx$$

$$= \frac{2}{kl} \int_0^{kl} f(x) \cos \frac{sk\pi x}{kl} dx$$

The above equation shows that $a_s = a_{sk}$, which is the amplitude of the harmonic with wave length $\frac{2l}{s} = \frac{60}{s}$.

Since only the high frequency terms of the Fourier series expansion are considered, the series reduces to,

$$g(x) = \sum_{n=1}^{12} a_n \cos \frac{n\pi x}{30}, \quad (-\infty < x < \infty)$$

The above equation contains all information about the

geometric properties of the microrelief features associated with any profile that give rise to any specific type of roughness. It is not an exact representation of the profile, since only 12 terms are considered, but it contains information about the significant microrelief features. This may be processed to obtain the different roughness elements.

4.36. Mathematical Formulations of Roughness Elements

4.361. Relief Factor (M)

Let the high frequency terms of the profile be represented by the equation

$$g(x) = \sum_{n=1}^{12} a_n \cos \omega_n x ,$$

where: $\omega_n = \frac{n\pi}{30}$.

The expressions

$$\frac{1}{2L} \int_{-L}^L g(x) dx = \frac{1}{2L} \int_{-L}^L \sum (a_n \cos \omega_n x) dx = 0$$

and

$$\begin{aligned} \frac{1}{2L} \int_{-L}^L |g(x)|^2 dx &= \frac{1}{2L} \int_{-L}^L \sum (a_n a_s \cos \omega_n x \cos \omega_s x) dx \\ &= \frac{1}{2} \sum a_n^2 \end{aligned}$$

since the system of functions $\cos \omega_n x$, $n = 1, 2, \dots$, is orthogonal on the interval $-L \leq x \leq L$ for all n and s .

Assuming that the function $g(x)$ is a random variable on a probability space $-L \leq x \leq L$ with probability $P(x)$ $P(x) = \frac{1}{2L}$, then the expected value and the variance are given by the relationships,

$$E(g(x)) = 0, \text{ and}$$

$$\text{Var } (g(x)) = \frac{1}{2} \sum a_n^2$$

The quantity $\frac{1}{2} \sum a_n^2$, or simply $\sum a_n^2$, measures the dispersion of the values of $g(x)$ which has the expected value equal to zero. It also indicates the expected range of heights of microrelief features. The larger is this quantity, the taller are the microrelief features. As $\sum a_n^2 \rightarrow 0$, the surface becomes smoother with no microrelief features. Therefore,

$$\text{Relief factor } (M) = \sum a_n^2$$

4.362. Slope Factor (P)

Differentiation of function $g(x)$ yields,

$$g'(x) = -\frac{\pi}{30} \sum n a_n \sin \omega_n x,$$

Considering the function $g'(x)$ as a random variable on the interval $-L \leq x \leq L$, one can show that

$$E(g'(x)) = 0, \text{ and}$$

$$\text{Var}(g'(x)) = \frac{1}{2} \frac{\pi^2}{30^2} \sum n^2 a_n^2.$$

As the quantity $\frac{1}{2} \frac{\pi^2}{30^2}$ is a constant and is independent of the curve being considered, it can be ignored. Therefore, the expected range of slope of the microrelief features is defined by the relationship,

$$\text{Slope factor (P)} = \sum n^2 a_n^2.$$

From the above relationship, the larger is the value of the slope factor, the steeper are the microrelief features. If $\sum n^2 a_n^2 \rightarrow 0$, the surface tends to smoothness.

4.363. Structural Homogeneity Factor (K)

Stone and Dugundji (1965) define a discrepancy or difference function $D(\tau)$ which measures the difference of microrelief between the length x and $(x + \tau)$ as,

$$D(\tau) = \frac{1}{2L} \int_{-L}^L |g(x + \tau) - g(x)|^2 dx$$

Expansion gives,

$$\begin{aligned} D(\tau) &= \frac{1}{2L} \int_{-L}^L |g(x+\tau)|^2 dx + \frac{1}{2L} \int_{-L}^L |g(x)|^2 dx \\ &\quad - \frac{1}{L} \int_{-L}^L g(x) g(x+\tau) dx \end{aligned}$$

Since the functions are integrated for the entire period,

$$\int_{-L}^L |g(x+\tau)|^2 dx = \int_{-L}^L |g(x)|^2 dx ,$$

The equation reduces to

$$D(\tau) = \frac{1}{L} \int_{-L}^L |g(x)|^2 dx - \frac{1}{L} \int_{-L}^L g(x+\tau)g(x) dx$$

The second term of the above equation is the autocorrelation function $R(\tau)$, and the first is the autocorrelation function when $\tau = 0$. Therefore,

$$D(\tau) = R(0) - T(\tau) .$$

The difference function can be shown to have the following properties.

$$D(0) = 0$$

$$D(\tau) \geq 0 \text{ for all } \tau ,$$

$$|D(\tau)| \leq 2 R(0) \text{ for all } \tau , \text{ and}$$

$$D(\tau) = D(-\tau) \text{ for all } \tau .$$

The autocorrelation function of $g(x)$ representing a profile is given by the relationship,

$$\begin{aligned} R(\tau) &= \frac{1}{L} \int_{-L}^L g(x+\tau) g(x) dx , \\ &= \frac{1}{L} \int_{-L}^L \sum a_s a_n \cos \omega_n x \cos \omega_s (x+\tau) dx , \\ &= \sum a_n^2 \cos \omega_n \tau . \end{aligned}$$

By considering the autocorrelation function $R(\tau)$ and the difference function $D(\tau)$ as random variables in the probability space $-L \leq x \leq L$, one obtains the following relationships,

$$E(R) = 0 ,$$

$$\text{Var} (R) = \frac{1}{2} \sum a_n^4$$

$$E(D) = R(0)$$

$$= \sum a_n^2$$

$$\text{Var} (D) = \frac{1}{2} \sum a_n^4$$

Introduction of the above values in the Chebyshev inequality gives,

$$\text{Prob} \{ \tau | D(\tau) - R(0) | \geq R(0) \} \leq \frac{\text{Var}(D)}{[R(0)]^2} = \frac{1}{2} \frac{\sum a_n^4}{[\sum a_n^2]^2}$$

For the relation $|D(\tau) - R(0)| \geq R(0)$ to be valid, either $D(\tau) = 0$, or $D(\tau) = 2 R(0)$. If $D(\tau) = 0$, the function $g(x)$ coincides with itself when shifted to τ units to the left; if $D(\tau) = 2 R(0)$, then $R(\tau) = -R(0)$. This means that the curve $g(x+\tau)$ is negatively correlated to the function $g(x)$. Therefore, the quantity $\frac{1}{2} \frac{\sum a_n^4}{(\sum a_n^2)^2}$ reflects the tendency of the microrelief features to be repeated. The structural homogeneity factor is given by,

$$\text{Homogeneity factor } (K) = \frac{1}{2} \frac{\sum a_n^4}{(\sum a_n^2)^2}$$

The smaller the value of K , the more diverse are the microrelief features. It will also appear from the above relationship that for a smooth surface with no microrelief features, K is undefined.

4.364. Resistance Factor (ρ)

According to Theorem 4 of Stone and Dugundji (1965), the autocorrelation function and the difference function can closely be approximated by the following relationships which are algebraically easier to handle.

$$R(\tau) = R(0) - \frac{|R''(0)|}{2} \tau^2, \text{ and}$$

$$D(\tau) = \frac{|R''(0)|}{2} \tau^2$$

Let τ_p be the distance required for the autocorrelation function to become zero, at which point there is no correlation. The average rate of decrease in correlation provides a measure of overall irregularity of the profile. This rate has been termed the resistance factor (ρ). By equating $R(\tau) = 0$, τ_p can be computed to be,

$$\tau_p = \sqrt{\frac{2R(0)}{|R''(0)|}}$$

The rate of decrease in correlation is given by,

$$\rho = \frac{R(0)}{\tau_p}$$

Substituting the known values,

$$\rho = \sqrt{\frac{R(0) |R''(0)|}{2}}$$

Differentiating $R(\tau)$ twice, and evaluating $R''(\tau)$ at $\tau = 0$, and substituting,

$$\rho = \frac{\pi}{30} \frac{1}{\sqrt{2}} \sqrt{(\sum a_n^2) (\sum n^2 a_n^2)} .$$

Neglecting the constant term and the square root operation, the above equation reduces to,

$$\text{Resistance factor } (\rho) = (\sum a_n^2) (\sum n^2 a_n^2) .$$

The resistance factor is the product of the relief factor and the slope factor and this single quantity thus accounts for both the roughness elements. Obviously the larger the value of the resistance factor, the larger is the overall irregularity.

4.365. Cell Length (C_L)

The term cell length represents the length of a profile from any given origin which exhibits all the

existing microrelief features. The concept of the term and mathematical formulation is given below.

Consider the difference function $D(\tau)$, with expected value $R(0)$, where $R(0)$ is not equal to zero and therefore, $R(\tau)$ exists. The function $D(\tau)$ is periodic with $D(0) = D(L) = 0$. Let τ_G be the last time in the interval $0 \leq \tau \leq L$ that $D(\tau)$ attains its average value $R(0)$ after which the difference becomes smaller and finally goes to zero. At this point it may be said that all significant microrelief features have been accounted for or considered since after τ_G the difference is less than average initially and finally goes to zero. Therefore, the cell length can be defined by the distance $0 \leq x \leq \tau_G$, and is applicable to any periodic curve.

Let τ_0 be the distance required for the $D(\tau)$ to rise from zero to its average value $R(0)$ in the interval $0 \leq x \leq L$. Since $D(\tau)$ is assumed to be a periodic even function, τ_0 is also equal to the distance required for $D(\tau)$ to drop from its last average value $R(0)$ to zero. Therefore,

$$\tau_G = L - \tau_0 .$$

By definition, when $\tau = \tau_0$, $D(\tau) = R(0)$. Substituting in the above equation and solving for τ_0 ,

$$\tau_0 = \sqrt{\frac{2R(0)}{|R''(0)|}} ,$$

$$= \frac{30}{\pi} \sqrt{2} \sqrt{\frac{\sum a_n^2}{\sum n^2 a_n^2}}$$

Since $\frac{30}{\pi} \sqrt{2}$ is approximately equal to half the interval being considered, the relationship may be modified to make it applicable to any periodic function on any interval. That is,

$$\tau_0 = \frac{L}{2} \sqrt{\frac{\sum a_n^2}{\sum n^2 a_n^2}}$$

Substituting in the equation of cell length,

$$\text{Cell length } (C_L) = L \left(1 - \frac{1}{2} \sqrt{\frac{\sum a_n^2}{\sum n^2 a_n^2}} \right)$$

4.37. Summary of Roughness Components.

The mathematical relationships obtained for the roughness components are presented below. These will be used for computing roughness components of the selected profiles.

$$\text{Relief factor } (M) = \sum a_n^2$$

$$\text{Slope factor } (p) = \sum n^2 a_n^2$$

$$\text{Homogeneity factor } (K) = \frac{1}{2} \frac{\sum a_n^4}{(\sum a_n^2)^2}$$

$$\text{Resistance factor } (\rho) = \frac{1}{2} (\sum a_n^2) (\sum n^2 a_n^2)$$

$$\text{Cell length } (C_L) = L \left(1 - \frac{1}{2} \sqrt{\frac{\sum a_n^2}{\sum n^2 a_n^2}} \right)$$

5. THE STUDY AREA AND DATA ACQUISITION

5.1. THE STUDY AREA

5.1.1. Site Selection

In pursuance of the objectives of the present study an area was selected based on the following considerations.

1. Nearness of its location.
2. Representativeness of the area.
3. No outside disturbing elements.
4. Area large enough for the photographic coverage of the camera.

The area selected for the present study has been described in the following section.

5.1.2. Site Description

The site of the present study has been the runoff plots operated by the Department of Land Resources Science of the University of Guelph. These plots are located on the campus of the University and are on the north eastern slopes of a drumlin extending from the northwest to the southeast. The drumlin, a characteristic land form of southern Ontario, is composed of calcareous glacial till. During the course of time it has developed a well drained loam textured soil which has been classified by Ontario soil survey as Guelph loam (Ketcheson and Onderdonk 1973).

The climate of the area is classified as humid with

moderately cold winter and warm summer. The mean annual precipitation varies from 30-35 inches including five* to 10 inches of snowfall. The thunderstorms occurring during summer months are of high intensity. The temperature ranges from a minimum of -10° to -20° F to a maximum of 90° to 95° F.

Fig. 5.1 shows the plan of the hydrologic station including the runoff plots. There are 10 plots, each 0.05 acres in area, with a length of 145 feet and a width of 15 feet. The land slope on the average ranges from seven to nine percent. The spaces between the runoff plots are utilized for non-experimental cropping. These were available for the present investigation. During the year of the reported study, the runoff plots were under maize crop having different treatments.

The spaces between the plots shown as Block I, II, and III in Fig 5.1 were selected for the study. The tillage operations consisted of mould board plowing in fall and a disc harrowing in spring followed by smoothing of the surface with a spike tooth harrow. These are the standard tillage operations required for planting of corn in this area. The plots selected for this study were kept bare throughout the period of investigation. The sporadic growth of weeds was controlled by the application of herbicide. Dead plants were removed from the plots to avoid any possible obstruction to overland flow.

* snowfall is expressed as water equivalent

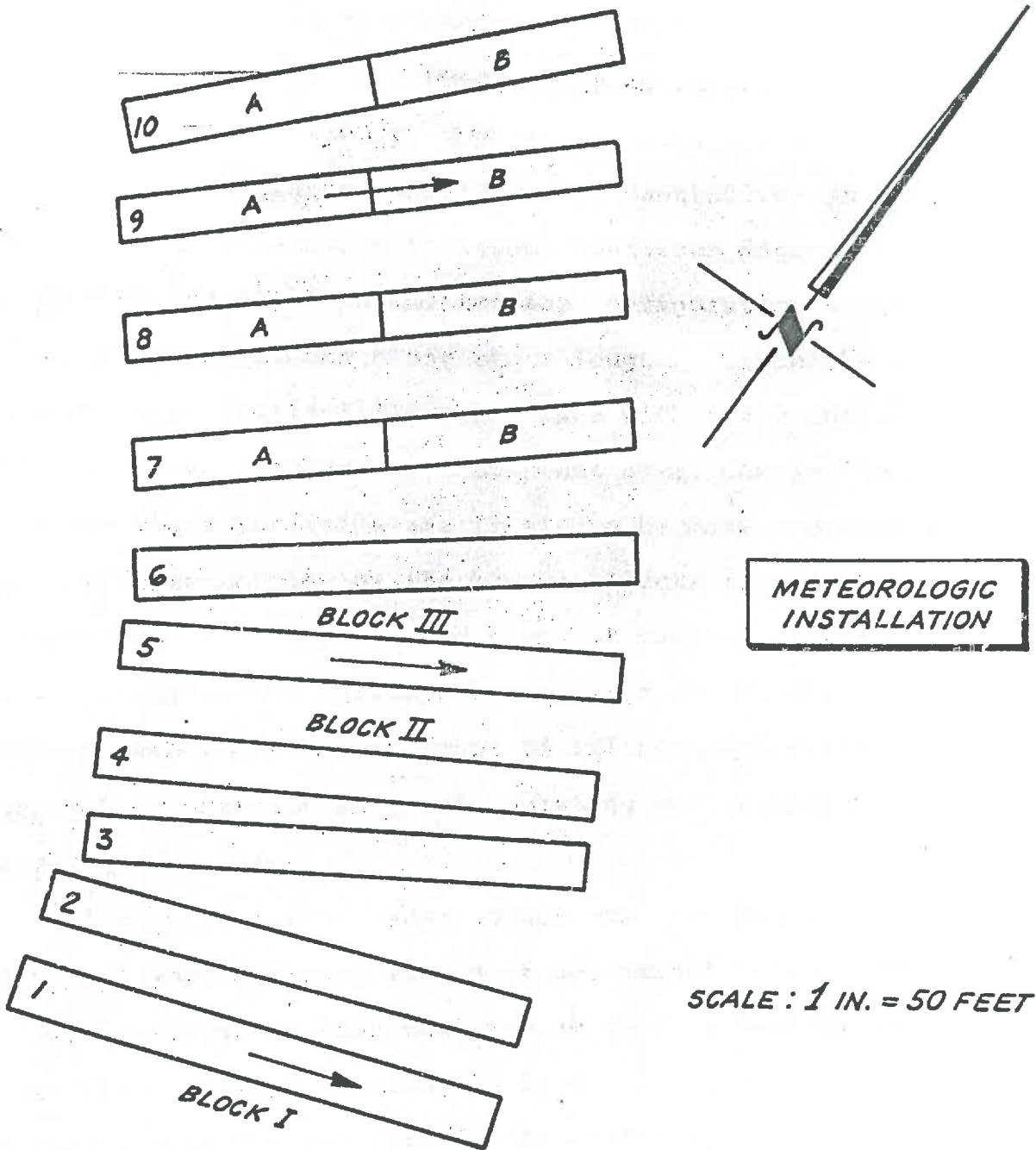


FIG. 5.1 - HYDROLOGIC STATION
UNIVERSITY OF GUELPH
ONTARIO, CANADA

5.13. Sample Plots

Three blocks having comparable slopes were selected with a view to study the homogeneity of the surface configuration in relation to depression storage and roughness and to draw inferences about the representativeness of the data. It is reasonable to assume that some degree of variability exists in slope and surface configuration even in the individual blocks along their length. Since the duration and depth of overland flow increases with every increment in length due to increase in catchment area, changes in surface characteristics are likely to be more pronounced in the lower portion of the blocks. Blocks II and III lie between the runoff plots and have got varying widths along their length. The narrower sections of the blocks imposed some restraint on the movement of tillage implements which might have contributed to the existing variability of the surface properties.

The stereometric camera which was used had a specific coverage when operated from a predetermined height. The camera coverage in this case was about five feet by seven feet from a height of about 10 feet. The limited coverage of the camera did not justify the photographing of the entire length of blocks because of time, labour and cost. The only choice left was to sample the block in such a way as to account for any such variabilities in the surface configuration.

Five sample plots of about seven feet by seven feet size were selected in each block. The first sample plot was located at a distance between 10 feet and 15 feet from the upper boundary of the block. Similarly the fifth sample plot was located above the lower boundary of the block. The sample plots 2, 3 and 4 were located approximately at equal distances between the sample plots 1 and 5. The size of the sample plots was selected on the basis of the expected coverage of the camera from a height of 10 feet. The height of 10 feet was considered adequate in terms of the expected coverage, scale of the photograph and operational efficiency. The number of sample plots and their spatial distribution were considered adequate to represent the block. The number of sample plots though small could be subjected to statistical analysis. The lay out of sample plots is shown in Fig. 5.2.

5.2. DATA ACQUISITION

5.2.1. Sample Plot Lay Out

The lay out and demarcation of sample plots was considered necessary in order to know the exact location required for proper orientation of the camera while taking the initial and also subsequent photographs. A clearly marked boundary of sample plots was also necessary to avoid any possible accidental disturbance to the surface. This was accomplished with the help of a string. The centre

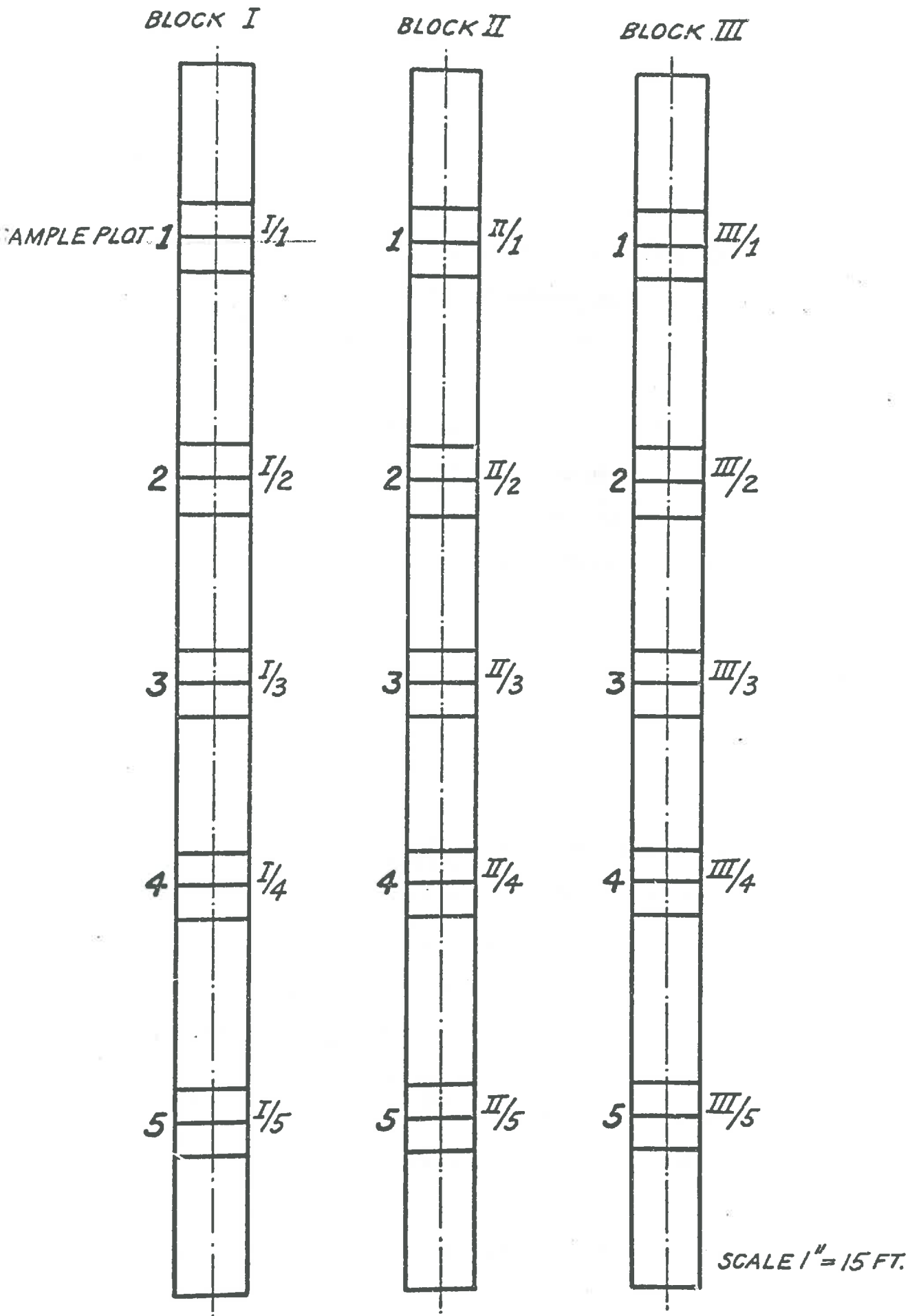


FIG. 5.2 - LAYOUT OF SAMPLE PLOTS

line of each block was demarcated with a tightly stretched string running along the length and securely tied at both ends. The boundary of the block was similarly marked by two parallel running strings approximately seven feet apart. The location of the centre of the sample plot was marked with two iron pins fixed in the ground at the boundary lines.

The sample plots were numbered as 1, 2, 3, 4 and 5, starting from the top of the block, for proper recording and identification of data to be subsequently collected. These were identified by block number and plot number as shown in Fig. 5.2.

5.22. Ground Control Points

Ground control points are required to establish the position and orientation of each photograph in space in relation to the ground or any other reference system. These control points are identified on the photograph and subsequently used in compilation of the topographic maps. The position of a ground control point is established by its horizontal position with respect to a horizontal datum or by its elevation with respect to any vertical datum or both.

The ground control points in this study consisted of a network of nine target pins located as shown in Fig. 5.3 (a,b) to cover the expected coverage of the camera. The target pins were 25 centimeters long and made of about 1

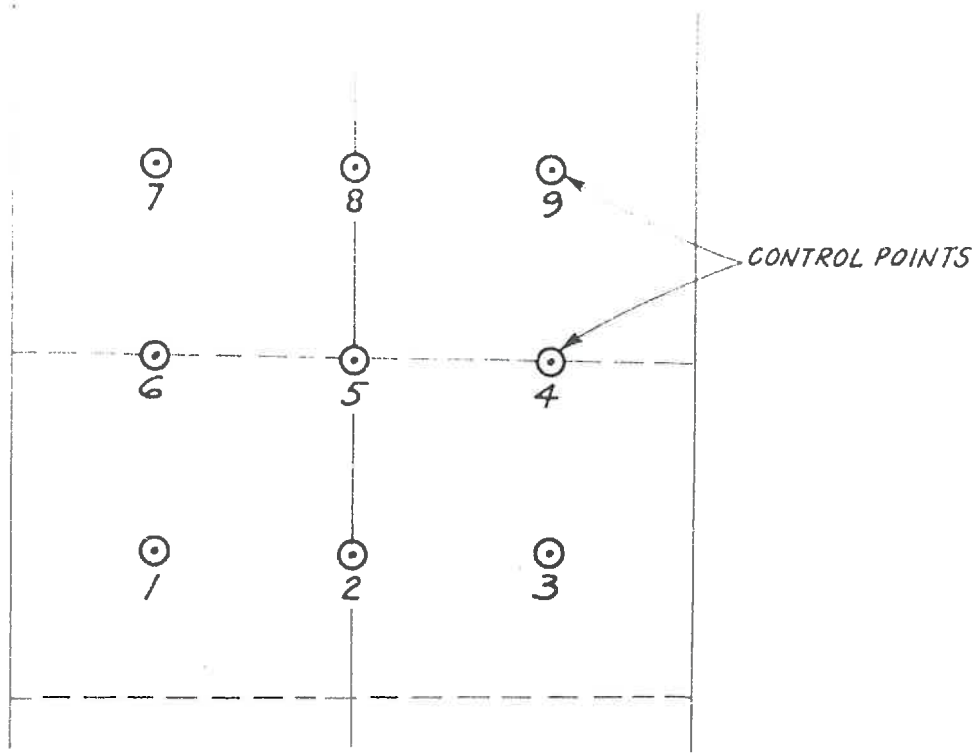


FIG. 5.3(a) - LOCATION OF CONTROL POINTS IN THE SAMPLE PLOT

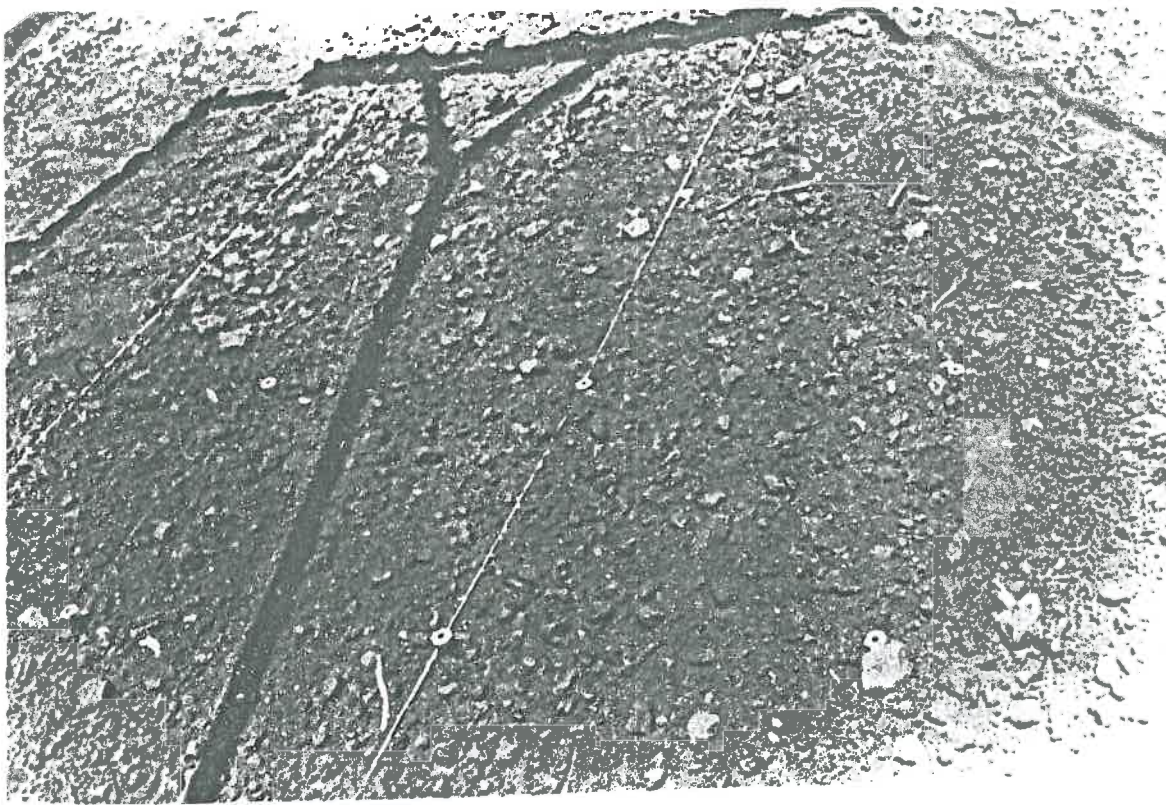


FIG. 5.3(b) - PHOTOGRAPH OF SAMPLE PLOT SHOWING LOCATION OF CONTROL POINTS.

centimeter diameter iron rod. The pins were provided with a 2.5 centimeters flat circular head. The top of each pin was painted white with a 0.50 centimeter diameter black circle in the centre to provide a sharp and well defined image in the photograph. The target pins were positioned and fixed in the ground with the help of a 4 feet by 4.5 feet rectangular iron rod frame to ensure that all the points were within the stereoscopic coverage of the camera. The pins projected up from the ground and their elevations with respect to the ground surface had random variations. The number of control points was considered adequate for accurate mapping since only four photo control points were required in the overlapped area to compute the elements of exterior orientation of each pair of overlapping photographs (Moffitt 1967).

5.23. Camera and Auxiliary Equipment

The major requirement of the stereophotogrammetric method is that the areas to be mapped have complete stereoscopic coverage of such configuration that the required accuracy can be obtained. In order to obtain stereo pairs, two cameras are required where quasistatic or dynamic photography is to be used. Furthermore the successive pairs of photographs must be exposed simultaneously to ensure the reliability of measurements on the photographs. Brief details of the camera and other auxiliary equipment used in this study are given in the following sections.

5.231. Camera

The Wild stereometric camera was obtained from the National Research Council, Ottawa. This camera, developed for the specific purpose of close range photography, was used in this investigation along with a specially designed tripod for mounting the camera and shutter release mechanism. The stereometric camera, shown in Fig. 5.4, consists of two cameras fixed at both ends of a base tube 120 centimeters long with parallel optical axes and coplanar focal planes (Zeller 1952). The base tube sits on a tripod and is locked in place with a clamp which when loosened permits the rotation of the base tube in any desired direction, the camera axes still remaining normal to it. A spring bolt above the base tube allows a fixed amount of tilt to be given to the base tube and hence the camera.

Each camera is provided with a view finder to adjust the orientation of the camera in relation to the object. The controls for the diaphragms and the shutters are at the centre of the base tube facing the operator. The left hand control is for adjusting the exposure timing which ranges from B to 1/250 seconds. The settings for the aperture opening are 12, 18, 24 and 36 and are set by the right hand control. The control in the middle is for winding the shutters. When the control is turned to wind the shutters a white dot appears on the control knob which disappears after the shutters are released.



FIG. 5.4 - WILD STEREO METRIC CAMERA

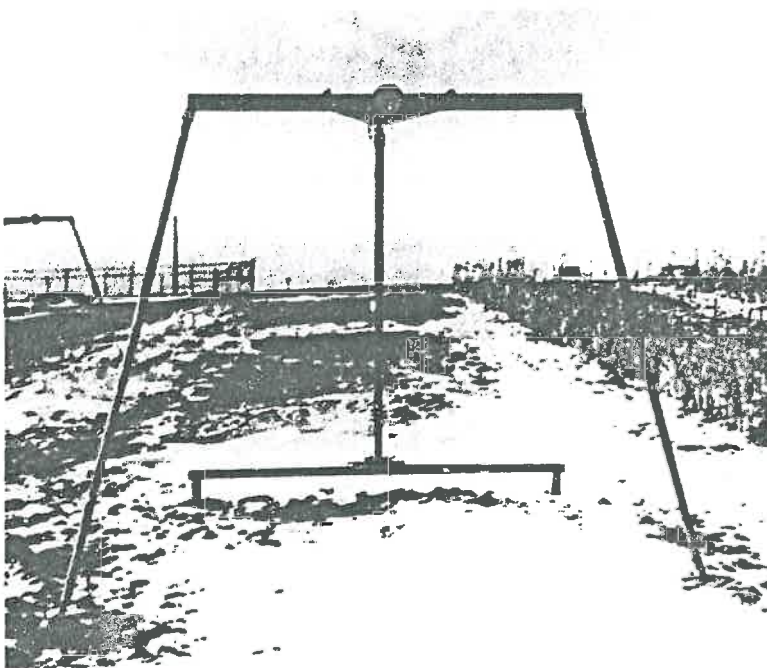


*FIG. 5.5 - TRIPOD OF THE STEREO METRIC CAMERA
FOR VERTICAL PHOTOGRAPHY.*

The base tube can be raised to about eight feet from the ground with the help of a crank which when turned raises a vertical tube which supports the base tube. The vertical setting of the camera is checked by means of a circular level bubble fitted to it.

The stereometric camera was calibrated by the National Research Council of Canada in 1954 and the calibrated principal distances of the left and right camera was reported to be 91.77 millimeters and 91.84 millimeters respectively (Wijk in personal communication 1972). The camera was again calibrated for the present study. For this purpose a set of two photographs were taken from a height of approximately 10 feet with 20 ground control points consisting of pins fixed on the ground at various heights in the overlapped area. The measurements made on a stereocomparator were used for the calibration of the camera by the method proposed by Harley (1966) (Natarajan 1972). The principal distances of the left and the right camera were found to be 91.91 millimeters and 91.97 millimeters respectively. The mean value of 91.94 was subsequently used in the computer program for establishing photo coordinates of the measured points. The lenses of the camera remain fixed with respect to the focal plane which ensures absolute maintenance of interior orientation.

The plates of size 65 millimeters by 90 millimeters are pressed on to the focal plane frame by springs in the

sides of each camera. The shutters are released with the help of a wire release which can be temporarily fixed in a socket on the base tube. There are two fiducial marks in both the right and the left focal planes of the camera. These are used to determine the principal points of the photographs.

5.232. Tripod

The tripod provided with the camera was designed for taking photographs in horizontal or slightly tilted positions and therefore was not suitable for the present study where the ground surface was to be photographed. A tripod, shown in Fig. 5.5, was fabricated to mount the base tube in such a way that the lens axes were vertical in order to photograph the surface from a height of 10 feet. The considerations in the design of the tripod were mechanical stability, convenience in operation, least amount of shadow on the surface to be photographed, and no disturbance to the surface of sample plots while operating the camera.

The tripod consisted of a triangular shaped iron frame with a clamp at the centre of the base of the triangular frame to rigidly hold the base tube of the camera in such a way that when the frame was horizontal the camera faced vertically downward. Both ends of the base of the frame holding the camera were welded at a

suitable angle to two adjustable telescopic legs made of iron pipe. The third end of the frame was securely bolted to a similar type of leg in such a way as to allow to-and-fro movement to help in positioning and leveling the camera. The concentric pipes forming the legs were provided with holes at a six inches interval for part of the length to enable the tripod to be raised to the desired height. The finer adjustment of the height while leveling the camera could be done with the help of a leveling screw threaded to the bottom of each leg. The leveling screws of the front two legs rested on the iron plates at the ground surface outside the sample plot. The leveling screw of the rear leg rested on a similar plate bolted to a seven feet long raised iron platform provided to avoid disturbance to the surface of the plot.

The shutter release wire for the camera was clamped on one side of the triangular frame and provided with a simple mechanism which could release the shutters when a string was pulled from the ground.

5.233. Photographic Plates

In selecting a photo sensitive material for use in photographic mapping it is desirable to choose an emulsion with highest resolution consistent with the camera aperture and the shutter speed. Since in close range photography both the terrain and the camera remain

fixed it is possible to employ a slow shutter speed and consequently high resolution emulsion. The stereometric camera used in this study was equipped with camera backs which received plate holders containing the glass plates. The glass plates are in fact more suited to ensure planarity of the image at the instant of the exposure and to preclude distortion due to possible film buckling in the focal plane.

Kodak metallographic plates of four inches by five inches were cut to 64 centimeters by 9 centimeters to be used with the camera. Sensitometric tests for average gradient of 0.6 to 0.65 indicated that a meter setting of 50 ASA would produce satisfactory exposure with a Kodak neutral gray test card. The average gradient is the slope of the line joining the toe contrast point and the upper scale contrast point on a characteristic curve known as $D - \log E$ curve. The characteristic curve is obtained by plotting density on Y axis and logarithm of the exposure on X axis. The toe contrast point was located at 0.10 density unit above the base plus fog density of an unexposed processed area of the glass plate. The upper scale contrast point was obtained by intersecting the characteristic curve with an arc having a radius of 1.5 log exposure unit with the centre at the toe contrast point.

5.24. Field Work

5.241. Positioning of Control Points.

The control points were numbered from 1 to 9 as shown in Fig. 5.3a. The same sequence of numbering was followed in all photographs. The elevations of the control points were measured with respect to a bench mark having an assumed elevation with a dumpy level. The bench mark was located at the side wall of the drop box of the H-type flume installed in runoff plot 1. The horizontal distance between the control points was carefully measured with a steel tape. These measurements were taken before photographing the surface and recorded on the data sheet separately provided for each sample plot. The elevations and horizontal distances were subsequently used to determine the X, Y, and Z values of each control point with respect to an arbitrarily selected coordinate system. The accuracy of horizontal and vertical measurements was estimated as 0.05 centimeters which is considered reasonable for a reliable mapping.

5.242. Camera Setting

The camera was securely clamped on the tripod and the shutter release wire fixed in place. The tripod was then lifted from the ground by four persons, carried to the sample plot to be photographed and installed there

keeping the front two legs away from the plot. After inserting the glass plates in the camera, aperture opening and exposure times were set with the help of an exposuremeter. The shutter was then cocked. The numbers on the plate holders were recorded on the respective data sheet for the identification of right and left plates. The camera on the right hand side of the observer facing up the slope was referred to as right camera and that on the left hand side as left camera. The corresponding plates were labelled as right and left plates.

The legs were then raised to a predetermined point which corresponded to a camera height of about 10 feet from the ground surface. The external orientation of the camera in relation to the plot boundary and the ground control points was checked and legs adjusted so that the camera was approximately above the centre of the plot. This operation was facilitated by the use of three plumb bobs hanging from the frame below the camera in such a way that when the camera was properly oriented these were just above the control points number 4, 5, and 6. The frame holding the camera was then levelled with the help of levelling screws and checked with a spirit level on a frame hanging from the sides of the triangular frame. Fig. 5.6 shows the setting of the camera over a sample plot.

After the horizontal and vertical orientation of the

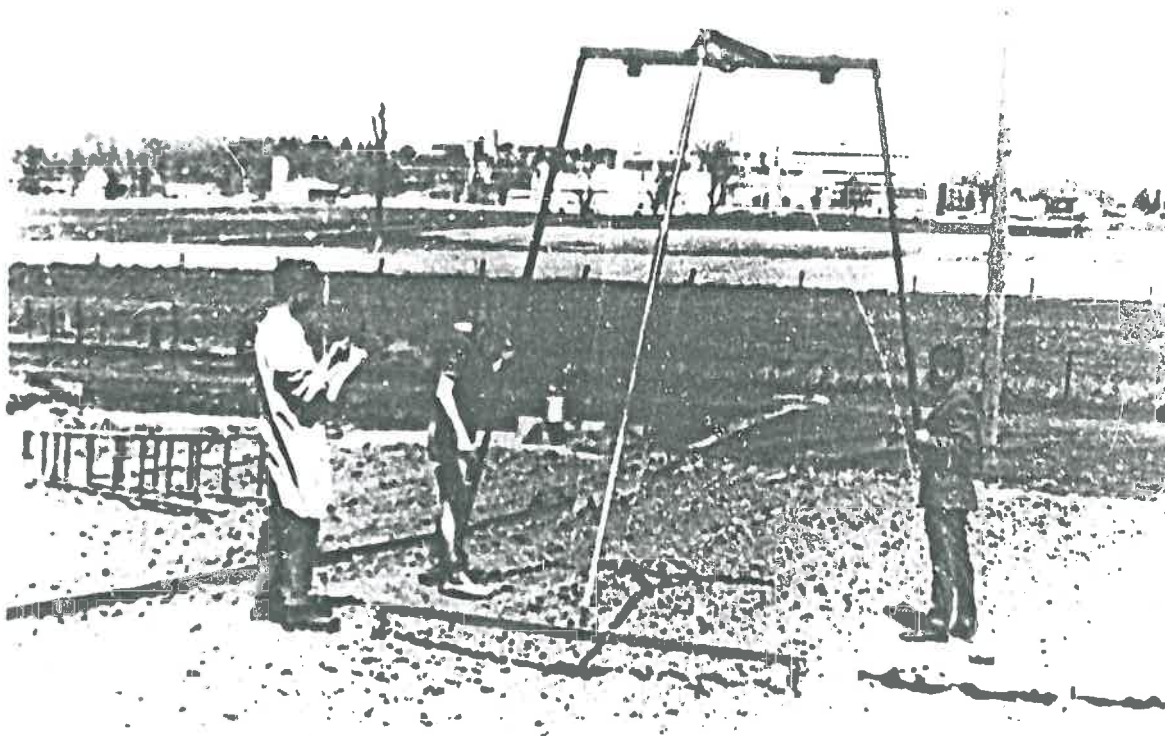


FIG. 5.6 - SETTING OF THE CAMERA OVER A SAMPLE PLOT.

camera were completed the camera was ready for making exposure. To expose the plates in the camera a string was carefully pulled from one side of the plot to actuate the shutter release wire without shaking the camera.

After taking the photograph the camera was lowered and the glass plates taken out from the camera and kept in a box. The numbers on the plates were rechecked with the record on the data sheet. The tripod was then lifted and moved to the next sample plot. The same operations were repeated until all the plots were photographed.

The system worked satisfactorily except that it was heavy and required four persons to operate. The time taken for one setting of the camera ranged from 20 minutes to 30 minutes.

5.25 Sequence of Observations

The first 15 sets of photographs were taken in the month of May, 1972 immediately after the completion of tillage operations required for planting of corn. Plots 2 and 4 in each block were subsequently photographed in the months of July and October, 1972 to study the effect of season on the surface properties. In all, 27 sets of photographs were taken.

5.26. Developing Glass Plates

The glass plates were developed in the air-photo laboratory of the School of Engineering of the University of Guelph. The procedure used was as follows:

The exposed plates were taped to the bottom of a developing tray 11 inches by 14 inches in size. Two litres of Kodak developer D.K. 50 with 1 : 1 dilution ratio at 70 degrees F. was added in the tray. The developing time was five minutes with ASA tray agitation. The plates were then fixed in Kodak fixer for a duration of five minutes to 10 minutes and washed for about 30 minutes, and rinsed with water treated with a wetting agent to promote even drying. The plates were then placed on edge at room temperature to dry.

The negatives on the glass plates thus obtained were satisfactory in their optical qualities. The control points had well defined and sharp images. These plates were measured on a stereocomparator for producing digital surface models. The method adapted for the purpose has been described in Chapter 6.

6. DEVELOPMENT AND ANALYSIS OF DIGITAL SURFACE MODEL

6.1. GENERAL

Before discussing the methods used in developing a digital surface model it is appropriate to present a formal definition of this term and briefly mention its scope and limitations.

A digital topographic surface model consists of a collection of points of known coordinates (X, Y, Z) selected to closely represent the surface configuration and stored in the computer memory or compiled in a form amenable to subsequent analysis by the computer when needed. In other words it is a numerical representation of the surface it represents. The suitability or appropriateness of any such model depends on how closely it represents the configuration of the surface which are of interest to an investigator. For a close representation it is essential that the spacing of the data points constituting the digital surface model should be compatible with the size of the surface features of interest. Therefore, the scale of the topographic variations, relevant to any specific problem, will dictate the spacing of points constituting the model.

A digital surface model is assumed to adequately portray the surface configuration and, therefore, is capable of providing any required quantitative information about the surface. In fact it is the only information that is available about the surface. And so any information about

the surface features derived or extracted from the model is considered to closely represent the actual. Anything that is more accurate than the model is the surface itself. This is not true in the analytical surface models. Analytical techniques of surface fitting such as polynomial functions, least squares, and double Fourier series do not provide any additional information to what is available in the digital surface model. Since these techniques basically use the information about the surface as contained in the digital surface model the analytically fitted surface expressed as mathematical functions can not be as close to the actual surface as the basic data itself.

The above assumption that a good digital surface model closely represents a surface and is capable of providing information about the surface features is not unrealistic. The appropriateness of a model has to be ascertained in terms of the scale of the surface features of interest and spacing of the data points of the model. This is not an adverse reflection or a limitation of the digital surface model since it is a fundamental requirement of any mapping system.

In the present study where small microtopographic variations on the surface were of interest in determining surface storage and roughness elements a spacing of 2.5 centimeters was considered adequate to provide a good digital surface model.

The methods used in developing a digital surface model and in analysing it to determine the storage and roughness properties of a surface are mentioned in the following sections.

6.2. DEVELOPMENT OF DIGITAL SURFACE MODEL

6.2.1. Sample Plot Index

The photo plates obtained for each sample plot were represented by arbitrarily assigned model numbers for identification and subsequent reference. Table 6.1 gives the model number assigned to each sample plot along with the plot number and block number. The symbols used for the sampling plots are also shown.

Table 6.1. Model Numbers of Sample Plots

Block No.	Plot No.	Months					
		May, '72		July, '72		October, '72	
		Model No.	Symbol	Model No.	Symbol	Model No.	Symbol
I	1	01-02	I/1	-	-	-	-
	2	03-04	I/2	31-32	I/2 (1)	49-50	I/2 (2)
	3	05-06	I/3	-	-	-	-
	4	07-08	I/4	41-42	I/4 (1)	45-46	I/4 (2)
	5	09-10	I/5				
II	1	11-12	II/1	-	-	-	-
	2	13-14	II/2	33-34	II/2 (1)	47-48	II/2 (2)
	3	15-16	II/3				
	4	17-18	II/4	35-36	II/4 (1)	43-44	II/4 (2)
	5	19-20	II/5	-	-	-	-
III	1	21-22	III/1	-	-	-	-
	2	23-24	III/2	37-38	III/2 (1)	51-52	III/2 (2)
	3	25-26	III/3				
	4	27-28	III/4	39-40	III/4 (1)	53-54	III/4 (2)
	5	29-30	III/5	-	-	-	-

6.22. Coding of Photo Plates

For systematic measurements of the photo plates it was necessary to recognize the types of points to be measured and code them with numerical numbers for identification and reference. Coding of points also facilitates rapid

measurements and compilation of the digitized data. The coding system followed in this study is similar to that adopted by other investigators (Natarajan 1969 and Van der Vliet 1969) using the same stereocomparator. There were three types of points measured on the photographs; fiducial points, ground control points and other points on the surface.

Each of the points was numerically represented by eight digit numbers for complete identification in relation to model number, type of point and serial number. The first four numbers from the left represent model number assigned to the photographic plates of each plot as presented in Table 6.1. The left plate of a stereo pair was assigned two digit odd numbers beginning from 01 and right plate was given even numbers beginning from 02. The first model for example, consisting of plates 01 and 02 was represented by 0102, the next by 0304 and so on up to 5354 which represented the last set of the photographs measured in this study.

Following the model number was a code number assigned to the following types of points measured on the photographs.

- 0 indicates fiducial point
- 1 indicates ground control point
- and
- 2 indicates other points on the ground surface

The last three numbers indicated the serial number of the

points. The following are the examples of the coding system.

1300	0	001	First fiducial point on the left plate number 13.
1314	1	007	Ground control point number 7 on model number 1314 consisting of left plate number 13 and right plate number 14.
1314	2	156	Point number 156 on the ground surface in model number 1314.

6.23. Measurement on the Stereocomparator

The photo plates were measured on a Wild S.T.K. 1 stereocomparator in the photogrammetric laboratory of the University of Toronto. The comparator is accompanied by a number panel machine, typewriter and a punch card machine. The measuring precision of the comparator is 1 micron. The standard of accuracy followed was that the difference in two or more readings of the same point should not exceed 3 microns. The procedure followed in the measurement is outlined below.

The glass plates with their emulsion side down were carefully placed on the respective picture carriers and fixed in place with the help of tape applied on the edges to avoid covering of the overlapped area. The plate carriers were then adjusted to obtain proper alignment and complete stereoscopic coverage. The floating mark's magnification selected was 11 which gave satisfactory result for pointing. The number panel machine was set according to the specified design of the numerical coding

of the points and all the switches were turned on.

The fiducial marks were measured first with monocular observation. By fixing the positions of X parallax wheel (P_x) and Y parallax wheel (P_y) for the dials to read 1000.00 it facilitated quick viewing from the left plate to the right plate and vice versa while measuring the fiducial points. For measuring fiducial points with mono setting the floating mark was fixed exactly centering the fiducial point by moving the X and Y wheels. When the floating mark was properly set the switch on the number panel machine or on the stereocomparator was pressed to get all measurements (X , Y , P_x , and P_y) typed and punched on a card.

After completing the measurements of the fiducial points the ground control points were measured in a proper order i.e., 1, 2, 3, --- 9 with stereo vision. The procedure followed in stereoscopic measurement was as follows. The left floating mark was fixed on the point of measurement with the help of X and Y wheels while sighting with only the left eye. Then the right floating mark was brought to the same point by adjusting P_x and P_y wheels while sighting with only the right eye. The same point was then viewed with both eyes to check the fusion of both the floating marks which indicated correct placing of the floating mark in three dimensions. In case of any error X , Y , P_x and P_y wheels were adjusted to get a good pointing.

After completion of the target points all other points selected on the ground surface while viewing the model were measured stereoscopically. The measurement was started from the top of the left hand side of the overlapped area moving in X direction keeping Y axis fixed. All those points were measured where significant change in slope was observed. The measurement was continued up to the end of the right hand side of the overlapped area. The Y axis was changed to a new position and the measurement continued from right to left. The procedure was repeated till the entire overlapped area was covered. The measurements were taken at a distance of about 3 to 5 cm. depending upon the irregularity of the surface. Comments if any about poor image in some part of a model, absence of any ground control point were recorded manually on the typed data sheet coming out of the typewriter. In all, 27 sets of photographs were measured on the stereocomparator. The number of points measured on each model ranged from 500 to 650 depending upon the extent of the overlapped area and the surface configuration. The size of the overlapped area ranged from about 2400 sq. cm. to 3000 sq. cm. The overlapped area is shown in Fig. 6.1(a,b).

6.24. Data Processing

6.241. General

The data obtained from the stereocomparator were

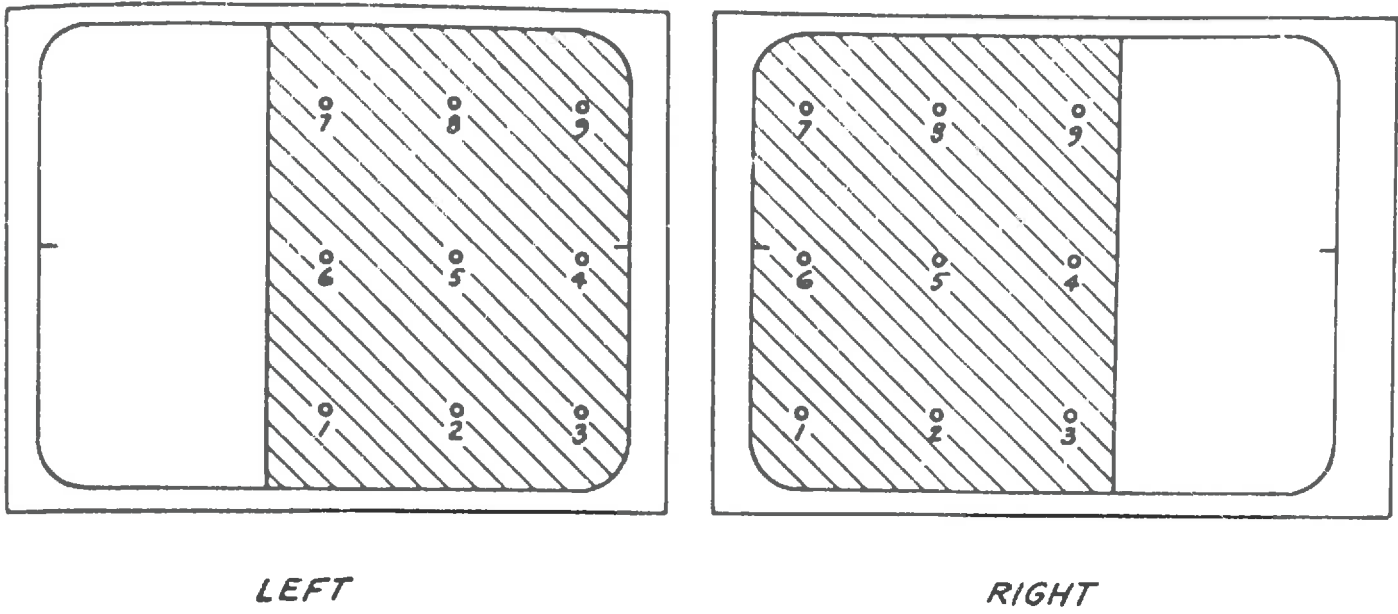


FIG. 6.1(a) - PLATES AS FIXED IN COMPARATOR SHOWING OVERLAPPED AREA

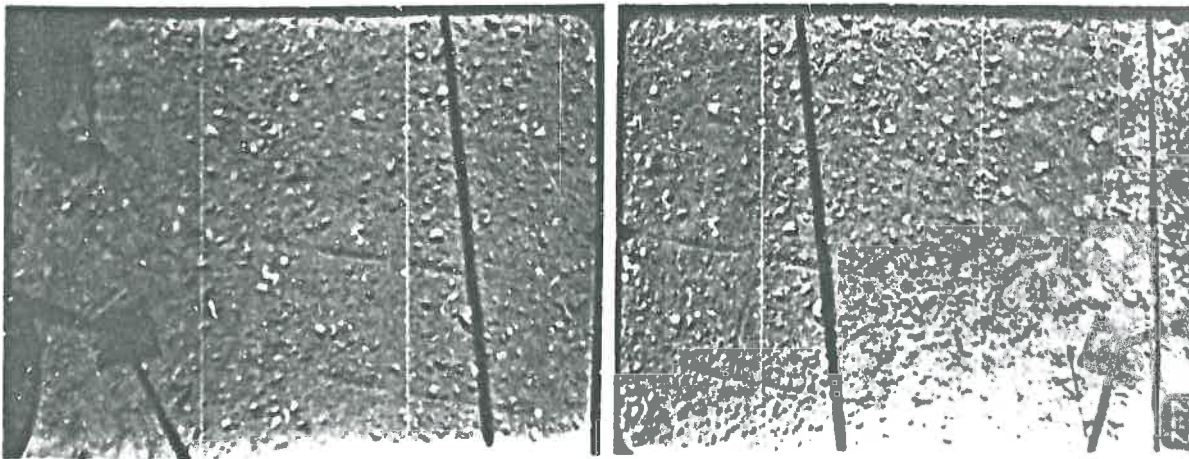


FIG. 6.1(b) CONTACT PRINT OF A SET OF GLASS PLATES

processed by using the available computer programs to obtain the ground co-ordinates of all the measured points on the photographs in order to produce the digital surface model. Computer processing of data involved four stages. The first program edited the data from the comparator and gave an output which was used as an input to the second program. The second and third programs developed by Dr. Schut (1966, 1966) of the National Research Council, Ottawa, have been successfully used at the University of Toronto (Natarajan 1969, 1972). The second program gives the photo coordinates of the measured points with reference to an arbitrarily selected origin and the third program converts the photo coordinates of the measured points to ground coordinates with the help of the known values of the coordinates of the ground control points. The fourth program obtained from the Institute of Computer Science of the University of Guelph was used to generate 2.5 cm. grid data by utilizing the output of the third program and to produce the digital surface model for all the plots photographed in this study. The details of the computer program including their functions are briefly mentioned below.

6.242. Data Preparation

The existing program compiled at the University of Toronto was used to edit the cards obtained from the stereo-

comparator to detect and eliminate any serious mistake introduced during measurements. It also calculated the arithmetic averages of coordinates of all measured points and their standard deviations. Also for each plate it calculated the coordinates of the principal points and the coordinates of points X' , Y' , X'' , and Y'' with respect to the instrument origin in the left and the right plates using the comparator coordinates X' , Y' , P_x and P_y . The computer program used for data preparation is shown in Appendix B.

After checking and correction of the mistakes the relevant control card was changed and the program rerun to get the punched output for use with the second program.

6.243. Strip Triangulation

The output of the data preparation program is used as input to Schut's "Analytical Strip Triangulation Program" published by the National Research Council of Canada (Schut 1966). The output of the program gives the strip coordinates X , Y and Z of all measured points and the want of intersection figure at each point. The same card also contains the strip and model number. The want of intersection figure is a useful indication for the internal precision of each model. A smaller figure exceeding a predetermined value were not included in the adjustment of the strip. A value of 25 micron was considered satisfactory in such measurements. The computer program

is shown in Appendix B.

6.244. Strip and Block Adjustment

The output of the Strip Triangulation program is used as input to Schut's "Polynomial Adjustment of Strips and Blocks" published by the National Research Council of Canada (Schut 1966). The computer program shown in Appendix B uses measured coordinates of ground control points. This program converts the photo coordinates of the measured points obtained as output of program 2 to ground coordinates X, Y and Z by using the known coordinates of the ground control points. Any mistake in the ground control values will show up in large residual errors which need to be checked and rectified. In the case of a residual exceeding 1 cm. the ground control point was rejected. In most cases the residual values were very small indicating satisfactory adjustment. The output consisted of irregularly spaced points with known coordinates spread over the sample plot.

6.245. Uniform Grid Data

The output from the strip and block adjustment program consisting of a set of scattered data points was used as input to a Fortran program compiled by the Institute of Computer Science of the University of Guelph to generate uniform (2.5 cm. x 2.5 cm.) grid data. The algorithm used is heuristic and the method used is as follows.

The area surrounding each grid intersection is divided into octants. The closest data point in each octant is selected and the value of the intersection is set equal to the average of the selected data points weighted by $1.0/d^2$ where d is the distance from the data point to the grid intersection being evaluated. If more than four octants do not contain data points the grid intersection value is not evaluated; but is set to a large negative $-0.1000E\ 32$ which helps in identifying an undefined area.

In the process of generating the grid data there is certain amount of smoothing of the maxima and minima points on the surface. Since the size of the grid is small, the amount of smoothing is considered to be too small to introduce any significant error in the estimates of depression storage and roughness components.

Based on the above method the computer program calculated the elevation data for all grid points spaced 2.5 centimeters apart in both the X and the Y direction. The grid was superimposed on the area represented by the scattered data points. The undefined points were provided with a large negative number. All the 27 sets of data were run with this program to obtain the grid data. The output of the program consisted of elevation data of grid points punched on cards.

The grid data on punched card constituted a digital surface model which was assumed to closely represent the surface. These models were subsequently analysed to obtain

information on the geometric properties of depressions and surface roughness.

6.246. Accuracy

The accuracy of digital surface models obtained by photogrammetric technique depends on the precision of the stereocomparator, accuracy of pointing, and the accuracy of measurements of the ground control points. The stereocomparator used in the present investigation is a precise instrument with an accuracy of one micron. The pointing precision was estimated to be ± 3 microns for the single pointings. The estimated error of measurements of the ground control points was of the order of ± 0.05 inches which is larger than the pointing error. It is evident from the above that the accuracy of measurements of the ground control points determines the overall accuracy of a digital surface model. According to Moffitt (1967) the accuracy of ground measurements required to establish the positions of the control points determines the accuracy of the final results since the photogrammetric measurements are generally considered more accurate. This is true for large photographic scale as the one used in the present study. The accuracy of ± 0.05 inches is considered reasonable for such investigations. The accuracy of the specially designed point gauges is also of the same order.

6.3. ANALYSIS OF DIGITAL SURFACE MODEL

6.31. Geometric Properties of Depressions

The computer program developed and described in Chapter 4 was used to analyse each digital surface model to obtain information on the geometric properties of depressions existing on the respective sample plots. The input to the program consisted of digital surface model with elevation data arranged by rows on the input cards.

The program consisted of a self contained set of Fortran routines run under O.S. Fortran. Two parameter cards were required to run the program. The first card contained grid dimensions and the other card had variable format specification. This specification gave the format of the input data. The computer program is given in Appendix B to provide further information about its operation.

All the 27 digital surface models were run to obtain the required information on the geometric properties of depressions. The time taken by the computer to analyse each set of data ranged from about 20 seconds to less than 30 seconds depending upon the number of data points and number of both simple and complex depressions. A sample output of the computer program is shown in Appendix B.

6.32. Computation of Roughness Components

Profiles along the direction of the Y axis running along the slope of the sample plot were considered for

computation of roughness components. This choice was dictated by the fact that since the roughness characteristics of a surface control overland flow, the direction of movement of water was of primary importance in an analysis of surface roughness. The direction of profiles may not be so important in the case of depression storage where any direction could be used.

The length of profiles ranged from about 175 centimeters to about 200 centimeters depending upon the grid dimensions of the model and the number of undefined points along any profile. A length of 180 centimeters containing 73 data points was considered for computing roughness components. The first step for any computer program was to ascertain the suitability of any profile in terms of its length since the profiles with inadequate length were not to be included in the analysis. In the case of profiles having required length the portion of it in excess of 180 centimeters was ignored. The roughness components were then computed using a computer program based on the method described below.

The Harman subroutine available in the Institute of Computer Science of the University of Guelph was modified to develop a computer program for computing the coefficients a_n with a set of points $Y(I)$, $I = 1, 2, \dots, k$, corresponding to a set x_i , $i = 1, 2, \dots, k$ of equally spaced arguments. The calculation of the coefficients is based on the relation-

ship shown in the equation given below.

$$a_n = \frac{2}{k} \sum_{I=1}^k Y(I) \cos \frac{2\pi}{k} n(I-1)$$

$$n = 1, 2, \dots, M, \text{ and}$$

$$I = 1, 2, \dots, k.$$

where M is the number of harmonics to be computed which was 12 in this study and k was equal to 13 equivalent to 30 centimeters length of a profile. The computed values of a_n were then used to compute the coefficients a_g for the entire length of the profile using the relationship given in Chapter 4. These coefficients were used to compute the required roughness components of the individual profile.

It may be mentioned that the numerically obtained coefficients were not true Fourier coefficients because of the expected discrepancies in the description of the function $y(x)$ by a set of discrete points. But since the purpose of computing the coefficients was to get a few parameters for subsequent comparison with similarly computed parameters, and not a mathematical fitting of the curve, any such discrepancy will not in any way adversely affect the results.

The computer program was designed to make use of the digital surface model as input data to ascertain the suitability of a profile in terms of the required number of

points and then to compute the roughness components. The profiles with inadequate length were skipped. The output of the program consisted of the data read, a_n , a_s , roughness components of each profile and mean values of roughness coefficients for the plot along with the standard deviation. The number of profiles analysed and the number of profiles skipped for want of adequate length were also given in the output. The program was designed to analyse any selected profile or profiles.

The roughness components of any profile represented the degree of roughness of the sample plot along that profile. In order to get roughness coefficients of a sample plot an arithmetic average of the roughness coefficient values of all the measured profiles (about 60 in this study) was considered as a fairly reasonable estimate since the profiles were spaced only 2.5 centimeters apart. The results of a preliminary analysis indicated that the mean value of roughness coefficients based on every third profile was within five percent of the mean value of all the measured profiles. It was therefore decided to use every third profile for computing the values of roughness coefficients of sample plots. The number of such profiles ranged from 18 to 21. On a relatively less variable surface it is expected that a much smaller number of profiles will need to be analysed to obtain a representative value for a sample plot or an area.

All the 27 sets of digital surface models were analysed using the above computer program to obtain the mean values of roughness components of the respective sample plots. The standard deviations of the roughness components were also computed to get an idea about the variability of roughness within the plot. The results of the analysis are presented in the next chapter.

7. ANALYSIS OF DATA AND DISCUSSION OF RESULTS

7.1. GENERAL

The analysis has been separated into two sections: one dealing with the geometric properties of depressions, and the other with surface roughness. Each section contains data, analyses of data, results, and a discussion of the results for each analysis. Applications of the results are presented separately at the end of the chapter. In view of the varied nature of the analysis, the sequence of the presentation of the results is briefly outlined below.

The section regarding geometric properties of depressions starts with an examination of the total number of depressions on the sample plots and the nature of their spatial distribution. This is followed by the results of a test of homogeneity of the sample plots in relation to the total volume of storage, required to establish the representativeness of the plots. The total volume of depression storage is then considered in relation to the average slope of the sample plots. The three geometric properties, i.e., volume, depth and surface area, which characterize a depression, have been found to be correlated and the functional relationships existing between them are presented. This is followed by an examination of the observed frequency distributions of these properties. The results of verification of a hypothesis that the observed distributions can be approximated by some known probability distribution models are then given.

The second section presents the numerical values of roughness components for all the sample plots. This is followed by an examination of the correspondence between the surface structure, exhibited by the plotting of a profile, and roughness components. The results of the test of homogeneity of the sample plots in relation to surface roughness are then considered and a discussion of the possible relationship between depression storage and roughness components presented.

The effect of season on changes in the surface properties, i.e., both depression storage and roughness, is considered. Then the application of all results are discussed in relation to practical problems.

7.2. GEOMETRIC PROPERTIES OF DEPRESSIONS

7.21. Number and Spatial Distribution of Depressions

The locations of low points, as observed in Plot No. I/2 and shown in Fig. 7.1, reveal the spacial distribution of the depressions. The depressions are distributed fairly uniformly over the entire plot except in a portion of the plot where the density of depression is relatively high. The location of the depressions in relation to the Y axis appears to be oriented to the direction of the tillage operation along the slope with almost regular spacing in the X direction up to $X = 40$ cm., after which the trend disappears. Hence, the spatial distribution of the depressions, found to be similar in the other plots, is partly

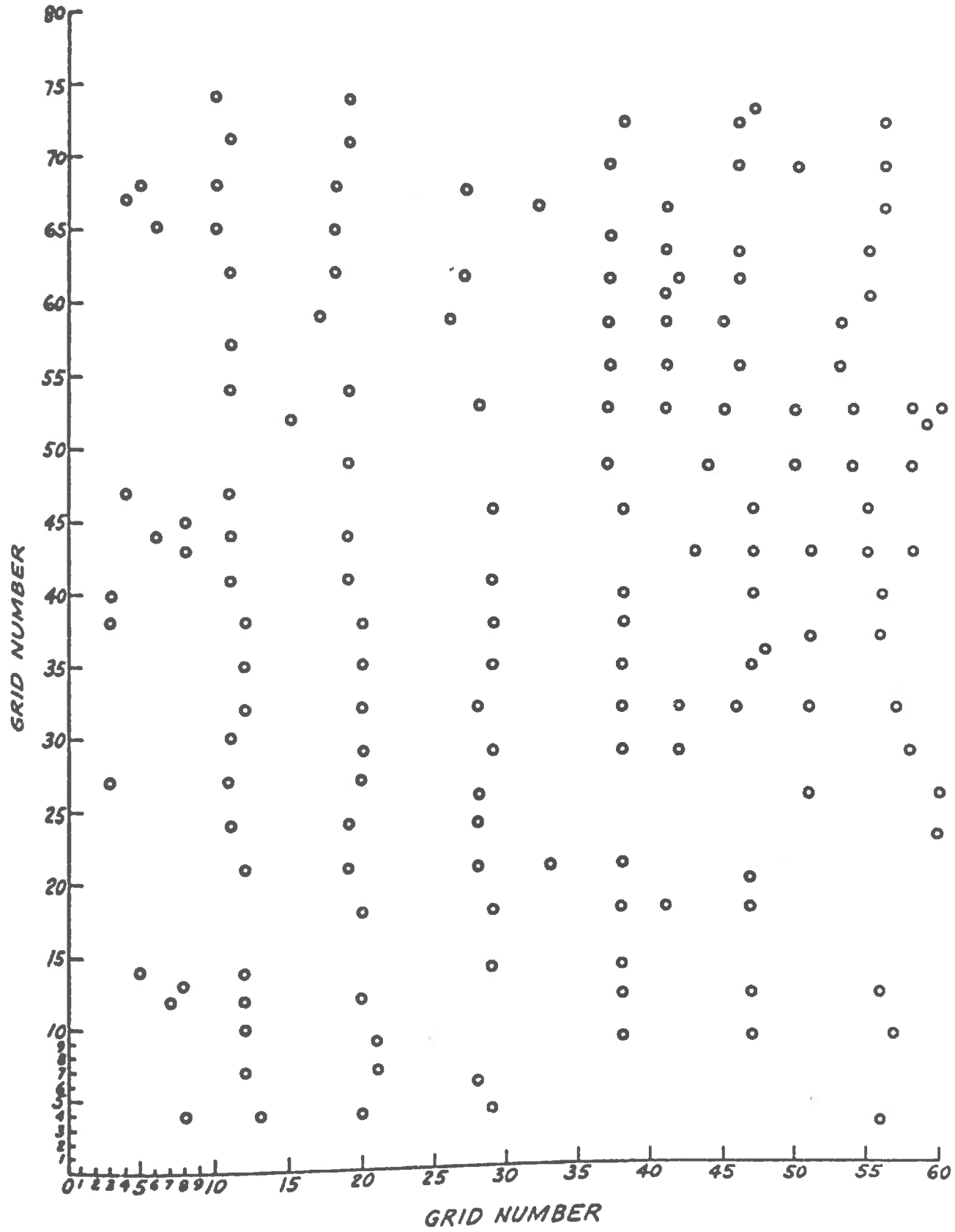


FIG. 7.1 - LOCATION OF DEPRESSIONS IN PLOT I/2

influenced by tillage operations with an added random component. This pattern is likely to be more pronounced with less rough surfaces and visible tool marks as was the case in the plots under study. In plots with rough surfaces having point variations of a few inches without tool marks, the spatial distribution of depressions is likely to be more random.

Table 7.1 gives the total number of depressions as obtained in all the 15 plots. The number ranges from 89 to 181 with means of 165, 126 and 119 in Blocks I, II, and III respectively. The total number of depressions in general reflects the magnitude of the volume of depression storage expected on a plot. The larger the number of depressions the greater is the expected storage. The observed variability in the number of depressions in each plot appears to be partly explained by the slope of the plots. Fig. 7.2 shows the plots of the number of depressions against the corresponding average slope of the plot for all three blocks. There is a consistent trend of decreasing number with increase in slope.

7.22. Volume of Depression Storage.

The total volume of depression storage obtained by summing the volumes of the individual depressions in respect to 15 sample plots is given in Table 7.1 along with the average slope of each plot and the number of depressions.

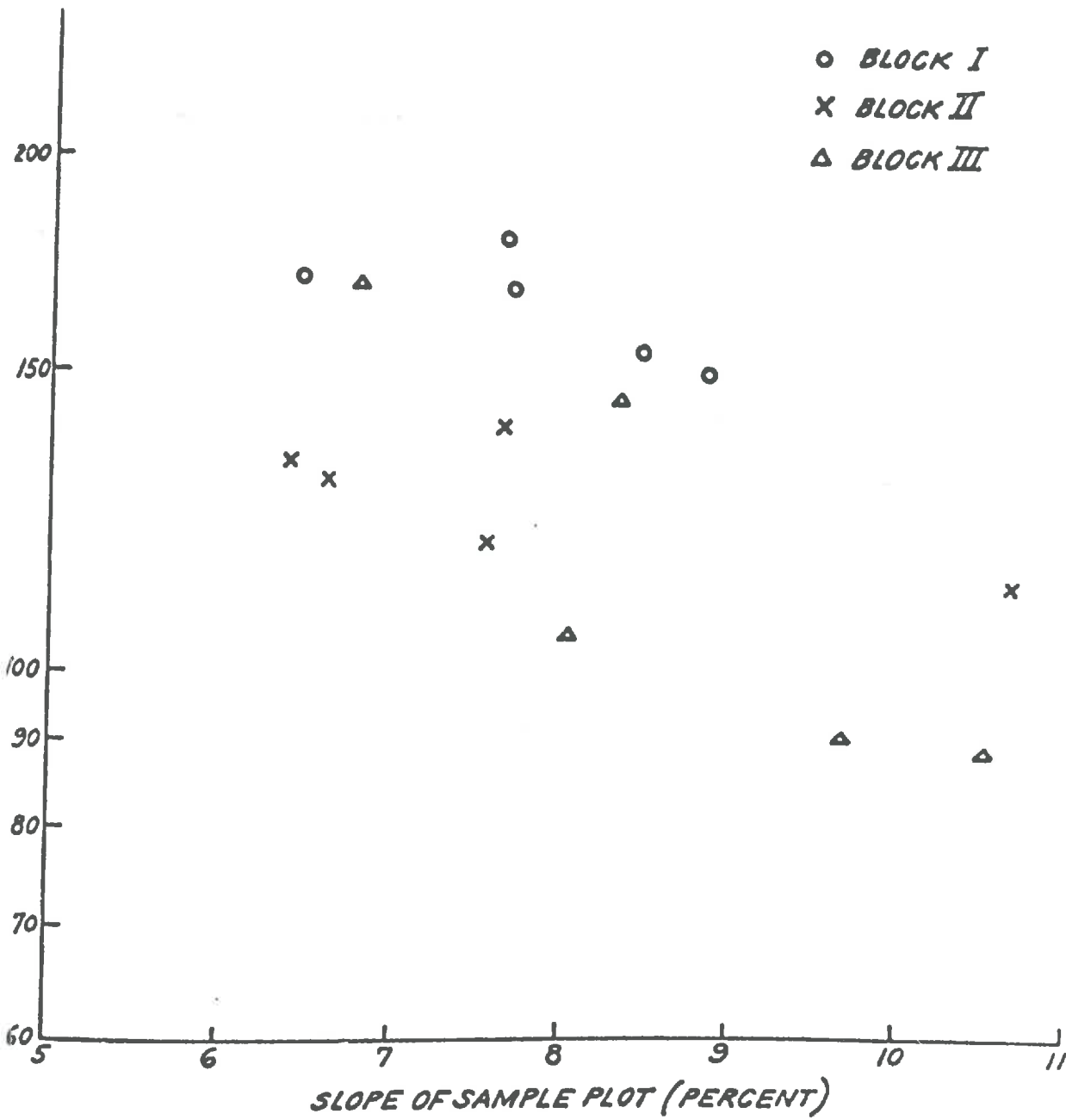


FIG. 7.2 - RELATION BETWEEN NUMBER OF DEPRESSIONS AND SLOPE OF SAMPLE PLOT.

Table 7.1. Volume of Depression Storage

Plot No.	Slope %	No. of Depression	Volume (cc.)	Average Volume per Depression (cc.)
I/1	8.45	156	471	3.02
I/2	8.85	151	370	2.45
I/3	7.62	181	1199	6.63
I/4	6.42	170	779	4.58
I/5	7.68	169	1486	8.79
Average	7.80	165	861	5.21
II/1	6.60	130	419	3.22
II/2	7.62	140	410	2.93
II/3	6.38	133	481	3.62
II/4	7.54	120	295	2.46
II/5	10.67	113	213	1.89
Average	7.76	126	367	2.91
III/1	6.79	169	755	4.47
III/2	8.31	145	685	4.72
III/3	8.03	103	341	3.25
III/4	9.69	91	149	1.63
III/5	10.51	89	118	1.33
Average	8.67	119	409	3.47

The slope of the sample plots is based on the average of the slopes of a few selected profiles. An examination of the slope values reveals a different pattern of the distribution of average slope for the sample plots in the three Blocks. In Block I the slope gradually decreases from the upper portion of the block to the lower portion. In Block II the pattern is not distinct, but there is a tendency toward increasing slope in the lower segment of the block with sample plot II/5 having the highest slope of 10.67%. In Block III there is a distinct pattern of increasing slope in the direction of the general slope of the block which is just the reverse of the slope pattern of Block I. The average slope of the sample plots and its distribution pattern in each block may partly explain the observed variability in total volume of depression storage.

The total volume of depression storage ranges from 118 cc. (0.05 mm.) to 1486 cc. (0.59 mm.) with a mean of 545 cc. (0.22 mm.). The mean volumes of storage for Blocks I, II, and III are 861 cc., 367 cc. and 409 cc. respectively. The volume of depression storage available on the surface under study is very small because of the relative smoothness of the surface. As mentioned earlier the plots were smoothed with a harrow after fall plowing resulting in a surface which did not have any depression having a maximum depth of more than 2 cm.

As discussed in Chapter 5 on the study area, the

three blocks had comparable physiographic conditions and experienced the same type of tillage operations. It was therefore expected that they would exhibit similar surface conditions and as a consequence comparable magnitudes of depression storage volumes. The large variabilities observed in the depression storage volumes within the sample plots of each block and also between the three blocks do not apparently conform to the assumption of similar surface conditions. In view of the apparent differences it was considered necessary to ascertain whether the differences in means could be attributed to chance or whether these were indicative of actual differences in the means of the corresponding blocks. An analysis of variance was selected to test the difference in means for statistical significance based on the sample data.

7.2.2. Test of Homogeneity of Surface

The analysis of variance separates the variance of all observations into parts, each part indicating the variability attributable to internal variation of the several populations and the variation from one population to another. Consider Blocks I, II and III as three distinct populations with means μ_1, μ_2 and μ_3 . The sample plots 1 to 5 form the random samples from each population with means \bar{x}_1, \bar{x}_2 and \bar{x}_3 respectively. The simplest model of the analysis of variance, known as "single variable classification", was applied to develop and test a hypothesis that the means are

equal, i.e., $\mu_1 = \mu_2 = \mu_3$ with the alternate hypothesis of inequality of means, i.e. $\mu_1 \neq \mu_2 \neq \mu_3$. The results are shown in Table 7.2.

Table 7.2. Analysis of Variance of Data of Depression Storage Volume

Source of Variation	Sum of Squares	Degrees of Freedom	Mean Square	F	F _{.95}
Between means	756143	2	378071	3.48	3.89
Within Samples	1304045	12	108670		
Total	2060188	14	-	-	-

Since the calculated F value of 3.48 is less than the tabular value of $F_{.95}(2,12) = 3.89$, it can be concluded that the hypothesis of equal means implying that all the samples were taken from the same population is justified at a 5% level of significance. In other words, the observed differences in the magnitude of storage volumes are not statistically significant. The test of significance using the F distribution in the analysis of variance of single variable of classification is based on the assumption that the observations are taken from a normally distributed population with equal variances. The available data is not adequate to test the validity of the above assumptions but it is felt that the assumption is not seriously violated because the sample plots are located in an area having similar surface conditions. According to Dixon and Massey (1957) any moderate violation

of the above assumptions has been found to have a very little effect in changing the results of the analysis. It is, therefore, not unrealistic to conclude that the sample plots come from the same population and are representative of the area under study. The results of the analysis based on the sample plots data can, therefore, be used to draw inferences about the depression storage property of the area under investigation.

It is evident from Table 7.1 and the results of the above analysis that there is a large variability in depression storage volume in sample plots of each block especially in Blocks I and III. This variability may be due to several physical factors including the slope of the sample plots. An examination of the slopes of the sample plots and the corresponding volumes of storage given in Table 7.1 indicates the existence of a relationship which may partly explain the observed variability in storage volumes of the sample plots in each block.

7.24. Storage Volume and Land Slope Relationship

Even though the sample size of 5 is very small for establishing any reliable functional relationship between the slope of the sample plot and depression storage volume, an attempt was made to investigate the degree of correlation and the form of the functional relationship that exists between the two sets of variables. A plot of depression storage volume (Y) against the corresponding

value of slope (X) indicated a non-linear relationship between X and Y. A logarithmic transformation of the dependent variable Y eliminated the non-linear behaviour of the plotted data as shown in Fig. 7.3. In spite of some scatter in the plotted points there is a good indication of the existence of a relationship between X and log Y for all the three blocks. The lines of best fit were drawn through the plotted points by the standard method of least squares. The exponential regression of the line is of the form:

$$Y = a e^{-bX}$$

where: Y is the predicted value of depression storage, in cc.,

X is the slope, %, and

a and b are statistical parameters.

The results of the analysis are summarized in Table 7.3.

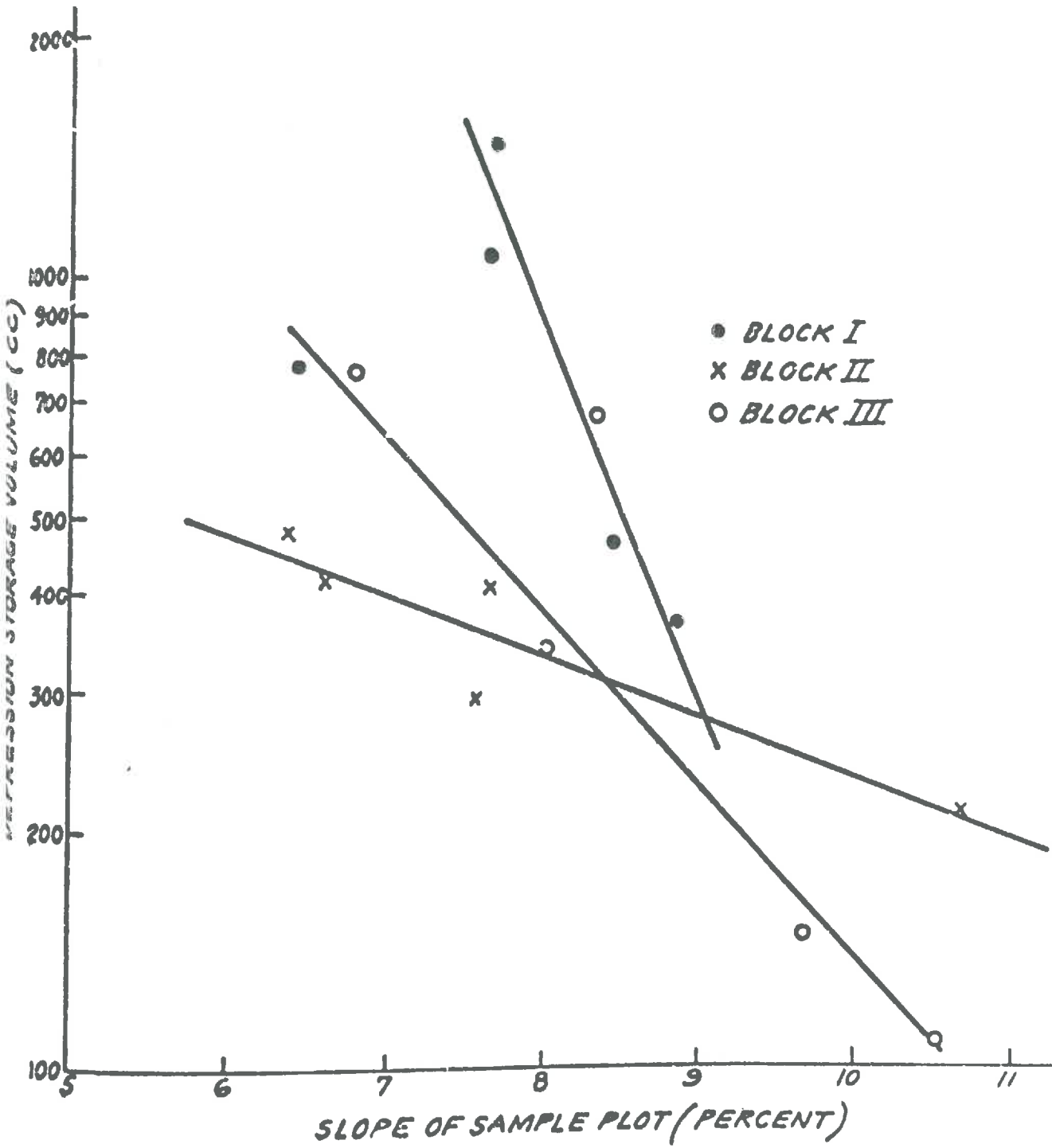


FIG. 7.3 - SLOPE-VOLUME RELATIONSHIP

Table 7.1. Results of Regression Analysis

Block	No. of Observation	Regression equation	Coefficient of Correlation	Standard Error (cc.)
I	5	$Y = 12841 e^{-0.3634X}$	0.3269	-
	4	$Y = 6483165 e^{-1.1128X}$	0.9549	197.44
II	5	$Y = 1369 e^{-0.1760X}$	0.8436	54.57
III	5	$Y = 32294 e^{-0.5343X}$	0.8380	-
	4	$Y = 21215 e^{-0.5030}$	0.9852	48.36

The low coefficient of correlation in the case of Block I is obviously due to one outlying point. The same trend is observed in Block III where a single point greatly reduces the coefficient of correlation. By ignoring these points in each of Blocks I and III, the correlation is substantially improved.

The general magnitude of the coefficients of correlation indicates a significant relationship between the slope and the depression storage volume. In the case of Blocks I and III, more than 90% of the variability in depression storage volumes is explained by the independent variable slope, whereas the coefficient of determination is 71% in the case of Block II.

The decrease in depression storage volume with increase in slope is due to a decrease in the number of depressions and also to a decrease in the depth of storage. An

exact mathematical relationship between the depth and slope can be obtained provided the depression is assumed to have a regular geometric form. However, such an assumption is physically unrealistic and may lead to misleading results. Fig. 7.4 shows a plot of the average maximum depth of the depressions versus the slope. In the case of Blocks I and III in spite of some scatter, there exists a relationship between slope and depth. The slope in Block II is not discernible. This observed relationship is likely to be more pronounced in the case of depressions having depths of a few inches. A similar trend is exhibited in the plot of slope and number of depressions for all three blocks shown in Fig. 7.2. Therefore, the decrease in the number of depressions and depth of storage with an increase in slope of the plot explains the relationship that exists between the slope and volume. This form of relationship conforms with the result reported by Lee (1972) who developed an exponential relationship between the slope and depression storage based on empirically determined storage values. Willeke (1966) and Viessman (1968) obtained a similar relationship between the loss, which is equivalent to active potential depression storage on an impervious area, and the slope.

The variation in the total volume of depression storage between the blocks, though statistically not significant, warrants some explanation regarding the possible reasons

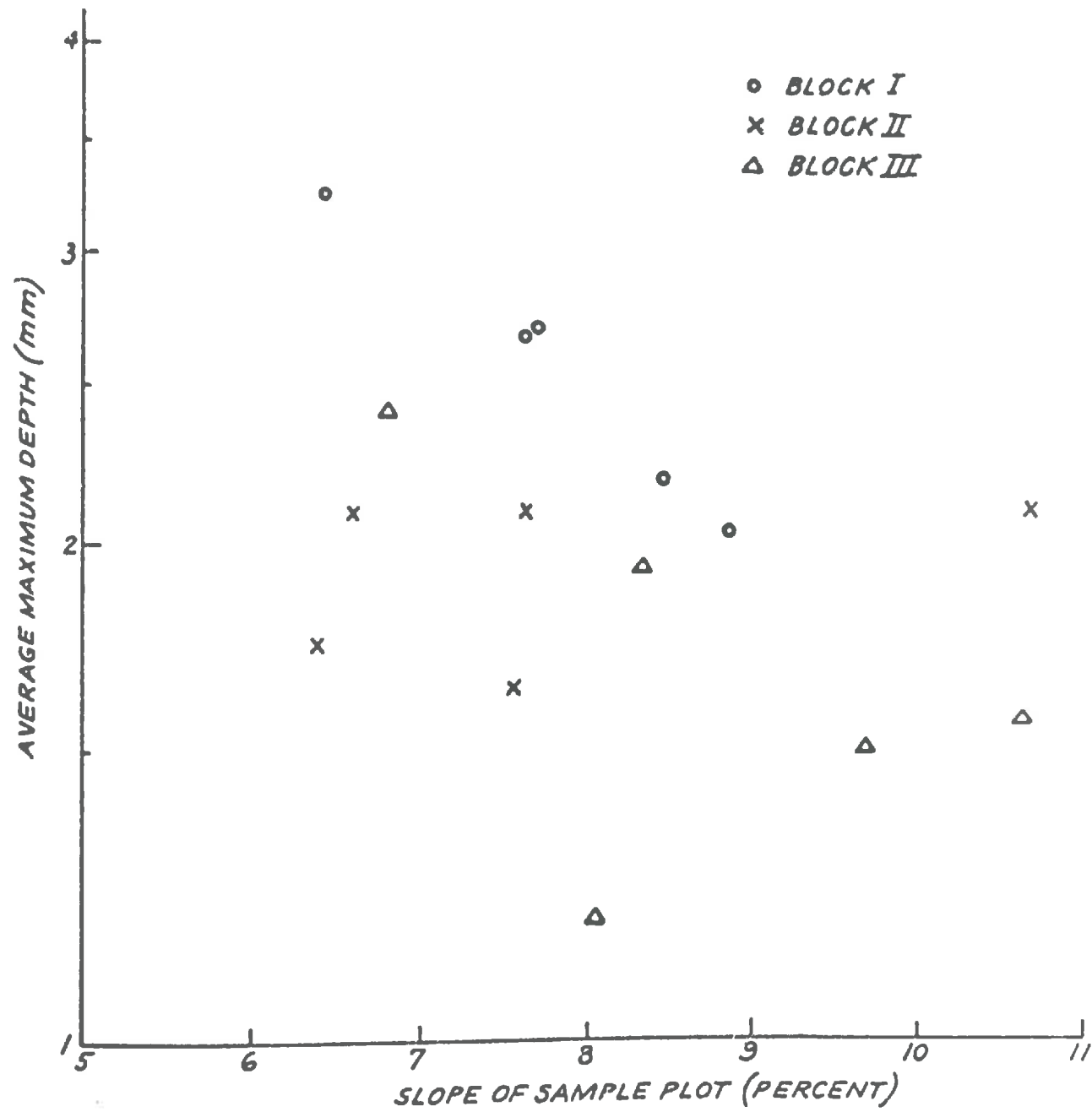


FIG. 7.4 - AVERAGE MAXIMUM DEPTH AND SLOPE RELATIONSHIP

to which it could be attributed. The differing distribution pattern of the slope along the length of each block is one of the possible reasons for the observed variations. The slope is an overridingly important factor in influencing the hydraulic behaviour of overland flow and the associated erosional processes occurring on any sloping surface. Since each block is an independent hydrologic unit, the existing slope pattern along its length is bound to influence the overall hydraulic behaviour of the surface giving rise to specific surface structure. The erosional processes may also modify the physical nature of the soil forming the surface at different points along the length. Such a situation would result in a different response in terms of depression storage and surface roughness to the same tillage operation.

Another possible reason may be the effect of the location of each block. Blocks II and III are narrow strips located between the runoff plots which offer some restraint on the movement of tillage equipment due to insufficient width along the entire length of the block. The degree of restraint being a variable because of the varying width might be responsible for creating some differences in the surface structure. Some of the plots in Block II and III have been observed to have a multiple direction slope and relatively more irregular surface which apparently has been caused by the restraint on the movement of the tillage implements. The above reasons

seem logical for explaining the variation in storage volume. But there is no quantitative data to support such reasonings.

7.25. Volume - Depth - Surface Area Relationships

A depression is characterized by its maximum volume, maximum depth, and surface area at the pour point level which corresponds to maximum water area when it is filled to its capacity. It is logical to assume the existence of some relationship between these three geometric properties of the individual depressions. An attempt has been made to investigate the form of functional relationships and the degree of correlation that exists between the three properties. Since the volume and depth of the depressions have the same form of relationship with the slope, it is not unrealistic to assume that the relationship between the three geometric properties of the individual depressions will not change materially from one sample plot to another. With this assumption 40 depressions were randomly selected from Block I to almost cover the observed range of volume, depth, and surface area. The mean and standard deviation of the properties of the selected depressions are given in Table 7.4.

Table 7.4. Mean and Standard Deviation of the Geometric Properties of Selected Depressions

Geometric Property	No. of Depression	Mean	Standard Deviation
Volume	40	14.12 cc.	29.03 cc.
Depth	40	0.48 cm.	0.20 cm.
Surface Area	40	35.62 sq. cm.	45.95 sq. cm.

An arithmetic plot of depth, D , as independent variable and volume, V , as dependent variable indicated a non-linear relationship. A logarithmic transformation of both the variables resulted in a linear relationship as shown in Fig. 7.5. The line of best fit was drawn through the plotted points by the method of least squares. The functional relationship is of the form:

$$V = a D^b$$

or in logarithmic form

$$\log V = \log a + b(\log D)$$

where: V is the predicted value of maximum volume, in cc.,

D is the maximum depth of storage, in mm., and

a and b are parameters to be determined statistically.

The depth-volume relationship is expressed by the following equation:

$$V = 0.7610 D^{1.4762}.$$

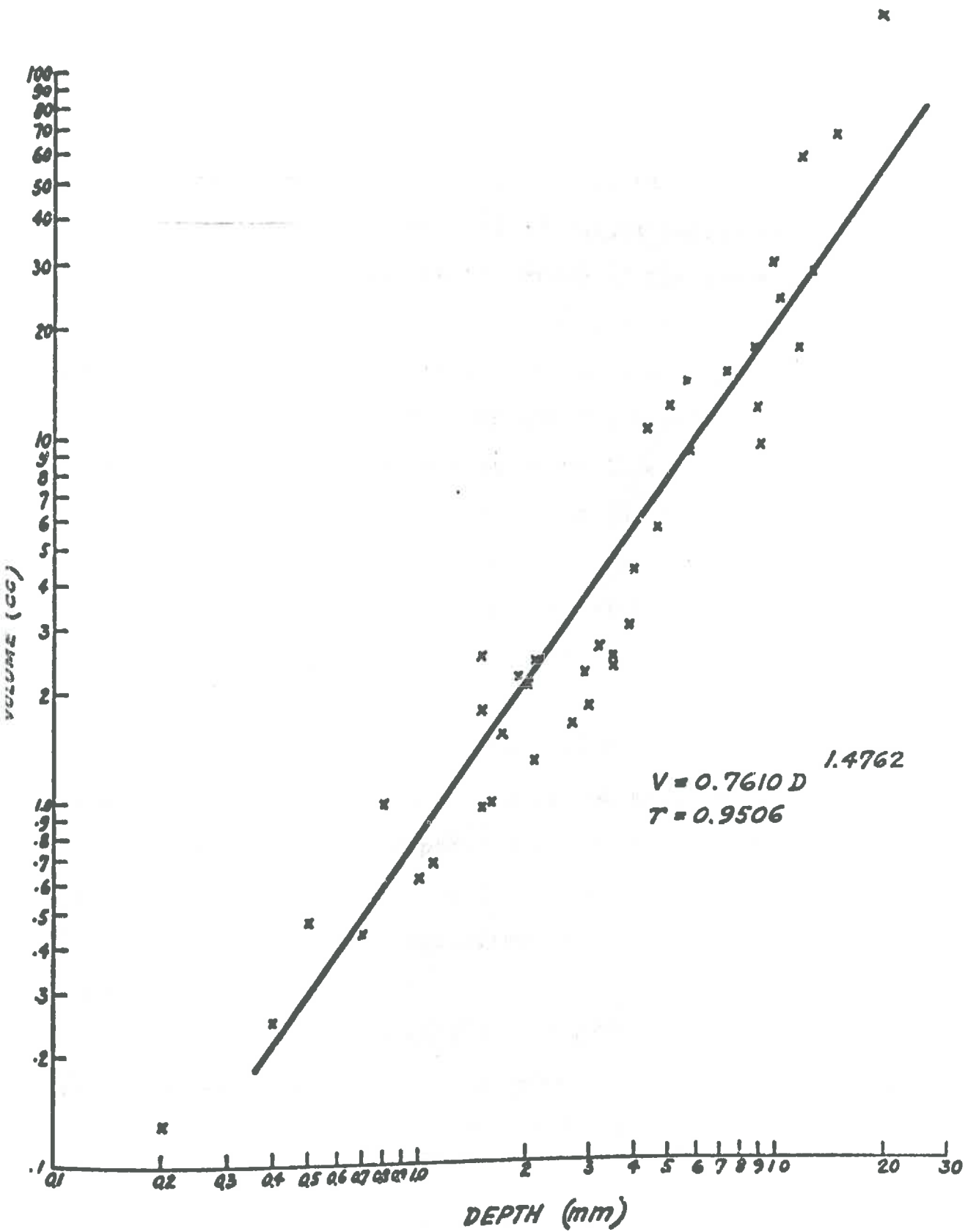


FIG. 7.5 - VOLUME - DEPTH RELATIONSHIP

The coefficient of correlation, r , is 0.9506 and the standard error of estimate is 1.64 cc., indicating a significant relationship between the depth and volume.

An examination of the plotted points indicates the existence of a break in the trend of the plotted points at a depth of about 3 mm. This suggests that the plotted points could be better fitted with two lines instead of one as obtained above. This trend and the trend of the exact plotting of some points on a straight line, especially at lower depths, is due to the use of constant values of surface area for a range of lower values of depth. Since the surface area can take a minimum value of 6.25 square cm., equivalent to the grid area, and any other value which is a multiple of 6.25, the volume becomes directly proportional to the depth for any constant value of surface area. At lower depths up to 3 mm., the surface area does not increase much with depth, resulting in a slow increase in volume. After a depth of 3 mm., the slope of the plotted points becomes steeper indicating a rapid increase in surface volume with depth.

In spite of the scatter in the plotted points, there exists a definite relationship between the depth and volume which could be used satisfactorily for predicting one in terms of the other. On the surfaces with depressions having depths of a few inches, the relationship between depth and volume is likely to be still more significant than

the present analysis where the depth is very small.

Fig. 7.6 shows the plot of surface area, SA, as independent variable and volume, V, as dependent variable on log-log paper, indicating a linear relationship between log SA and log V. The relationship is of the same form as obtained in the case of depth and volume. The resulting regression equation is

$$V = .0735 (SA)^{1.4914}$$

The relationship has a coefficient of correlation, r, of 0.9391 and a standard error of 1.78 cc. There is a relatively large scatter in the plotted points for the lower values of surface area which gradually decreases with the increase in surface area. The maximum scatter in volume at SA = 6.25 is due to varying depth and constant surface area, already noted in the depth-volume relationship. As is evident from the magnitude of the coefficient of correlation there exists a significant relationship between the surface area and volume of storage.

The relationship between the depth of storage, D, as independent variable and surface area, SA, as dependent variable, shown in Fig. 7.7, is of the same form as obtained in the case of depth-volume and surface area-volume. As expected there is a lot of scatter in the plotted points on the depth axis, due to the constant values of surface area for a range of depth values

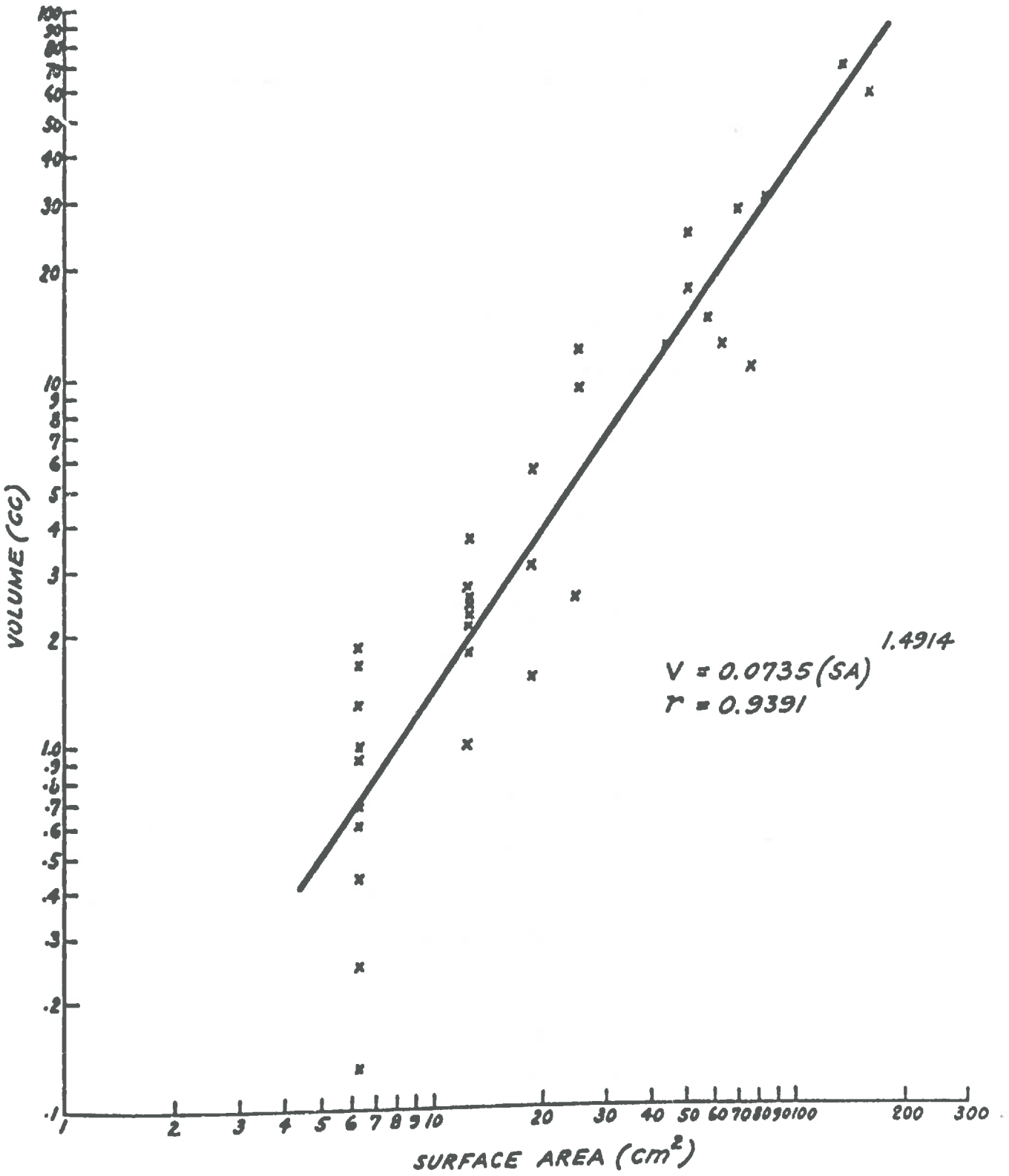


FIG. 7.6 - VOLUME-SURFACE AREA RELATIONSHIP

and the fact that the surface area can take only a value multiple of 6.25. The scatter gradually reduces as the depth increases indicating an increase in surface area with increasing depth. The equation of the regression line is given as

$$SA = 8.1120 D^{0.8055}$$

The coefficient of correlation of the prediction equation is 0.8274 and the value of standard error is 1.81 sq. cm. Though the coefficient is relatively low compared to that obtained in depth-volume and surface area-volume relationships, there is a strong indication of a usable relationship between the depth and surface area of the depressions.

From the results of the analysis it is evident that there are significant relationships between the three geometric properties of the depressions which can be used reliably to predict one in terms of another. The effect of surface area being a multiple of 6.25 is more pronounced in giving rise to a specific type of scatter in the plotted points for depths lower than 3 mm. The scatter gradually decreases with increasing depths showing a better fit of data. The depth of 3 mm. is in fact very small for any significant contribution to the total depression storage volume on any surface. It is felt that for the depressions having relatively higher depths of a few inches, the above relationships between the three geometric

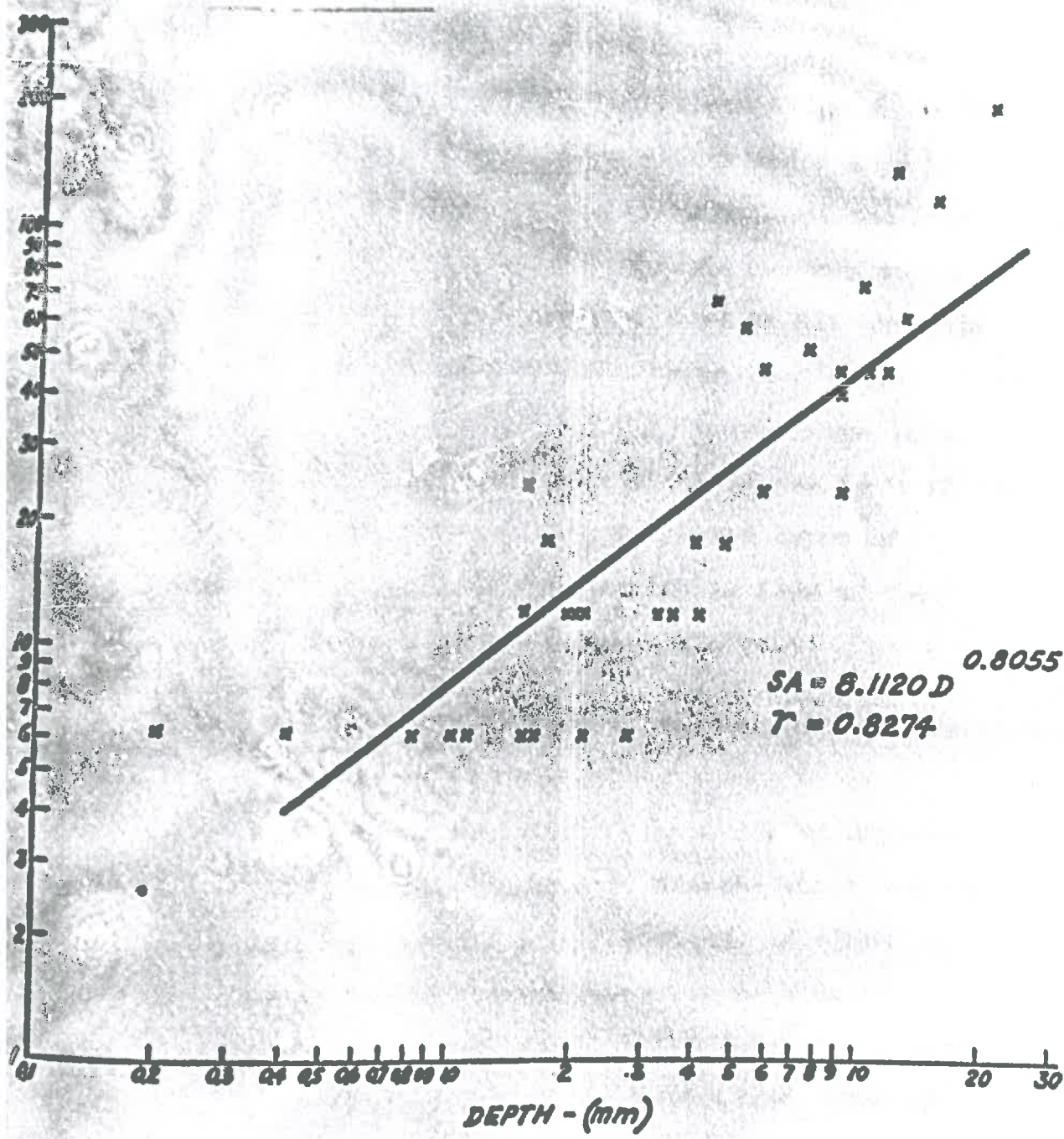


FIG. 7.7 - SURFACE AREA - DEPTH RELATIONSHIP

properties under investigation are likely to be more consistently significant.

There is no data yet available on the geometric properties of the individual depressions and the existing relationships in the scientific literature which could be used to compare the results. Haan (1967) reported a similar form of functional relationship between the depth and volume with an 'r' value of 0.89, and between surface area and volume with an 'r' value of 0.96 in his study on potholes. The mean maximum volume, depth, and surface area were 2.05 acre ft., 1.09 ft., and 2.29 acres respectively. It is interesting to note the similarity of the form of the relationship between two entirely different types of depressions. The degree of correlation is also of the same order as obtained in the present analysis.

7.26. Frequency Distribution of the Geometric Properties

7.261. General

The raw data on the geometric properties of depressions consist of unorganized lists of numbers which are not amenable to any statistical interpretation. A first necessary step is to make use of suitable methods of organizing, presenting, and reducing the observed data to facilitate their interpretation and evaluation. One of the most commonly used methods consists of the formation of frequency distributions. In this method, the raw data is classified into suitable groups or classes and

properties under investigation are likely to be more consistently significant.

There is no data yet available on the geometric properties of the individual depressions and the existing relationships in the scientific literature which could be used to compare the results. Huan (1967) reported a similar form of functional relationship between the depth and volume with an 'r' value of 0.89, and between surface area and volume with an 'r' value of 0.96 in his study on potholes. The mean maximum volume, depth, and surface area were 2.05 acre ft., 1.09 ft., and 2.29 acres respectively. It is interesting to note the similarity of the form of the relationship between two entirely different types of depressions. The degree of correlation is also of the same order as obtained in the present analysis.

7.26. Frequency Distribution of the Geometric Properties

7.261. General

The raw data on the geometric properties of depressions consist of unorganized lists of numbers which are not amenable to any statistical interpretation. A first necessary step is to make use of suitable methods of organizing, presenting, and reducing the observed data to facilitate their interpretation and evaluation. One of the most commonly used methods consists of the formation of frequency distributions. In this method, the raw data is classified into suitable groups or classes and

the number of items falling in each is tabulated. The plotting of the frequency in each class as a bar yields a histogram. The height of the bar represents the number of the frequency in that class. The treatment of the data up to this stage does not depend on the assumption that the data constitutes a random sample of any mathematical probability model. The method in fact is a simple aid for the reduction of the raw data and only helps to discern the shape of an underlying distribution. The frequency distributions of volume, depth, and surface area for all sample plots are discussed in the subsequent paragraphs.

7.262. Volume

The volume or storage capacity of the individual depressions observed in the three blocks ranged from a minimum of .06 cc. to a maximum of 439 cc., indicative of a very large variation. Since the volumes of more than 95 percent of the measured depressions were less than 22 cc., it was considered appropriate to use a class interval of 1 cc. in order to draw some inference about the underlying probability distribution. The volumes of depressions in classes higher than 20 cc. were in all cases less than 100 cc. except one which had a capacity of 161 cc.

It is interesting to note from the histograms in Fig. 7.8 (a to f). that the distribution pattern is identical for all the plots, with the maximum number of depressions

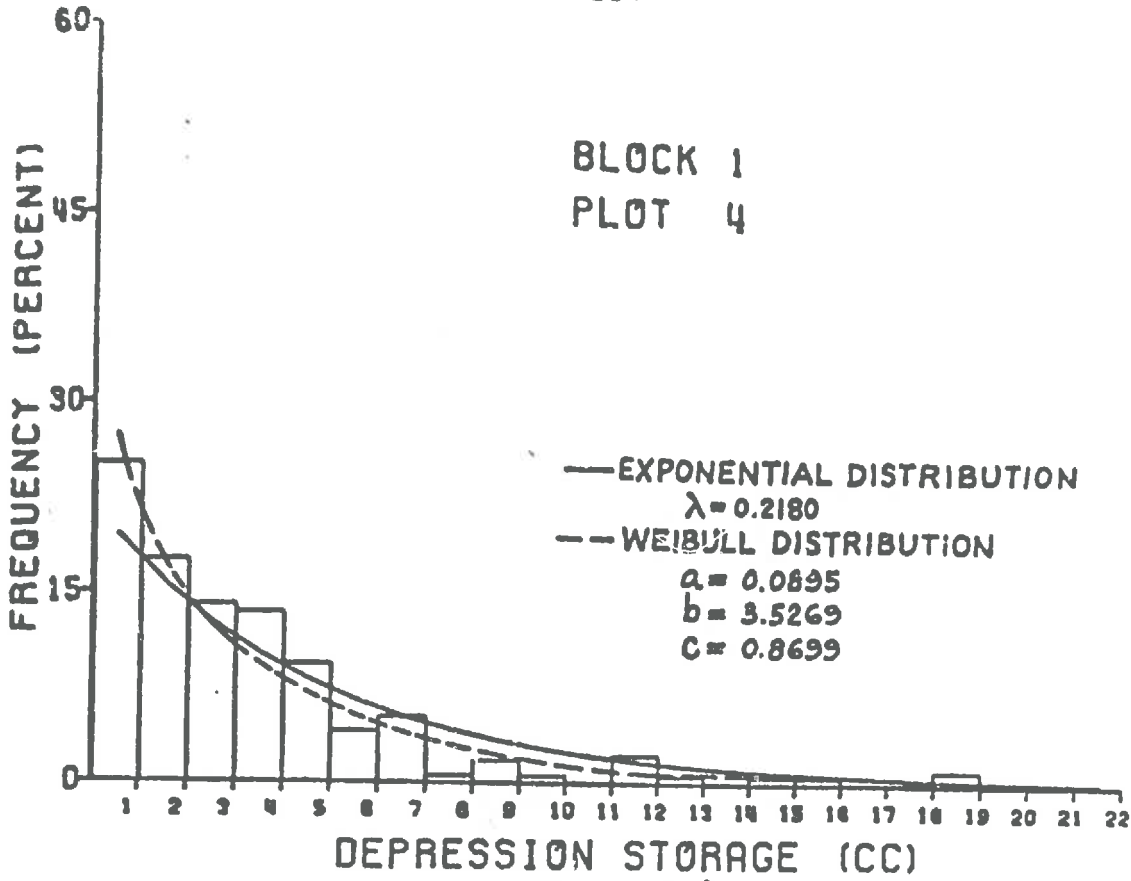


Fig. 7.8 (a)

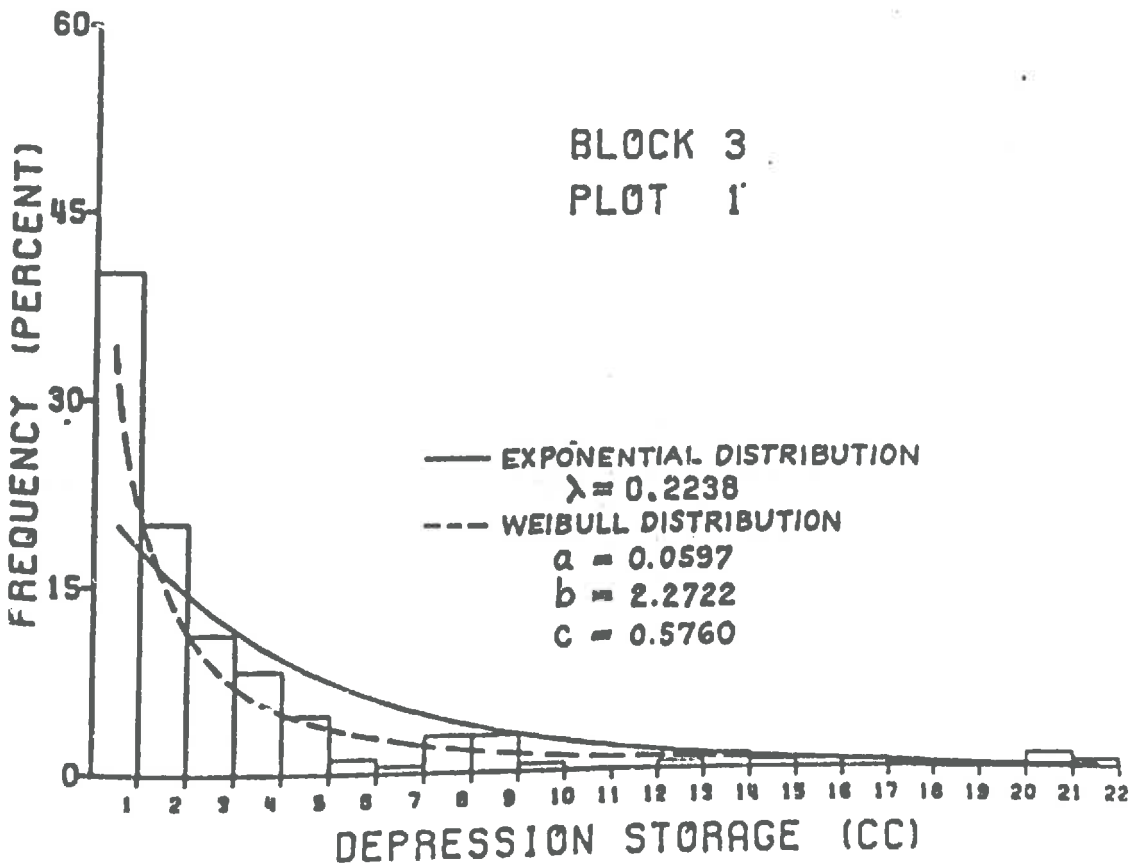


Fig. 7.8 (b)

FIG. 7.8 - HISTOGRAM OF VOLUME AND THEORETICAL CURVES

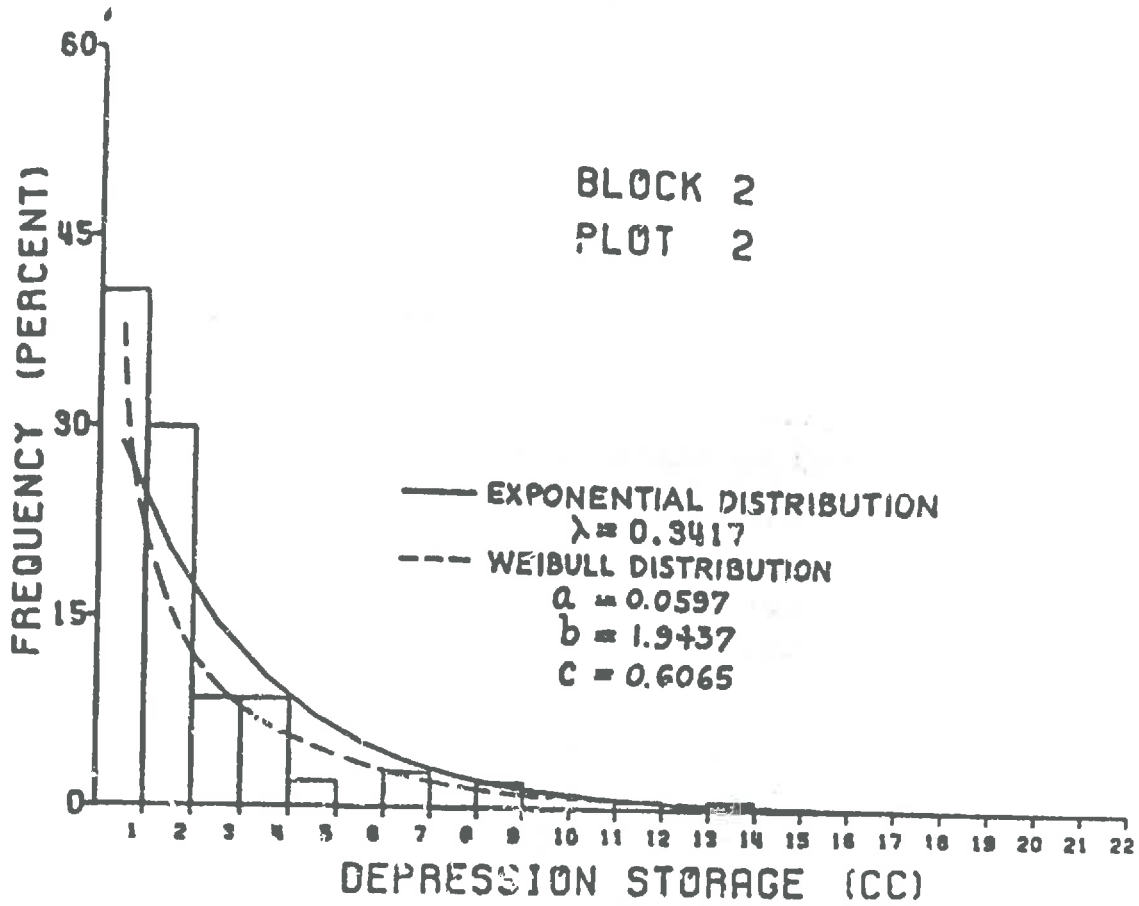


Fig. 7.8 (c)

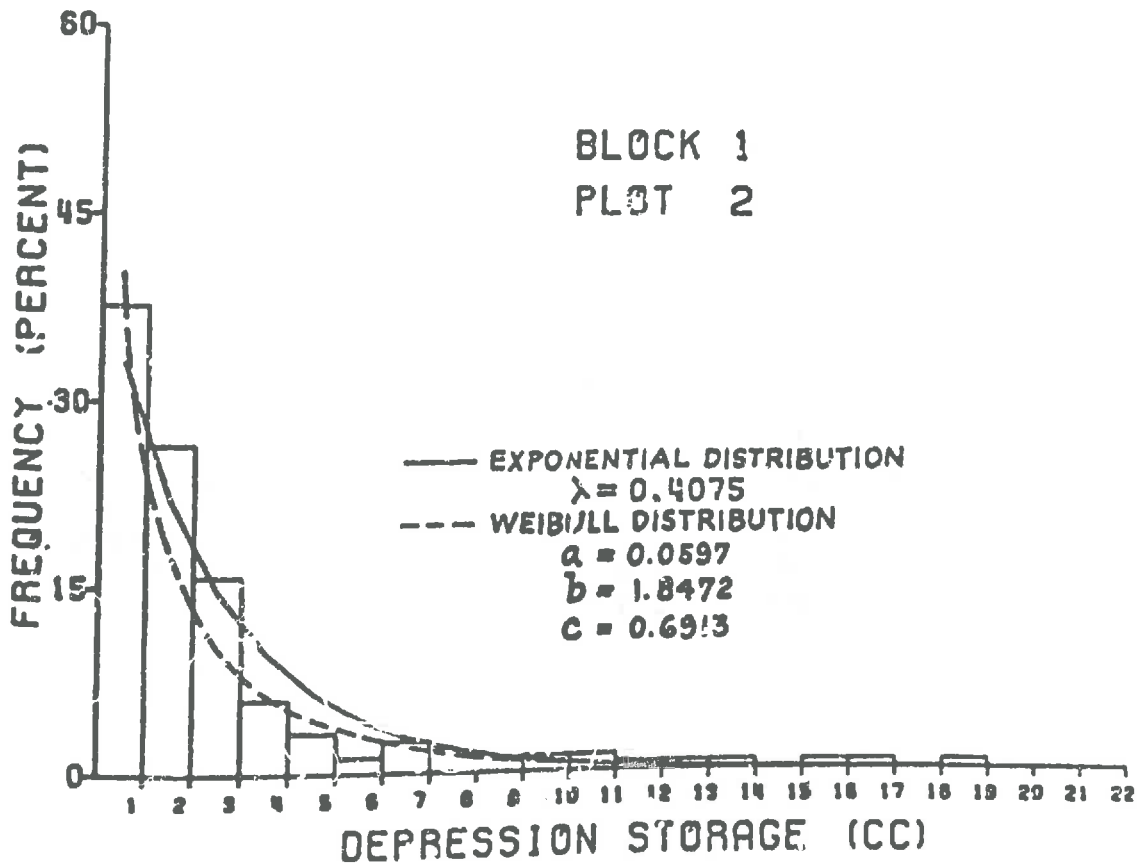


Fig. 7.8 (d)

FIG. 7.8 - HISTOGRAM OF VOLUME AND THEORETICAL CURVES

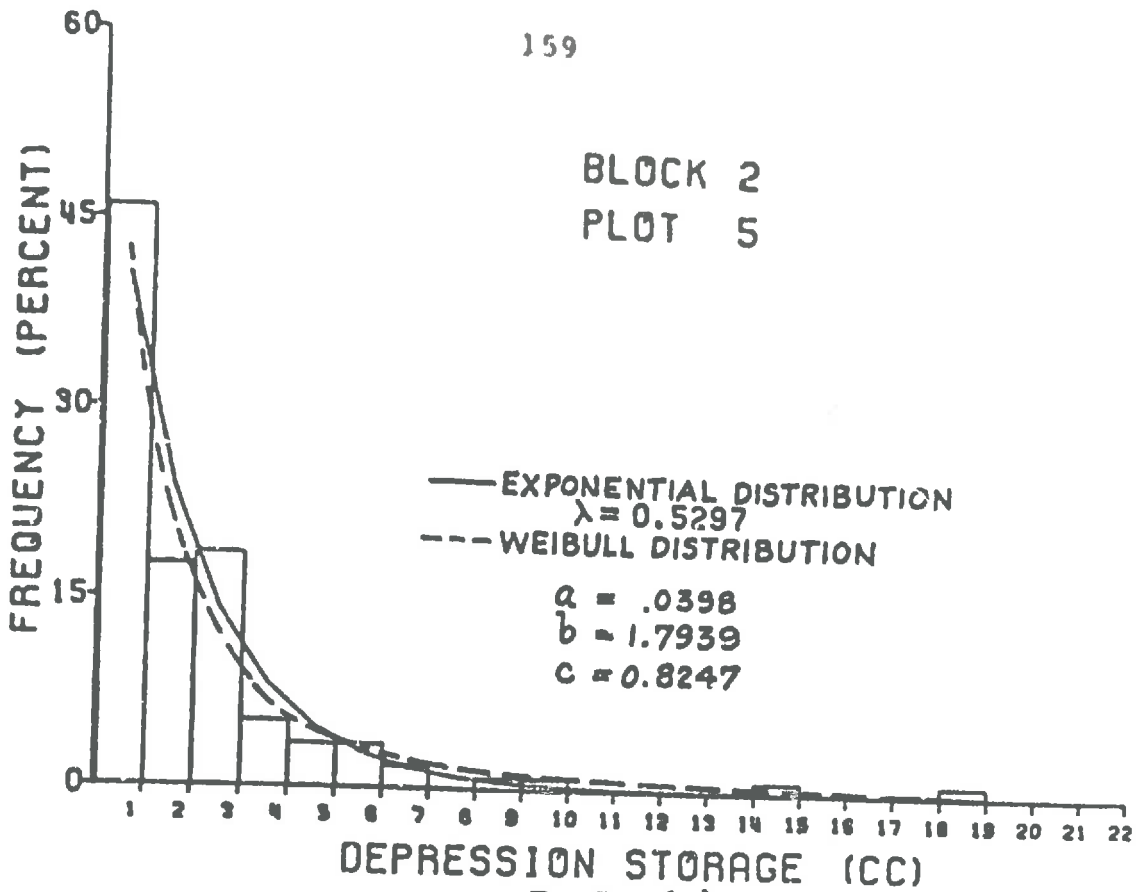


Fig. 7.8 (e)

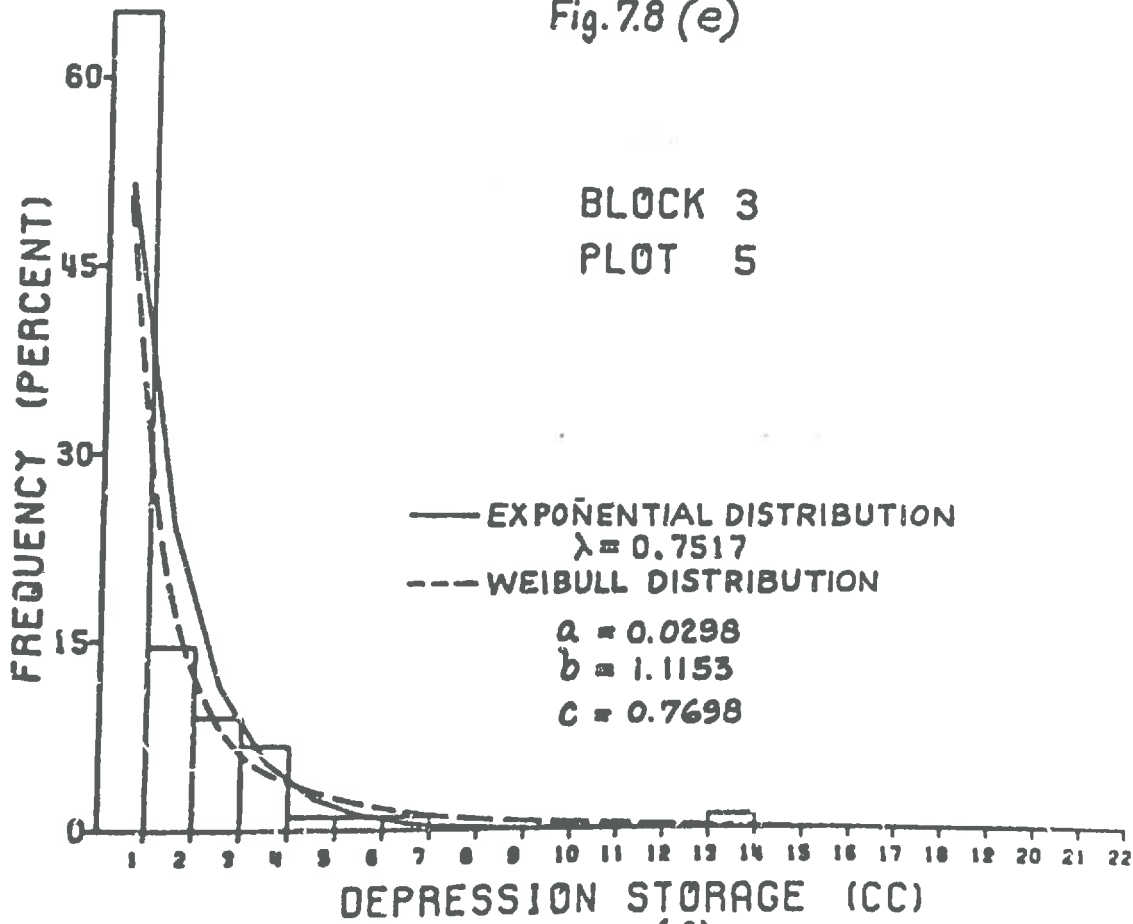


Fig. 7.8 (f)

FIG. 7.8 - HISTOGRAM OF VOLUME AND THEORETICAL CURVES.

falling in the lowest class of 0-1, rapidly decreasing up to the 4th class, and then gradually decreasing up to the highest class. Though there is a general similarity in the distribution pattern, a comparison of the frequencies in each class indicates variations from plot to plot which is not unexpected because of the large variations in total volume observed in sample plots.

In view of the observed variations in total volume of depression storage in sample plots, it is appropriate to investigate implications regarding the frequency distributions. The mean volume of depressions in the sample plots ranged from 1.33 cc. to 8.80 cc. Figures 7.8 (a to f) show plots of the histograms of volume with respect to a few sample plots selected to cover the observed range of the mean volume. Examination of the histograms reveals that with an increase in the mean volume the frequency of the lowest class decreases from more than 60 percent in Fig. 7.8f to about 30 percent in Fig. 7.8a. Additionally, the rate of decrease of frequencies in higher classes is gradual for plots of high mean volume, whereas the decrease is abrupt in the case of plots with relatively small mean values. Also in plots with higher mean values the number of frequencies in higher classes are relatively more, giving rise to a more even distribution in the entire range of classes.

7.263. Depth

The observed maximum depths of depressions ranged from 0.1 mm. to a maximum of 27.9 mm. The frequency dist-

ributions of depth reveal that all other depressions fall within the highest class of 21-22 mm. Considering the range of depths and the number of depressions it was decided to use a class interval of 1 mm. An examination of the histograms in Fig. 7.9(a to d) reveals that the distribution pattern is similar to that obtained for the case of volume except that the reduction in the frequencies in higher classes is relatively more gradual in almost all sample plots with varying mean values. The variation in mean depth values is much less than that obtained for the mean values of volume. The frequency distributions of the depth are, therefore, likely to have relatively small variations. This is apparent from the histograms of depths of a few plots selected on the basis of the mean values and shown in Fig. 7.9(a to d).

7.264. Surface Area.

The surface areas of the depressions ranged from a minimum of 6.25 sq. cm. to a maximum of 412.5. sq. cm. The total surface area of depressions on sample plots ranged from about 3 to 10 percent of the total plot area. The extent of area under the depressions bears a direct relation to the total volume of storage for the sample plot. This was evident from the surface area-volume relationship shown in Fig. 7.6

As mentioned earlier, the basic algorithm used for determining the volumes of depressions considers the area of a grid as a unit with the result that the surface area

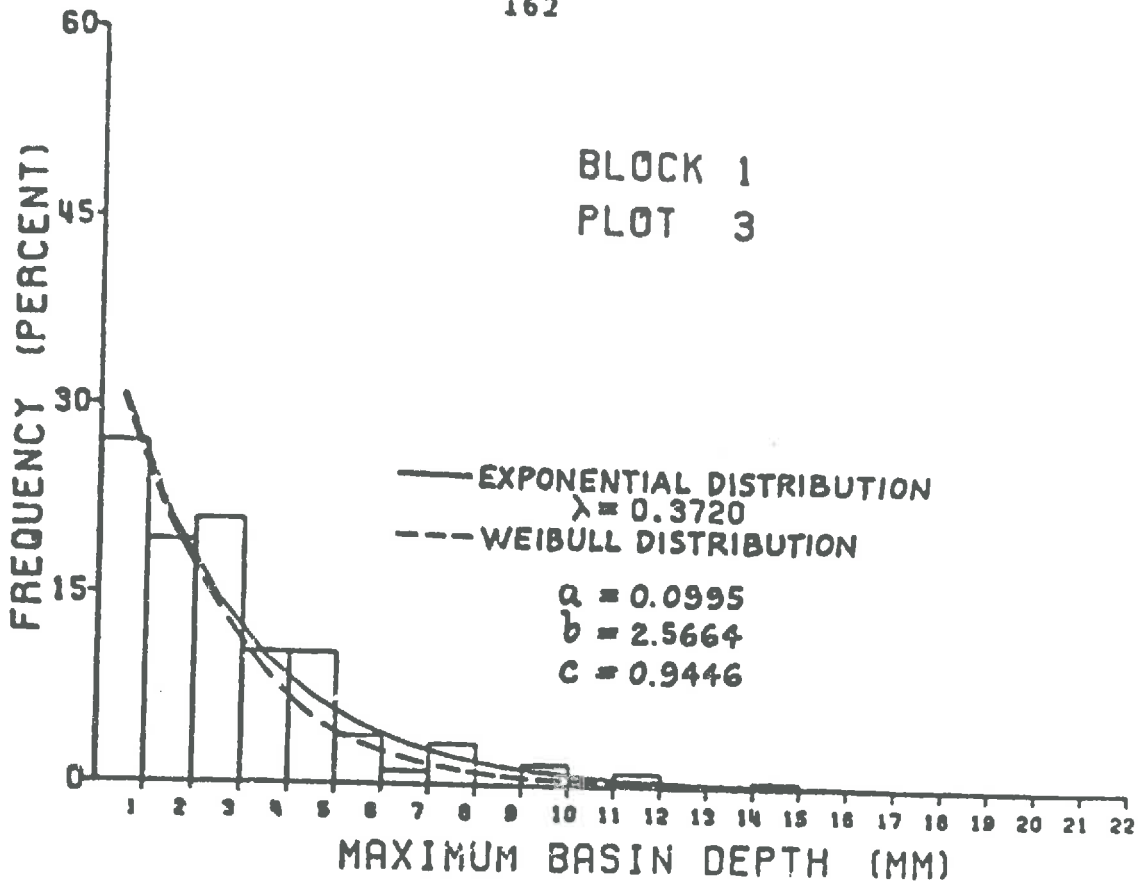


Fig.7.9 (a)

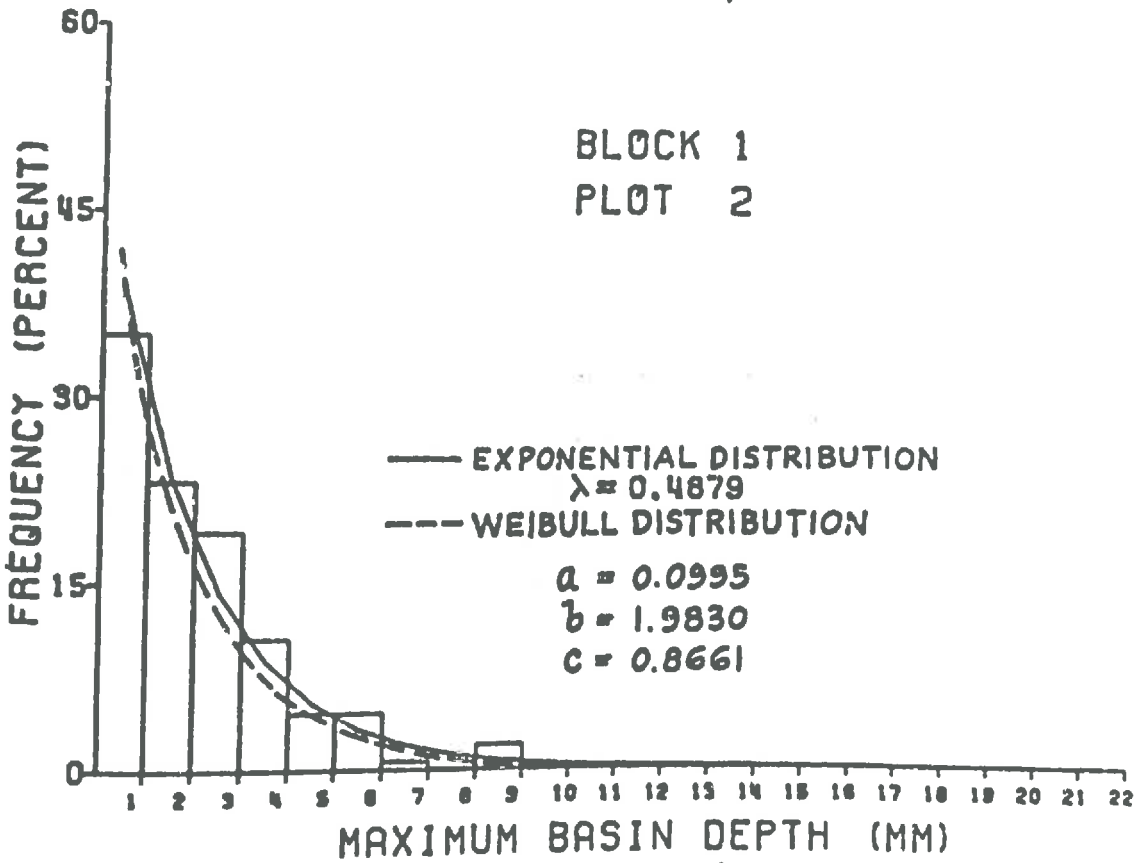


Fig.7.9 (b)

FIG.7.9 - HISTOGRAM OF DEPTH AND THEORETICAL CURVES

BLOCK 2
PLOT 3

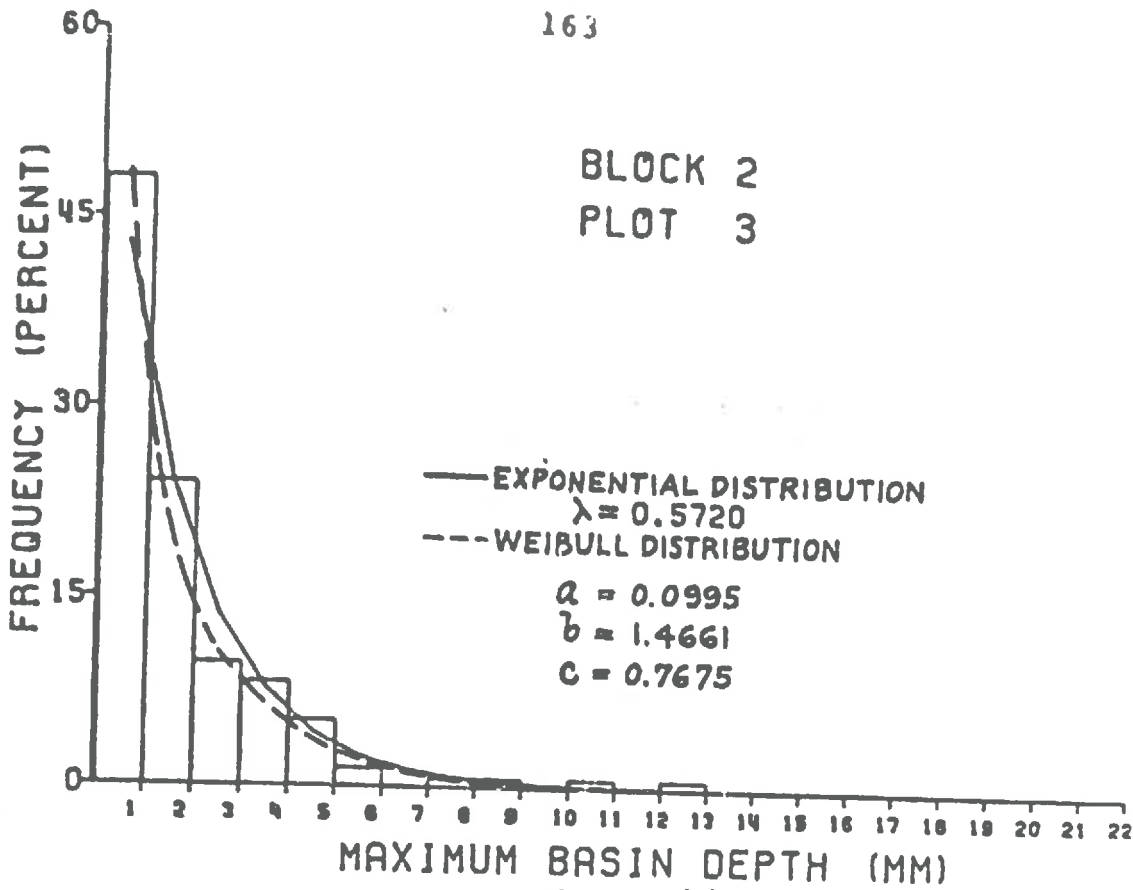


Fig. 7.9 (c)

BLOCK 3
PLOT 5

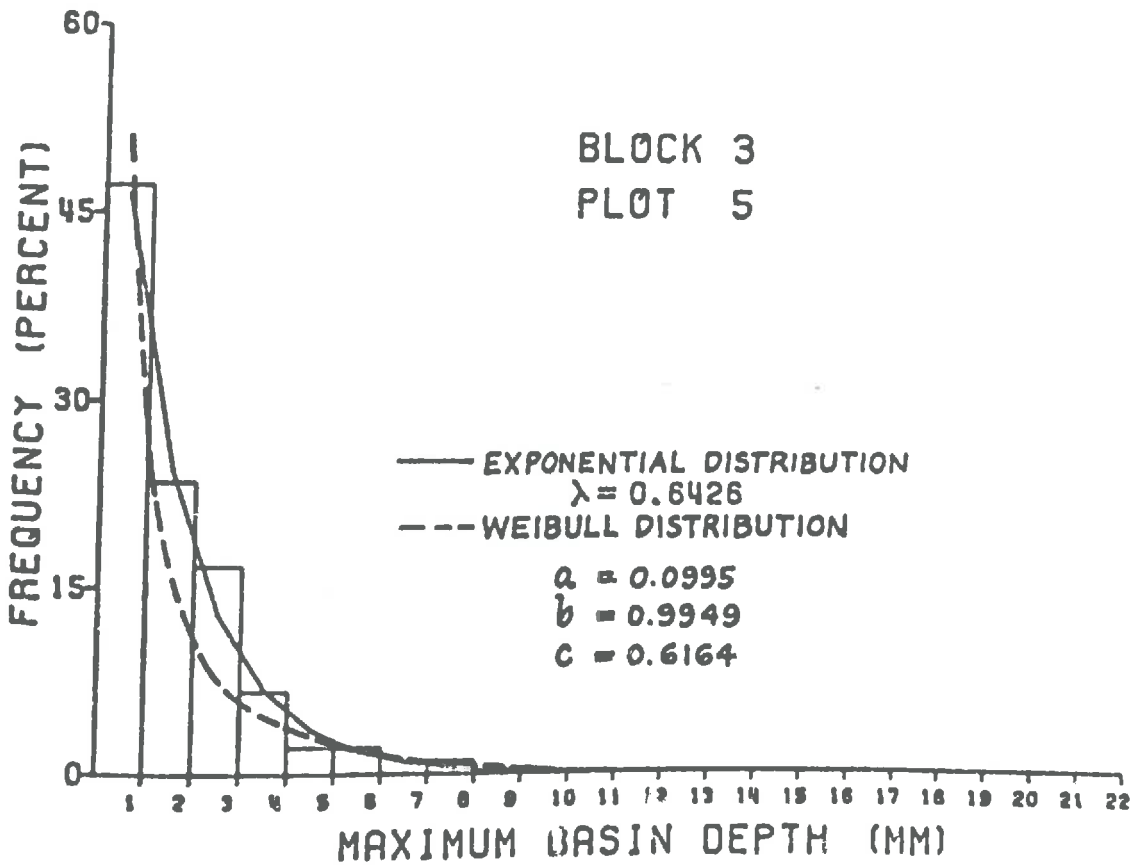


Fig. 7.9 (d)

FIG. 7.9 - HISTOGRAM OF DEPTH AND THEORETICAL CURVES

can take only values which are multiples of 6.25. In view of this limitation, 6.25 sq. cm. was considered as a class interval for the frequency distribution.

The frequency distribution of the surface area of depressions termed as basin area is shown in Fig. 7.10 (a,b) for a few plots. Examination of the frequencies reveals that all the depressions except a few have surface areas less than 125 sq. cm. It is also evident that the lowest class has relatively higher frequencies compared to the volume and depth. Also the reduction in frequencies in higher classes is relatively more abrupt in all the plots. The number of frequencies in each class with respect to all of the sample plots appears to be of comparable order. Considering each class as a unit equivalent to 6.25 sq. cm., the means of the surface area obtained for different sample plots ranged from 1.66 to 2.78. The small range in means is due to the small range of surface areas, restricted by the fact that it could take only values which were multiples of 6.25. The small difference in means therefore does not indicate that the variation in the frequency distribution as obtained in different plots is small. Examination of the histograms reveals the variations in the frequencies falling in classes higher than 2 units.

It is evident from the above discussion that all three geometric properties of depressions have specific patterns of frequency distribution which, in general, are

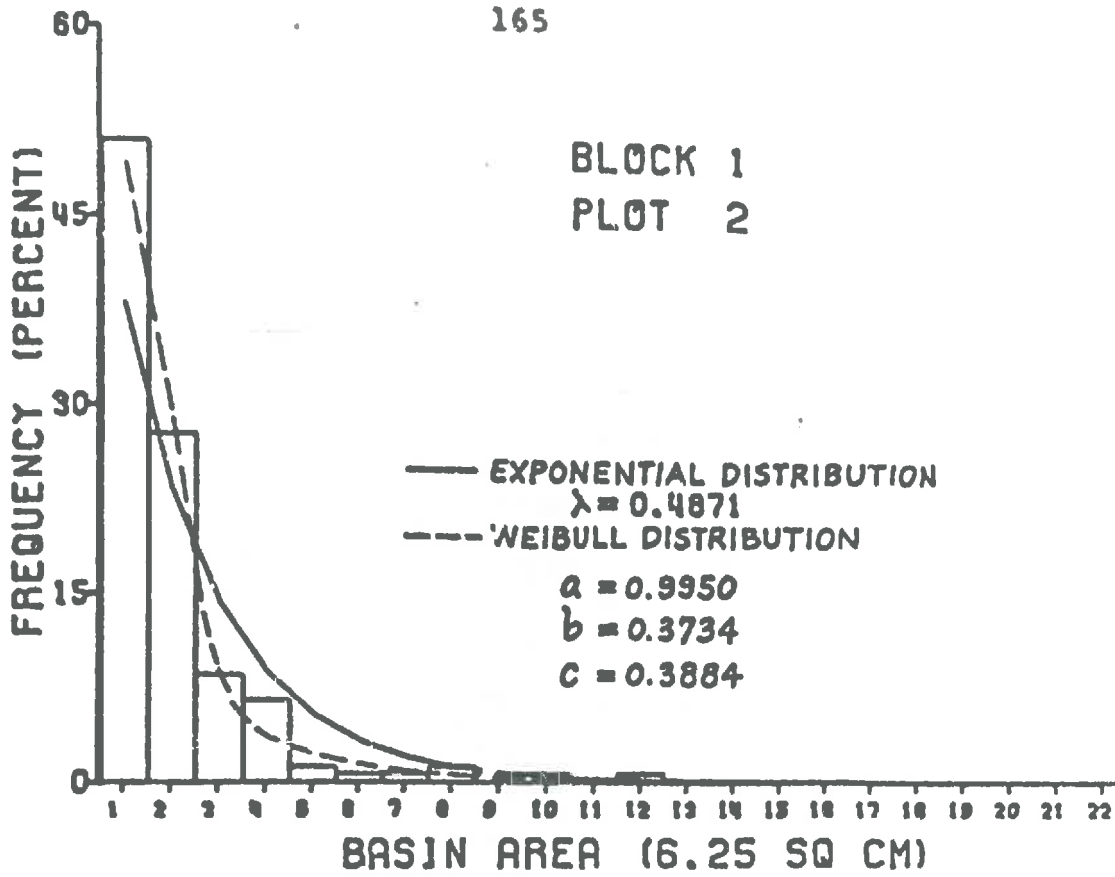


Fig. 7.10 (a)

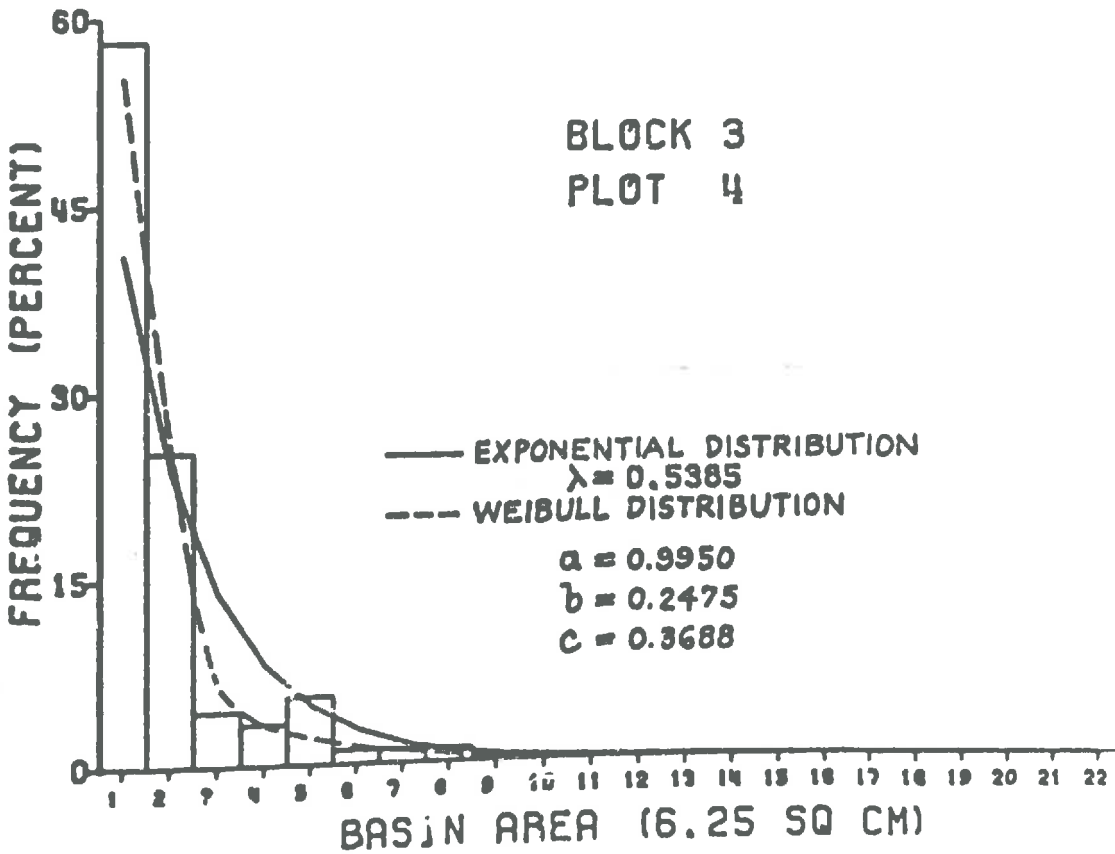


Fig. 7.10 (b)

FIG. 7.10 - HISTOGRAM OF SURFACE AREA & THEORETICAL CURVES

similar. There is also evidence of varying degrees of variations in the frequencies falling in each class in different sample plots. For a rational analysis of such data, it is advantageous to represent the frequency histograms with mathematical functions so that expected frequencies may be determined for desired classes. Such an approach could then be used in a theoretical or applied investigation related to the synthesis of watershed models. It was, therefore, considered desirable to investigate the applicability of known mathematical probability models for a description of the geometric properties of depressions.

7.27. Theoretical Probability Distribution Models

7.271. Exponential Distribution

From the above analysis it is evident that as the area, depth, or volume of depression decreases, the number of depressions, N , with that area, depth, or volume increases. Considering the limit, as SA, D or $V \rightarrow 0$, $N \rightarrow \infty$. Also, the number of depressions decreases with increasing values of area, depth, or volume. That is, as SA, D , or $V \rightarrow \infty$, $N \rightarrow 0$. One of the probability distribution models which could fit the above description is the exponential distribution. The exponential density function $f(x)$ is given by the relationship:

$$f(x) = \lambda e^{-\lambda x}, \quad x \geq 0 \text{ and } \lambda > 0$$

The mean μ_x of the distribution is given by the equation,

$$\mu_x = E(x) = \int_0^{\infty} x e^{-\lambda x} dx .$$

Integrating within the limits and solving for μ_x we get,

$$\mu_x = \frac{1}{\lambda}$$

Hence the parameter λ as a function of the moment is equal to

$$\lambda = \frac{1}{\mu_x}$$

By both methods of moments and maximum likelihood it can be shown that the unbiased estimator of the population mean μ is the sample mean \bar{x} . Therefore, the corresponding unbiased estimator of the parameter λ is given by the relationship:

$$\hat{\lambda} = \frac{1}{\bar{x}}$$

The parameter $\hat{\lambda}$ was determined for each of area, depth, and volume for all the sample plots. Substituting the value of $\hat{\lambda}$ in the above equation gives the required probability density function which is expected to fit the data. As an example, the equation describing the distribution of volume for sample plot 1/2 is given by the following relationship:

$$f(x) = 0.4075 e^{-0.4075 x}$$

where x is the volume in cc.

Relationships were developed for all geometric properties for all plots. These equations, given in Appendix A, were then used to determine the expected frequencies for each histogram class. The results are plotted on the histograms shown in Figures 7.8, 7.9 and 7.10 for volume, depth and surface area or basin area respectively.

Examination of the histograms of the observed data of volume, depth, and surface area and the corresponding theoretical curves indicates varying degrees of discrepancies in the fitting of data. As will appear from Fig. 7.8 b the occurrence of a few extreme values creates large discrepancies in the fitting of data in the first few classes. The exponential distribution, having only one parameter, lacks flexibility to account for a large range in magnitude of volume as observed in a few plots. This limitation is also evident from Fig. 7.8 c. In plots with a relatively small range in volume, the theoretical curve fits the observed data fairly well.

In the case of depth, where the range is relatively small and the distribution pattern of the frequencies in different classes is fairly comparable, the theoretical curves fit the observed data remarkably closely as can be seen in Fig. 7.9 (a, b, c and d).

In the case of surface area, the occurrence of a few extreme values in some of the sample plots resulted in an apparently poor fit of data. Also, the number of frequencies falling in the lowest classes is large compared to the volume and depth. The distribution of the frequencies is also characterized by the fact that the frequencies in the lower classes drop down more abruptly with the result that the discrepancies in the fit of data are more pronounced in the lowest class followed by class 3 onward as is evident in Fig. 7.10 (a and b). In this situation a distribution function which could provide a more steeply falling curve is likely to result in a better fit of the data.

In view of the varied nature of the frequency distribution of the observed data and the limitations of the exponential distribution it was felt that a distribution with a greater flexibility would be more appropriate to describe the distribution of the geometric properties of depressions. The Weibull distribution (Weibull 1938) which is known for its extreme flexibility in fitting exponentially distributed and also skewed data was considered an appropriate choice for investigation.

7.272. The Weibull Distribution:

The Weibull distribution function, though lacking a sound theoretical basis, has successfully been applied not only to life expectancy problems for which it was originally

intended but also to other fields such as breaking strength, reliability studies, etc. (Weibull 1938; Henderson 1965). The application of this distribution in the field of hydrology has so far been limited. Hann (1967) used this distribution function to describe the geometric properties of potholes to synthesize a watershed model. The Weibull distribution which is based on the weakest link concept is of the same form as the Fisher-Tippet type III extreme value distribution for the smallest values (Henderson 1965). The cumulative distribution function is given by the relationship:

$$F(x) = 1 - \exp\left[-\left(\frac{x-a}{b}\right)^c\right] \quad (7.1)$$

Differentiating the above equation we get the probability density function:

$$f(x) = \frac{c}{b} \left(\frac{x-a}{b}\right)^{c-1} \exp\left[-\left(\frac{x-a}{b}\right)^c\right] \quad (7.2)$$

where a , b , and c are the location, scale and shape parameters and ' x ' is a random variable. The quantity ' a ' corresponds to the position of the mode, the quantity ' b ' is the scale parameter analogous to standard deviation and the term ' c ' represents the skewness.

Lehman (1962, 1963) developed an equation for determining the parameters of the Weibull distribution by the method of maximum likelihood. Henderson (1965), after establishing the similarity between the form of the two parameter Weibull distribution and the extreme value distribution, used the

same approach for determining the parameters which is used for the extreme value distribution for large values. Hann and Beer (1967) presented a numerical method for solving the equations of the maximum likelihood estimators. The equations can be obtained as follows.

$$\text{Let } a = \left(\frac{1}{b}\right)^c \quad (7.3)$$

This transformation reduces equation 7.2 to

$$f(x) = c \alpha (x-a)^{c-1} \exp(-\alpha(x-a)^c) \quad (7.4)$$

The maximum likelihood function for the density function in equation 7.4 is given by the relationship:

$$L(a, \alpha, c) = \prod_{i=1}^n f(x_i; a, \alpha, c)$$

Substituting $f(x)$ and rearranging we get

$$L(a, \alpha, c) = c^n \frac{n}{\alpha} \prod_{i=1}^n (x_i - a)^{c-1} \prod_{i=1}^n \exp(-\alpha(x_i - a)^c) \quad (7.5)$$

The best linear unbiased estimator of the parameter a , α , c are obtained when the value of the likelihood function is a maximum. Also $L(a, \alpha, c)$ and $\log(L(a, \alpha, c))$ have their maximum at the same values of a , α , c . It is sometimes convenient to find the maximum of the logarithm of the likelihood function $L^*(a, \alpha, c)$. Taking logarithms of equation 7.5 we get

$$L^*(a, \alpha, c) = n \ln c + n \ln \alpha + (c-1) \sum_{i=1}^n \ln (x_i - a) - \alpha \sum_{i=1}^n (x_i - a)^c \quad (7.6)$$

Differentiating L^* with respect to a , α , c and setting to zero, we get 3 sets of equations which need to be solved to determine the estimators a , α , and c .

$$\frac{\partial L^*}{\partial a} = (1-c) \sum \frac{1}{(x_i - a)} + c\alpha \sum (x_i - a)^{c-1} = 0$$

or

$$(1 - c) \sum \frac{1}{(x_i - a)} + c \alpha \sum (x_i - a)^{c-1} = 0 \quad (7.7)$$

Again

$$\frac{\partial L^*}{\partial c} = \frac{n}{c} + \sum \ln (x_i - a) - \alpha \sum (x_i - a)^c \ln(x_i - a) = 0$$

Solving the above equation for c ,

$$c = \frac{n}{\alpha \sum (x_i - a)^c \ln(x_i - a) - \sum \ln(x_i - a)} \quad (7.8)$$

Similarly

$$\frac{dL}{da} = \frac{n}{a} - \sum (x_i - a)^{-c} = 0$$

Solving for a :

$$a = \frac{n}{\sum (x_i - a)^{-c}} \quad (7.9)$$

As will appear from the above, these equations cannot be solved directly for the unknowns a , α , and c .

Combining equations 7.8 and 7.9 and eliminating α we get:

$$c = \frac{n}{\frac{n}{\sum (x_i - a)^{-c}} \left[\sum (x_i - a)^{-c} \ln (x_i - a) - \sum \ln (x_i - a) \right]} \quad (7.10)$$

Equation 7.10 is solved for c for a specified value of 'a' and then α computed from the equation 7.9. The values of a , α , and c are then substituted in equation 7.6 to compute L^* . The procedure is repeated until the function L^* is maximized. A computer program has been developed at the Iowa State University which solves equation 7.11 iteratively using different values of c for a given value of 'a' until 'z' is approximately equal to zero (Hann and Beer 1967).

$$z = \frac{n}{\frac{n}{\sum (x_i - a)^{-c}} \left[\sum (x_i - a)^{-c} \ln (x_i - a) - \sum \ln (x_i - a) \right]} - c \quad (7.11)$$

The computer program obtained from Iowa State University was used to compute the parameters of the Weibull distribution for volume, depth, and surface area for all plots. These parameters are given in Appendix A. These values, when substituted in equation 7.7, give the required probability density function to determine the expected theoretical frequencies for all classes. For example the probability density function of volume for plot I/1 is given below.

$$f(x) = \frac{0.6913}{1.8472} \left(\frac{x - 0.0597}{1.8472} \right)^{-0.3087} \exp\left(-\left(\frac{x - 0.0597}{1.8472}\right)^{0.6913}\right)$$

where x is volume in cc. The program is shown in Appendix B.

The theoretical frequencies have been plotted on the histograms along with the exponential curves shown in Figures 7.8, 7.9, and 7.10. Examination of the curves for the case of volume shown in Fig. 7.8 clearly indicates that the Weibull distribution fits the observed data much better in the entire range. The occurrence of a few extreme values and an irregular distribution of observed frequencies which produced discrepancies in the exponential fit of data appear to be well accounted for by the flexibility of the Weibull distribution.

Comparison of the two curves and the observed data for depth shown in Fig. 7.9(a,b) indicates that the Weibull

distribution curve follows very closely to the exponential curve in the entire range of data. As will appear from Figure 7.9(c,d) there are minor discrepancies between the two curves in the first few classes after which the curves almost coincide. Both the theoretical distributions apparently provide a close fit of data but it is difficult to establish from visual comparison which fits the observed data better.

It is interesting to note from the plot of theoretical frequencies obtained from the two distributions shown in Fig. 7.10(a,b) that the Weibull distribution distinctly fits the observed data of surface area very closely in the entire range of classes. The specific pattern of the observed data characterized by the occurrence of a large frequency in the lowest class and an abrupt drop in frequencies in the lower classes, which produced discrepancies in the fit of the exponential curve, fit better with the Weibull distribution.

The apparent fit of data from the graphical comparison provides some qualitative indications about the appropriateness of a theoretical distribution for describing an observed frequency distribution. In order to arrive at an acceptable conclusion regarding the suitability of a distribution model, it is essential to statistically ascertain the goodness of fit between the model and the data.

7.28. Goodness of Fit Significance Test

Testing the closeness of a set of observed data and theoretical frequencies is a problem of testing a statistical hypothesis which requires a test statistic. The chi-square χ^2 statistic is appropriate for this study. The value χ^2 tests whether the observed frequencies of any phenomenon differ significantly from the frequencies which might be expected according to some assumed hypothesis. The test statistic χ^2 is defined by the relationship

$$\chi^2 = \sum_{i=1}^m \frac{(f_i - e_i)^2}{e_i}$$

where f_i is the observed frequency and e_i is the expected or theoretical frequency. The test statistic has χ^2 distribution with $(m-1)-k$ degrees of freedom where m is the number of comparisons and k is the number of unknown parameters of the theoretical distribution estimated from the sample data. The null hypothesis is that the difference between the two sets of frequencies are not statistically significant at the desired level of significance. The tabulated value of χ^2 is used as a criterion for rejecting the null hypothesis. If

$$\chi^2 = \sum_{i=1}^m \frac{(f_i - e_i)^2}{e_i} \geq \chi^2_{(m-1)-k, 1-\alpha}$$

we reject the null hypothesis.

The χ^2 values were computed for the data of volume, depth, and surface area for all the plots as shown in Appendix A. The number of groups of frequency ranged from 5 to 10 for volume, 5 to 9 for depth, and 5 to 8 for surface area. The number of groups were reduced because of pooling of the frequencies in order to have an observed frequency of 5 in each class. In this test it is also considered desirable to have about 10 classes but this requirement lacks universal agreement (King 1969). The data under study obviously did not meet this requirement in most cases. The computed χ^2 values were compared with the tabulated values at 95% and 99% levels for establishing statistical significance of the fit of data.

Examination of the χ^2 values for the volume distribution reveals that there is no significant difference between the observed frequency and expected frequency computed by the exponential density function in plots I/2 and I/5 at the 5% level of significance and in III/5 at the 1% level of significance. In the rest of the plots the differences are significant, indicating that the data does not fit the exponential distribution. The Weibull distribution fits the observed distribution at the 5% level of significance for plot I/4 and at the 1% level for plot II/5. The differences in the rest of the plots are significant implying the inability of the Weibull

distribution to fit the observed data. Comparison of the two sets of χ^2 values indicates that the χ^2 values based on the Weibull distribution are closer to the tabulated values for most plots. Also the χ^2 values are relatively uniform for all sample plots compared to those obtained by the exponential distribution. The above two points reflect on the ability of the Weibull distribution to better approximate the observed frequency distribution because of its inherent flexibility. It is also not unrealistic to assume an improved fit of data with an increase in the number of classes which in the present study seriously limit the degrees of freedom.

In the case of depth, the exponential distribution fits the observed data at the 5% level of significance for 11 sample plots and at the 1% level for 3 plots. Only in one plot are the differences significant. The corresponding numbers for the Weibull distribution are 7 and 3 respectively whereas in the remaining 5 plots the differences are significant, reflecting the inability of the Weibull distribution to fit the observed data. The remarkable performance of the exponential distribution to closely fit the observed data indicates that in this situation the one parameter distribution may be as good or better than the two or three parameter distribution. It does not adversely reflect on the appropriateness of the Weibull distribution, which also fits the observed

data in about two-thirds of the plots.

Examination of the χ^2 values in the case of surface area indicates that χ^2 values based on the exponential distribution are much larger in most of the plots compared to those obtained by the Weibull distribution. The exponential distribution does not fit the data in all the plots except one where also the significance level is 1%. It is interesting to observe that the Weibull distribution fits the observed data for 9 plots at the 5% level of significance and 4 plots at the 1% significance level. It does not fit the data in two plots where the χ^2 values are much less than those obtained by the exponential distribution. The appropriateness of the Weibull distribution to describe the frequency distribution of surface area is amply demonstrated by the results of the analysis.

As will appear from the above discussions the Weibull distribution can satisfactorily be used to describe the distribution of the three geometric properties of depressions, i.e., volume, depth and surface area. The exponential distribution may possibly prove better in the case of the frequency distribution of depth. It may be legitimately argued that the lack of an adequate fit of data does not justify the conclusion regarding the suitability of the Weibull distribution for fitting the data of volume. But considering the restraint imposed by

the limited number of classes, and the relative closeness of χ^2 values to the tabulated values, and in absence of any other suitable distribution, it is realistic to suggest that the Weibull distribution could be used for describing the geometric properties of depressions.

7.3. SURFACE ROUGHNESS

7.31. Roughness Components for the Plots

The number of profiles available for computing roughness components ranged from 57 to 62 in the sample plots under study. The means of the components of all the profiles were considered to closely represent the roughness components for the plots. In order to economize the computing time it was considered desirable to reduce the number of profiles included in the computation of the roughness components without sacrificing the accuracy of the results. With this in view the roughness components were computed for all 57 profiles of plot I/1. The means of the roughness components were computed by taking the average of 57 profiles. The means of the components were also computed for different size samples within a range of 3 to 57 in order to select a suitable sample size for subsequent analysis. The percent deviations of the sample means from the plot mean were computed and plotted against the sample size. Based on the trend of the plotted points it was decided to use about 20 profiles

for a reasonable representation of the plot mean. The percent deviation is expected to be less than 5% which seems to be reasonable in view of the observed variability in the structure of the profiles reflected in the computed values of the roughness components. It may be mentioned that the same degree of accuracy could be obtained by taking samples smaller than 20 in situations where the microtopographic variations within the plot are smaller than those observed in the plots under study.

Roughness components for every alternate profile were computed and the mean and the standard deviation determined for each plot. The number of such profiles ranged from 18 to 21. Table 7.5 shows the mean and the standard deviation of the five components of roughness: relief factor (M), slope factor (P), structural homogeneity factor (K), resistance factor (ρ), and cell length (C_L) for all the 15 sample plots.

Table 7.5. Surface Roughness Components

Plot No.	Roughness Components*									
	M		P		K		ρ		C _L	
	Mean	Sd	Mean	Sd	Mean	Sd	Mean	Sd	Mean	Sd
I/1	0.3152	0.0681	19.364	7.428	0.0813	0.0220	6.582	4.280	168.30	1.163
I/2	0.3068	0.0636	17.212	6.400	0.0816	0.0141	5.575	3.201	167.72	1.255
I/3	0.2867	0.0974	19.062	9.502	0.0884	0.0178	6.265	5.283	168.49	1.491
I/4	0.1803	0.0421	11.028	5.395	0.0931	0.0213	2.160	1.574	167.97	1.771
I/5	0.2626	0.0555	14.410	4.577	0.0875	0.0126	3.910	1.751	167.61	1.541
II/1	0.2243	0.0847	13.712	7.020	0.0840	0.0092	3.528	2.940	167.97	1.617
II/2	0.2733	0.0806	17.445	7.908	0.0803	0.0115	5.340	4.838	168.49	0.905
II/3	0.2563	0.0473	16.256	4.745	0.0813	0.0093	4.353	1.899	168.49	1.052
II/4	0.2219	0.0633	12.591	3.062	0.0849	0.0080	2.854	0.950	167.87	1.295
II/5	0.4308	0.0780	26.895	8.140	0.0875	0.0073	12.085	5.463	168.39	1.194
III/1	0.2103	0.0745	11.401	4.727	0.0854	0.0168	2.670	1.960	167.44	1.994
III/2	0.2796	0.0822	16.728	7.558	0.0849	0.0096	5.237	3.731	168.00	1.098
III/3	0.2845	0.0585	18.157	5.898	0.0835	0.0116	5.463	2.773	168.51	1.043
III/4	0.3785	0.0635	22.558	6.343	0.0851	0.0062	8.867	3.931	168.14	1.106
III/5	0.4486	0.0554	28.435	7.194	0.0855	0.0076	13.090	5.019	168.54	0.854

*M = Relief factor
P = Slope factor
K = Structural homogeneity factor
ρ = Resistance factor
C_L = Cell length

7.32. Correspondence Between Surface Structure and Roughness Components

Since the roughness components are based on the specific geometric properties of the microrelief features present on any surface, the numerical values are expected to be compatible with the physical structure of the profile. It is then possible to make visual comparison of the magnitude of each component and the corresponding property of the microrelief features exhibited by a profile taken on any surface when it is plotted on a graph. If so, it would reflect on the ability of the roughness components to quantitatively describe the specific geometric properties of the microrelief features and thereby the structure of the surface. With this premise an attempt was made to establish the expected correspondence between the surface structure exhibited by the plotted profiles and the roughness components.

Fig. 7.11 shows plottings of 5 profiles for sample plot I/1 having different geometric properties of microrelief features selected for the purpose of visual comparison. The relief factor which reflects the height of the microrelief features has a value of 0.5273 for profile No. 25. This profile exhibits microrelief features of maximum height. This is followed by profile No. 10. The least amount of roughness in terms of height is exhibited by profile No. 31 which has the lowest value of relief factor

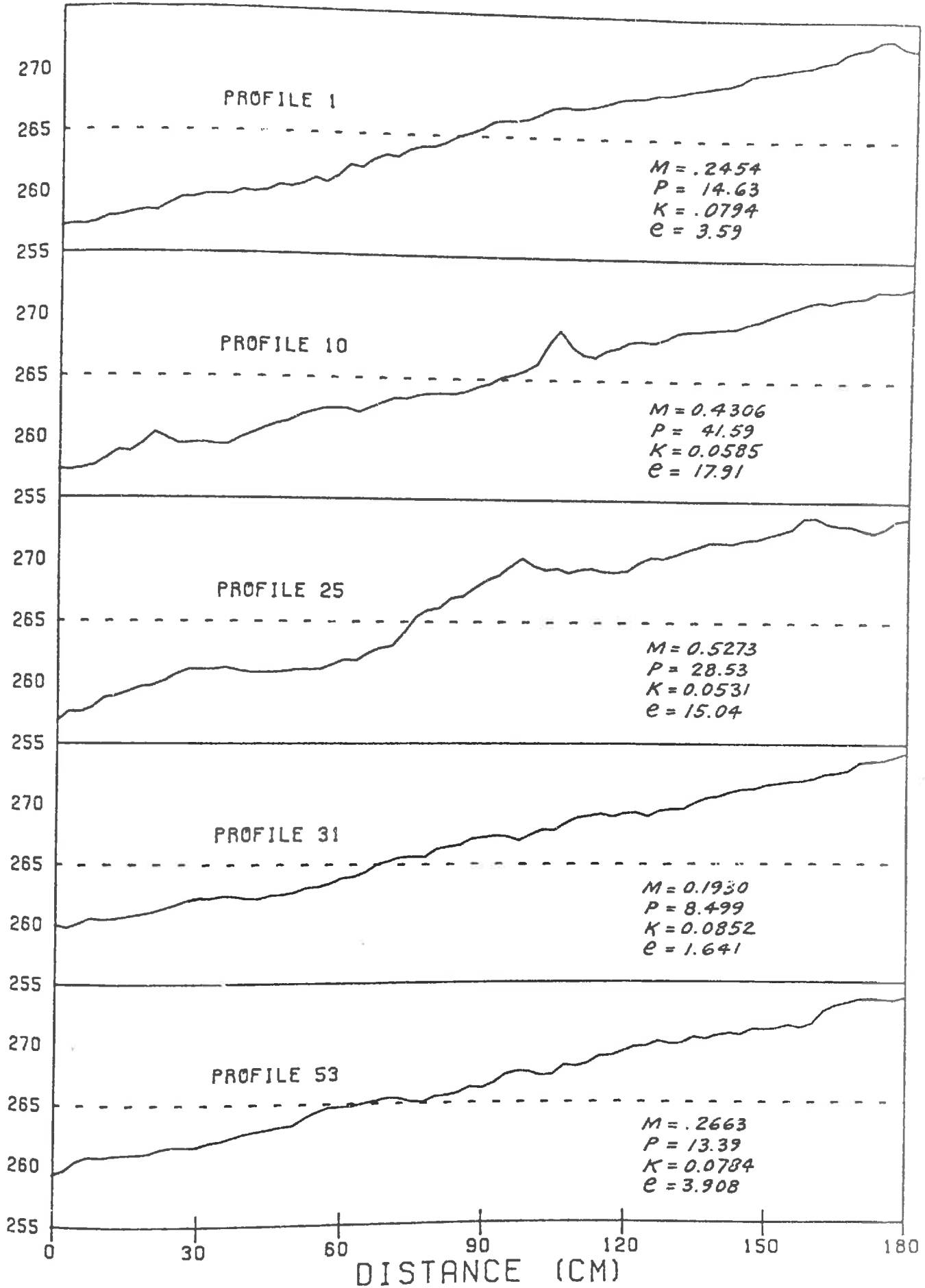


FIG. 7.11 - PLOTTINGS OF PROFILES FOR SAMPLE PLOT I/1

as, 0.1930. Profile No. 53 is rougher in terms of height than profile No. 1.

Comparison of roughness in terms of slope factor shows that profile No. 10 has the steepest slope of the microrelief features, and has the highest value of slope factor which is equal to 41.59. This is followed by profile No. 25. It could also be seen from the plotting of profile No. 31 that it has the smallest slope of the microrelief features, which is reflected in its lowest value of slope factor. Also the examination of the plotted profiles reveals that profile No. 1 is rougher than profile No. 53.

The structural homogeneity factor K , which reflects the repetitive tendency of the microrelief features, has the highest value of 0.0852 in case of profile No. 31 which otherwise has the lowest roughness both in terms of slope factor and relief factor. This is followed by profiles No. 1 and 53. The repetition of the relatively small microrelief features present in the above profiles can easily be seen in the respective plottings. Profile No. 25, which has the smallest value of the homogeneity factor, clearly indicates a small degree of repetition of the microrelief features. A similar trend is revealed by the plotting of profile No. 10 where the microrelief features having relatively large heights are not frequently repeated. It may be mentioned that the structural homogeneity factor

is not an overridingly important component of roughness in comparison with the relief and slope factors. In the case the two surfaces having similar values of the relief and slope factors, the structural homogeneity factor may help in sorting out the relative roughness. It certainly provides additional useful information about the structure of the surface.

The relative roughness of the profiles in terms of the resistance factor, which is the product of the relief factor and the slope factor, accounts for both height and slope of the microrelief features. The numerical values of the resistance factor are also comparable with the visually observed roughness of the plotted profiles. Profile No. 31, which has the lowest resistance factor, appears to have lowest roughness also. Similarly, profile No. 10 has a higher overall roughness than profile No. 25. Profile No. 1 is rougher than profile No. 53 in terms of resistance factor, which is also evident from the plottings of the profiles.

There is a very small variation in the numerical values of the cell length in all the profiles which is not explainable in terms of the apparent surface properties exhibited by the plottings of the profiles. As discussed earlier it is not an important component of roughness but provides some additional information about the surface.

The results discussed above are summarized in Table 7.6, wherein profile numbers are listed in order of increasing roughness separately in terms of four roughness components.

Table 7.6. Roughness Order of the Selected Profiles

Roughness Component	Profile No.				
Relief Factor	31	1	53	10	25
Slope Factor	31	53	1	25	10
Homogeneity Factor	25	10	53	1	31
Resistance Factor	31	1	53	25	10

It is evident from the above discussion that the roughness components truly portray the surface structure in terms of the geometric properties of the microrelief features which could be reliably used for a quantitative description of a surface.

7.33. Variability of Roughness Components

An examination of the figures of the standard deviation given in Table 7.5 reveals that there is large variation in the roughness components between the profiles within selected plots. Recalling the physical description of the

sample plots regarding the limitation of size and its possible effect on the microtopographic variability, the observed variability in the roughness components is not unexpected and in fact is compatible with visual observations of the surface. Relatively higher values of relief factor and slope factor in the case of plots II/5, III/4 and III/5 are obviously due to large irregularities of the surface. It is further noted from the figures of the standard deviation, that the variability is smaller in relief factor as compared to slope factor. The coefficient of variation of relief factor on the average ranges from 20 to 30 percent, whereas it ranges from 30 to 40 percent in the case of slope factor. Since the resistance factor is the product of relief and slope factors, the coefficient of variation is understandably higher. It ranges from 60 to 70 percent.

The variability in roughness coefficients within the sample plots is relatively smaller than that observed in the profiles of the individual plots. The magnitude of the roughness coefficients in general is comparable in most of the plots. There also does not appear to be any discernible evidence of any differing pattern in the values of roughness coefficients for the plots in each block. This was further confirmed by the results of the analysis of variance which was used to test the hypothesis of equal means for relief factor, slope factor, and

resistance factor. The results of the analysis of variance are shown in Table 7.7a, b and c.

Table 7.7. a. Analysis of Variance of Data of Relief Factor

Source of Variation	Sum of Squares	Degrees of Freedom	Mean Square	F	F _{.95}
Between Means	0.0070	2	0.0035	0.5468	3.89
Within Samples	0.0763	12	0.0064		
Total	0.0833	14	-	-	-

Table 7.7. b Analysis of Variance of Data of Slope Factor

Source of Variation	Sum of Squares	Degrees of Freedom	Mean Square	F	F _{.95}
Between Mean	26.9437	2	13.4718	0.4732	3.89
Within Samples	341.6289	12	28.4690		
Total	368.5726	14	-	-	-

Table 7.7.c Analysis of Variance of Data of Resistance Factor

Source of Variation	Sum of Squares	Degrees of Freedom	Mean Square	F	F _{.95}
Between Mean	12.1478	2	6.0739	0.5526	3.89
Within Samples	131.9138	12	10.9928		
Total	144.0616	14	-	-	-

Since the observed F value is less than the tabulated value of $F_{.95}(2,12)$ in all three cases, the hypothesis of equal means would be accepted at 5 percent level of significance. The results of the analysis clearly indicate that there is no significant difference between the blocks with respect to roughness components in the constituent sample plots. It is therefore realistic to conclude that the sample plots are representative of the surface under study with regard to roughness components.

7.34. Roughness Components and Depression Storage.

As discussed earlier the variability in the roughness components within the plots is much smaller than that observed in the case of depression storage volume. Also the observed differences are not statistically significant

in both cases of roughness coefficients and depression storage volume. These facts suggest that the differences in depression storage are not large enough to be detected by the roughness components. This is based on the assumption that the roughness components are related to depression storage which is not physically an unrealistic assumption though yet to be validated. Comparison of the figures of roughness components in Table 7.5 with corresponding values of depression storage given in Table 7.1 does not reveal any consistent trend which could suggest the existence of any relationship within the range of data.

7.4. SEASONAL CHANGES

7.41. General

The surface properties such as roughness, geometry, and the spatial distribution of depressions, etc. are highly time dependent. In this regard, the most important contributing factor is rainfall. The degree of change in properties depends on the size and stability of soil clods and aggregates, form roughness, particle roughness, and the characteristics of rainfall which provide the energy for change. The present study is confined to a quantitative evaluation of the cumulative effect of rainfall over a period of time in changing the surface properties. No attempt has been made to relate the causative factors to the degree of change occurring on a surface in relation to depression storage and surface roughness.

7.42. Depression Storage

Table 7.8 gives the depression storage volumes of six sample plots which were photographed twice subsequent to the initial photographing of 15 plots. The time intervals between the three sets of photographs were selected so as to cover the season from May to October. The initial values of depression storage are also given for comparison.

Table 7.8. Volume of Depression Storage

Date*	Plot No.	No. of Depressions	Total Volume (cc.)	Average Vol./Depression (cc.)
10-5-72	I/2	151	370.0	2.45
27-7-72	I/2(1)	55	35.4	0.64
10-10-72	I/2(2)	108	74.1	0.70
	I/4	170	779.0	4.58
	I/4(1)	138	151.2	1.10
	I/4(2)	144	157.2	1.10
	II/2	140	410.0	2.93
	II/2(1)	91	66.6	0.72
	II/2(2)	108	80.4	0.74
	II/4	120	295.0	2.46
	II/4(1)	56	24.4	0.44
	II/4(2)	66	40.3	0.61
	III/2	145	685.0	4.72
	III/2(1)	61	28.3	0.46
	III/2(2)	90	60.5	0.67
	III/4	91	149.0	1.63
	III/4(1)	74	53.6	0.72
	III/4(2)	84	65.1	0.70

*Initial measurement on 10-5-72 and subsequent measurements on 27-7-72 and 10-10-72.

An examination of the values of depression storage volume indicates a large seasonal reduction from the initial values to those obtained on 27-7-72. The reduction in volume of storage is due to both a substantial reduction in the number of depressions and the reduced depth and surface area, as is evident from the values of average volume per depression.

A further comparison of the sets of data in Table 7.8 reveals that there is a small increase in depression storage volume from 27-7-72 to 10-10-72 which is contrary to the expected trend of decreasing storage with time. The increase in volume is explained by an increase in the number of depressions, which consistently increased in all the sample plots. Even though the observed increase is insignificantly small, the consistency in trend calls for an explanation. A comparison of the figures of average volume per depression for both sets of data does not show any consistency in trend as to suggest any change in the geometric properties of depressions. The increase in volume is therefore due to an increase in the number of depressions. The increase in number of small depressions was apparently due to the effect of some disturbance to the surface of the sample plots caused by the earthworms and other insects which burrow in the soil. This remark is based on actual visual observation taken during the photographing of the plots. The increase in depression

storage is too small to suggest any significant contribution by these natural disturbances to the recovery of potential storage.

The substantial decrease of depression storage during the first part of the year suggests that it is unrealistic to assume that depression storage can be revived to its initial capacity, after infiltration and evaporation of the stored water, as done in some of the studies reviewed earlier. The assumption of a constant value of depression storage is therefore not justified. Every hydrologically significant rainfall event is likely to modify the geometric properties of depressions, resulting in a decrease in depression storage. In this process, the smaller size depressions may disappear whereas relatively large size depressions may be reduced in size.

The results of this analysis suggest that there is a rapid decrease in the volume of depression storage during the initial periods of rainfall, and at a certain point in time the potential storage capacity attains a more or less constant value. The magnitude of the final storage capacity will depend upon the initial storage capacity, soil type, slope, and rainfall characteristics. The available data in this study is not adequate to develop any mathematical expression for describing the rate of decrease of initial storage capacity with time.

It is felt that an exponential decay type curve used to describe infiltration rate might be an appropriate form of this relationship.

7.43. Geometric Properties of Depressions

Examination of the data of geometric properties of depressions indicated a considerable reduction in the values of depth and surface area and consequently storage capacity. In fact, the reduction in the total volume of depression storage was due more to a reduction in depth and surface area than to a reduction in the number of depressions. The volume of individual depressions was observed to be less than 8 cm. in most of the cases. Also most of the depressions had depths less than 0.5 cm. compared to 2 cm. observed in the initial measurements. Similarly the surface areas of depressions were less than 37.5 sq. cm., a very small area as compared to that obtained in the initial data.

The frequency distributions of volume, depth, and surface area exhibited similar patterns, with the largest frequency in the lowest class and a relatively abrupt decrease in the next lower classes. On the average, more than 85 percent of the frequencies fell in the lowest class. The remaining frequencies were distributed in the next four to five lower classes. The general trend of the frequency distributions can be seen in Fig. 7.12

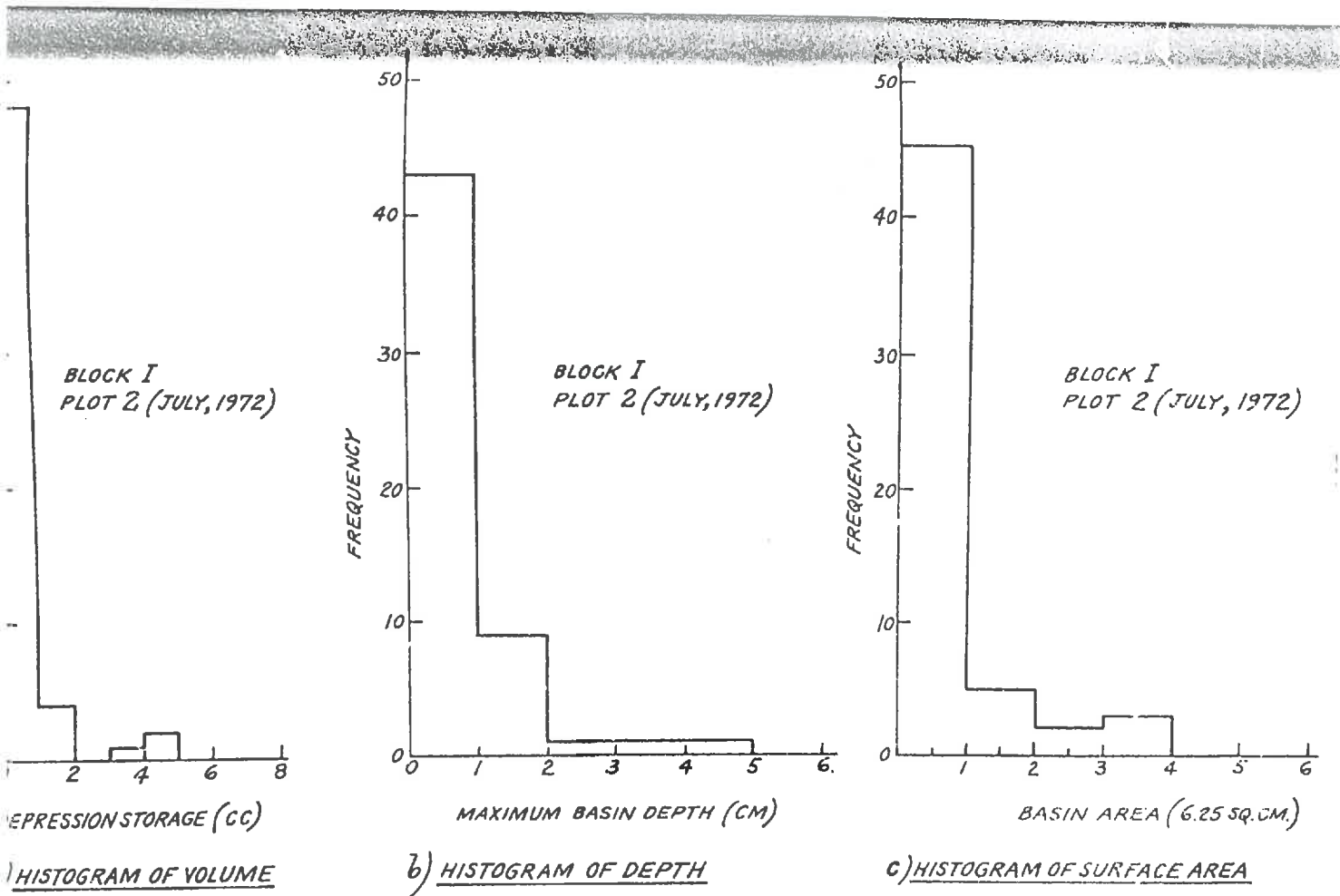


FIG. 7.12 - HISTOGRAM OF VOLUME, DEPTH AND SURFACE AREA

(a, b, and c) which show the histograms of volume, depth, and surface area, with respect to plot I/2(1). The shape of the histograms suggested that the Weibull density function could be used to approximately describe the observed frequency distribution. The fitting of a theoretical distribution was not attempted, because of an insignificant amount of depression storage and negligibly small depths and surface areas of depressions.

The relatively large size of depressions observed in the initial measurements of the surface partly or completely lost their capacity due to the process of degredation of higher points enclosing the depressions, thus lowering the pour point, and aggradation of depressional area. In effect, both these processes generated by the rainfall and overland flow occurring simultaneously in different parts of the surface jointly lead to the reduction in maximum depth and surface area of depressions. This results in the reduction of depression storage.

7.44. Surface Roughness

The roughness components of the selected sample plots were computed as done in the case of initial data. The results are shown in Table 7.9. The corresponding values of roughness components based on the initial measurements are also shown for the purpose of comparison.

Table 7.9. Roughness Components of Selected Plots.

Plot No.	Roughness Components				
	M	P	K	ρ	C_L
I/2	.3068	17.212	.0816	5.575	167.72
I/2(1)	.2649	14.331	.0825	3.836	167.71
I/2(2)	.2910	15.866	.0823	4.737	167.71
I/4	.1803	11.028	.0931	2.160	167.97
I/4(1)	.1597	9.804	.0843	1.653	168.43
I/4(2)	.1880	11.896	.0844	2.436	168.37
II/2	.2733	17.445	.0803	5.340	168.49
II/2(1)	.2509	14.426	.0837	3.739	168.07
II/2(2)	.2910	15.896	.0844	4.681	168.27
II/4	.2219	12.591	.0849	2.854	167.87
II/4(1)	.3145	19.242	.0824	6.130	168.44
II/4(2)	.3297	20.639	.0842	7.329	168.34
III/2	.2796	16.728	.0849	5.237	168.00
III/2(1)	.3285	20.420	.0853	6.902	168.48
III/2(2)	.3245	20.687	.0873	7.345	168.48
III/4	.3785	22.558	.0851	13.091	168.54
III/4(1)	.4437	27.632	.0844	12.641	168.51
III/4(2)	.3737	22.446	.0819	8.613	168.29

An examination of the values of roughness components given in Table 7.9 does not reveal any marked reduction in subsequent measurements of the surface which could be attributed to the smoothing effect of rainfall and overland flow reflected in the geometric properties of depressions. Also, the differences in the magnitude of the roughness components based on three sets of measurements do not indicate any consistent pattern or trend which could lead to an inference regarding the response of the surface to rainfall events.

A comparison of the first two sets of data indicated a small reduction in the values of relief factor, slope factor, and resistance factor for plots I/2, I/4, and II/2. This trend was reversed in plots II/4, III/2, and III/4, indicating increased roughness after rainfall. The magnitude of relief factor, slope factor, and resistance factor based on the third measurements were consistently larger by a small amount than the corresponding values based on the second measurement, except in plot III/4.

The increase in the values of roughness components after rainfall, observed in plots II/4, III/2, and III/4, was possibly due to the fact that these surfaces were subjected to varying degrees of erosion due to relatively steep slope and overall irregularity of the surface. The occurrence of erosion was evident by the existence of rill, dissections, falls, etc. in some of the plots, giving rise to a more uneven surface which was reflected in the larger values of roughness components.

This also explains the observed small increase in the values of roughness components based on the third measurement when compared to the second set of data. The results of this analysis further establishes the validity of the concept of roughness components and its appropriateness in physically describing a surface and identifying changes taking place in response to external forces.

7.45. Depression Storage and Surface Roughness

It appears from the above results that the geometric properties of depressions change noticeably with time during the year, but roughness components do not exhibit any significant change over the same interval. This trend suggests that the dynamic responses of depression storage and surface roughness are not related for the range of data under study. The differential behaviour of the two surface properties in response to the same seasonal factors calls for an objective analysis keeping in view the geometric properties of the surface and the physical processes involved.

It may be recalled that the roughness components describe the surface roughness of the entire plot studied based on the average characteristics for selected profiles. They account for irregularities of the surface caused by all microrelief features occurring within a horizontal distance of 5 to 60 cm. This range includes the irregularities caused by depressions. As mentioned earlier, the surface area of

the plots occupied by storage depressions was only 3 to 10 percent of the total area. As a result of seasonal changes, the extent of area under depressions was subsequently reduced to less than 5 percent. Thus, the proportion of the plot area involved in depression storage was very small, and although the storage characteristics may vary considerably from season to season, the influence on the total area due to depressional storage changes cannot be large.

A distinction has also to be made between a micro-relief feature contributing to roughness and forming a depression, and depression storage itself which is controlled by a pour point. The elevation of a pour point defines the boundary of a depression within the extent of a micro-relief feature. The depressional area is thus bounded by higher points of the microrelief feature which, though significantly contributing to roughness, do not contribute to depression storage. The height and extent of micro-relief features are generally larger than the depth and surface area of the depression storage elements. In the case of a lowering of the pour point by erosion, the depth and surface area of the depression would be substantially reduced with little change to the microrelief features. The extent of such changes in the geometric properties of microrelief features and the associated depression storage elements will depend on the relative differences between

their sizes. This may lead one to expect differing responses from surfaces with different depressional storage characteristics.

Under comparable soil and topographic conditions the rate and amount of such changes in time will very much depend on the size of depressions and possibly the orientation of pour points in relation to the direction of flow. Small size depressions are likely to change much faster as has been experienced in the present investigation where the depth of depressions ranged from 0.01 cm. to 2.79 cm. Since the range of depth was considerably smaller than the heights of the microrelief features, shown in Fig. 7.11, the smaller depressions completely disappeared and relatively larger depressions were reduced in size resulting in substantial reduction in depression storage with no apparent change in roughness. In situations where the depressions are relatively larger in size the results are likely to be different both in terms of contribution to overall roughness and seasonal changes. The large size depressions associated with a surface tilled with heavier implements will occupy greater a proportion of the total surface area. Also, the geometric properties of the depressional storage elements will be comparable in size with the microrelief features. Under these conditions the contribution of depressions to surface roughness of the plot is likely to be significant and may be reflected in the roughness

components. Also the rate of change in the geometric properties of depressions is likely to be relatively slow compared to small size depressions. Even in this situation, the seasonal changes in depression storage will be more pronounced, compared to changes in surface roughness, because of the vulnerability of pour points to erosion. The aggradation of depressional areas is an additional factor which reduces the depth of depressions but does not affect microrelief features.

The effect of erosional processes occurring on a surface during and after rainfall invariably results in some reduction in the geometric properties of depressions because of lowering of pour points and sedimentation of depressional areas. This may not always be true in the case of surface roughness. In fact, erosional processes may sometimes lead to higher roughness with the formation of rills and gullies. In such a situation, it may not be surprising to expect higher roughness components and substantially reduced depression storage over a period of time. In view of the observed differential behaviour of depression storage and surface roughness and the points discussed above surface roughness does not appear to be a good index of depression storage.

7.5. APPLICATION of RESULTS

It is appropriate at this stage to summarize the

salient points brought out in the discussion of the results and to make an objective assessment of their usefulness. The application of results is presented in the light of the deficiency in knowledge about the depression storage as revealed in the review of literature. It is not an attempt to describe the details of how these results can be applied but a projection of the hydrologic situations where the results of the analyses could be used with advantage. In some of the applications proposed herein the usefulness of the results of this study may have to be experimentally established.

It may be recalled that depression storage has indirectly been considered in many hydrologic investigations including conceptual hydrologic models. The direct measurement of depression storage on a natural surface has not been attempted before this study. The present study not only provides a simple technique of computing depression storage for any surface using a digital surface model but also provides information on geometric properties of individual depressions. The method is applicable to both microsurfaces and macrosurfaces.

The study reveals that the proposed technique of developing a digital surface model using a photogrammetric approach is simple, fast, and adaptable to any type and size of surface. The microsurfaces requiring estimates of

depression storage or roughness components can be photographed from close range, whereas macrosurfaces can be photographed by an airborne camera from any predetermined height. The choice of height will depend upon the required scale of the photographs which in turn will depend on the size of topographic variations of interest to the investigator. The photographs can then be used to develop a digital surface model.

The photogrammetric method requires the use of a stereocomparator or other similar instrument for measuring photographs and for digitizing data. The high cost of such instruments may be considered as an apparent disadvantage of this method. However, these instruments are generally available in a photogrammetric laboratory as part of basic laboratory equipment and so cannot be considered to be a limitation. In contrast, the especially designed point gauges referred to in the literature, in addition to being expensive, have serious limitations such as limited coverage and adaptability to different types of surfaces. They are also time consuming, and lack sufficient control after the instrument is set for any grid distance. The photogrammetric approach does not suffer from any of the above limitations.

The results of the reported study make it possible to directly measure depression storage on any surface. This includes small size depressions associated with micro-

surfaces and large size natural or artificial depressions existing on macrosurfaces. The only data required is a digital surface model. The measured values of depression storage, when used in a general storage equation, will allow a more realistic relationship to be developed between detention storage and runoff for any area. This will also eliminate the error introduced by an arbitrarily selected value of depression storage in hydrologic data analysis including simulation models.

Depression storage materially varies from watershed to watershed and also within any given watershed, depending upon the geomorphic setting, topographic features, and management practices. The spatial variability of depression storage calls for some type of classification of the watershed area. Since the systems of land form, evolved under the same geomorphic processes, exhibit a certain degree of geometric similarity, their description is amenable to classification. The area under each geomorphic class can be further subdivided on the basis of slope, vegetation, and management practices. Some of the classifications such as soil-cover complex (Chow 1964), land capability classification (Klingebiel and Montgomery (1961), and geomorphic grouping of soil (England and Onstad 1968; England and Holtan 1969; and England 1970) can satisfactorily be used to delineate hydrologic response units for the determination of depression storage. The

depression storage values for all such units may then be weighted to compute depression storage for a watershed. This will yield a realistic estimate for use in any investigation dealing with the response of a hydrologic system.

The study also reveals that significant relationships exist between the three important geometric properties of depressions, ie. volume, depth, and surface area. The form of the relationship is applicable to any size of depression indicating similarity of physical processes involved in the forming of a depression. For example, an increase in depth will require an increase in surface area within the constraints imposed by the soil properties. These relationships could be usefully utilized in computing one with the help of the other.

Additionally, the data regarding geometric properties of individual depressions can be processed to obtain relevant frequency distributions. This will not only provide information on the total volume of depression storage but the contribution by depressions of different size groups to the total storage and total depressional area. This information may be incorporated in simulation models for developing an appropriate parameter of depression storage and its time distribution.

For a realistic simulation of watershed response, a

conceptual hydrologic model must account for the rate of accretion to and depletion from depression storage. This is possible only if the information on geometric properties and their frequency distribution are available. The availability of such data will provide information on the total area under depressions which will initially not contribute to runoff. As the rainfall continues, smaller depressions will be filled up and part of the surface area under depressions will start contributing to runoff. With the passage of time, larger size depressions will be filled up and will start contributing to runoff. This process will continue till practically all the area under depression will start contributing to runoff. With a reliable estimate of excess rainfall ($P - F$) and the rates of inflow to the depressions, it is possible to almost reproduce the runoff generation process. The rate of inflow to a depression will depend upon its drainage area which has to be determined for each depression. Though it has not been attempted in this study, it is possible to use a similar logic for determining the catchment areas of all depressions.

As pointed out by Linsley (1967), it is not the flow routing technique which is responsible for the present inability of hydrologic models to reproduce watershed response, but the lack of quantitative data about the hydrologic processes such as depression storage and infiltration rate. The present study provides a technique of determining most

of the information about depression storage required in the analysis of hydrologic data. It is now possible to develop realistic parameters of the hydrologic models based on the measured values of depression storage. For example, the approach suggested by Claborn and Moore (1970) using a hypothetical distribution of depression storage could be used with the measured data as briefly discussed below.

Claborn and Moore (1970) assumed a parabolic relationship between the area producing runoff via depression storage and the fraction of volume in depression storage to describe the time distribution of storage in their proposed watershed simulation model. The relationship is shown in Fig. 7.13. This was based on a preliminary analysis involving hypothetical size distributions of depressions visualized to exist on watershed surfaces. Normalized area-volume histograms, considered in the above relationship, are shown in Fig. 7.14. Since the above relationship was not based on observed data, it was considered worthwhile to use the data of the geometric properties of depressions presented in this study for checking the validity of the above assumptions.

Instead of a normalized area-volume histogram, as given by Claborn and Moore (1970), a depth-surface area histogram was drawn using data of sample plot I/1. Since depth was found to be linearly related to volume, the shapes of the histograms may be expected to be similar. The resulting histogram was comparable to basin 'a' of Claborn and Moore

Fraction Depression Storage Oriented Area Producing Runoff to Stream

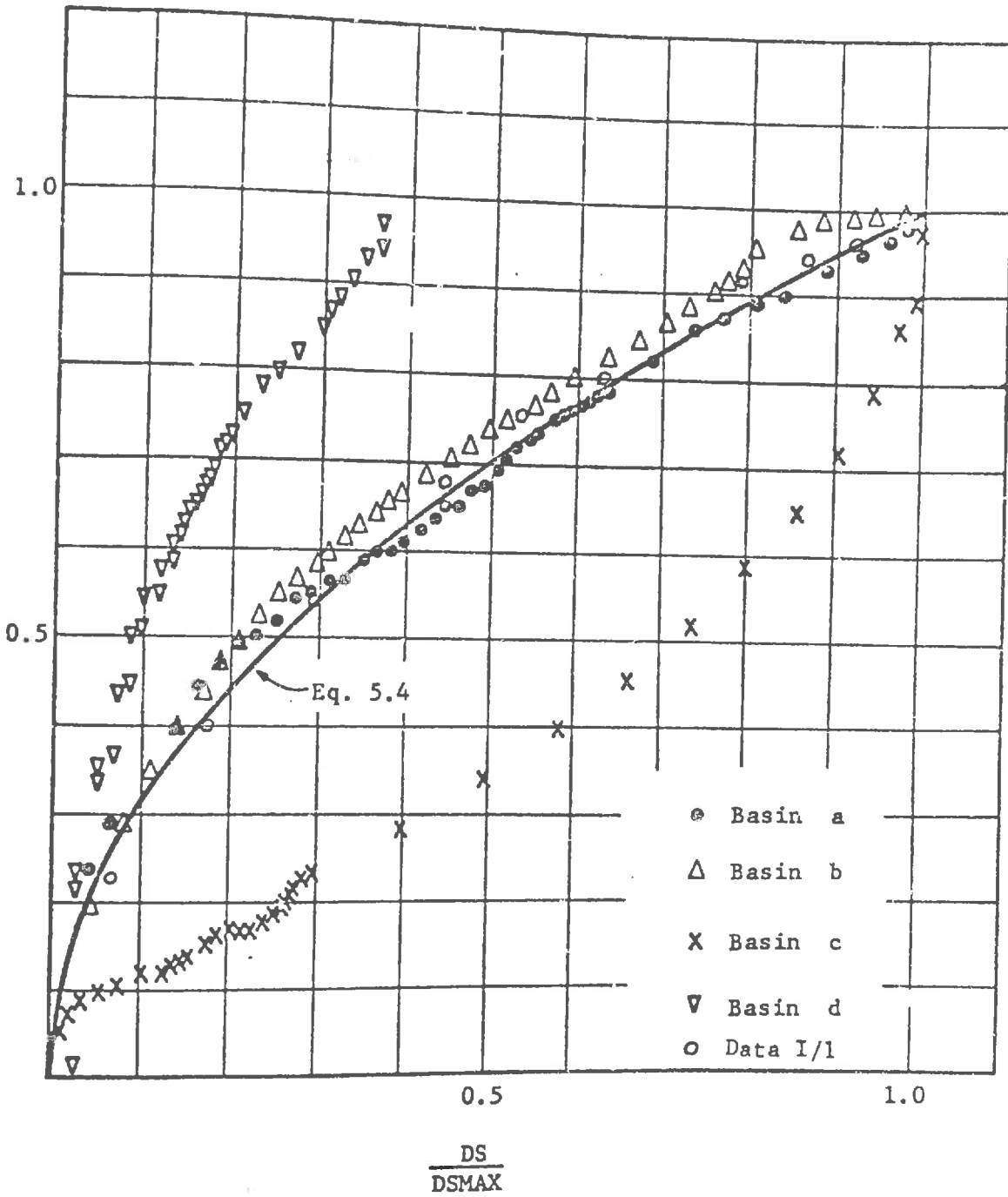


FIGURE 7.13. INFLUENCE OF DEPRESSION STORAGE CHARACTERISTICS ON FRACTION OF AREA PRODUCING RUNOFF. (After Claborn and Moore 1970)

Note: The units of depth are L where the volume has units of L^3

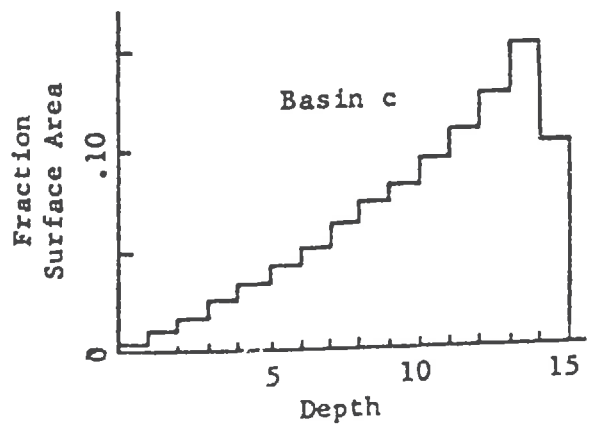
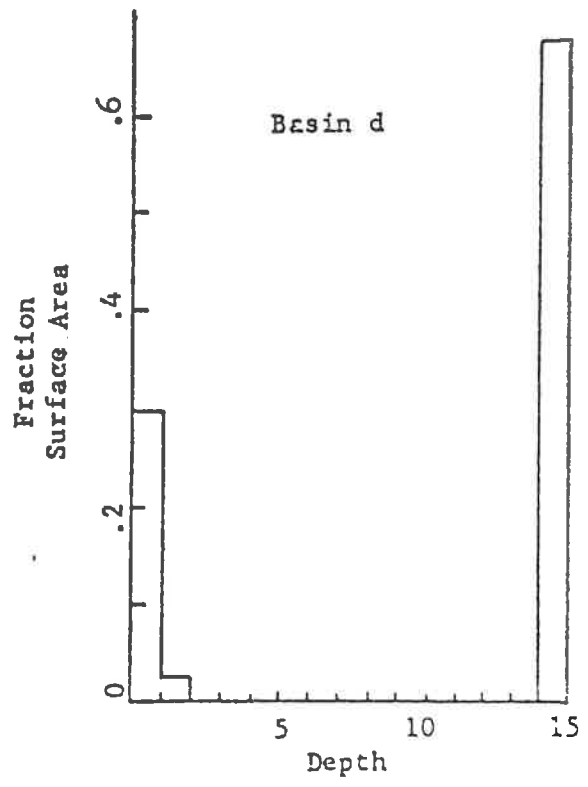
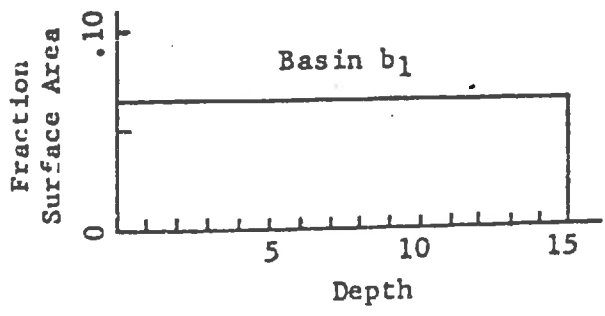
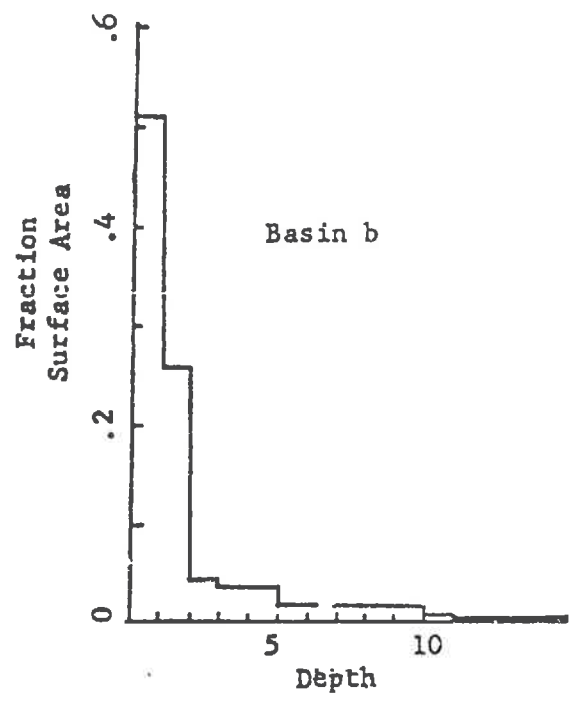
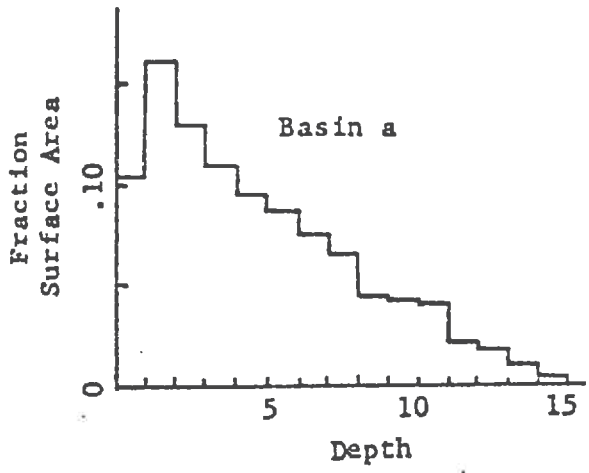


FIGURE 7.14. NORMALIZED AREA-VOLUME HISTOGRAMS. (After Claborn and Moore 1970)

(1970), except for class 1 which had the highest proportion. It is evident from this result and the frequency distribution of geometric properties discussed earlier that basins 'a' and 'b' of Claborn and Moore (1970) reflect reasonable assumptions for depression storage.

Using the same data, ratios of the actual volume of depression storage to the maximum volume were plotted against the corresponding fraction of depressional area producing runoff, as shown in Fig. 7.13. The closeness of the plotted points to the theoretical curve again supports the validity of the assumed relationship. The above application of the results strengthens the earlier assertions that information on the geometric properties of depressions, existing relationships between the three properties, and their statistical distributions, can be usefully utilized in the development of model parameters. The time distribution of volume and surface area on any surface can satisfactorily be described by their cumulative distribution functions. In fact Claborn and Moore (1970) suggested the use of an exponential function to describe the time distribution in basins 'c' and 'd'.

It has been established by the results of this study that the frequency distribution of geometric properties can be satisfactorily described by the exponential and Weibull density functions. Again these theoretical distributions appear to be applicable to all types and sizes of depressions. This information can then be used in a theoretical investigation, using a computer model of a watershed, to

evaluate the effect of depression storage on the system response. It may be recalled that Crawford (1969) reported a significant effect of depression storage on the watershed response. The availability of quantitative data will make such investigations more realistic and purposeful. For example, it may be desirable in some situations to manipulate a surface to increase depression storage in order to obtain a desired system response.

The results of the present study also reveal that roughness components based on the Fourier series analysis closely portray the physical structure of a surface and therefore provide a useful method of quantitatively describing a surface. Since the roughness components represent specific physical properties of a surface, it is possible to compare the relative roughness of two or more surfaces in terms of any geometric property.

As pointed out earlier, the two surface properties, ie. depression storage and surface roughness, control the response of a surface system. The physical description in terms of roughness components can be used to compare two or more surfaces having differing hydrologic responses. The observed variabilities in the hydrologic responses could be explained in terms of any specific geometric property associated with any surface which will be reflected in the magnitude of roughness components. This would lead to a better understanding of the runoff process occurring on

a surface.

Despite considerable efforts devoted to overland flow investigations, using equations of motion and continuity, it has not been possible to develop any method of estimating the hydraulic roughness of a surface under study. A reasonable estimate of roughness of a watershed surface is all the more difficult. Since the surface irregularities which contribute to hydraulic roughness are reflected in the roughness components, it may be possible to experimentally obtain a relationship between the roughness components and the corresponding hydraulic roughness. These relationships could then be used to compute hydraulic roughness with the help of roughness components.

The information on the physical description of a surface could also be utilized in the development of a physical watershed model. The usefulness of such a model is at present limited partly because it fails to represent a natural surface and also because there is no way to evaluate it. The comparison of roughness components obtained on any natural surface and the surface of a corresponding physical model may provide a basis for evaluating the representativeness of the physical model surface. If this could be achieved, the usefulness of a physical model for evaluating the hydrologic response under different surface conditions would be much enhanced.

8. CONCLUSIONS

The study reported in this thesis leads to the following conclusions.

1. The photogrammetric approach used to develop a digital surface model is well adapted to both microsurfaces and macrosurfaces for determining surface properties.
2. The spatial distribution of depressions on a surface has both random and direction oriented components.
3. The proposed method of determining depression storage, using a digital surface model, is simple, fast, reliable, and adaptable to any type of surface. The method provides information on important geometric properties of depressions i.e. volume, depth, and surface area.
4. The available data indicate a significant relationship between land slope and total volume of depression storage. The reduction in total volume of storage with increasing slope was both due to reduction in the number of depressions and reduced depths and surface areas of depressions.
5. There exist definable relationships among the three geometric properties of depressions

which could be used to compute one with the help of the other. The form of the relationships appears to be applicable to all sizes of depressions.

6. The frequency distribution of the three geometric properties can be approximated by a three parameter Weibull probability density function.
7. Roughness components based on Fourier series analysis adequately portray the physical structure of a surface and therefore provide a good method of quantitative description of surface roughness.
8. There is no relationship between depression storage and surface roughness within the range of data reported in this study.
9. Seasonal effects are very pronounced in reducing the volume of depression storage.

REFERENCES

- Adamowski, K. (1969). Stochastic analysis of daily river flow time series. Unpublished Ph.D. Thesis, University of Guelph, Guelph, Ontario, p. 73
- Allmaras, R.R., R.E. Burwell, W.E. Larson and R.F. Holt (1966). Total porosity and random roughness of the interrow zone as influenced by tillage. Conservation Res. Report No. 7. A.R.S., U.S.D.A., Washington, D.C.
- A.S.C.E. (1969). Design and construction of sanitary and storm sewers. W.P.C.F. manual of practice No. 9. American Society of Civil Engineers and Water pollution Control Federation, Washington, D.C.
- Barron, N.A. (1971). Soil surface depression storage calculated by geometrical models. Unpublished M.Sc. Thesis, University of Illinois at Urbana-Champaign, Urbana, Illinois.
- Beckmann, P. and A. Spizzichino (1963). The scattering of electromagnetic waves from rough surfaces. International Series of Monographs on electromagnetic waves, Vol. 4, Macmillan Co., p. 503.
- Bogdanoff, J.L. and F. Kozin (1962). On the statistical properties of the ground contour and its relation to the study of land locomotion. Report No. 7823, LL78. U.S. Army Tank-Automobile Centre, Detroit Arsenal, Centre line, Michigan.
- Bogdanoff, J.L. et al. (1966). Atlas of off-road ground roughness P.S.D.'s and report on data collection technique. Technical Report No. 9387, LL109. Land Locomotion Laboratory. U.S. Army Tank Automotive Centre, Warren, Michigan.
- Boughton, M.E. (1966). A mathematical model for relating runoff to rainfall with daily data. Civil Engineering Transactions, The Institution of Engineers, Australia, Vol. CE8:1, pp. 83-97.
- Brater, E.F. and S. Sangal (1969). Effects of urbanization on peak flows. Published in "Effects of watershed changes on streamflow". Edited by W.L. Moore and C.W. Morgan, University of Texas Press, Austin and London.

- Burwell, R.E., and R.R. Allmaras and M. Amemiya (1963).
A field measurement of total porosity and surface
microrelief of soils. Proc. Soil Sci. Soc. Amer.,
Vol. 27, pp. 697-700.
- Chow, V.T. (1964). Handbook of Applied Hydrology.
McGraw-Hill Book Company, Inc., Toronto.
- Claborn, B.J. and W.L. Moore (1970). Numerical sim-
ulation of watershed hydrology. Tech. Rep.
HYD14-7001. Hydraulic Engineering Laboratory,
Department of Civil Engineering, The University of
Texas at Austin.
- Crawford, N.H., and R.K. Linsley (1966). Digital
simulation in hydrology: The Stanford Watershed
Model IV. Technical Report 39, Department of
Civil Engineering, Stanford University, p. 212.
- Crawford, N.H. (1969). Analysis of watershed changes.
Published in "Effects watershed changes on streamflow."
Edited by W.L. Moore and C.W. Morgan, University
of Texas Press, Austin and London.
- Currence, H.D. and W.G. Lovely (1969). The analysis
of soil surface roughness. Presented at the 1969
annual meeting, American Society of Agricultural
Engineers, Purdue University, W. Lafayette, Indiana.
June 22-25, 1969.
- Dixon, W.J. and F.J. Massey, Jr. (1957). Introduction
to statistical analysis. McGraw-Hill Book Company,
Inc., Toronto.
- Dunin, F.X. (1969). A model for rainfall routing during
initial abstraction. J. Hyrdol., Vol. 7, pp. 57-72.
- England, C.B. and C.A. Onstad (1968). Isolation and
characterization of hydrologic response units
within agricultural watersheds. Water Resources
Research, Vol. 4, No. 1. pp. 73-77.
- England, C.B. and H.N. Holtan (1969). Geomorphic group-
ing of soils in watershed engineering. J. Hydrol.,
Vol. 7, pp. 217-225.
- England, C.B. (1970). Land capability: A hydrologic
response unit in agricultural watersheds. A.R.S.
41-172, Agricultural Research Service, U.S. Dept.
Agr. p. 12.

- Ghosh, A.K. (1971). A study of natural wiggly lines in hydrology. Unpublished Ph.D. Thesis, University of Illinois at Urbana-Champaign, Urbana, Illinois. p. 250.
- Haan, C.T. (1967). Hydraulics of watersheds characterized by depressional storage. Unpublished Ph.D. Thesis, Iowa State University of Science and Technology. p. 186.
- Haan, C.T. and C.E. Beer (1967). Determination of maximum likelihood estimators for the three parameter Weibull distribution. Iowa State Journal of Science, Vol. 42, No. 1, pp. 37-42.
- Harbaugh, J.W. and D.F. Merriam (1968). Computer applications in stratigraphic analysis. John Wiley and Sons, Inc., New York, p. 282.
- Harley, I.A. (1966). The calibration of cameras for non-topographical photogrammetry. Paper presented at Symposium of the ISP, Commission V. Tokyo, Oct. 13-18, 1966.
- Henderson, A.J. (1965). The Weibull distribution and industrial property mortality experience. Unpublished M.S. Thesis, Iowa State University Library, Ames, Iowa.
- Hicks, W.I. (1944). A method of computing urban runoff. Trans. Am. Soc. Civil Engrs., vol. 109, pp. 1217-1253.
- Hills, R.C. (1971). The influence of land management and soil characteristics on infiltration and the occurrence of overland flow. J. Hydrol., Vol. 13, pp. 163-181.
- Hobson, R.D. (1967). Fortran IV programs to determine surface roughness in topography for the CDC 3400 computer. Computer contribution No. 14. State Geological survey. The University of Kansas, Lawrence, U.S.A.
- Holtan, H.N. (1945). Time condensation in hydrograph analysis. Trans. Am. Geophys. Union, Vol. 26, pp. 407-413.
- Horner, W.W. and C.L. Lloyd (1940). Infiltration capacity values. Trans. Am. Geophys. Union, Vol. 21, pp. 522-541.

- Horton, R.E. (1939). Analysis of runoff-plat experiment with varying infiltration capacity. Trans. Am. Geophys. Union, vol. 20, pp. 693-711.
- Houbolt, J.C. (1961). Runway roughness studies in the aeronautical field. Jour, Air Transport Div., Am. Soc. Civil Engrs. 87(AT-1), pp. 11-31.
- Ketcheson, J.W. and J.J. Onderdonk (1973). Effect of Corn Stover on phosphorous in runoff from non-tilled soil. Agron. J. Vol. 65, pp. 69-71.
- King, L.J. (1969). Statistical analysis in geography. Prentice-Hall, Inc., Englewood Cliffs, N.J. p. 288.
- Klingebiel, A.A. and P.H. Montgomery (1961). Land-Capability Classification. U.S. Department Agr. Handbook 210.
- Kozin et al. (1964). Statistical studies of stable ground roughness. Report No. 8391, LL95. U.S. Army Tank-Automotive Centre, Warren, Michigan.
- Kozin et al. (1968). Supplement to the Atlas report of off-road ground roughness. Technical Report No. 10316, LL130, Land Locomotive Command, Warren, Michigan.
- Kuipers, H. (1957). A reliefmeter for soil cultivation studies. Netherlands Journ. of Agr. Sci. Vol. 5, pp. 255-267.
- Lee, R.J. (1972). Some relationships between the surface energy budget and the water budget. Publication in Meteorology No. 106. Arctic Meteorology Research group, Department of Meteorology, McGill University, Montreal.
- Lehman, E.H. (1962). Estimation of the scale parameter in the Weibull distribution using samples censored by time and by number of failures. The Institute of Statistics, North Carolina State University. Technical paper No. 1. (Mimeo).
- Lehman, E.H. (1963). Shapes, moments and estimators of the Weibull distribution. IEEE Trans., Reliability, R-12. pp. 32-38.
- Linsley, R.K., Jr., M.A. Kohler, and J.L.H. Paulhus (1949). Applied Hydrology. McGraw-Hill Book Company, Inc., New York.

- Linsley, R.K. (1967). The relation between rainfall and runoff. *J. Hydrol*, Vol. 5, pp. 297-311.
- Luttrell, D.H. (1963). The effect of tillage operations on bulk density and other physical properties of soil. Unpublished Ph.D. dissertation, Iowa State University of Science and Technology, Ames, Iowa.
- Merva. G.E., R.D. Brazee, G.O. Schwab and R.B. Curry (1970). Theoretical considerations of Watershed surface description. *Trans. Am. Soc. Agri. Engrs.*, Vol. 13, No. 4. pp. 462-465.
- Mitchell, J.K. (1970). Microrelief surface depression storage. Unpublished Ph.D. Thesis, University of Illinois at Urbana-Champaign, Urbana, Illinois. 203 pp.
- Mitchell, J.K. and B.A. Jones, Jr. (1971). "Clodhopper" helps with soil studies. *Illinois Research*, Fall, pp. 10-11.
- Moffitt, F.H. (1967). *Photogrammetry*. International Textbook Co., Scranton, Pa., Second Edition.
- Moffitt, F.H. 1968. Wave surface configuration. *Photogrammetric Engineering*. Vol XXXIV, No. 2. p. 179.
- Natarajan, T. (1969). Analytical block triangulation with increased overlaps. Unpublished M.A.Sc. Thesis, University of Toronto, Toronto, Ontario.
- Natarajan, T. (1972). Digital terrain analysis. Unpublished Ph.D. Thesis, University of Toronto, Toronto, Ontario. pp. 302.
- Paulin, A.O. (1961). Photogrammetry and frost action. *The Military Engineer*, July-August. p. 268.
- Press, H. and J.W. Tukey (1963). Power spectral methods of analysis and their application to problems in airplane dynamics. *AGARD Flight Text Manual*. Vol. IV, Part IVC (Revised).
- Rice, S.O. (1951). Reflection of electromagnetic waves from slightly rough surfaces. *Comm, on Pure and Applied Mathematics*. Vol. IV.
- Riley, J.P. and V.V.D. Narayana (1969). Modelling the runoff characteristics of an urban watershed by means of an analog computer. Published in "Effects of watershed changes on streamflow". Edited by W.L. Moore and C.W. Morgan, University of Texas Press, Austin and London.

- Rosenfield, G.H. (1966). Various applications of photogrammetry. Chapter XX in "Manual of photogrammetry", edited by M.M. Thompson, Vol. II, 3rd ed. Published by the American Society of Photogrammetry, 6269, Leesburg, Pike Falls Church, Va. pp. 961-998.
- Scheidegger, A.E. (1964). Some implications of statistical mechanics in geomorphology. Internat. Assoc. Sci. Hydrol., Bull., V. 9, No. 1, pp. 12-16.
- Schut, G.H. (1966). A Fortran program for the adjustment of strips and blocks by polynomial transformations. N.R.C. Ottawa, Publication NRC-9625.
- Schut, G.H. (1966). An introduction to analytical strip triangulation with a Fortran program. N.R.C., Ottawa, Publication NRC-9369.
- Sharp, A.L., and H.N. Holtan (1940). A graphical method of analysis of sprinkled-plot hydrographs. Trans. Am. Geophys. Union, Vol. 21, pp. 558-570.
- Sharp, A.L., and H.N. Holtan (1942). Extension of graphic methods of analysis of sprinkled-plot hydrographs to the analysis of hydrographs of control plots and small homogeneous watersheds. Trans. Am. Geophys. Union, Vol. 23, pp. 578-593.
- Sherman, L.K. (1940). Derivation of infiltration capacity from average loss rates. Trans. Am. Geophys. Union, Vol. 21, pp. 541-550.
- Stammers, W.N. (1956). The effect of slope and microtopography on depression storage and surface detention. M.Sc. Thesis, University of Guelph, Guelph, Ontario.
- Stammers, W.N., and H.D. Ayers (1957). The effect of slope and microtopography on depression storage and surface detention. International Association of Hydrology. Proceedings, General Assembly, Toronto, Ontario.
- Stone, R.O. and J. Dugundji (1965). A study of microrelief - its mapping, classification, and quantification by means of a Fourier analysis. Eng. Geol., Vol. 1(2), pp. 89-187.
- Thakur, R.T. (1970). Statistical models of river meanders. Unpublished Ph.D. Thesis, University of Illinois at Urbana-Champaign, Urbana, Illinois. p. 151.

- Tholin, A.L. and C.J. Keifer (1960). The hydrology of urban runoff. Trans. Am. Soc. Civil Engrs., Vol. 125, pp. 1308-1379.
- Viessman, W. Jr. (1968). Runoff estimation for very small drainage areas. Water Resour. Res., 4(1), pp. 87-93.
- Van der Vliet, A.D. (1969). An application of analytical photogrammetry to a cadastral survey. Unpublished M.A.Sc. Thesis, University of Toronto, Toronto, Ontario.
- Weibull, W. (1938). Investigations into strength properties of brittle materials. Proc. The Roy. Swedish Inst. for Engr. Res. Nr. 149.
- Wijk, M.C. Van. (1972). National Res. Council of Canada, Ottawa, Ontario. (In personal communication).
- Willeke, G.E. (1966). Time in urban hydrology. Hydraul. Div. J. Am. Soc. Civil Engrs., 92, No. HYI, Proc. Paper 4615, pp. 13-29.
- Zeller, M. (1952). Translated by E.A. Miskin and R. Powell. Text Book of Photogrammetry. H.K. Lewis and Co. Ltd., London.

ACKNOWLEDGEMENTS

The author wishes to express his deep sense of gratitude and appreciation to Dr. W.T. Dickinson, who supervised this study, for his unfailing help, guidance and encouragement. He is also indebted to Prof. S.H. Collins for his helpful suggestions which were very valuable. Thanks are also due to Dr. J. W. Ketcheson of the department of Land Resource Science for his suggestions and time in going through the manuscript. The help and encouragement received from Prof. H.D. Ayers, Director of the School of Engineering is gratefully acknowledged.

The author also wishes to express his grateful thanks to his friends and fellow students particularly R.J. Shillum, A.G. Bobba, P. Stewart, and R. MacMillan for their help in operating the camera and processing of photographs.

The author expresses his sincere thanks to Dr. T. Natarajan of the University of Toronto for his help in digitizing and processing of photo plates in the photogrammetric laboratory.

Thanks and appreciations are also due to Dr. A. Sheth, S. Hayes and S. Field of the Institute of Computer Science of the University of Guelph for their help in developing a computer program.

Financial assistance received from the National Research Council of Canada is acknowledged with thanks.

Finally the author wishes to gratefully acknowledge the

cooperation, understanding and sacrifices of his family, particularly his wife, which meant a difference between success and failure.

APPENDIX - A

Parameters of Probability Distribution Models

Parameter of Exponential Distribution* for Volume, Depth and Surface Area of Depressions.

Sample Plot No.	Parameter λ		
	Volume	Depth	Surface A
I/1	0.3314	0.4561	0.4657
I/2	0.4075	0.4879	0.4871
I/3	0.1509	0.3720	0.3935
I/4	0.2180	0.3080	0.3953
I/5	0.1136	0.3670	0.4092
II/1	0.3104	0.4779	0.4676
II/2	0.3417	0.4762	0.3857
II/3	0.2762	0.5720	0.4555
II/4	0.4062	0.6091	0.4959
II/5	0.5297	0.4718	0.5459
III/1	0.2238	0.4157	0.3588
III/2	0.2117	0.5133	0.4662
III/3	0.3074	0.8366	0.4816
III/4	0.6124	0.6618	0.5385
III/5	0.7517	0.6426	0.6013

*Exponential distribution function,

$$f(x) = \lambda e^{-\lambda x}, \quad x \geq 0.$$

Parameters of Weibull Distribution* for Volume, Depth and Surface Area of Depressions.

Sample Plot No.	Parameters, a, b, c.								
	Volume			Depth			Surface Area		
	a	b	c	a	b	c	a	b	c
I/1	0.0597	1.8825	0.6635	0.0995	2.0023	0.8819	0.9950	0.3812	0.3869
I/2	0.0597	1.8472	0.6913	0.0995	1.9830	0.8661	0.9950	0.3734	0.3884
I/3	0.0597	2.7873	0.6744	0.0995	2.5664	0.9446	0.9950	0.7036	0.4233
I/4	0.0895	3.5269	0.8699	0.0798	3.4938	1.3312	0.9950	0.7704	0.4484
I/5	0.0398	2.6859	0.6938	0.0971	2.6444	1.0413	0.9950	0.4062	0.3706
II/1	0.0597	1.7500	0.6314	0.0995	1.7958	0.7684	0.9950	0.5416	0.4114
II/2	0.0597	1.9437	0.6065	0.0995	1.8683	0.8635	0.9950	0.4751	0.3863
II/3	0.0597	1.3951	0.5861	0.0995	1.4661	0.7675	0.9950	0.3029	0.3718
II/4	0.0597	1.1658	0.5759	0.0995	1.2696	0.7340	0.9950	0.3427	0.3872
II/5	0.0398	1.7939	0.8247	0.0995	1.9121	0.8841	0.9950	0.3043	0.3933
III/1	0.0597	2.2722	0.5760	0.0995	2.0861	0.8056	0.9950	0.5290	0.3636
III/2	0.0597	1.4818	0.5279	0.0995	1.6251	0.7931	0.9950	0.2143	0.3541
III/3	0.0597	0.8224	0.4911	0.0995	0.8704	0.6371	0.9950	0.1942	0.3472
III/4	0.0398	1.1989	0.6896	0.0995	1.1824	0.7490	0.9950	0.2475	0.3688
III/5	0.0298	1.1153	0.7698	0.0995	0.9999	0.6164	0.9950	0.2389	0.3953

*Weibull distribution function $f(x) = \frac{c}{b} \left(\frac{x-a}{b}\right)^{c-1} \exp\left(-\left(\frac{x-a}{b}\right)^c\right)$

Data of Test For Goodness of Fit of Volume, Depth and Surface Area.

Sample Plot No.	Computed χ^2 Statistic ^ψ					
	Volume		Depth		Surface Area	
	Exponential	Weibull	Exponential	Weibull	Exponential	Weibull
I/1	25.83	23.57	3.67**	5.16**	22.76	3.79**
I/2	11.61**	22.44	7.88**	11.10*	21.57	5.96**
I/3	105.27	29.54	11.22**	13.34*	24.99	26.22
I/4	19.18	11.65**	32.16	9.08**	26.39	11.40*
I/5	192.27	28.49	12.74*	11.64*	44.09	17.78
II/1	26.75	17.67	2.07**	7.87**	11.30*	6.77*
II/2	30.28	40.22	10.69*	15.49	36.95	5.88**
II/3	86.95	33.95	4.11**	6.03**	28.71	0.63**
II/4	33.10	26.59	2.00**	8.99	24.38	3.79**
II/5	5.31**	7.19*	12.08*	34.60	18.45	4.66*
III/1	60.02	24.33	5.01**	7.36**	38.22	23.62
III/2	136.43	52.39	3.73**	7.56**	45.51	4.64**
III/3	103.50	55.31	4.01**	19.05	32.98	1.81**
III/4	14.95	15.24	2.59**	2.79**	17.02	2.37**
III/5	8.08*	13.76	3.30**	24.98	12.51	3.21**

$$\psi \quad \chi^2 = \sum_{i=1}^m \frac{(f_i - e_i)^2}{e_i}$$

- ** Difference between observed and theoretical frequencies is not significant at the 5% level of significance.

- * Difference between observed and theoretical frequencies is not significant at the 1% level of significance.

APPENDIX - B
Computer Programs

Line No.	Column	Statement	Model No.	IDN No.	PT. No.	OBSN.	LEFT X	RIGHT Y	STD. DEVIATION(S, /)
0001		DIMENSION A(10,4),B(1,4),C(8),D(8,4),X(4),Y(4),PP(4)							
0002	8	READ(5,9) IPTUN							
0003	9	FORMAT (I4)							
0004	2	WRITE (6,7)							
0005	7	FORMAT (I1)							
0006		NF=0							
0007		K=1							
0008		I=1							
0009		IF I=1							
0010		KEVEN=G							
0011		Y AXIS=-1							
0012		READ(5,4) IST,IM,IFF,INTER							
0013	4	FORMAT (I10)							
0014		IF ((IM/2)*2-IM) 13,12,13							
0015	12	KEVEN=1							
0016	13	IF (IST.DD.-2) GO TO 85							
0017		WRITE (6,1)							
0018	1	FORMAT(107H STRIP NO. MODEL NO. IDN NO. PT.NO. OBSN. LEFT X 1 LEFT Y RIGHT X RIGHT Y STD.DEVIATION(S, /)							
0019	6	READ(5,5) IPT1,(A(I,M),M=1,4)							
0020	5	FORMAT(I10,10X,4F10.3)							
0021		IPT=IPT1-10000							
0022		A(I,3)=A(I,1)-A(I,3)							
0023		A(I,4)=A(I,2)-A(I,4)							
0024	10	I=I+1							
0025		READ(5,5) IPT2,(A(I,M),M=1,4)							
0026		A(I,3)=A(I,1)-A(I,3)							
0027		A(I,4)=A(I,2)-A(I,4)							
0028		IF (IPT1-IPT2) 15,10,15							
0029	15	DO 20 M=1,4							
0030	20	B(I,M)=A(I,M)							
0031		N=I-1							
0032		FN=N							
0033		DO 40 M=1,4							
0034		SUM=0							
0035		IF (N.EQ.1) GO TO 35							
0036		DO 25 I=1,N							
0037	25	SUM=SUM+A(I,M)							
0038		AV=SUM/FN							
0039		SUMSQ=0.							
0040		DO 30 I=1,N							
0041		DIF=1000*(AV-A(I,M))							
0042	30	SUMSQ=SUMSQ+DIF**2							
0043		SD=SQRT(SUMSQ/(FN-1.))							
0044		C(I)=AV							
0045		C(M+4)=SD							
0046		GO TO 40							
0047	35	C(M)=A(I,M)							

UNIVERSITY OF GUELPH,

0049	40	CONTINUE
0050		C(2)=-C(2)*Y AXIS
0051		C(4)=-C(4)*Y AXIS
0052		IF (IFID=0) 41,42,41
0053	42	NF=NF+1
0054		DO 43 M=1,4
0055		D(NF,M)=C(M)
0056	41	IPT=IPT1-IFF*10000
0057		IF (IFID.EQ.1) IPT=0
0058		IF ((INTER.GT.0).AND.(KEVEN.EQ.1)) GO TO 46
0059		GO TO 51
0060	46	TEMP1=C(1)
0061		TEMP2=C(2)
0062		C(1)=C(3)
0063		C(2)=C(4)
0064		C(3)=TEMP1
0065		C(4)=TEMP2
0066		TEMP1=C(5)
0067		TEMP2=C(6)
0068		C(5)=C(7)
0069		C(6)=C(8)
0070		C(7)=TEMP1
0071		C(8)=TEMP2
0072	51	IF (IPUN) 44,44,49
0073	49	IF (K=9) 44,47,47
0074	47	WRITE(7,6P) IST,IM,IPT,(C(I),I=1,4)
0075	48	FORMAT (2I2,16,4F10.3)
0076	44	WRITE (6,45) IST,IM,IPT1,IPT,N,(C(I),I=1,8)
0077	45	FORMAT(1X,14,110,114,17,15,4F12.4,1X,4F5.1)
0078		I=1
0079		DO 50 M=1,4
0080	50	A(I,M)=B(I,M)
0081		IF (IPT2.EQ.-1) GO TO 60
0082		IF (IPT2.EQ.0) GO TO 55
0083		IPT1=IPT2
0084		K=K+1
0085		GO TO 10
0086	55	IF ID=0
0087		I=1
0088		K=K+1
0089		GO TO 6
0090	60	L=1
0091	65	IF ((L/2)+2-2) 70,75,70
0092	70	DO 71 I=1,4
0093		X(I)=D(I,1)
0094	71	Y(I)=D(I,2)
0095		GO TO 73

UNIVERSITY OF GUELPH

0096	75	DD 72 I=1,4
0097		X(1)=D(1)+4,3)
0098	72	Y(1)=D(1)+4,4)
0099	73	F13=(Y(1)-Y(3))/(X(1)-X(3))
0100		F42=(Y(4)-Y(2))/(X(4)-X(2))
0101		F=F13-F42
0102		XP=(Y(2)-Y(3)-F42*X(2)+F13*X(3))/F
0103		YP=F13*(XP-X(3))+Y(3)
0104		IF (L-2) 74,76,74
0105	74	PP(1)=XP
0106		PP(2)=YP
0107		L=L+1
0108		GO TO 65
0109	76	PP(3)=XP
0110		PP(4)=YP
0111		IDPP=0
0112		K=K-R
0113		IF ((INTER.GT.0).AND.(KEVEN.EQ.1)) GO TO 77
0114		GO TO 84
0115	77	TEMP1=PP(1)
0116		TEMP2=PP(2)
0117		PP(1)=PP(2)
0118		PP(2)=PP(4)
0119		PP(3)=TEMP1
0120		PP(4)=TEMP2
0121	94	IF (IPUM) 79,79,83
0122	83	WRITE(7,82) IST,IM,IDPP,(PP(I),I=1,4),K
0123	82	FORMAT (2I2,16,4F10.3)
0124	79	WRITE(6,80) IST,IM,IDPP,(PP(I),I=1,4)
0125	80	FORMAT(2I2,16,4F10.3)
0126		WRITE (6,81) K
0127	81	FORMAT(3I2,16,4F10.3)
0128		GO TO 2
0129	85	STOP
0130		END

UNIVERSITY OF GUELPH,

C ANALYTICAL STRIP TRIANGULATION.
 C N.P.C. PROGRAM OF DECEMBER 1966 - G.H.S.
 C

0001	DOUBLE PRECISION R(9), AR(12), AL(9), W(4), PP(4), T(9), S(20), CLIST(162), SLIST(10), PHC(404)	S.0001
0002	DOUBLE PRECISION R1,R2,R3,R4,R5,R6,R7,R8,R9, AR1,AR2, 1 AR3,AR4,AR5,AR6,AR7,AR8,AR9, BX,BY,BZ, AL1,AL2,AL3, 2 AL4,AL5,AL6,AL7,AL8,AL9, U1,V1,U2,V2, PP1,PP2,PP3, 3 PP4, T1,T2,T3,T4,T5,T6,T7,T8,T9, A1,A2,A3,OBZ,DBZ, 4 X1,Y1,Z1,X2,Y2,Z2, PX,PY,PZ, DELR,WANT, F,CX,CY,BX1, 5 CE,CR	S.0002
0003	DOUBLE PRECISION DSORT	S.0003
0004	DIMENSION IC(101),LIST(10),LYST(10)	S.0004
0005	COMMON P1,R2,K3,R4,R5,R6,R7,R8,R9, AR1,AR2, 1 AR3,AR4,AR5,AR6,AR7,AR8,AR9, BX,BY,BZ, AL1,AL2,AL3, 2 AL4,AL5,AL6,AL7,AL8,AL9, U1,V1,U2,V2, PP1,PP2,PP3, 3 PP4, T1,T2,T3,T4,T5,T6,T7,T8,T9, S	S.0005
0006	EQUIVALENCE (R1,R(1)),(AR1,AR(1)),(AL1,AL(1)), 1 (U1,W(1)), (PP1,PP(1)), (T1,T(1)), (A1,S(16)), 2 (A2,S(17)), (A3,S(18)), (DBZ,S(19)), (DBZ,S(20))	S.0006
0007	1 FORMAT (14,I5,F7.3,2F7.5,F7.0,F7.3,F7.4,I7,20X,I2)	S.0007
0008	2 FORMAT (14, F5.1, 9F7.2, 6X, I2)	M.0008
0009	3 FORMAT (14,2X,I4, 4F10.3,I3)	M.0009
0010	4 FORMAT (1H, 14,5X,5F15.9)	
0011	5 FORMAT(14,I5,4I9)	M.0011
0012	6 FORMAT (1H, I4, I5, 4I9)	S.0012
0013	6 FORMAT (6HOERRDR 12, 14H, EXIT AT CARD216)	S.0013
0014	9 FORMAT (1H1)	

C
C
C
C
C
C

BLOCK A INITIALIZE THE TRIANGULATION

READ CODES, FOCAL LENGTH, ETC

0015	1000 READ (5,1) KK, KKK, F, CX, CY, BX1, CE, CR, NUCRD, K7	M.0019
0016	CR = CR / 1000.	S.0020
0017	CE = (CE / 12756. + CR) / (F*F)	S.0021
0018	WRITE (6,9)	M.0022
0019	KK = KK + 1	S.0023
0020	K8 = 1	S.0024
0021	IF (KK) 2901, 2901, 1001	S.0025
0022	1001 IF (KK-5) 1010, 1010, 2901	S.0026
	READ CORRECTION TABLE	
0023	1010 K1 = 1	S.0027
0024	1011 K2 = K1 + 8	S.0028
0025	READ (5,2) K3, T3, (CLIST(1), I=K1, K2), K5	M.0029

C
C
C

UNIVERSITY OF GUELPH,

0026 IF (K1-1) 1011, 1012, 1014

0027 1012 K6 = K3

0028 DELR = T3

0029 K8 = 2

0030 IF (K6-162) 1014, 1014, 2902

C
C
C

CHECK CARD SEQUENCE

CHE

0031 1014 K7 = K7 + 1

0032 K8 = 3

0033 IF (K5-K7) 2902, 1015, 2902

0034 1015 K1 = K1 + 9

0035 IF (K6-K2) 1016, 1016, 1011

C
C
C

DIVIDE RADIAL CORRECTION BY INTERVAL

0036 1016 DO 1017 I = 1, K6

0037 1017 CLIST(I) = CLIST(I) / (DELR * 1000.)

C
C
C

READ FIRST CARD OF FIRST MODEL

0038 K4MAX = 100

0039 READ (5,3) 101, 102, (PF(I), I=1,4), K6

0040 1018 K4 = K6

0041 MOD = 1

0042 K3 = 1

0043 PX=200000.

0044 PY=400000.

0045 PZ=600000.

C
C
C
C
C

BLOCK B PERFORM THE RELATIVE ORIENTATION

FIRST ITERATION

0046 1100 K = 1

0047 KA = 1

0048 K2 = 1

0049 KK1 = 1

0050 WRITE (6,55)

0051 DO 1101 I=1,10

0052 1101 LIST(I) = -1

0053 LI = 1

0054 K5 = K4MAX

0055 IF (K4 = K4MAX) 1102, 2030, 2030

0056 1102 K5 = K4

0057 K8 = 4

0058 IF (K4-6) 2903, 2030, 2030

S.0030
S.0031
S.0032
S.0033
S.0034

S.0035
S.0036
S.0037
S.0038
S.0039

S.0040
S.0041

S.0042
M.0043
S.0044
S.0045
S.0046
S.0047
S.0048
S.0049

S.0050
S.0051
S.0052
S.0053
M.0054
S.0055
S.0056
S.0057
S.0058
S.0059
S.0060
S.0061
S.0062

Line No.	Code	Description	Symbol
		READ FIRST GROUP OF ORIENTATION POINTS	
0059	C	1110 K1=1	M.0063
0060	C	GO TO 2010	S.0064
0061	C	1111 DO 1112 I = 1,4	S.0065
0062	C	PHC(K2) = W(I)	S.0066
0063	C	1112 K2 = K2 + 1	S.0067
		TAG POINT FOR SCALING NEXT MODEL	
0064	C	IF (LI-10) 1113, 1113, 1120	S.0068
0065	C	1113 IF (K6 - 1) 1120, 1114, 1120	S.0069
0066	C	1114 LIST(LI) = ID(K1)	S.0070
0067	C	LI = LI + 1	S.0071
0068	C	K1 = 2	S.0072
		CORRECTION EQUATION FOR FIRST ITERATION	
		T2 IS THE COEFFICIENT OF 2A2&0EZ	
		T6 IS IN SECCND PART OF EQUATION	
0069	C	1120 T1 = V1 * V2 + 1.	S.0073
0070	C	T2 = -V1 * U2	S.0074
0071	C	T3 = -U2	S.0075
0072	C	T4 = U2 - U1	S.0076
0073	C	T5 = U1 * V2	S.0077
0074	C	T6 = V2 - V1	S.0078
		FOR THE CONTRIBUTION TO THE NORMAL EQUATIONS,	
0075	C	GO TO 2090	S.0079
0076	C	1121 K1=K1+1	M.0080
0077	C	IF(K1.LE.K5)GO TO 2010	M.0081
		TO SOLVE THE NORMAL EQUATIONS,	
0078	C	GO TO 2100	S.0081
0079	C	1150 BY = DBY	S.0082
0080	C	BZ = DBZ	S.0083
0081	C	DO 1151 I=1,9	S.0084
0082	C	1151 AR(I) = R(I)	S.0085
		TEST SIZE OF CORRECTIONS	
0083	C	DO 1152 I=16,20	S.0086
0084	C	IF (30. * S(I)) 1200, 1152, 1200	S.0087
0085	C	1152 CONTINUE	S.0088
0086	C	GO TO 1300	S.0089

UNIVERSITY OF GUELPH

Line No.	Code	Description	Reference
	C	SECOND ITERATION, USED ONLY IF	
	C	FIRST CORRECTIONS ARE LARGE	
0087	C	1200 K = 2	S.0090
0088	C	1201 K2 = 1	S.0091
0089	C	GO TO 2030	S.0092
	C	USE FIRST GROUP OF ORIENTATION POINTS	
0090	C	1202 K1=0	M.0093
0091	C	1205 K1=K1+1	M.0094
0092	C	DO 1203 I=1,4	S.0094
0093	C	W(I) = PHC(K2)	S.0095
0094	C	1203 K2 = K2 + 1	S.0096
0095	C	GO TO 2040	S.0097
0096	C	1204 IF(K1-K5)1205,1206,1206	M.0098
0097	C	1206 GO TO (2999, 2100, 1302, 1602), K	M.0099
	C	FINAL ITERATION	
0098	C	1300 K = 3	S.0100
0099	C	KB = 1	S.0101
0100	C	GO TO 1201	S.0102
0101	C	1301 GO TO (1204, 1303), KB	S.0103
	C	USE REMAINING ORIENTATION POINTS, IF ANY	
0102	C	1302 KB = 2	S.0104
0103	C	K1 = K4MAX + 1	S.0105
0104	C	KB = K5	S.0106
0105	C	1303 KB = KB + 1	S.0107
0106	C	IF (KB-K4) 2010, 2010, 2100	S.0108
	C	BLOCK C SCALE THE MODEL	
0107	C	1400 KA = 2	S.0109
0108	C	GO TO (1450, 1401), MOD	S.0110
0109	C	1401 KD = 1	S.0111
0110	C	BX = 1.	S.0112
0111	C	J = 0	S.0113
0112	C	TO COMPUTE SCALE FACTORS, GO TO (1410, 1430), KK2	S.0114
	C	USE SPECIFIED REGULAR POINT SEQUENCE	

0113	C	1410	KKB = 3		S.0115
0114			GO TO (2999, 1411, 1412, 1414, 1413), KK		S.0116
0115		1411	KKP = 2		S.0117
0116		1412	KKA = 2		S.0118
0117			GO TO 1420		S.0119
0118		1413	KKB = 4		S.0120
0119		1414	KKA = 1		S.0121
0120		1420	M2=KKA		M.0122
	C		REPLACE DISTANCE IN SLIST BY SCALE FACTOR		S.0123
0121	C	1421	DD 1422 I = 1,4		S.0124
0122			K7 = 4 * M2 - 4 + I		S.0125
0123		1422	W(I) = PHC(K7)		
	C		FOR X2, X1, D, B*X2, LAMBDA1, AND 0,5 LAMBDA3,		S.0126
0124	C		GO TO 2040		
	C	1423	J = J + 1		S.0127
0125			SLIST(J) = SLIST(J) / T6		S.0128
0126			GO TO (1424, 1432), KK2		S.0129
0127		1424	M2=M2+1		M.0130
0128			IF (M2-KKA)1421,1421,1440		M.0131
0129					
	C		SCALE WITH TAGGED POINTS		
	C	1430	M1=0		M.0132
0130		1435	M1=M1+1		M.0133
0131			IF (LYST(M1)) 1440, 1421, 1431		S.0133
0132		1431	M2=0		M.0134
0133		1436	M2=M2+1		M.0135
0134			IF (10*(M2)-LYST(M1)) 1432,1421,1432		S.0135
0135		1432	IF (M2-K5)1436,1437,1437		M.0136
0136		1437	IF (M1-10)1435,1440,1440		M.0137
0137					
	C		MEAN THE SCALE FACTORS		S.0137
	C	1440	T1 = 0.		S.0138
0138			BX = 0.		S.0139
0139		DD 1443	I = 1,J		S.0139
0140			IF (SLIST(I)) 1443, 2999, 1442		S.0140
0141		1442	BX = BX + SLIST(I)		S.0141
0142			T1 = T1 + 1.		S.0142
0143		1443	CONTINUE		S.0143
0144			BX = BX / T1		S.0144
0145					
	C		DISCARD ANOMALOUS SCALE FACTORS		
	C				
	C				

```

0146 T2 = 0.
0147 DO 1455 I = 1, J
0148 IF (SLIST(I)) 1455, 2999, 1451
0149 1451 T3 = SLIST(I) - BX
0150 IF (T3) 1452, 1455, 1453
0151 1452 T3 = -T3
0152 1453 IF (T3 - .9999999999 * T2) 1455, 1454, 1454
0153 1454 K7 = I
0154 T2 = T3
0155 1455 CONTINUE
0156 IF (T2 / BX - .0005) 1500, 1500, 1456
0157 1456 SLIST(K7) = -SLIST(K7)
0158 WRITE (6,55) K7
0159 GO TO 1440
C
0160 1460 BX = BX1
C
C
C
C
C
C
0161 BLOCK D COMPLETE THE ABSOLUTE ORIENTATION
0162 BASE COMPONENTS AND ORIENTATION MATRIX
0163
0164 1500 BY = BX * BY
0165 BZ = BX * BZ
0166 GO TO (1510, 1501), MOD
0167 1501 DO 1502 I = 1, 9
0168 1502 R(I) = AL(I)
0169 J = 12
0170 GO TO 2210
C
C
C
0171 PRINT MATRIX AND COORDINATES OF CENTRES
0172
0173 1510 DO 1511 I=1,3
0174 1511 WRITE (6,4) ID1, AR(I), AR(I+3), AR(I+6)
0175 WRITE (6,55)
0176 K7 = 0
0177 GO TO (1512, 1514), MOD
0178 1512 IX = PX
0179 IY = PY
0180 IZ = PZ
0181 WRITE (6,55) ID1, K7, IX, IY, IZ
0182 IF (NDCRD) 1514, 1513, 1514
0183 1513 PUNCH 5, ID1, K7, IX, IY, IZ
0184 1514 IX = PX + BX
0185 IY = PY + BY
0186 IZ = PZ + BZ
0187 WRITE (6,55) ID1, K7, IX, IY, IZ
0188 IF (NJCRD) 1520, 1515, 1520
    
```

S.0145
S.0146
S.0147
S.0148
S.0149
S.0150
S.0151
S.0152
S.0153
S.0154
S.0155
S.0156
M.0157
S.0158
S.0159

S.0160
S.0161
S.0162
S.0163
S.0164
S.0165
S.0166

S.0167
M.0168
M.0169
S.0170
S.0171
S.0172
S.0173
S.0174
M.0175
S.0176

S.0177
S.0178
S.0179
M.0180
M.0181
S.0182

UNIVERSITY OF GUELPH,

0184 1515 PUNCH 5, ID1, K7, IX, IY, IZ

	C				
	C				
	C	BLOCK E	COMPUTE STRIP COORDINATES		
	C		INITIALIZE TRIANGULATION		
0185	C	1520	KD = 2		S.0184
	C		SET COUNTERS FOR THE COMPUTATION OF DISTANCES		
0186	C		GO TO (1521, 1527), KK1		S.0185
0187	C	1521	KKB = 5		S.0186
0188	C		GO TO (1600, 1526, 1523, 1524, 1525), KK		S.0187
0189	C	1523	KKB = 7		S.0188
0190	C		KKA = 6		S.0189
0191	C		GO TO 1527		S.0190
0192	C	1524	KKB = 6		S.0191
0193	C		KKA = 4		S.0192
0194	C		GO TO 1527		S.0193
0195	C	1525	KKB = 8		S.0194
0196	C	1526	KKA = 5		S.0195
0197	C	1527	KKC = 1		S.0196
	C		TRIANGULATE STORED POINTS		
0198	C	1600	K = 4		S.0197
0199	C		KB = 1		S.0198
0200	C		K2 = 1		S.0199
0201	C		GO TO 1202		S.0200
	C		TRIANGULATE ADDITIONAL POINTS		
0202	C	1602	KB = 2		S.0201
0203	C		K1 = K4MAX + 1		S.0202
0204	C	1603	GO TO 2010		S.0203
	C		POSITION VECTOR AND WANT OF INTERSECTION		
0205	C	1610	IX = T4 + PX		S.0204
0206	C		IY = T5 + PY		S.0205
0207	C		IZ = T6 + PZ		S.0206
	C		ROUND OFF PROPERLY		
0208	C		K7 = WANT * DSQRT(T9) + .5		S.0207
0209	C		IF (WANT) 1611, 1612, 1612		S.0208
0210	C	1611	K7 = K7 - 1		S.0209

UNIVERSITY OF GUELPH

0211	1612 WRITE (6,55) ID1, ID(K1), IX, IY, IZ, K7	M.0211
0212	IF (N)CRD) 1614, 1613, 1614	S.0212
0213	1613 PUNCH 5, ID1, ID(K1), IX, IY, IZ, K7	S.0214
0214	1614 GO TO (1620, 1603), KB	
C	STORE DISTANCE FOR SCALING NEXT MODEL	
C		
C		
0215	1620 GO TO (1621, 1630), KK1	S.0215
0216	1621 GO TO (1204, 1622, 1622, 1622, 1622), KK	S.0216
0217	1622 IF (KKA-K1) 1623, 1623, 1204	S.0217
0218	1623 IF (K1-KKB) 1624, 1624, 1204	S.0218
0219	1624 SLIST(KKC) = AR7*(T4-BX) + AR8*(T5-BY) + AR9*(T6-BZ)	S.0219
0220	KKC = KKC + 1	S.0220
0221	GO TO 1204	S.0221
C		
0222	1630 IF (KKC-10) 1631, 1631, 1204	S.0222
0223	1631 IF (LIST(KKC)-ID(K1)) 1204, 1624, 1204	S.0223
C		
C		
C	BLOCK F PREPARE FOR NEXT MODEL	
C		
0224	1700 K8 = 5	S.0224
0225	GO TO (2904, 1701), KA	S.0225
0226	1701 ID1 = 102	S.0226
0227	IF (ID1) 1000, 2999, 1702	S.0227
0228	1702 ON 1703 I=1,4	S.0228
0229	1703 PP(I) = W(I)	S.0229
0230	GO TO (1704, 1706), KK1	S.0230
0231	1704 GO TO (1018, 1706, 1705, 1706, 1705), KK	S.0231
0232	1705 K8 = 6	S.0232
0233	IF (KKB - K4) 1706, 1706, 2904	S.0233
0234	1706 K4 = K6	S.0234
0235	ON 1707 I = 1,10	S.0235
0236	1707 LYST(I) = LIST(I)	S.0236
0237	KK2 = KK1	S.0237
0238	PX = PX + BX	S.0238
0239	PY = PY + BY	S.0239
0240	PZ = PZ + BZ	S.0240
0241	ON 1708 I = 1,9	S.0241
0242	1708 AL(I) = AK(I)	S.0242
0243	MOD = 2	S.0243
0244	GO TO 1100	S.0244
C		
C		
C	SUBROUTINES	
C		
C	READ A POINT	
C		

UNIVERSITY OF GUELPH,

0245	2010	READ (5,3) ID2, ID(K1), (W(I), I=1,4), K6	S.0245
0246		IF (ID2-ID1) 1700, 2011, 1700	S.0246
0247	2011	U1 = (U1 - PP1) * CX	S.0247
0248		V1 = (V1 - PP2) * CY	S.0248
0249		U2 = (U2 - PP3) * CX	S.0249
0250		V2 = (V2 - PP4) * CY	S.0250
		C C C CORRECT PHOTOGRAPH COORDINATES	
0251		KC = 1	S.0251
0252		T1 = U1 * U1 + V1 * V1	S.0252
		C C C USE FIRST POINT TO DEFINE POSITION OF PHOTOGRAPH	
0253		GO TO (2012, 2021), K3	S.0253
0254	2012	K3 = 2	S.0254
0255		IF (U2-U1) 2013, 2013, 2021	S.0255
		C C C FOR ROTATION TO NEGATIVE POSITION	
0256	2013	F = -F	S.0256
0257	2021	T2 = DSORT (T1)	S.0257
0258		J = T2 / DELR + 1.	S.0258
0259		T3 = J	S.0259
0260		T3 = DELR * T3 - T2	S.0260
0261		T4 = (T3 * CLIST(J) + (DELR - T3) * CLIST(J+1)) / T2 + CR + CE * T1	S.0261
0262		K7 = KC + 1	S.0262
0263		DO 2022 I = KC, K7	S.0263
0264	2022	W(I) = (W(I) + W(I) * T4) / F	S.0264
0265		GO TO (2024, 2999, 2025), KC	S.0265
0266	2024	KC = 3	S.0266
0267		T1 = U2 * U2 + V2 * V2	S.0267
0268		GO TO 2021	S.0268
0269	2025	GO TO (1111, 2999, 2040, 2040), K	S.0269
		C C C ZERO THE NORMAL EQUATIONS	
0270	2030	DO 2031 M1 = 1, 20	S.0270
0271	2031	S(M1) = 0.	S.0271
0272		GO TO (1110, 1202, 1202), K	S.0272
		C C C VECTOR X2	
0273	2040	X2 = AR1 * U2 + AR4 * V2 + AR7	S.0273
0274		Y2 = AR2 * U2 + AR5 * V2 + AR8	S.0274
0275		Z2 = AR3 * U2 + AR6 * V2 + AR9	S.0275
0276		GO TO (2050, 2230), KA	S.0276
		C	

CORRECTION EQUATION FOR SECOND ITERATION

Line No.	Code	Statement	Address
0277	C	2050 CROSS PRODUCT B * U1	S.0277
0278	C	T7 = BY - V1 * BZ	S.0278
0279	C	T8 = U1 * BZ - 1.	S.0279
	C	T9 = V1 - U1 * BY	
0280	C	CROSS PRODUCT X2 * T8 * U1	S.0280
0281	C	T1 = Y2 * T9 - Z2 * T8	S.0281
0282	C	T2 = Z2 * T7 - X2 * T9	S.0282
	C	T3 = X2 * T8 - Y2 * T7	
0283	C	CROSS PRODUCT U1 * X2 AND U1 * X2 . B	S.0283
0284	C	T4 = X2 - U1 * Z2	S.0284
0285	C	T5 = U1 * Y2 - V1 * X2	S.0285
0286	C	T6 = Y2 - V1 * Z2 - T4 * BY - T5 * BZ	S.0286
	C	GO TO (2999, 2090, 2051), K	
	C	APPLY WEIGHT	
0287	C	2091 IF (KKK), 2090, 2090, 2052	S.0287
0288	C	2052 T7 = 1./((.14+U1*U1+V1*V1)**2+(.14+U2*U2+V2*V2)**2)	S.0288
0289	C	T7 = DSQRT(T7)	S.0289
0290	C	DO 2053 I = 1,6	S.0290
0291	C	2053 T(I) = T7 * T(I)	S.0291
	C	FORM THE NORMAL EQUATIONS	
0292	C	2090 M3 = 1	S.0292
0293	C	DO 2091 M1 = 1,5	S.0293
0294	C	DO 2091 M2 = M1,6	S.0294
0295	C	S(M3) = S(M3) + T(M1) * T(M2)	S.0295
0296	C	2091 M3 = M3+1	S.0296
0297	C	GO TO (1121, 1204, 1301), K	S.0297
	C	SOLVE THE NORMAL EQUATIONS	
	C	ELIMINATION	
0298	C	2100 K7 = 0	S.0298
0299	C	DO 101 L1 = 2,5	S.0299
0300	C	M1 = K7 + 1	S.0300
0301	C	K7 = M1 + 7 - L1	S.0301
0302	C	M3 = K7	S.0302
0303	C	M4 = M1 + 1	S.0303
0304	C	M5 = K7 - 1	S.0304
0305	C	DO 102 L2 = M4, M5	S.0305
0306	C	T1 = S(L2) / S(M1)	S.0306
0307	C	DO 103 M2 = L2, K7	S.0307

UNIVERSITY OF GUELPH,

```

0308      M3 = M3 + 1
0309      103 S(M3) = S(M3) - T1 * S(M2)
0310      102 S(L2) = T1
0311      101 S(K7) = S(K7) / S(M1)
0312      DBZ = DBZ / S(19)

```

S.0308
S.0309
S.0310
S.0311
S.0312

C
C
C

BACK SUBSTITUTION

```

0313      M1 = 20
0314      DO 105 L1 = 2,5
0315      M1 = M1 - 1
0316      M2 = 20
0317      M3 = M3 - 2
0318      S(M1) = S(M3)
0319      DO 105 L2 = 2,L1
0320      M3 = M3 - 1
0321      S(M1) = S(M1) - S(M2) * S(M3)
0322      105 M2 = M2 - 1
0323      GO TO (120, 2200, 2200), K
0324      120 A2 = A2 - DBZ

```

S.0313
S.0314
S.0315
S.0316
S.0317
S.0318
S.0319
S.0320
S.0321
S.0322
S.0323
S.0324

C
C
C

ORTHOGONAL MATRIX, COLUMNWISE

```

0325      2200 WRITE (6,4) K, (S(I),I=16,20)
0326      T1 = .5 * A1
0327      T2 = .5 * A2
0328      T3 = .5 * A3
0329      R1 = T2 * A2 + T3 * A3
0330      R5 = T3 * A3 + T1 * A1
0331      R9 = T1 * A1 + T2 * A2
0332      R2 = T1 * A2 + A3
0333      R4 = T1 * A2 - A3
0334      R3 = T3 * A1 - A2
0335      R7 = T3 * A1 + A2
0336      R6 = T2 * A3 + A1
0337      R8 = T2 * A3 - A1
0338      T8 = 1. + .5 * R9 + T3 * T3
0339      DO 2201 I=1,9
0340      2201 R(I) = R(I) / T8
0341      R1 = 1. - R1
0342      R5 = 1. - R5
0343      R9 = 1. - R9

```

M.0325
S.0326
S.0327
S.0328
S.0329
S.0330
S.0331
S.0332
S.0333
S.0334
S.0335
S.0336
S.0337
S.0338
S.0339
S.0340
S.0341
S.0342
S.0343

C
C
C
C
C

FOR ACCURATE LAST DIGIT, COMPUTE INSTEAD

```

T7 = .5 * R9 + T3 * A3
T8 = 1. / T8 + T7
T8 = T8 + .5 * T8 - T8 + .5 * T8 - T7 * T8 / T8 + T7
DO 2201 I=1,9

```

14/32/12

DATE = 72348

MAIN

FORTRAN IV G LEVEL 21

```

C2201 R71< #P71<*T8
C R1 #.5 - R1 G.5
C R5 #.5 - R5 G.5
C R9 #.5 - R9 G.5

```

S.0344
S.0345

0344
0345

```

C J = 9
C GO TO (1150, 2210, 2210), K

```

```

C C REPLACE MATRIX AR<< BY MATRIX PRODUCT R<< * AR<<
C

```

S.0346
S.0347
S.0248
S.0349
S.0350
S.0351
S.0352
S.0353

0346
0347
0348
0349
0350
0351
0352
0353

```

C2210 DO 2211 I = 1, J, 3
C T1 = AR(I)
C T2 = AR(I+1)
C T3 = AR(I+2)
C AR(I) = R1 * T1 + R4 * T2 + R7 * T3
C AR(I+1) = R2 * T1 + R5 * T2 + R8 * T3
C2211 AR(I+2) = R3 * T1 + R6 * T2 + R9 * T3
C IF (J-9) 2999, 2220, 1510

```

S.3354
S.0355
S.0356

0354
0355
0356

```

C2220 HY = BY + D3Y
C BZ = BZ + DBZ
C GO TO (1300, 1300, 1400), K

```

```

C C POSITION VECTOR IN STPIP COORDINATE SYSTEM
C X # P1 G LAMPDA1 X1 E 0.5 LAMBDA3 D
C VECTOR X1
C

```

S.0357
S.0358
S.0359
S.0360
S.0361
S.0362
S.0363
S.0364
S.0365

0357
0358
0359
0360
0361
0362
0363
0364
0365

```

C2230 GO TO (2231, 2232), MOD
C2231 X1 = U1
C Y1 = V1
C Z1 = 1.
C GO TO 2234
C2232 GO TO (2231, 2233), KU
C2233 X1 = AL1 * U1 + AL4 * V1 + AL7
C Y1 = AL2 * U1 + AL5 * V1 + AL8
C Z1 = AL3 * U1 + AL6 * V1 + AL9

```

S.0366
S.0367
S.0368
S.0369

0366
0367
0368
0369

```

C CROSS PRODUCT U # X1 * X2, AND O.D
C2234 T1 = Y1 * Z2 - Z1 * Y2
C T2 = Z1 * X2 - X1 * Z2
C T3 = X1 * Y2 - Y1 * X2
C T4 = X1 * X1 + Y1 * Y1 + Z1 * Z1

```

S.0370
S.0371
S.0372

0370
0371
0372

```

C CROSS PRODUCT U # X2
C T4 = BY * Z2 - BZ * Y2
C T5 = BZ * X2 - BX * Z2
C T6 = BX * Y2 - HY * X2

```

UNIVERSITY OF GUELPH,

0373 0374 0375	C	LAMBDA1, LAMBDA3, AND 0.5 LAMBDA3 T7 = (T4 * T1 + T5 * T2 + T6 * T3) / T9 WANT = (BX * T1 + GY * T2 + BZ * T3) / T9 T8 = 0.5 * WANT	S.0373 S.0374 S.0375
0376 0377 0378 0379	C C	POSITION VECTOR, REFERRED TO ORIGIN IN FIRST CENTRE T4 = T7 * X1 + T8 * T1 T5 = T7 * Y1 + T8 * T2 T6 = T7 * Z1 + T8 * T3 GO TO (1423, 1610), KD	S.0376 S.0377 S.0378 S.0379
0380	C C C	ERROR MESSAGES 2901 K5 = K7	S.028
0381 0382 0383	C	2902 WRITE (6,6) K8, K5 2910 READ (5,3) ID2 2911 IF (ID2) 1000, 2999, 2910	M.0391 M.0392 S.0383
0384 0385 0386 0387	C	2903 WRITE (6,6) K8, ID1, ID2 GO TO 2910 2904 WRITE (6,6) K8, ID2, ID(K1) GO TO 2911	M.0394 S.0385 M.0386 S.0387
0388 0389	C	2999 STOP END	M.0391 S.0392

UNIVERSITY OF GUELPH,

C
C
C
C

BLOCK NO.1, PLOT NO.1
POLYNOMIAL ADJUSTMENT OF STRIPS AND BLOCKS
NRC PROGRAM OF JANUARY 24 1967

0001	DOUBLE PRECISION	FL(301),GL(301),HL(301), T(20), TT(11),S(209),	M.0001
0002	1G(65),XL(1600),YL(1600),ZL(1600),TB(9),TC(9),R(9),A(24),		
0003	2 T7,T8,TD, XA,YA,ZA,XB,YB,ZB,XC,YC,XS,XZ, W, XX(,)		
0004	DIMENSION LE(301),LH(300),LS(1600),LP(1600),MY(101),MZ(101)		S.0002
0005	EQUIVALENCE (R(10),A(1)), (S(66),G(1)),		S.0003
0006	1 (ZB,XX(1)), (XA,XX(2)), (YA,XX(3)), (ZA,XX(4))		
0007	1 FORMAT(I4,15,3F9.5)		
0008	21 FORMAT (1H,2I6,2X,3P3F10.2,2X,3P3F10.2)		
0009	22 FORMAT (1H,2I6,2X,3P3F10.2,2X,3P3F10.2)		
0010	24 FORMAT(2X,2I6,2X,3P3F15.2,2X,3P3F10.2)		S.0007
0011	8 FORMAT (1H1 17)		S.0008
0012	91 FORMAT (23H TOO FEW CONTROL POINTS)		S.0009
0013	92 FORMAT (32H NORMAL EQUATIONS ARE UNSOLVABLE)		S.0010
0014	93 FORMAT (16H MEMORY OVERFLOW)		
0015	26 FORMAT(14,3P3F12.2,3P3F10.2)		
0016	C		
0017	C		
0018	C		
0019	C		
0020	C		
0021	C		
0022	C		
0023	C		
0024	C		
0025	5000 I1 = 1		S.0016
0026	I2 = 1		S.0017
0027	4000 READ (5,1) LS(1), LE(11), FL(11), GL(11), HL(12)		M.0018
0028	IF(LS(1)) 4007,4001,4001		S.0019
0029	4001 IF (HL(12)) 4002, 4004, 4002		S.0020
0030	4002 IF (I2=300) 4003, 4003, 404		S.0021
0031	4003 LH(I2) = LE(11)		S.0022
0032	I2 = I2 + 1		S.0023
0033	4004 IF (GL(11)) 4005, 4000, 4005		S.0024
0034	4005 IF (I1=300) 4006, 4006, 404		S.0025
0035	4006 I1 = I1 + 1		S.0026
0036	GO TO 4000		S.0027
0037	C		
0038	C		
0039	C		
0040	INITIATE BLOCK ADJUSTMENT		S.0028
0041	4007 LP(1) = LE(11)		S.0029
0042	XL(1) = FL(11)		S.0030
0043	ITER = 1		S.0031
0044	MAXIT = 1		S.0032
0045	IF (LE(11)) 4011, 4011, 4008		S.0033
0046	4008 IF (LE(11) - 20) 4010, 4010, 4009		S.0034
0047	4009 LE(11) = 20		

0032	4010	MAXIT = LE(I1)	S.0035
0033		WRITE (6,8)	M.0036
0034	4011	YL(?) = SL(I1)	S.0037
0035		ZL(1) = HL(I2)	S.0038
0036		I1 = I1 - 1	S.0039
0037		I2 = I2 - 1	S.0040
0038		I3 = I1	S.0041
0039		I4 = I2	S.0042
0040		I5 = 1	S.0043
0041		I = 1	S.0044
0042		GO TO 5012	S.0045
	C		
	C		
	C	BLOCK B READ CARDS FOR COMPUTATION OF FORMULAS	
	C		
	C	READ AND STORE CODES	
	C		
0043	5010	KREAD * 1	S.0046
0044		GO TO 400	S.0047
0045	5011	IF (LS(I5)) 5012, 5000, 5010	S.0048
0046	5012	IF (LS(I5)+9) 5013, 5000, 5010	S.0049
0047	5013	K11 = -LS(I5) / 100	S.0050
0048		IA = -LS(I5) - 100 * K11	S.0051
0049		K22 = IA / 10	S.0052
0050		K33 = IA - 10 * K22	S.0053
0051		IF (ITER-1) 5015, 5014, 5015	S.0054
0052	5014	LP(I5) = 1	S.0055
0053	5015	IF (MAXIT - ITER) 5016, 5017, 5016	S.0056
0054	5016	WRITE (6, 21) LS(I5), LP(I5), XL(I5), YL(I5), ZL(I5)	M.0057
0055		GO TO 5020	S.0058
0056	5017	WRITE (6, 8) LS(I5)	M.0059
	C		
	C	INITIATE MATRICES R AND A	
	C		
0057	5020	I8 = I5 + 1	S.0060
0058		DO 5021 K = 1, I8	S.0061
0059	5021	R(K) = 0.	S.0062
0060		A(1) = 1.	S.0063
0061		A(5) = 1.	S.0064
0062		A(?) = 1.	S.0065
	C		
	C	SET IA FOR TESTS, STORE TO	
	C	IF NEEDED, READ TWO AXIS POINTS	
	C		
0063		IA = IA - 11	S.0066
0064		TD = 0.	S.0067
0065		IF (XL(I5)) 5024, 5023, 5024	S.0068
0066	5023	IF (IA) 5029, 5029, 5026	S.0069

0067	5024	IF (LP(I5) - 1) 5025,5025,5026	S.0070
0068	5025	TD = 1.7 * (2. * XL(I5))	S.0071
0069	5026	KRFAD = 2	S.0072
0070		K = 0	M.0073
0071	1001	I = K + 1	M.0074
0072		GO TO 400	S.0074
0073	5027	IF (LS(I5)) 5049, 5028, 5028	S.0075
0074	5028	IF (K.LT.2) GO TO 1001	M.0076
0075	5029	KR = 1	S.0077
0076		ISUM = 0	S.0078
0077		I7 = I5 + 1	S.0079
	C	READ THE CONTROL POINTS, FIND E,N, AND H	
	C		
	C		
0078	5030	KRFAD = 3	S.0080
0079		GO TO 400	S.0081
0080	5035	J1 = I - I7 + 1	S.0082
0081		IF (LS(I)) 5040,5040,530	S.0083
0082	5032	ISUM = ISUM + 1	S.0084
0083	5033	IF (J1 - 100) 400, 400, 5034	S.0085
0084	5034	I5 = I5 + 1	S.0086
0085		LS(I5) = -8	S.0087
0086	5040	I6 = I5 - 1	S.0088
0087		IF (ISUM - K11) 5049, 5049, 5041	S.0089
0088	5041	ISUM = 0	S.0090
0089		I = I7 - 1	M.0091
0090	1002	I = I + 1	M.0092
0091		J1 = I - I7 + 1	S.0092
0092		GO TO 540	S.0093
0093	5042	ISUM = ISUM + 1	S.0094
0094	5044	IF (I-16) 1002,1003,1003	M.0095
	C	STORE TRANSLATIONS IN A-ARPA	
	C		
	C		
0095	1003	A(I10) = 0.5 * (XL(I8) + XL(I8+1))	M.0096
0096		A(I11) = 0.5 * (YL(I8) + YL(I8+1))	S.0097
0097		A(I12) = 0.5 * (ZL(I8) + ZL(I8+1))	S.0098
0098		J = MY(I)	S.0099
0099		A(I13) = FL(J)	S.0100
0100		A(I14) = GL(J)	S.0101
0101		J = MZ(I)	S.0102
0102		A(I15) = HL(J)	S.0103
0103		IF (ISUM - K22 - K33) 5049, 5049, 5050	S.0104
	C		
0104	5049	WRITE (6,91)	M.0105
0105		GO TO 5011	S.0106
	C		
	C		

0140 5061 A(15) = A(15) + S(M1) S.0141

0141 C FOR IMPROVING THE PLANIMETRIC ADJUSTMENT S.0142
C GO TO 5100

0142 C 5069 A(13) = A(10) S.0143
0143 A(14) = A(11) S.0144
0144 A(15) = A(12) S.0145

0145 C COMPUTE FORMULAS FOR AXIS-OF-FLIGHT COORDINATES S.0146
C

0146 5070 IF (IA) 5300, 5300, 5071 S.0147
0147 5071 I = 18 + 1 S.0148
0148 KT = 3 S.0149
0149 GO TO 501 S.0150
0150 5073 T8 = DSQRT(XA**2 + YA**2) S.0151
0151 T7 = XA / T8 S.0152
0152 T8 = YA / T8 S.0153
0153 M1 = 0 S.0154
0154 S(1) = T7 - 1. S.0155
0155 G(1) = -T8 S.0156
GO TO 5051

0156 C SUBROUTINE FOR THE COMPUTATION OF NORMAL S.0157
C EQUATIONS FOR ALL PLANIMETRIC ADJUSTMENTS S.0158
C

0157 5100 N = K1 + 1 S.0159
0158 N1 = N + 1 S.0160
0159 W = DSQRT(1000. * YL(18-1)) S.0161

0160 5101 DO 5101 I = 1,130 S.0162
0161 S(I) = 0. S.0163
0162 T(I) = 1. S.0164
0163 TT(I) = 0. S.0165

0164 I = 17 - 1 S.0166
0165 I = I + 1 S.0167
0166 J1 = I - 17 + 1 S.0168
0167 J = MY(J1) S.0169
0168 IF(J) 5102, 5106, 5102 S.0170
0169 5102 GO TO (501, 5103), KB S.0171

0170 5103 XA = XL(I)
0171 YA = YL(I)

0172 C FORM A CORRECTION EQUATION FOR PLANIMETRIC ADJUSTMENT S.0172
C

0173 5104 DO 5105 M2 = 1-K1 S.0173
0174 K1 = M2 + 1 S.0174
T(M1) = XA * T(M2) - YA * TT(M2)

0175	5105	TT(M1) = YA * T(M2) + XA * TT(M2)	S.0175	
0176		T(N1) = FL(J) - A(13) - T(2)	S.0176	
0177		TT(N1) = GL(J) - A(14) - TT(2)	S.0177	
0178		TO FORM THE NORMAL EQUATIONS IF (J - 13) 110, 110, 114	S.0178	
0179	5106	IF (I-16) 1004,5107,5107	M.0179	
0180	5107	TO SOLVE THE NORMAL EQUATIONS GO TO 100	M.0180	
0181	5110	GO TO (5051, 5330), KB	S.0181	
0182	5200	SUBROUTINE FOR THE COMPUTATION OF NORMAL EQUATIONS FOR ALL H-ADJUSTMENTS	S.0182	
0183			N = K2 + K1 + 1	S.0183
0184			N1 = N - 1	S.0184
0185			W = DSORT(1000. * ZL(I-1))	S.0185
0186			KT = 2	S.0186
0187	5201		DO 5201 I = 1,209	S.0187
0188			S(I) = 0.	M.0188
0189			I = 17-1	M.0189
0190	1005		I = I+1	S.0189
0191			J1 = I - 17 + 1	S.0190
0192			J = NZ(J1)	S.0191
0193	5202		IF (J) 5202, 5207, 5202	S.0192
0194	5203		GO TO (501, 5203), KB	S.0193
0195			XA = XL(I)	S.0194
0196			YA = YL(I)	S.0195
0197			ZA = ZL(I)	S.0196
0197	5204	FORM A CORRECTION EQUATION FOR HEIGHT ADJUSTMENT DO 5205 M2 = 1,K2	S.0197	
0198		M1 = M2 + 1	S.0198	
0199	5205	T(M1) = XA * T(M2)	S.0199	
0200		XS = YA	S.0200	
0201	5206	DO 5206 M2 = 1,K3	S.0201	
0202		M1 = M2 + 1	S.0202	
0203		T(M1) = XS	S.0203	
0204	5206	XS = XS * XA	S.0204	
0205		T(N1) = HL(J) - A(15) - ZA - TD * (XA**2 + YA**2)	S.0205	
0206		TO FORM THE NORMAL EQUATIONS	M.0206	
0207	5207	IF (J - 14) 110, 110, 114 IF (I-16) 1005,5208,5208	M.0206	

Line No.	Code	Description	Labels
0208	C	TO SOLVE THE NORMAL EQUATIONS	M.0207
0209	C	5208 GO TO 100	S.0208
	C	5210 GO TO 15060, 53101, KH	
	C	BLOCK D HEIGHT ADJUSTMENT	
	C	FIRST, PERFORM THE LINEAR TRANSFORMATION	
0210	C	5300 KT = 5	S.0209
0211	C	I = 18 - 1	M.0210
0212	C	1006 I = I + 1	M.0211
0213	C	GO TO 501	S.0211
0214	C	5301 XL(I) = XA	S.0212
0215	C	YI(I) = YA	S.0213
0216	C	ZL(I) = ZA	M.0214
0217	C	IF (I-16) 1006, 1007, 1007	M.0215
0218	C	1007 K1 = K11	M.0216
0219	C	K2 = K22	S.0216
0220	C	K3 = K33	S.0217
0221	C	K8 = 2	S.0218
0222	C	FOR THE COMPUTATION OF THE FORMULAS GO TO 5200	S.0219
	C	STORE THE COEFFICIENTS	
0223	C	5310 A(I5) = A(I5) + S(M1)	S.0220
0224	C	DO 5311 I = 1, K2	S.0221
0225	C	M1 = M1 + 1	S.0222
0226	C	5311 TB(I) = S(M1)	S.0223
0227	C	DO 5312 I = 1, K3	S.0224
0228	C	M1 = M1 + 1	S.0225
0229	C	5312 TC(I) = S(M1)	S.0226
0230	C	IF (K2 - 1) 5313, 5313, 5314	S.0227
0231	C	5313 TB(2) = TD	S.0228
0232	C	K2 = 2	S.0229
0233	C	GO TO 5320	S.0230
0234	C	5314 TB(2) = TB(2) + TD	S.0231
	C	BLOCK E PLANIMETRIC ADJUSTMENT	
	C	FIRST, PERFORM THE HEIGHT ADJUSTMENT	
0235	C	5320 K5 = 1	S.0232
0236	C	I = 18 - 1	M.0233

UNIVERSITY OF GUELPH,

0237	1008	I = I + 1				M.0234
0238		XA = XL(I)				S.0234
0239		YA = YL(I)				S.0235
0240		ZA = ZL(I)				S.0236
0241		GO TO 502				S.0237
0242	5321	XL(I) = XB				S.0238
0243		YL(I) = YB				S.0239
0244		ZL(I) = ZB				M.0240
0245		IF (I-16) 1008,5323,5323				M.0241
0246	C	FOR THE COMPUTATION OF THE FORMULAS				
	C	GO TO 5100				M.0242
	C	STORE THE COEFFICIENTS				
	C					
0247	5330	J = 0				S.0242
0248		DO 5331 I = M1,LST				S.0243
0249		J = J + 1				S.0244
0250		S(I) = S(I)				S.0245
0251	5331	G(I) = G(I)				S.0246
0252		LP(I8-1) = LP(I8-1) + 1				S.0247
	C	BLOCK F TRANSFORMATION OF CONTROL POINTS				
	C					
	C					
0253	5400	KR = 2				S.0248
0254		I = I8 - 1				M.0249
0255	1009	I = I + 1				M.0250
0256		J1 = I - I7 + 1				S.0251
0257		XB = XL(I)				S.0252
0258		YB = YL(I)				S.0253
0259		ZB = ZL(I)				S.0254
0260		GO TO 507				S.0255
0261	5401	XL(I) = XC				S.0256
0262		YL(I) = YC				S.0257
0263		ZL(I) = ZB				S.0258
0264		IF (I - I7) 5415, 5461, 5461				
0265	C	COMPUTE RESIDUALS AND MEANS				S.0259
0266	C	J = MY(J1)				S.0260
0267	5402	IF (J) 5402, 5404, 5402				S.0261
0268		XA = XC - FL(J)				S.0262
0269		YA = YC - GL(J)				S.0263
0270	5441	IF (J - I3) 5441, 5441, 5442				S.0264
0271		XC = FL(J)				S.0265
0272		YC = GL(J)				S.0266
0273	5442	GO TO (5403, 5404), KS				S.0267

0274	5403	FL(J)	= XC						S.0268
0275		CL(J)	= YC						S.0269
0276		XA	= .5 * XA						S.0270
0277		YA	= .5 * YA						S.0271
0278		XC	= XC - XA						S.0272
0279		YC	= YC - YA						S.0273
	C								
0280	5404	J	= MZ(J1)						S.0274
0281		IF (J)	5405, 5407, 5405						S.0275
0282	5405	ZA	= ZB - HL(J)						S.0276
0283		IF (J - 14)	5443, 5443, 5444						S.0277
0284	5443	ZB	= HL(J)						S.0278
0285		GO TO	5407						S.0279
0286	5444	GO TO (5406, 5407)	KS						S.0280
0287	5406	HL(J)	= ZB						S.0281
0288		ZA	= .5 * ZA						S.0282
0289		ZB	= ZB - ZA						S.0283
	C								
	C								
	C								
		TO WRITE OR NOT / AND WHAT TO WRITE							
0290	5407	JJ	= 1						S.0284
0291		IF (MY(J1))	5445, 5446, 5445						S.0285
0292	5445	JJ	= JJ + 2						S.0286
0293	5446	IF (MZ(J1))	5447, 5448, 5447						S.0287
0294	5447	JJ	= JJ + 1						S.0288
0295	5448	IF (MAXIT - ITER)	5411, 5408, 5411						S.0289
0296	5408	IF (JJ - 2)	5409, 5410, 5409						S.0290
0297	5409	WRITE(6,21)	LS(I), LP(I), XC, YC, (XX(J), J=1, JJ)						M.0291
0298		WRITE(7,22)	LS(I), LP(I), XC, YC, (XX(J), J=1, JJ)						M.0291
0299		GO TO	5411						
0300	5410	WRITE (6,22)	LS(I), LP(I), XC, YC, ZB, ZA						S.0292
0301	5411	GO TO (5412, 5421)	KS						M.0293
0302	5412	IF (JJ - 1)	5414, 5414, 5415						S.0294
0303	5414	I1	= I1 + 1						S.0295
0304		IF (I1 - 300)	5451, 5451, 404						S.0296
0305	5451	LE(I1)	= LP(I)						S.0297
0306		FL(I1)	= XC						S.0298
0307		GL(I1)	= YC						S.0299
0308		I2	= I2 + 1						S.0300
0309		IF (I2 - 300)	5452, 5452, 404						S.0301
0310	5452	LH(I2)	= LP(I)						S.0302
0311		HL(I2)	= ZB						S.0303
0312	5415	IF (I1 - I6)	1009, 5420, 5420						S.0304
	C								M.0305
	C								
	C								
	C								
		BLOCK G TRANSFORMATION OF REMAINING POINTS							
0313	5420	I	= I6 + 1						S.0306

0314	KT = 6	S.0307
0315	KS = 2	S.0308
0316	WRITE (6,21)	S.0309
0317	GO TO 5422	S.0310
0318	5421 KREAD = 4	S.0311
0319	GO TO 400	S.0312
0320	5422 IF (LS(I)) 5423, 5900, 500	S.0313
0321	5423 IF (LS(I) + 9) 5012, 5900, 5421	S.0314
0322	C 5900 IS = 0	S.0315
0323	ITER = ITER + 1	S.0316
0324	IF (ITER - MAXIT) 5010, 5010, 5911	S.0317
0325	5901 WRITE (6,21)	M.0318
0326	IF (LS(I)) 5000, 5902, 5902	S.0323
0327	5902 STGP	M.0324
C C C C C C C C C		
SUBROUTINES		
0328	110 IF (W) 114, 114, 111	S.0325
0329	111 DO 113 M1 = 1, N1	S.0326
0330	T(M1) = T(M1) * W	S.0327
0331	GO TO (112, 113), XT	S.0328
0332	112 TT(M1) = TT(M1) * W	S.0329
0333	113 CONTINUE	S.0330
0334	114 M3 = 1	S.0331
0335	DO 117 M1 = 1, N	S.0332
0336	DO 117 M2 = M1, N1	S.0333
0337	GO TO (115, 116), KT	S.0334
0338	115 S(M3) = S(M3) + TT(M1) * TT(M2)	S.0335
0339	G(M3) = G(M3) + T(M1) * TT(M2) - TT(M1) * T(M2)	S.0336
0340	116 S(M3) = S(M3) + T(M1) * T(M2)	S.0337
0341	117 M3 = M3 + 1	S.0338
0342	T(1) = 1.	S.0339
0343	GO TO (5106, 5207), KT	S.0340
C C C		
SOLVE THE NORMAL EQUATIONS		
ELIMINATION		
0344	100 LST = 0	S.0341
0345	DO 101 L1 = 2, N	S.0342
0346	M1 = LST + 1	S.0343
0347	LST = M1 + N + 2 - L1	S.0344
0348	M3 = LST	S.0345
0349	M4 = M1 + 1	S.0346
0350	M5 = LST - 1	S.0347
0351	DO 102 L2 = M4, M5	S.0348
0352	IF (S(M1)) 140, 140, 120	S.0349

0353	120	GO TO (121,122), KT				S.0350
0354	121	XZ = G(L2) / S(M1)				S.0351
0355	122	XS = S(L2) / S(M1)				S.0352
0356		DO 103 M2 = L2, LST				S.0353
0357		M3 = M3 + 1				S.0354
0358		GO TO (123,103), KT				S.0355
0359	123	G(M3) = G(M3) - XS * G(M2) + XZ * S(M2)				S.0356
0360		S(M3) = S(M3) - XZ * G(M2)				S.0357
0361	103	S(M3) = S(M3) - XS * S(M2)				S.0358
0362		GO TO (124,102), KT				S.0359
0363	124	G(L2) = XZ				S.0360
0364	102	S(L2) = XS				S.0361
0365		GO TO (125,101), KT				S.0362
0366	125	G(LST) = G(LST) / S(M1)				S.0363
0367	101	S(LST) = S(LST) / S(M1)				S.0364
0368		IF (S(M3-1)) 140, 140, 126				S.0365
0369	126	GO TO (127,128), KT				S.0366
0370	127	G(M3) = G(M3) / S(M3-1)				S.0367
0371	128	S(M3) = S(M3) / S(M3-1)				S.0368
	C	BACK SUBSTITUTION				S.0369
0372		LST = M2				S.0370
0373		M1 = LST				S.0371
0374		DO 105 L1 = 2, N				S.0372
0375		M1 = M1 - 1				S.0373
0376		M2 = LST				S.0374
0377		M3 = M3 - 2				S.0375
0378		GO TO (131,132), KT				S.0376
0379	131	G(M1) = G(M3)				S.0377
0380	132	S(M1) = S(M3)				S.0378
0381		DO 105 L2 = 2, L1				S.0379
0382		M3 = M3 - 1				S.0380
0383		GO TO (133,134), KT				S.0381
0384	133	G(M1) = G(M1) - G(M3) * S(M2) - S(M3) * G(M2)				S.0382
0385		S(M1) = S(M1) + G(M3) * G(M2)				S.0383
0386	134	S(M1) = S(M1) - S(M3) * S(M2)				S.0384
0387	105	M2 = M2 - 1				S.0385
0388		GO TO (5110, 5210), KT				M.0386
0389	C	140 WRITE (6,92)				S.0387
0390		GO TO 5011				
	C	READ ALL CARDS, EXCEPT GROUND-CONTROL DECK				S.0388
0391	400	I5 = I5 + 1				S.0389
0392		I = I5				S.0390
0393		IF (ITER - 1) 401, 401, 403				S.0391
0394	401	IF (I5 - 1600) 402, 402, 404				S.0392
0395	402	READ (5,1) LS(I), L(I), XL(I), YL(I), ZL(I)				

0396		403 GO TO (5011, 5027, 5035, 5422), KREAD		S.0393
0397	C	404 WRITE (6,92)		S.0394
0398		GO TO 5302		S.0395
0399	C	LINEAR TRANSFORMATION		S.0396
0400	500	XL(I) = XL(I) - A(10)		S.0397
0401		YL(I) = YL(I) - A(11)		S.0398
0402		ZL(I) = ZL(I) - A(12)		S.0399
0403	501	DO 555 K = 1,3		S.0400
0404	555	XX(K+1) = A(K) * XL(I) + A(K+3) * YL(I) + A(K+6) * ZL(I)		S.0401
		GO TO (5004, 5204, 5073, 5073, 5301, 5021), KT		
0405	C	CORRECTION OF HEIGHT DEFORMATION		S.0402
0406	502	XB = 0.		S.0403
0407		YB = 0.		S.0404
0408		ZB = ZA		S.0405
0409		XS = XA		S.0406
0410		XZ = ZA		S.0407
0411	DO 503	K = 1, K2		S.0408
0412		XB = XB + TB(K) * XZ * FLOAT (K)		S.0409
0413		ZB = ZB + TB(K) * XS		S.0410
0414		XS = XA * XS		S.0411
0415	503	XZ = XA * XZ		S.0412
0416		YA = ZA		S.0413
0417	DO 504	K = 1, K3		S.0414
0418		YB = YB + TC(K) * XZ		S.0415
0419		ZB = ZB + TC(K) * XS		S.0416
0420		XS = XA		S.0417
0421	504	XZ = XZ * XA		S.0418
0422		YB = YB + 2. * TD * YA * ZA		S.0419
0423		ZB = ZB + TD * YA**2		S.0420
0424		XB = XA - XB		S.0421
0425		YB = YA - YB		S.0422
0426		ZB = ZB + A(15)		S.0423
0427		IF (IA) 506, 506, 505		S.0424
0428	C	TRANSFORMATION TO GROUND CONTROL		S.0425
0429	505	XZ = TB * XB + T7 * YB		S.0426
0430		XB = T7 * XB - TB * YB		S.0427
0431		YB = XZ		S.0428
		GO TO (5321, 5071), K5		
0432	C	CORRECTION OF PLANIMETRIC DEFORMATION		S.0429
0433	507	XC = S(1)		S.0430
0434		YC = G(1)		S.0431
		XA = XB		

```

0435      YA      = YB                      S.0432
0436      DO 508 K = 1,K1                  S.0433
0437      M1      = K + 1                    S.0434
0438      XC      = XC + S(M1) * XA - G(M1) * YA S.0435
0439      YC      = YC + G(M1) * XA + S(M1) * YA S.0436
0440      XS      = XA * XB - YA * YB        S.0437
0441      YA      = YA * XB + XA * YB        S.0438
0442      508    XA      = XS                S.0439
0443      XC      = XB + XC + A(13)          S.0440
0444      YC      = YB + YC + A(14)          S.0441
0445      GO TO (5401, 530), KS              S.0442

      C
      C SEARCH EASTING AND NORTHING
0446      530    DO 532 J = 1,11              S.0443
0447      IF (LP(J) - LE(J)) 532, 531, 532 S.0444
0448      531    MY (J) = J                    S.0445
0449      GO TO (5032, 540), KR                S.0446
0450      532    CONTINUE                       S.0447
0451      MY (J) = 0                           S.0448
0452      GO TO (5033, 540), KP                S.0449

      C
      C SEARCH HEIGHT
0453      540    DO 542 J = 1,12              S.0450
0454      IF (LP(J) - LH(J)) 542, 541, 542 S.0451
0455      541    HZ(J) = J                      S.0452
0456      GO TO (5042, 5401), KR                S.0453
0457      542    CONTINUE                       S.0454
0458      HZ(J) = 0                            S.0455
0459      GO TO (5044, 5401), KR                S.0456

      C
      C MATRIX MULTIPLICATION
0460      560    M      = 15                    S.0457
0461      DO 561 J = 1,7,3                     S.0458
0462      DO 561 I = 1,3                       S.0459
0463      M      = M + 1                        S.0460
0464      561    A(M)  = R(I)*A(IJ) + R(I+3)*A(J+1) + R(I+6)*A(J+2) S.0461
0465      DO 562 I = 1,9                       S.0462
0466      A(I)  = A(I) + 15                    S.0463
0467      GO TO (5053, 5061, 5300), KT          S.0464
0468      END
    
```

UNIVERSITY OF GUELPH

UNIVERSITY OF GUELPH

```

$JOB WATFIV 02410237 WAST ENGINEERING
C PROPERTIES OF DEPRESSIONS.
C THIS PROGRAM USES A DIGITAL SURFACE MODEL AND COMPUTES GEOMETRIC
C SURFACE VOLUME CALCULATION
COMMON /DIN/JJ, IZX, IZY, MAXIZX, MAXIZY, LPLEN, BLEN, PPLEN
REAL*4 Z(10,70), VOL(500), AREA(500), HTS(500), TOTVOL(200),
MINHT(200)
LOGICAL*1 ZFLG(100,70), FLAG, TRUF,
DATA ZFLG/7000, FALSE, NP/0, IF/1, LFVEL/1, N.L/0, SVGL/0.0/
INTEGER*2 PPL(1500,2), LPL(500,2), LVL(500), LPF(500), BNL(1500),
INL(200,2), NRM(200), BAS(200), NUM(200), NSUR(200,25), PPR(100,70),
2/7000*07, BNL2(1500)
INTEGER BLEN, PPLEN
DIMENSION IFMT(118)
C INPUT SURFACE MATRIX
READ MATRIX DIMENSIONS AND INPUT FORMAT
READ(5,1) IZX, IZY, IFMT1
IF(IZX.GT.MAXIZX) GO TO 60
IF(IZY.GT.MAXIZY) GO TO 70
FORMAT(13/18A1)
C READ MATRIX BY ROWS
DO 40 I=1,IZX
40 READ(5,IFMT1) (Z(I,J),J=1,IZY)
C LIST SURFACE DATA
WRITE(6,10) IZX,IZY
FORMAT(11H, ' INPUT SURFACE MEASURES ',15,' BY ',15)
DO 20 I=1,IZX
20 WRITE(6,IFMT2) (Z(I,J),J=1,IZY)
C SCAN SURFACE FOR INITIAL LOW POINTS
CALL IONS(Z,NL,LPL,LPF,LVL,HTS,650)
CALL RASINI(Z,LPL,IF,NL,VCL,ARFA,PPL,BAL,ZFLG,NP,BNL2,PPR,LVEL)
LEVEL=LPF(1)
CALL NFXILEVEL , NL,NP,NL,LPL,LVL,LPF,PPL,FLG,BNL,BNL,NEW,
IBNL2,PPR,630)
CALL SUMIN(L,ARFA,HTS,Z,BAS,NUM,NSUB,MINHT,BLE,NEW,VOL,LPL,LVL,
LPF,TOTVOL,NL,SVGL)
CONTINUE
90 FORMAT('1')
80 WRITE(6,90)
STOP
100 FORMAT(' DIMENSION OF DATA MATRIX EXCEEDS ',15,' INCREASE VALUE ',
1' OF MAXIZX')
60 PRINT 100,IZX
GO TO 80
110 FORMAT(' DIMENSION OF DATA MATRIX EXCEEDS ',15,' INCREASE VALUE ',
1' OF MAXIZY')
70 PRINT 110,IZY
GO TO 80
END
.....
BLKX DATA
COMMON/DIN/JJ, IZX, IZY, MAXIZX, MAXIZY, LPLEN, BLEN, PPLEN

```

```

00001500
00002200
00003100
00004400
00005500
00006550
00007600
00008700
00009800
00010900
00012000
00013100
00014000
00015000
00016000
00017000
00018000
00019000
00019500
00020000
00021000
00022000
00023000
00024000
00025000
00026000
00027000
00027500
00028000
00029000
00030000
00031000
00032000
00033000
00034000
00035000
00036000
00037000
00038000
00039000
00040000
00041000
00042000
00043000
00044000
00045000
00046000
00047000
00048000
00049000
00050000

```




Line No.	Code	Description	Address
39		INTEGER PPLEN,BLEN	00005400
40		DATA PPLEN,HLEN,LPLEN,MAXIX,MAXIZY,JJ	00005500
		1/1500,200,500,100, 70,25/	00005600
41		COMMON /OUTFMT/IFMT(4)	00005700
42		DATA IFMT/'(1H)', '(1J)', 'FU.3', '))' //	00005800
43		END	00005900
44	C	SUBROUTINE LOWS (Z,LEN,LPL,LPF,LVL,HTS,*)	00006000
	C	THIS ROUTINE ESTABLISHES INITIAL LOW POINTS FOR THE SURFACE	00006100
	C	*****	00006200
	C	INPUT Z THE SURFACE MATRIX	00006300
	C	IZX & IZY THE SIZE OF Z	00006400
	C	OUTPUT LEN - THE NUMBER OF LOW POINTS ON THE SURFACE	00006500
	C	LPL A LIST OF THE LOW POINT COORDS	00006600
	C	LPF LIST OF LOW PT FLAGS	00006700
	C	LVL LIST OF LOW PT LEVELS	00006800
	C	HTS LIST OF HEIGHTS OF LOW PTS	00006900
	C	*****	00007000
45		COMMON/DIM/JJ, IZX, IZY, MAXIX, MAXIZY, MAXLEN, BLEN, PPLEN	00007100
46		INTEGER BLEN, PPLEN	00007200
47		DIMENSION Z(MAXIX, MAXIZY)	00007300
48		INTEGER*2 LPL(MAXLEN, 2), LVL(MAXLEN), LPF(MAXLEN)	00007400
49		REAL*4 HTS(MAXLEN)	00007500
50		LEN=0	00007600
	C	SCAN MATRIX, INCREASING ROW COORDS WITHIN INCREASING COLUMN COORDS	00007700
	C	START AT (2,2), END AT (IZX-1, IZY-1)	00007800
51		ILIM=IZX-1	00007900
52		JLIM=IZY-1	00008000
53		DO 20 I=2, ILIM	00008100
54		DO 10 J=2, JLIM	00008200
55		POINT=Z(I, J)	00008300
	C	BRANCH IF HEIGHT UNDEFINED AT POINT	00008400
56		IF (POINT.LT.0.) GO TO 10	00008500
	C	COMPARE WITH ADJACENT POINTS, BRANCH IF NOT LOW	00008600
57		IF ((POINT.GT.Z(I, J-1)) .OR. (POINT.GT.Z(I-1, J))) GO TO 10	00008700
58		IF ((POINT.GE.Z(I, J+1)) .OR. (POINT.GE.Z(I+1, J))) GO TO 10	00008800
	C	ADD LOW POINT TO LOW POINT LIST	00008900
59		LEN=LEN+1	00009000
60		IF (LEN.GT.MAXLEN) GO TO 30	00009100
61		LPL(LEN, 1)=I	00009200
62		LPL(LEN, 2)=J	00009300
63		LVL(LEN)=1	00009400
64		LPF(LEN)=0	00009500
65		HTS(LEN)=Z(I, J)	00009600
66		CONTINUE	00009700
67		CONTINUE	00009800
	C	IF NO LOWS FOUND TERMINATE PROGRAM	00009900
68		IF (LEN.EQ.0) RETURN 1	00100000
	CC	OTHERWISE PRINT OUT LOWS AND RETURN	00100100
69		1 FORMAT ('1', 10X, 'OUTPUT DATA FOR STAGE 1- LEVEL 1')	00100200
70		WRITE(6, 1)	00100300
71		WRITE(6, 2) LEN, ((LPL(I, J), J=1, 2), I=1, LEN)	00100400
72		2 FORMAT ('//15', ' (N) IAL LOW POINTS FOR SURFACE : // (2I3)')	00100500
73		RETURN	00100600
74		WRITE(6, 3) MAXLEN	00100700
75		3 FORMAT (' NUMBER OF LOW POINTS EXCEEDS ' , 15, ' INCREASE VALUE OF	00100800
		LPLEN')	00100900
			00110000
			00111000

76	STOP	00011200
77	END	00011300
*****		00011400
78	SUBROUTINE BASIN(Z,LPL,IF,IL,VOL,AREA,PPL,BNL,ZFLG,NP,BNL2,PPH, LEVEL)	00011500
	C SUBROUTINE TO CALCULATE BASIN DATA FOR GIVEN LEVEL	00011550
	*****	00011600
	INPUT Z DATA MATRIX	00011630
	LPL LOW POINT LIST	00011660
	IF,IL - INDICES OF FIRST AND LAST LOW POINTS FOR LEVEL	00011690
	VOL - LIST OF BASIN VOLUMES	00011720
	AREA - LIST OF BASIN AREAS	00011750
	PPL - POUR POINT COORDINATES	00011780
	BNL - BASIN NUMBER LIST TO MATCH PP'S WITH BASINS	00011810
	NP - NUMBER OF POUR POINTS AT PREVIOUS LEVELS	00011840
	ZFLG - LOGICAL MATRIX INDICATING ACTIVE POUR POINTS	00011870
	Z - THE DATA MATRIX FILLED IN TO THE NEXT LEVEL	00011900
	LPL - LOW POINT LIST - UNCHANGED	00011930
	PPL POUR POINT COORDS WITH NEW POUR POINTS ADDED	00011960
	ZFLG - LOGICAL MATRIX INDICATING NEW ACTIVE POUR POINTS	00011990
	VOL - LIST OF VOLUMES - UPDATED	00012020
	AREA - LIST OF BASIN AREAS - UPDATED	00012050
	BNL BASIN NUMBER LIST - UPDATED	00012080
	WORK AREAS SPC-- LIST OF SURROUNDING POINT COORDS FOR EACH BASIN	00012110
	SPH - LIST OF SURROUNDING POINT HEIGHTS	00012140
	BPC - LIST OF BASIN POINTS FOR GIVEN BASIN	00012170
	BPH - LIST OF BASIN POINT HEIGHTS	00012200
	PRINTED OUTPUT FOR EACH BASIN INCLUDES -	00012230
	BASIN NUMBER, NUMBER OF BASIN POINTS, BASIN AREA, BASIN DEPTH	00012260
	BASIN POINT COORDS, AND BASIN POINT HEIGHTS BEFORE NEW LEVEL ESTAB	00012290
	*****	00012320
	DATA STRUCTURES, LINKAGE, AND INITIALIZATION	00012350
	COMMON/DIM/JJ, IZX, IZY, MAXIZX, MAXIZY, LPLLEN, BLLN, PPLEN	00012380
	COMMON DIST	00012410
	INTEGER PPLEN, BLEN	00012440
	DIMENSION Z(MAXIZX, MAXIZY), VOL(LPLEN), AREA(LPLEN)	00012470
	LOGICAL*1 ZFLG(MAXIZX, MAXIZY), FLAG/.TRUE./	00012500
	INTEGER*2 PPL(PPLEN,2), LPL(LPLEN,2), BNL(PPLEN), BNL2(PPLEN),	00012530
	1PPH(MAXIZX, MAXIZY)	00012560
	INTEGER*2 BLANK, PEE	00012590
	INTEGER SPLEN	00012620
	INTEGER*2 ADJ(4,2)/0.1,0,-1,1,0,-1,0/	00012650
	DATA HIGH/10E30/	00012680
	DATA BLANK/' /, PEE/' P '/	00012710
	*****	00012740
	DIMENSION BPH(100), SPH(400)	00012770
	INTEGER*2 BPC(100,2), SPC(400,2), PPIND(100)	00012800
	DATA MAXNP/100/	00012830
	INTEGER*2 LSAV(4)/4*0/	00012860
	*****	00012890
	SURF=DIST*DIST	00012920
	*****	00012950
	1 FORMAT('1',10X,'OUTPUT DATA FOR STAGE 2- LEVEL',I4)	00012980
	WRITE(6,1)LEVEL	00013010
	REPEAT CALCULATIONS FOR ALL LOWS ON GIVEN LEVEL	00013040
	NSAV=IL	00013070
	DO 100 INDX=IF,IL	00013100
	*****	00013130
	*****	00013160
	*****	00013190
	*****	00013220
	*****	00013250
	*****	00013280
	*****	00013310
	*****	00013340
	*****	00013370
	*****	00013400
	*****	00013430
	*****	00013460
	*****	00013490
	*****	00013520
	*****	00013550
	*****	00013580
	*****	00013610
	*****	00013640
	*****	00013670
	*****	00013700


```

C INITIALIZE FOR LOW POINT
99 L2=0
100 NCON=0
101 NPTS=0
102 SPLEN=1
103 HTLST=-1
104 SPC(I,1)=LPL(INDX,1)
105 SPC(I,2)=LPL(INDX,2)
106 SPH(I)=Z(SPC(I,1),SPC(I,2))
C*****
C FIND ALL BASIN POINTS ASSOCIATED WITH GIVEN LOW POINT
C*****
C FIND MINIMUM HEIGHT IN SPL
107 HTMIN=HIGH
108 DO 20 I=1,SPLEN
109 IF(HTMIN.LE.SPH(I)) GO TO 20
110 HTMIN=SPH(I)
111 LOCN=I
112 CONTINUE
20 C COMPARE MINIMUM HEIGHT WITH LAST BASIN POINT HEIGHT
113 IF(HTMIN-HTLST)50,40,25
C IF NEW BASIN POINT, UPDATE BASIN POINT LISTS
25 C
114 NPTS=NPTS+1
115 IF (NPTS.LE.MAXNP) GO TO 26
116 WRITE(6,27) MAXNP
117 27 FORMAT (' NUMBER OF BASIN POINTS EXCEEDS ',I5/
1 ' INCREASE MAXNP AND DIMENSIONS OF THE FOLLOWING VARIABLES: ',
2 ' BPH SPH BPC SPC PPIND')
26 BPC(NPTS,1)=SPC(LOCN,1)
118 BPC(NPTS,2)=SPC(LOCN,2)
119 BPH(NPTS)=SPH(LOCN)
120 HTLST=BPH(NPTS)
121 PPIND(NPTS)=BLANK
122 C SET HEIGHT HIGH IN SPH AND MATRIX TO EXCLUDE FROM FURTHER TESTS
123 SPH(LOCN)=HIGH
124 Z(SPC(LOCN,1),SPC(LOCN,2))=HIGH
C TERMINATE BASIN DEFINITION IF AT EDGE OF MATRIX
125 IF(BPC(NPTS,1).EQ.1)GO TO 31
126 IF(BPC(NPTS,1).EQ.1)GO TO 31
127 IF(BPC(NPTS,2).EQ.1)GO TO 32
128 IF(BPC(NPTS,2).EQ.1)GO TO 32
C UPDATE SURROUNDING POINT LISTS
129 DO 30 I=1,4
130 SPC(SPLEN+I,1)=SPC(LOCN,1)+ADJIT(I)
131 SPC(SPLEN+I,2)=SPC(LOCN,2)+ADJIT(I)
132 SPH(SPLEN+I)=Z(SPC(SPLEN+I,1),SPC(SPLEN+I,2))
133 SPLEN=SPLEN+4
30 C BRANCH BACK TO FIND NEXT MINIMUM
134 GO TO 10

```

```

00016000
00015900
00017000
00017100
00017200
00017300
00017400
00017500
00017600
00017700
00017800
00017900
00018000
00018100
00018200
00018300
00018400
00018500
00018600
00018700
00018800
00018900
00019000
00019100
00019200
00019300
00019400
00019500
00019600
00019700
00019800
00019900
00020000
00020100
00020200
00020300
00020400
00020500
00020600
00020700
00020800
00020900
00021000
00021100
00021200
00021300
00021400
00021500
00021600
00021700
00021800
00021900
00022000
00022100
00022200
00022300
00022400
00022500
00022600
00022700

```

```

C INITIALIZE FOR EACH LOW POINT
99 L2=0
100 NCON=0
101 NPTS=0
102 SPLEN=1
103 HTLST=-1
104 SPC(1,1)=LPL(INDX,1)
105 SPC(1,2)=LPL(INDX,2)
106 SPH(1)=Z(SPC(1,1),SPC(1,2))
C*****
C FIND ALL BASIN POINTS ASSOCIATED WITH GIVEN LOW POINT
C*****
C
C FIND MINIMUM HEIGHT IN SPL
107 10 HTMIN=HIGH
108 DO 20 I=1,SPLN
109 IF(HTMIN.LE.SPH(I)) GO TO 20
110 HTMIN=SPH(I)
111 LOCN=I
112 20 CONTINUE
C
C COMPARE MINIMUM HEIGHT WITH LAST BASIN POINT HEIGHT
113 IF(HTMIN-HTLST)50,40,25
C
C IF NEW BASIN POINT, UPDATE BASIN POINT LISTS
C
114 25 NPTS=NPTS+1
115 IF (NPTS.LE.MAXNP) GO TO 26
116 WRITE (6,27) MAXNP
117 27 FORMAT (' NUMBER OF BASIN POINTS EXCEEDS ',15/
1 ' INCREASE MAXNP AND DIMENSIONS OF THE FOLLOWING VARIABLES: ',
2 ' BPH SPH BPC SPC PPIND')
118 26 BPC(NPTS,1)=SPC(LOCN,1)
119 BPC(NPTS,2)=SPC(LOCN,2)
120 BPH(NPTS)=SPH(LOCN)
121 HTLST=BPH(NPTS)
122 PPIND(NPTS)=BLANK
C
C SET HEIGHT HIGH IN SPH AND MATRIX TO EXCLUDE FROM FURTHER TESTS
123 SPH(LOCN)=HIGH
124 Z(SPC(LOCN,1),SPC(LOCN,2))=HIGH
C
C TERMINATE BASIN DEFINITION IF AT EDGE OF MATRIX
125 IF(BPC(NPTS,1).EQ.12)GO TO 31
126 IF(BPC(NPTS,1).EQ.1)GO TO 31
127 IF(BPC(NPTS,2).EQ.12)GO TO 32
128 IF(BPC(NPTS,2).EQ.1)GO TO 32
C
C UPDATE SURROUNDING POINT LISTS
129 DO 30 I=1,4
130 SPC(SPLEN+I,1)=SPC(LOCN,1)+ADJ(I,1)
131 SPC(SPLEN+I,2)=SPC(LOCN,2)+ADJ(I,2)
132 30 SPH(SPLEN+I)=Z(SPC(SPLEN+I,1),SPC(SPLEN+I,2))
133 SPLEN=SPLEN+4
C
C BRANCH BACK TO FIND NEXT MINIMUM
134 GO TO 10
C*****

```

```

00016000
00016900
00017000
00017100
00017200
00017300
00017400
00017500
00017600
00017700
00017800
00017900
00018000
00018100
00018200
00018300
00018400
00018500
00018600
00018700
00018800
00018900
00019000
00019100
00019200
00019300
00019400
00019500
00019600
00019700
00019800
00019900
00020000
00020100
00020200
00020300
00020400
00020500
00020600
00020700
00020800
00020900
00021000
00021100
00021200
00021300
00021400
00021500
00021600
00021700
00021800
00021900
00022000
00022100
00022200
00022300
00022400
00022500
00022600
00022700

```

UNIVERSITY

Line No.	Code	Description	Value
	C	**ENTRY 40 **	00022800
	C	TWO EQUAL BASIN POINTS FOUND	00022700
	C	*****	00022600
	C	DETERMINE IF SURROUNDING POINT USED ALREADY	00022500
135	40	IF (Z(SPC(L,GN,1)), SPC(L,GN,2)).NE.0 HIGH 1 GO TO 41	00022400
136		SPH(L,GN)=HIGH	00022300
137		GO TO 10	00022200
	C	DETERMINE IF LAST BASIN POINT IS 1. AN ACTIVE P P FOR A PREVIOUS	00022100
	C	.. IF NOT BRANCH BACK FOR REGULAR PROCESSING TO NEW MINIM	00022000
138	41	IF (.NOT. ZPLG(BPC(INPTS,1), BPC(INPTS,2))) GO TO 25	00021900
139		IF (PPD(BPC(INPTS,1), BPC(INPTS,2)).NE.0) GO TO 25	00021800
	C	.. YES SET SPH HIGH AND SEARCH FOR OTHER P P'S	00021700
140		J=INPTS+4-2	00021600
141		L1=J+3	00021500
142		DO 77 L=J,L1	00021400
143		L2=L+1	00021300
144		IF (SPH(L).NE.0) H(INPTS) GO TO 77	00021200
145		Z(SPC(L,1), SPC(L,2))=HIGH	00021100
146		LSAV(L)=L	00021000
147		77 CONTINUE	00020900
148		GO TO 50	00020800
149		31 IF (BPC(INPTS,2), EQ, 1) GO TO 33	00020700
150		SPLN=SPLN+1	00020600
151		SPC(SPLN,1)=BPC(INPTS,1)	00020500
152		SPC(SPLN,2)=BPC(INPTS,2)+1	00020400
153		SPH(SPLN)=Z(SPC(SPLN,1), SPC(SPLN,2))	00020300
154		IF (BPC(INPTS,2), EQ, 1) GO TO 32	00020200
155		33 SPLN=SPLN+1	00020100
156		SPC(SPLN,1)=BPC(INPTS,1)	00020000
157		SPC(SPLN,2)=BPC(INPTS,2)-1	00019900
158		SPH(SPLN)=Z(SPC(SPLN,1), SPC(SPLN,2))	00019800
159		IF (BPC(INPTS,2), EQ, 1) GO TO 32	00019700
160		GO TO 35	00019600
161		32 IF (BPC(INPTS,1), EQ, 1) GO TO 34	00019500
162		SPLN=SPLN+1	00019400
163		SPC(SPLN,1)=BPC(INPTS,1)+1	00019300
164		SPC(SPLN,2)=BPC(INPTS,2)	00019200
165		SPH(SPLN)=Z(SPC(SPLN,1), SPC(SPLN,2))	00019100
166		IF (BPC(INPTS,1), EQ, 1) GO TO 35	00019000
167		34 SPLN=SPLN+1	00018900
168		SPC(SPLN,1)=BPC(INPTS,1)-1	00018800
169		SPC(SPLN,2)=BPC(INPTS,2)	00018700
170		SPH(SPLN)=Z(SPC(SPLN,1), SPC(SPLN,2))	00018600
171		35 IF (GN, EQ, 1) GO TO 55	00018500
	C	*****	00018400
	C	*****	00018300
	C	POINT POINT FOR BASIN FOUND ** FIND ANY OTHER EQUAL POINTS	00018200
	C	*****	00018100
	C	*****	00018000
	C	UPDATE PP LIST AND LOGICAL MATRIX FOR ACTIVE P P'S	00017900
172	40	NP=NP+1	00017800
173		IF (NP, GT, PPLN) GO TO 40	00017700
174		PPLN(1)=BPC(INPTS,1)	00017600
175		PPLN(2)=BPC(INPTS,2)	00017500

176	HNL(INP)=INDX	00028800
177	RNL2(INP)=INDX	00028900
	C GO BACK AND ADD PREVIOUS EQUAL POINTS TO PP LIST	00029000
178	INDXPP=NPTS	00029100
179	ISAV=NPTS	00029200
180	DO 53 I=1,NPTS	00029300
181	IF(I.EQ.NPTS)GO TO 54	00029400
182	J=NPTS-I	00029500
183	IF(RPH(J).NE.HTLST)GO TO 54	00029600
184	INDXPP=INDXPP-1	00029700
185	NP=NP+1	00029800
186	IF(NP.GT.PPLEN)GO TO 80	00029900
187	PPL(NP,1)=UPC(J,1)	00030000
188	PPL(NP,2)=UPC(J,2)	00030100
189	RNL(INP)=INDX	00030200
190	53 RNL2(INP)=INDX	00030300
	C ADD ALL EQUAL POINTS TO THE BASIN DEFINITION (IF INACTIVE)	00030400
191	54 I=1	00030500
	C TEST IF EQUAL TO PP HEIGHT	00030600
192	52 IF(Z(SPC(I,1),SPC(I,2)).NE.HTLST)GO TO 55	00030700
	C TEST IF CANDIDATE ALREADY A BASIN POINT FOR THIS BASIN	00030800
193	IF(HIGH.EQ.Z(SPC(I,1),SPC(I,2)))GO TO 55	00030900
194	NCON=1	00031000
	C UPDATE BASIN DEFINITION	00031100
195	NPTS=NPTS+1	00031200
196	BPC(NPTS,1)=SPC(I,1)	00031300
197	BPC(NPTS,2)=SPC(I,2)	00031400
198	RPH(NPTS)=HTLST	00031500
	C UPDATE POUR POINT LIST	00031600
199	NP=NP+1	00031700
200	IF(NP.GT.PPLFN)GO TO 80	00031800
201	PPL(NP,1)=BPC(NPTS,1)	00031900
202	PPL(NP,2)=BPC(NPTS,2)	00032000
203	RNL(INP)=INDX	00032100
204	RNL2(INP)=INDX	00032200
205	Z(SPC(I,1),SPC(I,2))=HIGH	00032300
	C TEST IF ASSOCIATED POINT IS ACTIVE IN A PREVIOUS BASIN	00032400
206	IF(.NOT.ZFLAG(SPC(I,1),SPC(I,2)))GO TO 58	00032500
207	IF(PPB(SPC(I,1),SPC(I,2)).NL.INDX)GO TO 55	00032600
	C UPDATE SURROUNDING POINT LIST TO INCLUDE THOSE AROUND NEW PP	00032700
	C INCLUDE TEST IF AT EDGE OF MATRIX	00032800
208	50 IF(BPC(NPTS,1).EQ.12X)GO TO 31	00032900
209	IF(BPC(NPTS,1).EQ.1)GO TO 31	00033000
210	IF(BPC(NPTS,2).EQ.12Y)GO TO 32	00033100
211	IF(BPC(NPTS,2).EQ.1)GO TO 32	00033200
212	DO 51 K=1,4	00033300
213	SPC(SPLEN+K,1)=SPC(I,1)+ADJ(K,1)	00033400
214	SPC(SPLEN+K,2)=SPC(I,2)+ADJ(K,2)	00033500
215	51 SPH(SPLEN+K)=Z(SPC(SPLEN+K,1),SPC(SPLEN+K,2))	00033600
216	SPLEN=SPLEN+4	00033700
217	I=I+1	00033800
218	IF(I.LE.SPLEN)GO TO 52	00033900
	C UPDATE LOGICAL MATRIX WITH NEW ACTIVE P P'S	00034000
219	DO 57 I=INDXPP,NPTS	00034100
220	PPIND(I)=PEE	00034200
221	57 ZFLAG(BPC(I,1),BPC(I,2))=FLAG	00034300
	C CALCULATE BASIN VOLUME AND AREA. ADD TO LISTS	00034400
		00034500
		00034600
		00034700
222	VOL(INDX)=0	


```

223 DO 56 I=1,INDXPP
224 56 VOL(INDX)=VOL(INDX)+(SURF*(HTLST-BPH(I)) )
225 AREA(INDX)=SURF*(INDXPP-I)
226 DEPTH=HTLST-BPH(I)
C*****
C SUMMARIZE BASIN INFORMATION AND ESTABLISH ALL POINTS AT PP LEVEL
C*****
C PRINT OUT DATA FOR BASIN
C WRITE(6,60) INDX,VOL(INDX), DEPTH , AREA(INDX),NPTS,
227 1 (BPC(I,1),UPC(I,2),BPH(I),PPIND(I),I=1,NPTS)
228 60 FORMAT(1H0,10X,' BASIN NUMBER =',I5/
1 15X,' VOLUME=',F8.3/
2 15X,' DEPTH=',F8.3/
3 15X,' AREA=',F8.3/
4 15X,' NUMBER OF POINTS=',I5/
5 15X,' COORDS HEIGHTS'/
6 15X,'I4,F8.3,2X,A?))
C SET ALL BASIN POINTS LEVEL WITH PP HEIGHT
229 DO 70 I=1,NPTS
230 70 Z(UPC(I,1),BPC(I,2))=HTLST
C RESET ADJACENT PTS TO SPH
231 DO 70 L=1,4
232 IF(LSAV(L).EQ.0)GO TO 79
233 Z(SPC(LSAV(L),1),SPC(LSAV(L),2))=SPH(LSAV(L))
234 LSAV(L)=0
235 79 CONTINUE
C BRANCH BACK FOR NEXT BASIN CALCULATIONS
236 100 CONTINUE
C*****
C TERMINATE BASIN DEFINITION FOR THIS LEVEL
237 IF(NSAVE+1
238 RETURN
239 80 PRINT 90,PPLLEN
240 90 FORMAT(' NUMBER OF POUR POINTS EXCEEDS ',I5,' INCREASE VALUE OF
1PPLLEN')
241 STOP
242 END
C*****
243 SUBROUTINE NEXTLEVEL,NL,NP,NLL,LPL,LVL,LPF,PPL,ZFLG,BNL,HLL,NEW,
1,NL2,PPR,*)
C DECLARE ALL DATA STRUCTURES
244 COMMON/DIM/JJ,IZX,IZY,MAXIZX,MAXIZY,LPLLEN,BLLEN,PPLLEN
245 INTEGER BLLEN,PPLLEN
246 INTEGER*2 LPL(LPLLEN,2),LVL(LPLLEN),LPF(LPLLEN),PPL(PPLLEN,2),
1BNL(BLLEN),HLL(BLLEN,2),NEW(BLLEN),BNL2(PPLLEN),
2PPB(MAXIZX,MAXIZY)
247 LOGICAL*1 ZFLG(MAXIZX,MAXIZY)
C SUBROUTINE TO DETERMINE LOW POINT LOCATIONS AT NEXT LEVEL
C*****
INPUT: LPL LOW POINT LIST
LVL LOW PT LEVEL LIST
LPF LOW PT FLAG LIST
PPL POUR POINT LIST
ZFLG POUR PT FLAG LIST

```

```

00034800
00034900
00035000
00035100
00035200
00035300
00035400
00035500
00035600
00035700
00035800
00035900
00036000
00036100
00036200
00036300
00036400
00036500
00036600
00036700
00036800
00036900
00037000
00037100
00037200
00037300
00037400
00037500
00037600
00037700
00037800
00037900
00038000
00038100
00038200
00038300
00038400
00038500
00038600
00038700
00038800
00038900
00039000
00039100
00039200
00039300
00039400
00039500
00039600
00039700
00039800
00039900
00040000
00040100
00040200
00040300
00040400
00040500
00040600
00040700
00040800
00040900
00041000

```

	C OUTPUT ONE BASIN NUMBER LIST	00041100
	C BNL2 INITIALLY IDENTICAL TO BNL BUT ITS ELEMENTS REPLACED BY NEW	00041200
	C PPR INITIALLY ZEROED OUT ITS ELEMENTS REPLACED BY NEW	00041300
	C ALL BASIN LINKED LIST	00041400
	C NEW LOW PT LIST ABOVE LEVEL ONE	00041500
	C PRINTED OUTPUT FOR STAGE J INCLUDES-	00041600
	C BASIN LINKED LIST WITH CORRESPONDING LOW PT	00041700
248	NSAVE=NLL	00041800
249	I=1	00041900
250	1 IF(I.EQ.NP)GO TO 3	00042000
	C IND=1 IMPLIES 'ON' CONDITION	00042100
251	IND=1	00042200
	C CHECK FOR ACTIVE STATES OF POUR PT AND ITS BASIN	00042300
252	IF(.NOT.ZFLG(PPL(I,1),PPL(I,2)).AND..TRUE.)GO TO 4	00042400
253	IF (LPP(BNL(I)).EQ.1) GO TO 4	00042500
254	J=I+1	00042600
255	2 IF(J.GT.NP) GO TO 4	00042700
	C CHECK FOR ACTIVE STATES OF NEXT POUR PT AND ITS BASIN	00042800
256	IF(.NOT.ZFLG(PPL(J,1),PPL(J,2)).AND..TRUE.)GO TO 5	00042900
257	IF(LPP(BNL(J)).EQ.1) GO TO 5	00043000
	C CHECK FOR SHARED POUR POINTS	00043100
258	IF(PPL(I,1).NE.PPL(J,1).OR.PPL(I,2).NE.PPL(J,2)) GO TO 5	00043200
259	IND=0	00043300
	C IND=0 IMPLIES 'OFF' CONDITION	00043400
	C INCREMENT NO OF BASIN PAIRS BY ONE	00043500
260	NLL=NLL+1	00043600
261	IF(NLL.GT.BLLEN)GO TO 40	00043700
	C CHECK TO SEE IF BASINS ARE ALREADY IN BLL	00043800
262	IF (NLL.EQ.1)GO TO 88	00043900
263	LOOP=NLL-1	00044000
264	DO 7 M=1,LOOP	00044100
265	IF(BNL(I).EQ.BLL(M,1).OR.BNL(I).EQ.BLL(M,2))GO TO 8	00044200
266	IF(BNL(J).EQ.BLL(M,1).OR.BNL(J).EQ.BLL(M,2))GO TO 8	00044300
267	7 CONTINUE	00044400
	C INCREMENT NO OF LOW PTS IN LPL	00044500
268	88 NL=NLL+1	00044600
269	IF(NL.GT.LPLEN)GO TO 30	00044700
	C UPDATE NEW LOW LIST	00044800
270	NEW(NLL)=NL	00044900
	C UPDATE LOW POINT LIST	00045000
271	LPL(NL,1)=PPL(I,1)	00045100
272	LPL(NL,2)=PPL(I,2)	00045200
	C UPDATE LOW PT FLAG LIST	00045300
273	LPP(NL)=0	00045400
	C UPDATE LOW PT LEVEL LIST	00045500
274	LVL(NL)=LEVEL	00045600
	C UPDATE BASIN LINK LIST	00045700
275	6 BLL(NLL,1)=BNL(I)	00045800
276	BLL(NLL,2)=BNL(J)	00045900
	C FIND BASINS IN BNL2	00046000
277	JC=1	00046100
278	11 IF(BNL2(JC).NE.BNL(I).AND.BNL2(JC).NE.BNL(J))GO TO 12	00046200
	C UPDATE BNL2 AND PPR	00046300
279	BNL2(JC)=NEW(NLL)	00046400
280	PPR(PPL(JC,1),PPL(JC,2))=NEW(NLL)	00046500
281	12 JC=JC+1	00046600
282	IF(JC.LE.NP)GO TO 11	00046700
283	5 J=J+1	00046800
284	GO TO 2	00046900
	C ALL LOW PTS AT THIS LEVEL DETERMINED	00047000

285	3 IF(NSAVE.EQ.NLL) GO TO 99	00047100
	C SET FLAGS IN LPF FOR BASINS ADDED TO BLL AT THIS LEVEL	00047200
286	LOOP=NSAVE+1	00047300
287	DO 9 M=LOOP,NLL	00047400
288	LPF(BLL(M,1))=1	00047500
289	LPF(BLL(M,2))=1	00047600
290	9 CONTINUE	00047700
291	33 I=NSAVE+1	00047800
292	IND=0	00047900
293	31 IF(I.LT.NLL)GO TO 32	00048000
294	IF(IND.EQ.1)GO TO 33	00048100
295	GO TO 38	00048200
296	32 K=I+1	00048300
297	34 J=1	00048400
298	37 IF(BLL(I,J).EQ.BLL(K,1).OR.BLL(I,J).EQ.BLL(K,2))GO TO 35	00048500
299	46 IF(J.EQ.2)GO TO 36	00048600
300	J=2	00048700
301	GO TO 37	00048800
302	36 K=K+1	00048900
303	IF(K.LE.NLL)GO TO 34	00049000
304	I=I+1	00049100
305	GO TO 31	00049200
306	35 IF(NEW(I)-NEW(K))41,46,43	00049300
307	41 J1=1	00049400
308	J2=K	00049500
309	GO TO 44	00049600
310	43 J1=K	00049700
311	J2=1	00049800
312	44 LPL(NEW(J2),1)=0	00049900
313	DO 51 L=1,NP	00050000
314	IF(BNL2(L).NE.NEW(J2))GO TO 51	00050100
315	BNL2(L)=NEW(J1)	00050200
316	PPL(PPL(L,1),PPL(L,2))=NEW(J1)	00050300
317	51 CONTINUE	00050400
318	NEW(J2)=NEW(J1)	00050500
319	IND=1	00050600
320	GO TO 46	00050700
321	38 I=1	00050800
322	52 IF(LPL(I,1).NE.0)GO TO 47	00050900
323	IF(I.EQ.NL)GO TO 48	00051000
324	LL=NL-1	00051100
325	DO 49 L=1,LL	00051200
326	LPL(L,1)=LPL(L+1,1)	00051300
327	LPL(L,2)=LPL(L+1,2)	00051400
328	LPF(L)=LPF(L+1)	00051500
329	49 CONTINUE	00051600
330	NL=NL-1	00051700
331	GO TO 52	00051800
332	47 I=I+1	00051900
333	IF(I.LE.NL)GO TO 52	00052000
334	GO TO 53	00052100
335	40 NL=NL-1	00052200
336	180 FORMAT('0',10X,'OUTPUT DATA FOR STAGE 3- LEVEL',14)	00052300
337	53 PRINT 180,LEVEL	00052400
338	IF(NLL.EQ.0)GO TO 10	00052500
339	120 FORMAT('0',16X,'LINK LIST',7,11X,'BASIN LINK',5X,'NEW LOW')	00052600
340	150 FORMAT('0',10X,2(15),7X,13)	00052700
341	PRINT 120	00052800
342	PRINT 150,(BLL(I,1),BLL(I,2),NEW(I),I=1,NLL)	00052900
343	RETURN	00053400



```

344 190 FORMAT('0',10X,'NO SHARED POOR PTS')
345 10 PRINT 190
346 99 RETURN
C IF POOR PT INACTIVE, NEXT PT IS EXAMINED
347 * I=I+1
348 IF(IND.EQ.1)GO TO 1
C SET FLAG IN ZFLG MATRIX TO 'OFF', IE FALSE
349 ZFLG(IPPL(I-1,1),PPL(I-1,2))=.FALSE.
350 GO TO 1
C UPDATE NEW LOW LIST
351 8 NEW(BLL)=NEW(M)
352 GO TO 6
353 110 FORMAT(' NUMBER OF BASIN PAIRS EXCEEDS ',15,' INCREASE VALUE OF
      1BLLEN')
354 40 PRINT 110,BLLEN
355 GO TO 50
356 30 PRINT 130,LPLLEN
357 130 FORMAT(' NUMBER OF LOW POINTS EXCEEDS ',15,' INCREASE VALUE IN
      1LPLEN')
358 50 STOP
359 END
C *****
C DECLARE ALL DATA STRUCTURES
360 SUBROUTINE SUBR(INLL,AREA,HTS,Z,BAS,NUM,NSUB,MINHT,BLL,NEW,VOL,
      1LPL,LVL,LPF,TOTVOL,NI,SVOL)
361 COMMON/DIM/JJ,IZX,IZY,MAXIZX,MAXIZY,LPLEN,BLLEN,PPLEN
362 INTEGER BLLEN,PPLEN
363 INTEGER*2 BLL(BLLEN,2),NFW(BLLEN),LPL(LPLEN,2),LVL(LPLEN),
      1LPL(LPLEN),BAS(BLLEN),NUM(BLLEN),NSUB(BLLEN,JJ)
364 REAL VOL(LPLEN),AREA(LPLEN),HTS(LPLEN),MINHT(BLLEN),
      1TOTVOL(BLLEN),Z(MAXIZX,MAXIZY)
C SUBROUTINE TO CALCULATE AND PRINT A SURFACE SUMMARY
*****
C INPUT
LVL LOW PT LEVEL LIST
LPF LOW PT FLAG LIST
BLL BASIN LINKED LIST
NEW LOW PT LIST ABOVE LEVEL ONE
VOL LIST OF BASIN VOLUMES
AREA LIST OF BASIN AREAS
HTS LIST OF LOW PT HTS AT LEVEL ONE
Z DATA MATRIX
C OUTPUT
BAS LIST OF BASINS ABOVE LEVEL ONE
NUM LIST OF NO OF SUBBASINS IN BASINS NOTED BY BAS
NSUB LIST OF SUBBASINS IN BASINS NOTED BY BAS
MINHT LIST OF MIN HTS OF SIMPLE SUBBASINS IN NSUB
TOTVOL LIST OF VOLUME OF BASINS NOTED BY BAS
C PRINTED OUTPUT FOR STAGE 4 INCLUDES-
C BASIN NUMBER- ITS VOLUME,AREA AND MAXIMUM DEPTH PLUS A LIST OF ITS SUR
      IF(INLL.EQ.0)GO TO 1
365 I=1
366 I8=0
367 2 NN=NFW(I)
368 IF(VOL(NN).NE.0)GO TO 20
369 LPF(BLL(I,1))=0
370 LPF(BLL(I,2))=0
371 GO TO 14
372 20 JB=1
373 IF(HTS.EQ.0)GO TO 3
374 8 IF(INN.EQ.BASIJ)GO TO 19
375

```

```

00053500
00053600
00053700
00053800
00053900
00054000
00054100
00054200
00054300
00054400
00054500
00054600
00054700
00054800
00054900
00055000
00055100
00055200
00055300
00055400
00055500
00055600
00055700
00055800
00055900
00056000
00056100
00056200
00056300
00056400
00056500
00056600
00056700
00056800
00056900
00057000
00057100
00057200
00057300
00057400
00057500
00057600
00057700
00057800
00057900
00058000
00058100
00058200
00058300
00058400
00058500
00058600
00058700
00058800
00058900
00059000
00059100
00059200
00059300

```


376	JB=JB+1	00059400
377	IF(JB.LI.IB)GO TO 8	00059500
378	3 ID=JB	00059600
379	C UPDATE BASIN (DEFINED AT LEVELS>1) NUMBER LIST BAS(JB)=NN	00059700
380	C INITIALIZE # OF ELEMENTS IN BAS, MINIMUM HEIGHT VALUE, TOTAL VOLUME VALUE	00059800
380	MINHT(JB)=10E30	00060100
381	TOTVOL(JB)=VOL(NN)	00060200
382	19 M=BL(1,1)	00060300
383	5 IF(NUM(JB).EQ.0)GO TO 9	00060400
384	C CHECK TO SEE IF BASIN ALREADY IN SUBBASIN LIST	00060500
385	LOOP=NUM(JB)	00060600
386	DO 90 K=1,LOOP	00060700
387	IF(NSUB(JB,K).EQ.M)GO TO 6	00060800
388	90 CONTINUE	00060900
388	C CHECK THAT BASIN IS LEVEL ONE	00061000
389	9 IF(LVL(M).EQ.1)GO TO 10	00061100
390	C IF NOT LEVEL ONE, FIND TOTVOL, NO OF SUBBASINS, AND SUBBASINS IN BASIN	00061200
391	J=1	00061300
392	12 IF(BAS(J).EQ.M)GO TO 11	00061400
393	J=J+1	00061500
394	IF(J.NC.IB)GO TO 12	00061600
395	200 FORMAT('0',10X,'*****NOTE: PROGRAM ERROR -MISSING LINKED PAIR -')	00061700
396	1'BASIN',IB)	00061800
397	PRINT 200,J	00061900
398	RETURN	00062000
399	11 TOTVOL(JB)=TOTVOL(JB)+TOTVOL(J)	00062100
400	NJB=NUM(JB)	00062200
401	NUM(JB)=NUM(JB)+NUM(J)	00062300
402	IF(NUM(JB).GT.UJ)GO TO 25	00062400
403	LOOP=NUM(J)	00062500
404	DO 13 K=1,LOOP	00062600
405	NSUB(JB,NJB+K)=NSUB(J,K)	00062700
406	13 CONTINUE	00062800
407	C UPDATE MINIMUM HT IF NECESSARY	00062900
408	IF(MINHT(J).LT.MINHT(JB))MINHT(JB)=MINHT(J)	00063000
409	C UPDATE NO OF SUBBASINS AND SUBBASINS LIST FOR BASIN 'M'	00063100
410	7 NUM(JB)=NUM(JB)+1	00063200
411	IF(NUM(JB).GT.UJ)GO TO 25	00063300
412	NSUB(JB,NUM(JB))=M	00063400
413	6 IF(M.EQ.BL(1,2))GO TO 14	00063500
414	M=BL(1,2)	00063600
415	GO TO 5	00063700
416	C IS EXAMINATION OF LINKED LIST THROUGH?	00063800
417	14 I=I+1	00063900
418	IF(I.LE.NLL)GO TO 2	00064000
419	C PRINT SURFACE SUMMARY	00064100
420	250 FORMAT('1',10X,'OUTPUT FOR STAGE 4 - SURFACE SUMMARY- ALL')	00064200
421	1'LEVELS')	00064300
422	PRINT 250	00064400
423	IF(TH.EQ.0)GO TO 1	00064500
424	16 J=BAS(1B)	00064600
425	C CHECK IF LOW PT FLAG ON	00064700
426	IF(LPF(J).EQ.1)GO TO 15	00064800
427	DEPTH=Z(LPL(J,1),LPL(J,2))-MINHT(1B)	00064900
428	210 FORMAT('1',10X,'**',1X,'BASIN NUMBER',15,' VOLUME='F8.3,	00065000
429	1' AREA='F8.3)	00065100
430	PRINT 210,J,TOTVOL(1B),AREA(J)	00065200
431	220 FORMAT('1',20X,'MAXIMUM DEPTH='F8.3)	00065300
432	PRINT 220,DEPTH	

423	230	FORMAT(' ',10X,'BASIN NUMBER',15,' CONTAINS BASINS',13, 117(7X,13))				00065400
424		LCOM=NUM(I1)				00065500
425		PRINT 210,J,J,(NSUB(I1,K),K=1,LOOP)				00065600
426		SVOL=SVOL+TOTVOL(J1)				00065700
427	15	I1=I1-1				00065800
428		IF(I1.GT.0)GO TO 16				00065900
429		C CHECK FOR UNLINKED LEVEL ONE BASINS				00066000
430		1 I=NL				00066100
431		18 IF(LVL(I).NE.1)GO TO 17				00066200
432		IF(LPF(I).EQ.1)GO TO 17				00066300
433		DEPTH=Z(LPL(I,1),LPL(I,2))-HTS(I)				00066400
434	240	FORMAT(' ',10X,'BASIN NUMBER',15,' VOLUME=',F8.3,' AREA=',F8.3)				00066500
435		PRINT 240,I,VOL(I),AREA(I)				00066600
436		PRINT 220,DEPTH				00066700
437		SVOL=SVOL+VOL(I)				00066800
438		17 I=I-1				00066900
439		IF(I.GT.0)GO TO 18				00067000
440	280	FORMAT(' ',10X,50(' '),				00067100
441	260	FORMAT(' ',10X,'TOTAL VOLUME OF BASINS LISTED ABOVE=',F8.3)				00067200
442		WRITE(6,280)				00067300
443		PRINT 260,SVOL				00067400
444		WRITE(6,280)				00067500
445		RETURN				00067600
446		C IF LEVEL ONE UPDATE TOTVOL AND MINIMUM HT LISTS				00067700
447		1 TOTVOL(J1)=TOTVOL(J1)+VOL(M)				00067800
448		IF(HTS(M).LT.(MINHT(J1))MINHT(J1)=HTS(M)				00067900
449		GO TO 7				00068000
450	25	PRINT 270,JJ				00068100
451	270	FORMAT(' NUMBER OF SUBBASINS EXCEEDS',15,' INCREASE VALUE OF JJ')				00068200
		STOP				
		END				



OUTPUT DATA FOR STAGE 1- LEVEL 1

171 INITIAL LOW POINTS FOR SURFACE :

3 7
 3 16
 3 23
 4 43
 4 56
 6 7
 6 14
 6 24
 6 33
 6 47
 9 7
 9 24
 9 42
 9 47
 12 7
 12 12
 12 22
 12 33
 12 38
 12 42
 12 46
 12 53
 14 40
 15 6
 15 10
 15 23
 15 32
 15 37
 15 46
 15 50
 15 55
 17 6
 17 23
 18 32
 18 37
 18 41
 18 46
 20 23
 20 41
 23 6
 23 12
 23 23
 23 46
 23 55
 26 6
 26 10
 26 12
 26 23
 26 36
 26 41
 26 46
 28 51
 29 6
 29 13
 29 21
 29 24

UNIVERSITY OF GUELPH,



OUTPUT DATA FOR STAGE 2- LEVEL 1

BASIN NUMBER - 1

VOLUME= 2.251
 DEPTH= 0.280
 AREA= 12.500

NUMBER OF POINTS= 3
 COORDS HEIGHTS
 3 7 256.130
 3 9 256.230
 2 7 256.410 P

BASIN NUMBER - 2

VOLUME= 3.374
 DEPTH= 0.340
 AREA= 12.500

NUMBER OF POINTS= 3
 COORDS HEIGHTS
 3 16 256.240
 3 15 256.380
 2 16 256.580 P

BASIN NUMBER - 3

VOLUME= 4.240
 DEPTH= 0.280
 AREA= 25.000

NUMBER OF POINTS= 5
 COORDS HEIGHTS
 3 33 258.810
 3 34 258.940
 4 33 258.940
 4 34 258.990
 2 33 259.090 P

BASIN NUMBER - 4

VOLUME= 1.064
 DEPTH= 0.100
 AREA= 12.500

NUMBER OF POINTS= 3
 COORDS HEIGHTS
 4 43 259.300
 3 43 259.330
 2 43 259.400 P

BASIN NUMBER - 5

VOLUME= 0.812
 DEPTH= 0.130
 AREA= 6.250

NUMBER OF POINTS= 2
 COORDS HEIGHTS
 4 56 259.440
 3 56 259.570 P

BASIN NUMBER - 6

VOLUME= 1.312
 DEPTH= 0.210
 AREA= 6.250

NUMBER OF POINTS= 2
 COORDS HEIGHTS
 6 7 257.000



OUTPUT DATA FOR STAGE 3- LEVEL 2

LINK LIST

BASIN	LINK	NEW	LOW
17	26	172	
89	90	173	
102	103	174	
120	124	175	
145	148	176	
147	158	177	
159	163	178	
160	162	179	
167	171	180	

OUTPUT DATA FOR STAGE 2- LEVEL 2

BASIN NUMBER - 172

VOLUME= 3.055
 DEPTH= 0.070
 AREA= 43.750

NUMBER OF POINTS= 8

	COORDS	HEIGHTS
14	22 259.700	
14	23 259.700	
15	22 259.700	
13	22 259.700	
15	23 259.700	
12	22 259.700	
12	23 259.700	
11	22 259.770	P

BASIN NUMBER - 173

VOLUME= 7.570
 DEPTH= 0.150
 AREA= 56.250

NUMBER OF POINTS= 11

	COORDS	HEIGHTS
42	47 267.560	
42	48 267.560	
42	46 267.560	
43	48 267.560	
42	45 267.560	
43	45 267.560	
42	44 267.560	
43	44 267.560	
41	45 267.700	
43	46 267.710	P
44	44 267.710	P

BASIN NUMBER - 174

VOLUME= 2.252
 DEPTH= 0.040
 AREA= 56.250

NUMBER OF POINTS= 11

	COORDS	HEIGHTS
48	20 268.260	
48	21 268.260	
48	19 268.260	
48	22 268.260	
49	21 268.260	
49	19 268.260	
48	18 268.260	
49	22 268.260	
49	18 268.260	
47	21 268.300	P
47	18 268.300	P

BASIN NUMBER - 175

VOLUME= 18.314
 DEPTH= 0.280
 AREA= 81.250

NUMBER OF POINTS= 14

	COORDS	HEIGHTS
55	47 269.340	
56	47 269.340	

OUTPUT DATA FOR STAGE 3- LEVEL 3

LINK LIST

BASIN	LINK	NEW	LOW
17	27	172	
89	90	173	
102	103	174	
120	124	175	
145	148	176	
147	153	177	
159	163	178	
160	162	179	
167	171	180	
94	173	181	

OUTPUT DATA FOR STAGE 2- LEVEL 3

BASIN NUMBER - 181

VOLUME = 12.115

DEPTH = 0.130

AREA = 106.250

NUMBER OF POINTS = 18

COORDS HEIGHTS

44	44	267.710
45	44	267.710
43	44	267.710
46	44	267.710
43	45	267.710
42	44	267.710
43	46	267.710
42	45	267.710
42	46	267.710
41	45	267.710
42	47	267.710
42	48	267.710
43	48	267.710
43	47	267.720
41	44	267.760
41	46	267.810
42	43	267.820
40	45	267.840

P



OUTPUT FOR STAGE 4- SURFACE SUMMARY- ALL LEVELS

* BASIN NUMBER 181	VOLUME= 32.026	AREA= 106.250				
MAXIMUM DEPTH= 0.680						
BASIN NUMBER 191	CONTAINS BASINS181		94	89	90	173
* BASIN NUMBER 177	VOLUME= 6.181	AREA= 37.500				
MAXIMUM DEPTH= 0.420						
BASIN NUMBER 177	CONTAINS BASINS177		147	158		
* BASIN NUMBER 175	VOLUME= 23.377	AREA= 81.250				
MAXIMUM DEPTH= 0.960						
BASIN NUMBER 175	CONTAINS BASINS175		120	124		
* BASIN NUMBER 174	VOLUME= 16.183	AREA= 56.250				
MAXIMUM DEPTH= 0.720						
BASIN NUMBER 174	CONTAINS BASINS174		102	103		
* BASIN NUMBER 172	VOLUME= 7.744	AREA= 43.750				
MAXIMUM DEPTH= 0.300						
BASIN NUMBER 172	CONTAINS BASINS172		17	26		
BASIN NUMBER 171	VOLUME= 0.250	AREA= 6.250				
MAXIMUM DEPTH= 0.040						
BASIN NUMBER 170	VOLUME= 0.0	AREA= 0.0				
MAXIMUM DEPTH= 0.0						
BASIN NUMBER 169	VOLUME= 1.062	AREA= 18.750				
MAXIMUM DEPTH= 0.130						
BASIN NUMBER 168	VOLUME= 0.812	AREA= 6.250				
MAXIMUM DEPTH= 0.130						
BASIN NUMBER 167	VOLUME= 0.563	AREA= 6.250				
MAXIMUM DEPTH= 0.090						
BASIN NUMBER 166	VOLUME= 1.064	AREA= 6.250				
MAXIMUM DEPTH= 0.170						
BASIN NUMBER 165	VOLUME= 3.062	AREA= 6.250				
MAXIMUM DEPTH= 0.490						
BASIN NUMBER 164	VOLUME= 1.813	AREA= 12.500				

BASIN NUMBER 162 VOLUME= 0.436 AREA= 6.250
MAXIMUM DEPTH= 0.070

BASIN NUMBER 161 VOLUME= 1.067 AREA= 12.500
MAXIMUM DEPTH= 0.110

BASIN NUMBER 160 VOLUME= 0.313 AREA= 6.250
MAXIMUM DEPTH= 0.050

BASIN NUMBER 159 VOLUME= 0.250 AREA= 12.500
MAXIMUM DEPTH= 0.030

BASIN NUMBER 157 VOLUME= 8.684 AREA= 31.250
MAXIMUM DEPTH= 0.570

BASIN NUMBER 156 VOLUME= 0.311 AREA= 6.250
MAXIMUM DEPTH= 0.050

BASIN NUMBER 155 VOLUME= 1.810 AREA= 12.500
MAXIMUM DEPTH= 0.270

BASIN NUMBER 154 VOLUME= 3.688 AREA= 18.750
MAXIMUM DEPTH= 0.270

BASIN NUMBER 153 VOLUME= 0.0 AREA= 0.0
MAXIMUM DEPTH= 0.0

BASIN NUMBER 152 VOLUME= 0.125 AREA= 6.250
MAXIMUM DEPTH= 0.020

BASIN NUMBER 151 VOLUME= 0.250 AREA= 6.250
MAXIMUM DEPTH= 0.040

BASIN NUMBER 150 VOLUME= 6.815 AREA= 25.000
MAXIMUM DEPTH= 0.310

BASIN NUMBER 149 VOLUME= 1.064 AREA= 6.250
MAXIMUM DEPTH= 0.170

BASIN NUMBER 148 VOLUME= 0.749 AREA= 6.250
MAXIMUM DEPTH= 0.120

BASIN NUMBER 147 VOLUME=

UNIVERSITY OF SINGAPORE

BASIN NUMBER 2 VOLUME= 3.374 AREA= 12.500
MAXIMUM DEPTH= 0.340

BASIN NUMBER 1 VOLUME= 2.251 AREA= 12.500
MAXIMUM DEPTH= 0.290

TOTAL VOLUME OF BASINS LISTED ABOVE= 470.635

1
2
3
4
5
6
7
8
9
10
11
12
13
14
15
16
17
18

19
20
21
22
23
24
25
26
27
28
29
30
31
32
33
34
35
36
37
38
39
40
41
42
43
44
45
46
47
48
49
50
51

```

C
  BLOCK NO.11, PLOT NO.1 SURFACE AREA
  DIMENSION A(500), I(100)
  READ(5,1) IO
  1 FORMAT (I4)
  READ(5,2) (A(I),I=1,100)
  2 FORMAT(40F2.0)
  WRITE(6,4) A
  4 FORMAT('0',5F10.2)
  DEL=1.
  XL=0.0
  J=22
  ITAB=1
  N=13
  CALL WEIBULL (A,M,AL,J,DEL,IO,ITAB,AP,B,C)
  WRITE(6,3) AP,B,C
  3 FORMAT('1X',4F10.5,3X',5F10.5,3X',5F10.5)
  STOP
  END

  SUBROUTINE WEIBULL(A,M,AL,J,DEL,IO,TABL,AP,B,C)
  SUBROUTINE WEIBULL
  THIS ROUTINE DETERMINES THE MAXIMUM LIKELIHOOD ESTIMATOR FOR THE
  PARAMETERS OF THE WEIBULL DISTRIBUTION

  DIMENSION N(60), CM(60), RE(60), PX(1=0), PXT(60), ER(60), T(60), A(500)
  DIMENSION I(100)
  COMMON DATA(500),N
  INTEGER TABLE
  XLTEMP = XL
  N=M
  DO 50 I=1,N
    DATA(I)=A(I)
    XR=10000.
    DO 13 I=1,M
      IF(A(I))=XR) I2, I3, I3
    12 XR=A(I)
    13 CONTINUE
    GO TO (70,70,71,71),TABLE
    71 CALL COETHM(CO1,CP,PL,C)
    AP=0
    GO TO 3
    70 FR=0.1
    KA=0.
    CALL REGO3(XA,XR,F,X1,Y1,X2,Y2,N,CP,PL)
    IF(Y1-Y2)1,1,2
    1 AP=X2
    GO TO 3
    2 AP=X1
    3 RP=(1./PL)*W(1./CP)
    B=RP
    C=CP
    GO TO (40,61,63,61),TABLE
    41 RETURN
    63 CONTINUE
    32 CM(I)=XL+DEL/2
    IF(CM(I)-AP)30,31,31
    30 XL =XL+DEL/2
  
```




```

52      OFL=DEL-DEL/2.7J
53      GO TO 32
54      31 XL=XL-DEL
55      DO 4 I=1,J
56      XL=XL+DEL
57      NF(I)=0
58      CH(I)=XL*(DEL/2.)
59      XP=XL*DEL
60      DO 5 K=1,N
61      IF(A(K)-XL)5,4,6
62      6 IF (A(K)-XR) 4,4,5
63      4 NF(I)=NF(I)+1
64      5 CONTINUE
65      AJ=J-1
66      XL=XL-(AJ*DEL)
67      DO 7 I=1,J
68      L=NF(I)
69      Z2=N
70      RF(I)=Z1/Z2
71      7 CONTINUE
72      CHISO=0
73      DO 8 I=1,J
74      PX(I)=RF(I)/DEL
75      C2=(CP/B
76      C3=(CM(I)-AP)/B
77      PXT(I)=C2*(C3**((CP-1.)/EXP(C3**CP)
78      ER(I)=PXT(I)-PXO(I)
79      T(I)=DEL*PXT(I)
80      CHISO=CHISO+(ER(I)**2)*DEL/PXT(I)
81      8 CONTINUE
82      WRITE(6,9) (I(I),I=1,ND),AP,B,CP,CHISO
83      9 FORMAT(1H1,10X,'FITTING THE WEIBULL DISTRIBUTION TO',//BOAL, /
C//IX,'A = 'E10.4,5X,'B = 'E10.4,5X,'C = 'E10.4//IX,'PIX) = (C/B)*
IX*CHISO = 'E14.
C//IX
CR, T, REL.FR, PIX) PIX) 'CLASS FREQ. O.REL.F
DO 10 I=1,J
WRITE(6,11) CH(I),NF(I),RF(I),T(I),PXO(I),PXT(I),ER(I)
11 FORMAT(1H0,1X,E11.4,3X,E3.4X,5(1X,E11.4))
10 CONTINUE
XL=XLTEMP
IF(AP)20,21,20
21 AP=0
CALL COETM1,001,CP,PL,AP)
GO TO 3
20 RETURN
END

```

SUBROUTINE LIKLH1AP,CP,PL,Y)
THIS EVALUATES THE LIKELIHOOD FUNCTION AT EACH LEVEL OF INPUT
AP = PARAMETER A
CP = PARAMETER C
PL = PARAMETER LAMBDA
N = NO. OF DATA POINTS SET BY COMMON
Y = VALUE OF THE LIKELIHOOD FUNCTION
DATA ARRAY IS COMMON WITH SUBROUTINE WEIBULL

SUBROUTINE LIKLH1AP,CP,PL,Y)
COMMON T1501,N



```

C
97      C1 = A*ALCG(CP) + (N*ALCG(PL))
98      SLMT = 0.
99      SUMLT = 0
100     DO 2 J=1,N
101     SLMT = SLMT + (J*(J)-AP)*CP
102     SUMLT = SUMLT + ALOGIT(J) - AP)
103     2 CONTINUE
104     Y = C1 - (PL*SUMTC) + ((CP-1.)*SUMLT)
105     RETURN
106     END

SUBROUTINE RECG3(XL,XP,F,X1,Y1,X2,Y2,N,CP,PL)
ZTEST = .001
ETA = 0.414033949
PSI = 1. - ETA
DELX = XP - XL
M = 2. + 1*ALCG(F)/ALCG(ETA)
X1 = (PSI*DELX) * XL
X2 = (ETA*DELX) * XL
AP = X1
CALL COETM(ZTEST,CP,PL,AP)
CALL LIKLH(AP,CP,PL,Y1)
AP = X2
CALL COETM(ZTEST,CP,PL,AP)
CALL LIKLH(AP,CP,PL,Y2)
J = M-2
DO 6 K=1,J
DELX = DELX*ETA
IF(Y2-Y1) 5,4,4
4 Y1 = Y2
X1 = X2
X2 = X1 + ((ETA - PSI)*DELX)
AP = X2
CALL COETM(ZTEST,CP,PL,AP)
CALL LIKLH(AP,CP,PL,Y2)
GO TO 6
5 Y2 = Y1
X2 = X1
X1 = X2 - ((LTA - PSI)*DELX)
AP = X1
CALL COETM(ZTEST,CP,PL,AP)
CALL LIKLH(AP,CP,PL,Y1)
6 CONTINUE
RETURN
END

SUBROUTINE COETM FOR THE WEIBUL SUBROUTINE
C
C
C
C
THIS SUBROUTINE DETERMINES THE MAXIMUM LIKELIHOOD ESTIMATORS FOR
AND LAMDA WITH A GIVEN.

SUBROUTINE COETM (CTCL ,C,L,A)
COMMON X(500),M
REAL L
NC = 4
CMIN = .2
CMAX = 10.
YA = CFNT(X,M,CMIN,A)

```




```

148       IF (ABS(YA)-CTOL*CMIN-.001)30,30,31
149       30 C=CMIN
150       GO TO 24
151       31 YB=CFNT(X,M,CMAX,A)
152       IF (ABS(YB)-CTOL*CMAX-.001)32,32,33
153       32 C = CMAX
154       GO TO 24
155       33 IF (YA*YB)3,3,1
156       1 WRITE(6,4) CMIN,CMAX
157       4 FORMAT(1,' IN THE INTERVAL 'E15.7,' TO 'E15.7,' THE
         C THAN ONE SOLUTION FOR C')
158       STOP
159       3 C2=(CMIN+CMAX)/2.
160       Y2=CFNT(X,M,C2,A)
161       IF (ABS(Y2)-CTOL*C2-.001)7,7,25
162       25 IF(YA*Y2)8,7,9
163       7 C=C2
164       GO TO 24
165       8 Y1=YA
166       C1=CMIN
167       GO TO 10
168       9 Y1=YB
169       C1=CMAX
170       10 N=NC-1
171       DO 20 I=1,N
172       C3=C2-(C2-C1)*Y2/(Y2-Y1)
173       Y3=CFNT(X,M,C3,A)
174       IF (ABS(Y3)-CTOL*C3-.001)11,11,26
175       26 IF (Y2*Y3)12,11,13
176       11 C=C3
177       GO TO 24
178       12 C1=C2
179       Y1=Y2
180       13 C2=C3
181       20 Y2=Y3
   C
   C
   C
182       23 IF (ABS(Y2)-CTOL*C2-.001)21,21,22
183       21 C=C2
184       GO TO 24
185       22 C3=C2-(C2-C1)*Y2/(Y2-Y1)
186       Y3=CFNT(X,M,C3,A)
187       C1=C2
188       Y1=Y2
189       C2=C3
190       Y2=Y3
191       GO TO 23
192       24 A1=0
193       A2=0
194       A3=0
195       DO 35 I=1,M
196       A1=A1+1./(X(I)-A)
197       A2=A2+(X(I)-A)**(C-1)
198       35 A3=A3+(X(I)-A)**C
199       L= M/A3
200       AFNT=(1.-C)*A1+C*L*A2
201       RETURN
202       ENC
   C
   FUNCTION CFNT

```

C
C
C

THIS EVALUATES EQUATION 8

```
203 FUNCTION CFN(X,M,C,A)
204 DIMENSION X(500)
205 A1=0
206 A2=0
207 A3=0
208 DO I =1,M
209 A1=A1+(X(I)-A)*C
210 A2=A2+(X(I)-A)*C*ALOG(X(I)-A)
211 A3=A3+ALOG(X(I)-A)
212 CFN= (M/((M/A1)*A2)-A3)-C
213 RETURN
214 END
```

